POLITECNICO DI MILANO

DEPARTMENT OF CIVIL AND ENVIRONMENTAL ENGINEERING

DOCTORAL PROGRAM IN ENVIRONMENTAL AND INFRASTRUCTURE ENGINEERING

ENVIRONMENTAL TECHNOLOGIES AREA

A RISK-BASED APPROACH FOR CONTAMINANTS OF EMERGING CONCERN IN DRINKING WATER PRODUCTION AND DISTRIBUTION CHAIN

Doctoral dissertation of:

Beatrice Cantoni

Supervisor:
Prof. Manuela Antonelli

Co-supervisor:
Dr. Andrea Turolla

Tutor:
Prof. Francesca Malpei

The chair of the doctoral program:
Prof. Riccardo Barzaghi

XXXIII cycle

2017-2020

ABSTRACT

The revision of the European drinking water (DW) Directive has introduced some contaminants of emerging concern (CECs) among the list of monitored parameters and highlighting the importance of the analysis of materials in contact with DW. Above all, these revisions are a direct consequence of the shift of the "drinking water production" paradigm promoted by the EU Directive. In fact, it designs a general framework in which the conventional approach, based on controlling the exceedance of regulation limits, is enslaved to a wider approach based on human health risk minimization throughout the whole supply system (from source to tap). Quantification of the risk consists of understanding the level of exposure concentrations with respect to health-based guideline levels derived from toxicological studies. However, the use of a risk-based approach is not easy to be achieved for CECs due to several knowledge gaps. In particular, it is difficult to evaluate CECs exposure levels in DW, firstly because of their low concentrations compared to the LOQ (Limit of Quantification) values of the analytical methods, which are in continuous refining; this results in monitoring databases characterized by high percentages of censored data, i.e. data below the LOQ. Moreover, uncertain estimation of CECs exposure levels in DW is also due to a lack of consolidated engineering knowledge about their fate throughout treatment processes in drinking water treatment plants (DWTPs) and in drinking water distribution networks (DWDNs). Finally, high uncertainty is related also to CECs toxicity that hinders the prioritization of CECs to be included in the regulations and also the limit to be proposed.

The goal of this PhD project is to contribute to fill the knowledge gaps in the field of risk assessment related to the spread of CECs in DW supply systems, providing effective tools for supporting water utilities in managing a reliable water supply system and decision-makers in CECs regulation prioritization. Specifically, the DW supply system was considered as made of 4 elements: (i) DW sources (e.g. groundwater, surface water), (ii) drinking water treatment plant, (iii) drinking water distribution network and (iv) point of use (i.e. the consumer's tap). Within this framework, lab-scale experiments have been combined with full-scale monitoring, development of predictive models and risk assessment procedures, and advanced statistical methods (i.e. sensitivity analysis, uncertainty analysis, factorial analysis, cluster analysis, etc.), to apportion the contribution of each element of the DW supply system in determining human health risk, in order to prioritize the interventions in view of an overall risk minimization.

Firstly, an advanced approach, based on Maximum Likelihood Estimation method for left-censored data (MLE_{LC}), was compared with the traditional methods used to handle censored data, that are their elimination or substitution with a value between 0 and LOQ. These methods have been applied on full-scale monitoring data of several micropollutants in samples collected throughout the whole DW supply system in a highly urbanized Italian area. Results demonstrated the benefits of MLE_{LC} method compared to the traditional ones, especially for high percentages of censored data, not only in terms of more accurate fit of concentration statistical distribution, but also in three data analysis applications, that are the estimation of concentrations time trend in source water, treatment removal efficiency and human health risk.

Secondly, a new probabilistic procedure, that is a quantitative chemical risk assessment (QCRA), was developed to assess human health risk related to the occurrence of CECs in DW, including all the uncertainties related to both exposure and hazard assessments. The QCRA quantifies the risk in terms of benchmark quotient probabilistic distribution, from estimated CECs concentration in DW, simulating source water treatment by granular activated carbon (GAC). Sensitivity and uncertainty analyses were performed to identify main factors affecting risk estimation, highlighting future research needs and directions, to improve reliability of risk assessment. QCRA was applied to bisphenol A as an example CEC and various GAC management options (intervention scenario). This demonstrated that QCRA is

more effective than deterministic CRA, in evaluating the effect of each scenario in risk minimization, permitting to select and prioritize the most appropriate interventions.

Since based on the QCRA outputs, it was found that modelling of GAC breakthrough curves has a relevant role in the accuracy of risk estimation, experimental work has been performed to more accurately model GAC performance towards CECs, in particular perfluoroalkyl substances (PFAS) and pharmaceutical active compounds (PhACs). GACs were tested by equilibrium batch experiments, providing isotherms, and rapid small-scale column tests (RSSCT), to calibrate CECs breakthrough curves. These studies were performed on 8 PFAS and 8 PhACs in 3 water matrices, that are tap water and two synthetic matrices at lower dissolved organic carbon (DOC) and two levels of conductivity. In addition, 4 commercial GACs were tested, differing for origin, micro- and mesoporous structure and surface charge. Finally, full-scale data collected through a monitoring campaign on PFAS were used for model validation. CECs removal was confirmed to rely on compounds hydrophobicity; GAC surface charge was demonstrated to have more influence than its porosity. Moreover, the interaction between CEC hydrophobicity and GAC porosity was found to have significant effect on performance. Finally, a correlation was found between the removal of the absorbance of UV at 254 nm and CECs removal, that was not dependent on the activated carbon nor the water matrix, but it was found to depend on the test scale.

Finally, potential recontamination events in the DWDN were studied with particular focus on BPA release from epoxy resins used to renovate pipelines. Lab migration tests were performed on three epoxy resins and designed with the Design of Experiments (DoE) method in order to build a BPA release model as a function of water chlorine concentration and chemical stability. BPA release over time was well described by the combination of two first-order kinetic models, where the first describes the release of free BPA due to incomplete polymerization and the second describes BPA release due to resins' deterioration. The calibrated BPA release model was combined with the hydraulic model of a highly urbanized Italian area, through EPANET MSX. The model allowed to simulate the current fate of BPA in the DWDN, identifying the most vulnerable areas; as a consequence, the combined model can be adopted to optimize monitoring and intervention plans, which can be site-specific customized to minimize the human health risk.

Contents

STATE OF THE ART

List of symbols and abbreviations

AC	Activated Carbon
BTZ	Bentazone
BPA	Bisphenol A
BQ	Benchmark Quotient
DCF	Diclofenac
CECs	Contaminants of Emerging Concern
CCL	Candidate Contaminant List
CRA	Chemical Risk Assessment
CBZ	Carbamazepine
DW	Drinking Water
DWTP	Drinking Water Treatment Plant
DWDN	Drinking Water Distribution Network
DWTL	Drinking Water Threshold Level
E1	Estrone
E2	17β-estradiol
EE2	17α-ethinylestradiol
E3	Estriol
EU	European Union
GAC	Granular Activated Carbon
GPS	Glyphosate

LOQ	Limits of quantification
MTBE	Methyl Tertiary-Butyl Ether
NOAEL	No-Observed-Adverse-Effect Level
NOM	Natural Organic Matter
NP	Nonylphenol
OP	Octylphenol
PFAS	Perfluoroalkyl substances
PFOA	Perfluorooctanoic acid
PFOS	Perfluorooctanesulfonic acid
PhACs	Pharmaceutical Active Compounds
PPCPs	Pharmaceuticals and Personal Care Products
PBDE	PolyBrominated Diphenyl Ethers
RfD	Reference Dose
RSSCT	Rapid Small Scale Column Test
t-OP	ter-octylphenol
UF	Uncertainty Factor
US-EPA	United States Environmental Protection Agency
VOC	Volatile Organic Chemicals
WHO	World Health Organization

1. Contaminants of emerging concern

In recent years, the presence of micropollutants in the aquatic environment has become an issue of growing global concern. Great attention is paid to the so-called contaminants of emerging concern (CECs), that belong to several families of chemicals discharged from households (e.g. pharmaceutical active compounds (PhACs), estrogens), agriculture (e.g. pesticides) and industrial processes (e.g. perfluorinated compounds, alkylphenols) (Stuart et al., 2012). CECs can be distinguished from conventional micropollutants being the formers currently not included in routine monitoring programmes or current regulations. However, they might become candidate for future regulations depending on research on their (eco)toxicity, potential health effects and on monitoring data regarding their occurrence in the various environmental compartments (Richardson and Kimura, 2016). Although these substances are potentially hazardous, as some are persistent and biologically active, they have been scarcely analyzed in the past due to their extremely low concentrations (ranging from ng L^{-1} to µg L^{-1}) that made them hard to detect and quantify (Valcárcel et al., 2011). The recently enhanced quantification analytical techniques allowed the identification of these substances in environmental samples, including drinking waters (DW) (Petrović et al., 2003; Schwarzenbach et al., 2006). CECs are usually present at trace concentrations as complex mixture of hundreds up to thousands of substances, posing significant human health and environmental threats (Coday et al., 2014). Consequently, regulations are being adopted worldwide to limit their presence.

The European Union (EU), in the Directive 2013/39/EU, listed 45 compounds as priority substances to be monitored in water, representing a significant risk to or via the aquatic environment, for which environmental quality standards have been defined (EU Parliament, 2013). The Australian Cooperative Research Centre for Contamination Assessment and Remediation of the Environment identified in 2014 the first-tier priority contaminants: two perfluorinated alkyl compounds (perfluorooctanesulfonic acid, PFOS, and perfluorooctanoic acid, PFOA), methyl tertiary-butyl ether (MTBE), benzo[a]pyrene,

weathered hydrocarbons and polybrominated diphenyl ethers (PBDE). Moreover, in 2016, the United States Environmental Protection Agency (US-EPA) announced the final Contaminant Candidate List CCL4 listing 97 chemicals or chemical groups and 12 microbial contaminants which are currently not subjected to any proposed or promulgated national primary drinking water regulations, but which are known or anticipated to occur in public water systems and may require future regulation, based on their health effects, occurrence, treatability and availability of analytical methods. This list included cyanotoxins, disinfection by-products, industrial chemicals (e.g. alkylphenols), inorganic chemicals, pesticides, Pharmaceuticals and Personal Care Products (PPCPs) and Volatile Organic Chemicals (VOCs) (EPA, 2016). Eight CECs, among estrogens and PhACs, are listed in the European Watch List (Decision 2018/840), as substances that may be regulated in the future based on their (eco-) toxicity, effects on human health and monitoring data related to their presence and persistence (EU Parliament, 2020a). Moreover, in the revision of Directive 98/83/EC on the quality of water intended for human consumption, the EU included concentration limits for bisphenol A (BPA) and perfluoroalkyl substances (PFAS), and suggested the integration of the Watch List with 17β-estradiol (E2) and nonylphenol (NP), since research and monitoring of these two compounds are recommended (EU Parliament, 2020b).

As shortly summarized above, different priority lists worldwide focused on a wide range of CECs, and several knowledge gaps are involved in their assessment. This makes difficult prioritizing CECs to be included in DW regulations and related mitigation actions.

2. Shift in the approach for DW supply systems management

In addition to the introduction of some CECs among the list of monitored parameters, the revision of the European DW Directive 98/83/EC promoted a shift of the "drinking water production" paradigm (EU Parliament, 2020b). In fact, it designed a general framework in which the conventional approach, based on the control of compliance with quality standards, is enslaved to a more comprehensive and wider approach based on human health risk minimization throughout the whole supply system (from source to tap). This risk-based approach is based on: i) the identification in the DW supply systems of potential hazards, that are events that can cause DW contamination and adverse effects on users' health, and ii) the quantification of the risk related to the identified hazard (WHO-IPCS, 2018). The risk can be quantified estimating the hazard likelihood of occurrence and severity of the consequences in case of hazard occurrence. The likelihood of a hazard, usually expressed as a frequency of occurrence, depends on the site-specific system conditions (e.g. pollution sources control measures, treatment processes, distribution maintenance and protection practices, frequency of extreme weather conditions). The severity of a hazard, and the consequent DW contamination, is estimated through the exposure and health effect assessment. The exposure assessment determines the size and nature of the exposed population and the route, amount and duration of the exposure to the hazardous contaminant; while the health effect assessment defines the relation between the contaminant dose and the resulting health effect (WHO, 2010). Therefore, a risk-based approach should be used for: (i) prioritization of substances to be included in regulations, and (ii) design and management of a resilient DW supply system. For the second application, the risk assessment should be performed to define a risk apportionment throughout the supply chain, in order to identify the main risk sources, and to evaluate the more appropriate mitigation actions in preventing and minimizing risks for the consumer along the entire DW production and distribution system, in compliance with the precautionary principle. In fact, the human health risk assessment for CECs is of major interest because, even considering the recent advances in treatment technologies, in the common practice DWTPs are not specifically designed and managed to remove CECs (Benotti et al., 2009; Simazaki et al., 2015; Vulliet et al., 2011). Therefore, it is important to assess whether the drinking water treatment plants (DWTPs), as currently designed, are able to deal with CECs, and, if not, which treatment is the most suitable to be integrated and address CECs removal. On the other end, the holistic approach now introduced in the revision of the EU DW Directive, puts attention on the

need to include in the assessment the Drinking Water Distribution Network (DWDN), looking at the materials in contact with DW, to evaluate whether a worsening in the treated DW occurs before approaching users tap.

The "Carcinogenic Risk Assessment Guidelines" (https://bit.ly/33582jl), drawn up by the US-EPA in the 1980s, are one of the first documents in which "risk assessment" is described for the evaluation of the negative effects on human health due to dangerous substances. In the document, the approach is identified as a decision supporting tool, which combines scientific evidence of experimental and/or modeling data with socio-economic, technical and political considerations to decide whether or how much controlling future exposure to substances with suspected carcinogenic effects (US EPA, 1986). This is in accordance with the World Health Organization (WHO) guidelines that state the importance of the implementation of a "framework for safe drinking water" as basic and essential requirement to ensure the safety of drinking water. This framework provides a preventive risk-based approach to manage water quality, composed of health-based targets established by a competent health authority. In particular, the recommendations confirm the need to regulate a list of selected parameters, among the hundreds of compounds for which WHO guideline risk-based values exist (Gorchev and Ozolins, 2011).

As for chemical risk assessment (CRA), the current procedure consists of three steps: (i) the exposure assessment, in which the route, magnitude and frequency of the exposure to the considered compound are quantified; (ii) the hazard assessment, in which the relationship between dose of exposure to the substance and the incidence and severity of an effect (depending on the assessed health endpoint) is estimated and a health-based guideline level, namely the Drinking Water Target Level (DWTL), is defined; (iii) the risk characterization, where the results of the previous two steps are integrated and combined to generate a quantitative or qualitative estimation of the incidence and severity of the adverse effects likely to occur in a human population due to actual or predicted exposure to the considered single substance (Bokkers et al., 2017). This is usually performed by a deterministic procedure computing the Benchmark Quotient (BQ), also referred to as Hazard Quotient (HQ), assumed as the ratio between the exposure concentration (C_{EXP}) to a substance and its health-based drinking water target level (DWTL) point values (Baken et al., 2018a) (Eq. 1).

$$\mathrm{BQ} = \frac{C_{EXP}}{\mathrm{DWTL}} \qquad \text{(Eq. 1)}$$

Hence, the BQ provides an indication of the risk level, depending whether its value is lower or higher than 1: a BQ lower than 1 indicates that the chemical exposure is less than the benchmark suggesting that the exposure is unlikely to result in an adverse effect; conversely, a BQ higher than 1 indicates that the exposure is greater than the benchmark and that the sources, pathways and routes of chemical exposure should be further evaluated (van Leeuwen & Vermeire, 2007).

However, the use of a risk-based approach for DW supply management is not easy to be achieved for CECs due to several knowledge gaps on both exposure and hazard assessments related to CECs in DW, as described in the following paragraphs.

3. CECs exposure from DW consumption

In the exposure assessment (step i in paragraph 2), the ingestion of drinking water is considered as route of exposure. Thus, the chemical concentration in the drinking water, typically the maximum one, is the exposure concentration, which can be obtained in three different ways: it can be directly measured in monitoring campaigns, generalized from existing literature data collected in similar case studies, or estimated using models (WHO, 2010). Anyway, all these methods include critical issues which generate uncertainties in estimating exposure concentration.

3.1. Direct measurements through CECs monitoring campaigns

Monitoring campaigns in the studied DW supply system generally provide the most accurate and relevant data, but are the most time and resource intensive. A major challenge for these activities, posed by the low concentrations of CECs, is the complexity of detection and quantification procedures. Therefore, when monitoring CECs in raw and treated water, it is important to consider the performance of the analytical methods adopted in terms of limits of quantification (LOQ), accuracy and precision, which define the minimum measurable concentration, the maximum observable removal efficiency and the associated error (Wang et al., 2016).

To evaluate current analytical methods capabilities, a literature review has been conducted by considering relevant research works, published from 2000, on the removal of several CECs with three treatment processes specifically addressing CECs removal, namely adsorption on activated carbon, separation by pressure-driven membranes (nanofiltration and reverse osmosis) and degradation by oxidation and advanced oxidation processes. Analyzed CECs were: (i) four alkylphenols, namely BPA, octylphenol (OP), ter-octylphenol (t-OP) and NP, (ii) four estrogens, including estrone (E1), E2, 17α-ethinylestradiol (EE2) and estriol (E3), (iii) two PhACs, namely carbamazepine (CBZ) and diclofenac (DCF), (iv) two PFAS, namely PFOA and PFOS, and two pesticides, namely glyphosate (GPS) and bentazone (BTZ). In detail, 251 bibliographic sources have been examined, consisting of research articles, literature reviews and books. Among the 251 examined references, only 40 studies reported the LOQ values of the adopted analytical methods, which are represented in Figure 1 as a function of the CECs. None of the research studies on BTZ reported the instrument LOQ for this compound.

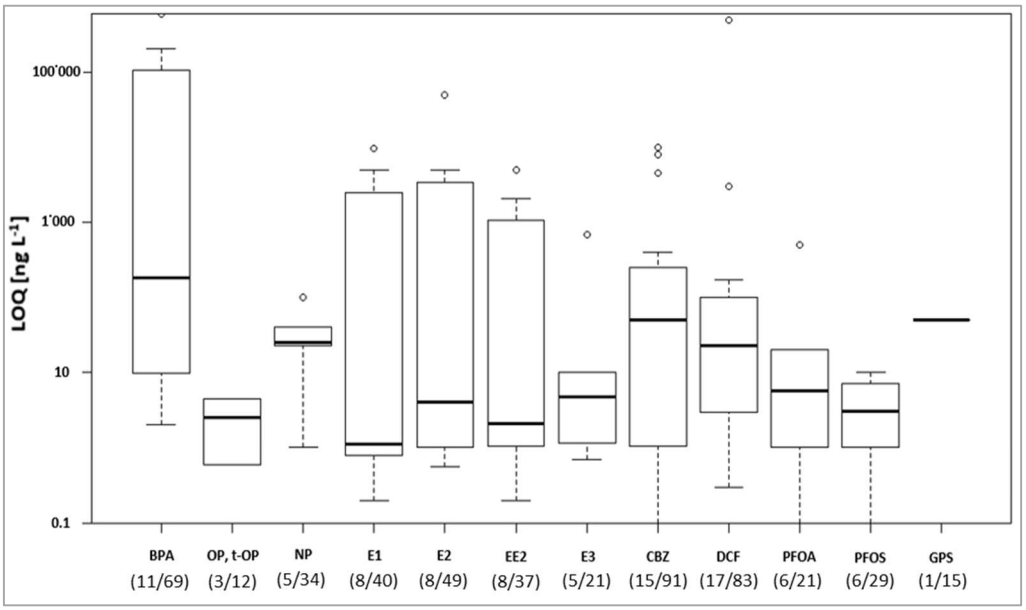

Figure 1. LOQ values (ng L^{-1}) reported in examined references (251 references about CECs removal by adsorption on GAC, nanofiltration, reverse osmosis, ozonation, advanced oxidation processes) as a function of the investigated CECs. In brackets are displayed the number of works reporting the analytical method LOQ with respect to the total number of studies analyzing the specific CEC.

A wide range of LOQ can be found for each CEC, varying from 0.1 ng L^{-1} to more than 0.1 mg L^{-1}. Advances in analytical techniques are still required to improve the performance of existing instruments in terms of detection and quantification limits, accuracy and precision. In fact, in many cases current analytical LOQ are in the same order of magnitude of CECs occurrence concentrations. As a consequence, the direct use of monitoring data in risk assessment is undermined by uncertainty, since water quality databases have high percentages of left-censored data, that are values lower than the LOQ of the adopted analytical

methods (Baccarelli et al., 2005). Conventionally, censored data are treated through their elimination or substitution with specific values, arbitrarily selected in the range between zero and LOQ. However, these methods lead to neglect, in case of elimination, or modify, in case of substitution, the information coming from the original dataset (Tekindal et al., 2017). Therefore, these conventional methods have some limitations and can lead to erroneous conclusions on the occurrence of CECs in DW and the associated human health risk (Kleywegt et al., 2011; Wang et al., 2016). As a consequence, it is important to apply advanced techniques for the proper treatment of databases with high percentages of censored data, such as in the case of CECs concentrations in DW (Rodríguez-Gil et al., 2018).

Another critical issue related to the use of measurements for exposure assessment for CECs in DW is due to the limited number of available data. In fact, currently, the monitoring of thousands of CECs throughout the whole DW supply chain is not feasible from an economic point of view. Although new methodologies, such as non-target screening (Singer et al., 2016), are becoming more and more consolidated, their cost is still too high to be adopted in routine monitoring campaigns. Consequently, the monitoring campaigns are carried out in specific points of the DW supply system with typically very low frequencies, producing discontinuous information that may not reflect the real level of CECs contamination and associated risk. In addition, when monitoring campaigns are referred to DWTPs, no information about removal processes are provided in most of the cases, making difficult comparing data and drawing general considerations. It should be stressed that, for several treatment processes, the performance is variable over time, with a decreasing time trend, as for example the adsorption onto granular activated carbon (GAC), where the removal efficiency depends on the time passed since the last regeneration of the filter bed (Denning and Dvorak, 2008). Therefore, when assessing the effectiveness of GAC filters for removal of CECs through the monitoring of full-scale plants, it is important to consider that adsorption is a dynamic process: the performance of different GAC filters towards a target compound can therefore differ only because collected samples represent two different moments in the operating time. Therefore, monitoring data have to be related to the instant of time in the operating time in which the sample has been collected in order not to draw wrong conclusions about the possibility of removal of a given contaminant.

Several case studies of CRA where exposure assessment is based on CECs measurement in DW are reported in literature. Schriks et al. (2010) evaluated the risk related to a selection of 50 CECs in surface water, considering as exposure concentration the maximum value reported in Rhine and Meuse river basins annual reports; however, water treatment processes and distribution network were not considered within the system boundaries, so that these aspects have not been evaluated within the risk assessment framework. Riva et al. (2018) assessed the risk related to CECs in DW considering single data deriving from a monitoring campaign performed at several DWTPs; for each contaminant, the CEC measured concentration at the outlet of the monitored DWTP was assumed as exposure concentration, but again no information were provided about the type of treatment systems and operating conditions in the analyzed DWTPs and the DWDN were not considered. Gaffney et al. (2014) studied the risk related to the occurrence of 31 PhACs along the DW supply system considering their concentration both in raw water and in water after the DWTP; in particular, the case with the raw water PhACs concentrations was considered as the worst-case scenario, assuming a potential operating malfunction in the DWTP resulting in the supply of untreated raw water. In this study, even if both the concentrations before and after the DWTP were considered, providing information about the applied treatments and their overall removal efficiency, no information were provided about the fate in the DWDN and the treatment performance variation over time, which could affect the final output estimation.

Summarizing, measurements for compounds that are not routinely monitored, such as CECs, do not describe appropriately the concentration variability in space and time and cannot be used as stand-alone tools for risk assessment unless accepting high uncertainties for the output (IPCS, 2000).

3.2. Expected CECs concentration based on literature data

To overcome measurements limitations, an option for exposure assessment (step ii in paragraph 2) is the estimation of expected CECs tap concentration based on existing literature data on CECs fate throughout treatment processes present in DWTPs and through the DWDN.

The low concentration and the different properties of CECs not only complicate detection procedures, but also create challenges for treatment processes (Luo et al., 2014). The prediction of removal efficiencies achievable with technologies available at full scale is a complex and contradictory topic. In fact, the prediction of CECs fate in treatment plants from existing literature data is characterized by wide uncertainties due to: (i) presence in complex and multi-component matrices; (ii) concentrations of contaminants that vary over time; (iii) published studies carried out under controlled or poorly representative conditions, or not-reported operating conditions; (iv) the already mentioned difficulty in the analysis due to low concentrations, coexistence in several phases and limited analytical accuracy.

Removal of different CECs in drinking water treatment plants (DWTPs) would need the integration of different unit processes in the treatment train, since only one unit is not expected to cope with this aim. The choice of the processes to be included in the risk assessment and optimization scenarios depends on the DW source and the target CEC. In case of the majority of CECs, the literature states that, among the available treatment processes currently applied in DWTPs, adsorption onto GAC was identified as the best available technology (Westerhoff et al., 2005). As a rule, activated carbon (AC) is used in granular form, in filters positioned in the terminal phase of the purification system, just before the final disinfection. This allows the removal of any present micropollutants, residual natural organic matter (NOM) and any by-products of an oxidation phase (Crittenden et al., 2012). Scientific literature provides a wide number of studies in which many combinations of ACs and CECs have been experimentally tested. AC performances have been determined in real waters or in synthetic matrices (e.g. deionized water or other real waters with addition of inorganics and/or background organic matter) by means of lab scale batch tests and continuous fixed bed tests (at lab , pilot or full scale). A summary of the removal efficiencies found through a literature review on relevant research works about removal of several CECs with adsorption on activated carbon published from 2000 (124 references), is reported in Figure 2.

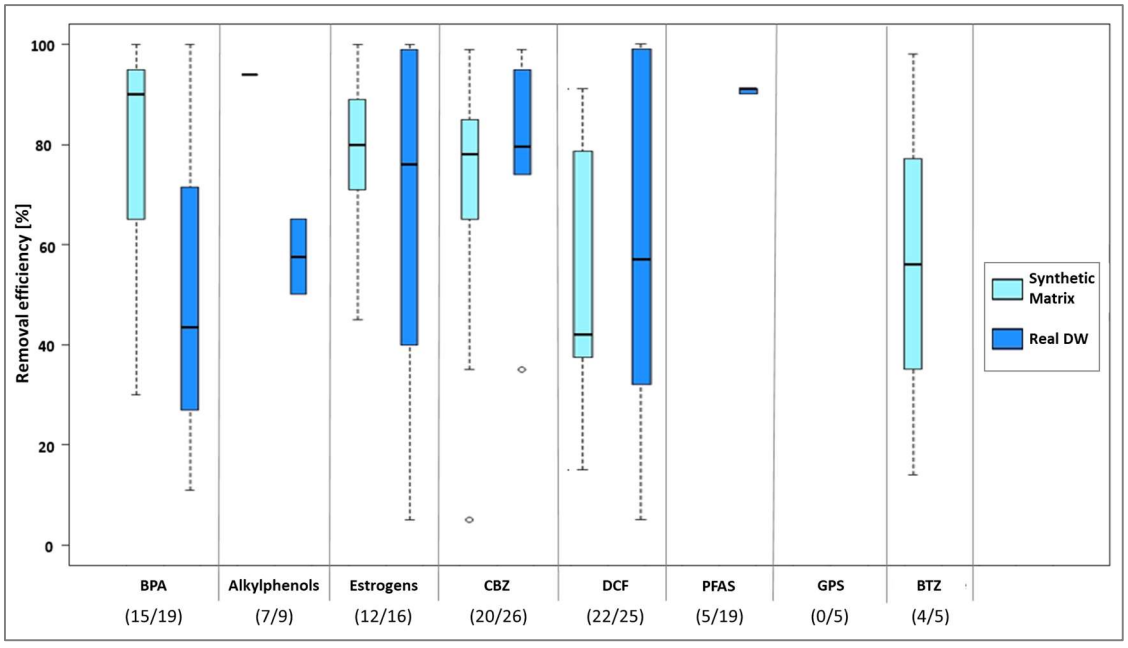

Figure 2. Range of removal efficiency [%] achieved by adsorption on activated carbon of some CECs in the examined literature (124 studies), as a function of the tested water matrix. In brackets are displayed the number of works reporting a removal efficiency with respect to the total number of studies analyzing the specific CEC.

There is a strong variability in the results reported in literature about the removal of CECs by adsorption on activated carbon, especially for some CECs: experimental outcomes range both among different compounds in the same water matrix and for the same compound in the various water matrices. Such behavior is mostly due to two peculiar aspects: the belonging of significantly different compounds to this group of pollutants and the strong influence of the operating conditions on process effectiveness. Among the investigated CECs, activated carbon is highly effective (median removal efficiency over 80%) on estrogens and CBZ in all the matrices, and BPA and alkylphenols in synthetic matrices. Only DCF exhibits a slightly lower adsorbability regardless of the operating conditions. Otherwise, despite the widespread diffusion in the environment, experimental data on GPS and BTZ are still scarce, being the totality of the research works in literature referred to high concentrations of these pollutants (order of mg L^{-1}), except for an article published by Mailler et al. (2016) (Mailler et al., 2016). Finally, although activated carbon was successfully applied on PFOS and PFOA, a limited number of studies in the literature reported analyzed removal efficiency.

Overall, the available studies show that activated carbon is effective in removing a wide range of compounds, having very different physical-chemical properties; however, the adsorption capacities determined in different studies cannot be easily compared due to three main aspects:

- differences in the studied process scale;
- differences in experimental conditions, such as adsorbent type, initial CEC concentration, water matrix composition, AC dose and contact time;
- differences in reporting experimental results, being expressed in terms of percentage removal efficiency for a given dose and contact time or in terms of isotherm parameters.

Therefore, it is important to identify if the experiments are performed at: (i) laboratory scale, usually in batch reactors; (ii) pilot scale, using low-flow reactors, or (iii) full scale DWTPs. In fact, the main concern for the lab- and pilot-scale studies is the effective transferability of the obtained results at the full scale with feasible engineering parameters. Moreover, when using literature data to predict CECs removal efficiency by GAC, great attention has to be paid to the water matrix used in the experiments, addressing to synthetic solutions or real water samples. In particular, this aspect refers to both CECs concentration and the presence of interfering/competing compounds, since they directly affect the removal performance (Siriwardena et al., 2019). Again, the main concern about the use of a synthetic solution is the transferability of the obtained results to real conditions. An overview of the literature, reported in Figure 3, shows that most of the experimental data on CECs was obtained by means of experimental activities performed at the laboratory scale, in completely mixed batch reactors or in rapid small scale columns, using water matrices usually constituted by synthetic solutions (prepared from deionized water) or natural water spiked with a single compound. In fact, the research works based on lab-scale experiments are almost 86% of the 124 examined studies, compared to the ones based on pilot- and full-scale experiments (10% and 4%, respectively). Almost 64% of the research works are based on experiments performed using synthetic solutions, while 25% on surface water samples; only few studies are focused on groundwater (6%) and drinking water (5%). Only in recent years, research works have been increasingly conducted by on-site positioned pilots or by monitoring full scale facilities, *inter alia* (Eschauzier et al., 2012; Löwenberg et al., 2014; Mailler et al., 2015). This shift is primarily due to the increased awareness about the importance of real operating conditions and the frequent poor transferability of laboratory outcomes on larger contact reactors.

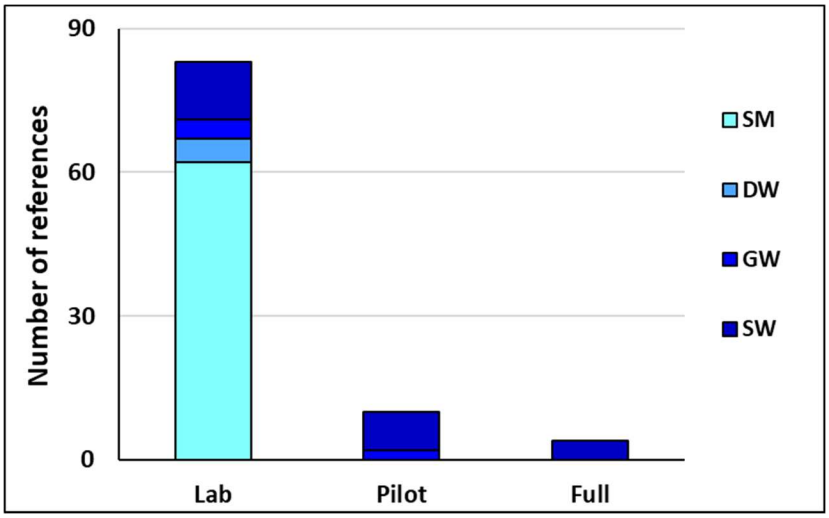

Figure 3. Distribution of examined literature studies about CECs adsorption on activated carbon (124 references) as a function of experimental scale and tested water matrix. SM: synthetic matrix; DW: drinking water; GW: groundwater; SW: surface water.

In addition to the water matrix, also the tested CECs concentration is a decisive parameter in determining the process effectiveness when considering a complex water matrix. Actually, when dealing with adsorption on activated carbon, it is of paramount importance to interpret the process as a dynamic equilibrium among the adsorbing solid phase and the solutes, constituted by a number of components including CECs having different physical-chemical properties and concentrations. Within this framework, the presence of compounds at concentrations differing by orders of magnitude is the key element in determining the extent of adsorption. For instance, NOM concentration in a treated water flow is commonly of the order of mg L^{-1}, while the concentration of regulated and routinely monitored micropollutants is of the order of μg L^{-1}, compared to concentrations of CECs which range between ng L^{-1} and μg L^{-1} (Snyder et al., 2007; Yoon et al., 2005; Yu et al., 2009). In detail, competitive phenomena occur at active sites and CECs are highly disadvantaged in multicomponent systems, due to the difference in concentration (Yu et al., 2012). This observation is fundamental when looking at the concentrations of CECs adopted in the experiments, summarized in Figure 4, ranging from few ng L^{-1} to several hundreds of mg L^{-1}. In fact, it can be noted that the tested initial concentrations in synthetic matrices is significantly higher than CECs concentration measured in real DW samples. Therefore, it is hard to transfer results obtained by tests in synthetic matrix for the prediction of real full-scale applications.

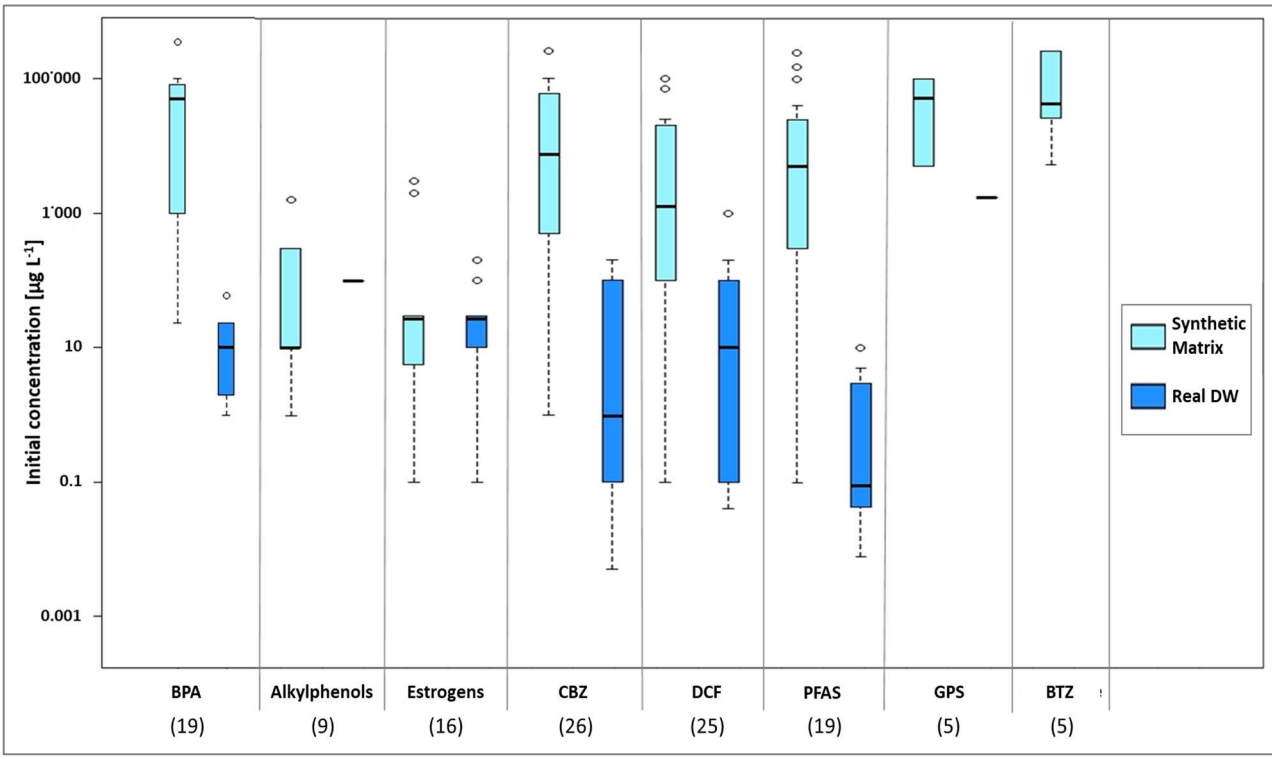

Figure 4. Adsorption on activated carbon of some CECs in the examined literature studies (124 references): range of initial concentration [µg/L] as a function of the studied CEC and the water matrix used in the experiments. In brackets the total number of studies analyzing each CEC is displayed.

Finally, since the experiment scale, the water matrix and operating conditions strongly affect the adsorption process, it is not easy to compare the results of different studies and use them for CECs exposure predictions in different case studies. However, literature data may allow to preliminary compare the adsorbability of different compounds and to roughly estimate the fate of different CECs through GAC filters in presence of a mixture of CECs.

3.3. Exposure prediction through the combination of experimental and modeling tools

To overcome measurements and literature data limitations, an option for exposure assessment (step iii in paragraph 2) is the combination of experiments and prediction models. In fact, models, including the ones estimating treatment processes performance, when properly calibrated and validated, provide precious information complementary to the existing measurements. In exposure models, the effect of specific system conditions can be simulated, allowing the prediction of the resulting exposure variability and identifying the parameters that have greater effects on the variability and accuracy of the exposure concentration (US EPA, 2010). Modeling CECs fate throughout the whole DW supply chain, including their removal in the DWTP treatment units and their potential recontamination in the distribution network, can be helpful to apportion the contribution of each element of the DW supply system in determining human health risk. CECs fate prediction requires reliable monitoring data, experimental data and modeling tools to be able to give an accurate estimate of the concentrations of CECs at the tap, to which end users are effectively exposed.

Considering activated carbon adsorption as removal process, to predict CECs fate through GAC filters it must be taken into account that removal efficiency is not constant over time, and its variability depends on system operating conditions; hence, breakthrough curves are typically used to model adsorption process, since they report the time trend of the outlet contaminant concentration, normalized to the inlet concentration, during filter operation (Denning and Dvorak, 2008). The most practical and

applicable approaches to model adsorption process performance are: (i) Rapid Small Scale Column Test (RSSCT) based on a similitude approach (Crittenden et al., 1987), or (ii) numerical simulations based on experimental isotherms and kinetics data. In RSSCT, the adsorption process performance is simulated in small-scale column to estimate the contaminants breakthrough curves (Senevirathna et al., 2010). The experimental RSSCT approach has been widely adopted for regulated and routinely monitored micropollutants and in few cases for CECs, since it allows convenient testing of various operating conditions of full-scale adsorbers over a reasonable timeframe without complicated mathematical modeling. Conversely, mathematical modeling allows a less time consuming evaluation of several non-tested operating conditions and consents a proper handling of the uncertainties related to isotherms and kinetics data, as well as operating conditions of the process, resulting in a more comprehensive tool able to predict adsorption performance (Athanasaki et al., 2015). Several equations for the mechanistic description of the process kinetics have been proposed for organic pollutants (Crittenden et al., 1991; Worch, 2008), including the intraparticle diffusion model, the homogeneous surface diffusion model and the pore and surface diffusion model, although their application to CECs is still limited, *inter alia* (García-Mateos et al., 2015; Kovalova et al., 2013). Furthermore, few research works were addressed so far to the modeling of multi-component systems including CECs (Sotelo et al., 2014; Yu et al., 2008). One of the first model to take into account the competition in a multi-component solution was the Ideal Adsorbed Solution Theory (Radke and Prausnitz, 1972), which is based on a combination of isotherm parameters obtained in mono-component solutions. Some attempts were carried out in the past on CECs (Sotelo et al., 2014). However, these models require an attentive calibration of the parameters, usually based on isotherms and kinetics tests in batch or in small column, but the very low initial concentrations of the target compounds can lead to the collection of not-reliable experimental data.

For the prediction of chemical recontamination events in the DWDN, it is important to evaluate the pipelines materials, since they affect the CECs that can be leached in DW. The fate of chemicals in the DWDN can be predicted combining water quality models to a hydraulic model in dynamic simulations (e.g. by softwares like EPANET, Infoworks) (Seyoum and Tanyimboh, 2017). However, water quality models need a calibration of the parameters, usually assessed through lab-scale migration tests, usually performed under standardized and not realistic conditions, contributing to uncertainties in the prediction of the effect of water quality and operating conditions on CECs leaching from different materials in real DWDNs.

Anyhow, it is worth mentioning that a stochastic approach is highly recommended to take into account the many factors affecting adsorption process performance and recontamination in the DWDN, especially for CECs, being input data for CECs affected by uncertainties (Stuart et al., 2012). Currently, there are no stochastic reliable models that allow to estimate: i) the concentration of CEC in raw water, ii) the removal efficiency in a DWTP, and iii) possible recontamination events along the distribution network. Therefore, mathematical models should be developed to propagate uncertainties associated with the measures and parameters/inputs of the models to provide the decision makers with a clear understanding of the impact of this uncertainty on any final quantitative risk estimate (WHO-IPCS, 2018). In this way, prediction modeling can be used when the scope is to carry out scenario analysis under uncertain conditions to understand the effects of an intervention in the performance of the system. This makes it possible to identify the most appropriate interventions and therefore to correctly allocate resources, including economic ones, to effectively reduce the overall human health risk.

4. CECs hazard assessment

In the hazard assessment step of the risk assessment procedure, the potential adverse health effects associated to a chemical compound are described through the definition of health-based guidance values, such as the Reference Dose (RfD) [mg/(kg day)], which provide an estimate of the amount of chemical that can be ingested by a person without appreciable health risk (Schriks et al., 2010). The RfD is developed from toxicological and epidemiological information: firstly, a No-Observed-Adverse-Effect Level (NOAEL) [mg/(kg day)], which is the highest dose of a constituent that causes no detectable adverse health effect, is identified based on a toxicological study typically conducted on animals; then, the RfD is obtained by dividing the NOAEL by an Uncertainty Factor (UF) which takes into account interspecies and intraspecies variability, as well as data quality, duration of exposure and other uncertainty sources (WHO, 2016). Once that the RfD is obtained, human exposure factors are considered, such as intake rates and allocation factors (corresponding to the percentage of human exposure allocated to the drinking water), in order to develop guideline values for chemicals in drinking water, or DWTLs, which express the chemical concentration in drinking water that does not exceed tolerable risk to the health of the consumer over a lifetime (WHO, 2010).

However, due to the relatively recent introduction or detection of CECs, there is not enough information on toxicity, impact, behavior data for these pollutants. Thus, there exists a lack of DWTLs computed starting from toxicological information, particularly regarding the potential human health risk associated with direct water ingestion (Baken et al., 2018b; Schriks et al., 2010). As a consequence, it is common to derive DWTLs based on the most recent toxicity data available for selected CECs (Riva et al., 2018). Nevertheless, deriving substance specific DWTLs is labor-intensive and available toxicity studies are often absent, incomplete and contradictory for CECs (Schriks et al., 2010). For example, regarding the adverse endocrine effects related to BPA occurrence in DW, EFSA reported in 2010 a RfD equal to 0.01 mg/(kg day), based on a NOAEL equal to 5 mg/(kg day) (Tyl et al., 2002), while Danish EPA (2014) computed a RfD equal to 0.0004 mg/(kg day), based on a NOAEL equal to 0.07 mg/(kg day) (Ryan and Vandenbergh, 2006), resulting in a two orders of magnitude difference between the two values.

5. Quantitative chemical risk assessment

Drinking water supply systems management and control are nowadays addressed through qualitative or deterministic risk assessments, through the Water Safety Plan (WSP), promoted by the World Health Organization (https://wsportal.org/). However, qualitative and deterministic approaches do not allow to take into account the knowledge-gaps (discontinuity of the measures, lack of toxicological informations, etc.) and uncertainties (measurement errors, not always consolidated toxicological data, removal efficiencies, etc.) typical of the contamination by CECs in DW supply systems, as highlighted in previous paragraphs.

Concerning how to deal with uncertainty within a risk assessment framework, few case studies are reported in literature, that provided a probabilistic quantification of the risk, including uncertainties, in applications other than drinking water. However, these applications include the uncertainty analysis just either in the exposure assessment (Caldas et al., 2006; Fryer et al., 2006; Kavcar et al., 2009) or in the hazard assessment (Baird et al., 1996; Renwick et al., 2004), resulting in a risk estimation that is not completely representative of the uncertainties characterizing the whole problem.

As a consequence, a stochastic approach, namely a quantitative chemical risk assessment, is highly recommended to include in the evaluation the uncertainties related to both the exposure and hazard assessment steps of the procedure, in particular for a class of contaminants as the CECs, where a gap of knowledge is certainly present (Chiu and Slob, 2015).

References

Athanasaki, G., Sherrill, L., Hristovski, K.D., 2015. The pore surface diffusion model as a tool for rapid screening of novel nanomaterial-enhanced hybrid ion-exchange media. Environ. Sci. Water Res. Technol. 1, 448–456. https://doi.org/10.1039/c5ew00108k

Baccarelli, A., Pfeiffer, R., Consonni, D., Pesatori, A.C., Bonzini, M., Patterson, D.G., Bertazzi, P.A., Landi, M.T., 2005. Handling of dioxin measurement data in the presence of non-detectable values: Overview of available methods and their application in the Seveso chloracne study. Chemosphere 60, 898–906. https://doi.org/10.1016/j.chemosphere.2005.01.055

Baird, S.J.S., Cohen, J.T., Graham, J.D., Shlyakhter, A.I., Evans, J.S., 1996. Noncancer Risk Assessment: A Probabilistic Alternative to Current Practice. Hum. Ecol. Risk Assess. An Int. J. 2, 79–102. https://doi.org/10.1080/10807039.1996.10387463

Baken, K.A., Sjerps, R.M.A., Schriks, M., Wezel, A.P. Van, 2018a. Toxicological risk assessment and prioritization of drinking water relevant contaminants of emerging concern. Environ. Int. 118, 293–303. https://doi.org/10.1016/j.envint.2018.05.006

Baken, K.A., Sjerps, R.M.A., Schriks, M., Wezel, A.P. Van, 2018b. Toxicological risk assessment and prioritization of drinking water relevant contaminants of emerging concern. Environ. Int. 118, 293–303. https://doi.org/10.1016/j.envint.2018.05.006

Benotti, M.J., Trenholm, R.A., Vanderford, B.J., Holady, J.C., Stanford, B.D., Snyder, S.A., 2009. Pharmaceuticals and endocrine disrupting compounds in U.S. drinking water. Environ. Sci. Technol. 43, 597–603. https://doi.org/10.1021/es801845a

Bokkers, B.G.H., Mengelers, M.J., Bakker, M.I., Chiu, W.A., Slob, W., 2017. APROBA-Plus: A probabilistic tool to evaluate and express uncertainty in hazard characterization and exposure assessment of substances. Food Chem. Toxicol. 110, 408–417. https://doi.org/10.1016/j.fct.2017.10.038

Caldas, E.D., Boon, P.E., Tressou, J., 2006. Probabilistic assessment of the cumulative acute exposure to organophosphorus and carbamate insecticides in the Brazilian diet. Toxicology 222, 132–142. https://doi.org/10.1016/j.tox.2006.02.006

Chiu, W.A., Slob, W., 2015. A unified probabilistic framework for dose–response assessment of human health effects. Environ. Health Perspect. 123, 1241–1254. https://doi.org/10.1289/ehp.1409385

Coday, B.D., Yaffe, B.G.M., Xu, P., Cath, T.Y., 2014. Rejection of Trace Organic Compounds by Forward Osmosis Membranes: A Literature Review. Environ. Sci. Technol. 48, 3612–3624. https://doi.org/10.1021/es4038676

Crittenden, J.C., Berrigan, J.K., Hand, D.W., Lykins, B., 1987. Design of rapid fixed-bed adsorption tests for nonconstant diffusivities. J. Environ. Eng. (United States) 113, 243–259. https://doi.org/10.1061/(ASCE)0733-9372(1987)113:2(243)

Crittenden, J.C., Reddy, P.S., Arora, H., Trynoski, J., Hand, D.W., Perram, D.L., Summers, R.S., 1991. Predicting GAC performance with rapid small-scale column tests. J. Am. Water Works Assoc. 77–87.

Danish EPA, 2014. Background for national legislation on bisphenol A (BPA) in EU and EFTA countries.

Denning, P., Dvorak, B.I., 2008. Maximizing sorbent life: A comparison of columns in parallel, lead-lag series, and with bypass blending. Am. Water Work. Assoc. - Am. Water Work. Assoc. Assoc. Annu. Conf. Expo. ACE 2008 81. https://doi.org/10.2175/106143008X325674

Environmental Protection Agency (EPA), 2016. Drinking water contaminant candidate list 4-Final. Fed. Regist. 81, 9–13.

Eschauzier, C., Beerendonk, E., Scholte-Veenendaal, P., De Voogt, P., 2012. Impact of treatment processes on the removal of perfluoroalkyl acids from the drinking water production chain. Environ. Sci. Technol. 46, 1708–15. https://doi.org/10.1021/es201662b

EU Parliament, 2020a. Decision (EU) 2020/1161 establishing a watch list of substances for Union-wide monitoring in the field of water policy pursuant to Directive 2008/105/EC of the European Parliament and of the Council, in: Off. J. Eur. Union. 2020. https://eur-lex.europa.eu/legal-content/EN/TXT/?uri=uriserv:OJ.L_.2020.257.01.0032.01.ENG&toc=OJ:L:2020:257:TOC

EU Parliament, 2020b. Directive of the European Parliament and of the Council on the quality of water intended for human consumption, in: Off. J. Eur. Union. 2020. https://doi.org/10.1017/CBO9781107415324.004

Fryer, M., Collins, C.D., Ferrier, H., Colvile, R.N., Nieuwenhuijsen, M.J., 2006. Human exposure modelling for chemical risk assessment: A review of current approaches and research and policy implications. Environ. Sci. Policy 9, 261–274. https://doi.org/10.1016/j.envsci.2005.11.011

García-Mateos, F.J., Ruiz-Rosas, R., Marqués, M.D., Cotoruelo, L.M., Rodríguez-Mirasol, J., Cordero, T., 2015. Removal of paracetamol on biomass-derived activated carbon: modeling the fixed bed breakthrough curves using batch adsorption experiments. Chem. Eng. J. 279, 18–30.

Gorchev, H.G., Ozolins, G., 2011. WHO guidelines for drinking-water quality. WHO Chron. 38, 104–108. https://doi.org/10.1016/S1462-0758(00)00006-6

IPCS, 2000. Human exposure assessment.

Jesus Gaffney, V. De, Almeida, C.M.M., Rodrigues, A., Ferreira, E., Jo, M., Vale, V., 2014. Occurrence of pharmaceuticals in a water supply system and related human health risk assessment 2, 1–10. https://doi.org/10.1016/j.watres.2014.10.027

Kavcar, P., Sofuoglu, A., Sofuoglu, S.C., 2009. A health risk assessment for exposure to trace metals via drinking water ingestion pathway 212, 216–227. https://doi.org/10.1016/j.ijheh.2008.05.002

Kleywegt, S., Pileggi, V., Yang, P., Hao, C., Zhao, X., Rocks, C., Thach, S., Cheung, P., Whitehead, B., 2011. Pharmaceuticals, hormones and bisphenol A in untreated source and finished drinking water in Ontario, Canada - Occurrence and treatment efficiency. Sci. Total Environ. 409, 1481–1488. https://doi.org/10.1016/j.scitotenv.2011.01.010

Kovalova, L., Knappe, D.R.U., Lehnberg, K., Kazner, C., Hollender, J., 2013. Removal of highly polar micropollutants from wastewater by powdered activated carbon. Environ. Sci. Pollut. Res. 20, 3607–3615. https://doi.org/10.1007/s11356-012-1432-9

Löwenberg, J., Zenker, A., Baggenstos, M., Koch, G., Kazner, C., Wintgens, T., 2014. Comparison of two PAC/UF processes for the removal of micropollutants from wastewater treatment plant effluent: process performance and removal efficiency. Water Res. 56, 26–36. https://doi.org/10.1016/j.watres.2014.02.038

Luo, Y., Guo, W., Ngo, H.H., Nghiem, L.D., Hai, F.I., Zhang, J., Liang, S., Wang, X.C., 2014. A review on the occurrence of micropollutants in the aquatic environment and their fate and removal during wastewater treatment. Sci. Total Environ. 473, 619–641.

Mailler, R., Gasperi, J., Coquet, Y., Buleté, A., Vulliet, E., Deshayes, S., Zedek, S., Mirande-Bret, C., Eudes, V., Bressy, A., Caupos, E., Moilleron, R., Chebbo, G., Rocher, V., 2016. Removal of a wide range of emerging pollutants from wastewater treatment plant discharges by micro-grain activated carbon in fluidized bed as tertiary treatment at large pilot scale. Sci. Total Environ. 542, 983–996. https://doi.org/10.1016/j.scitotenv.2015.10.153

Mailler, R., Gasperi, J., Coquet, Y., Deshayes, S., Zedek, S., Cren-Olivé, C., Cartiser, N., Eudes, V., Bressy, A., Caupos, E., Moilleron, R., Chebbo, G., Rocher, V., 2015. Study of a large scale powdered activated carbon pilot: Removals of a wide range of emerging and priority micropollutants from wastewater treatment plant effluents. Water Res. 72, 315–30. https://doi.org/10.1016/j.watres.2014.10.047

Petrović, M., Gonzalez, S., Barceló, D., 2003. Analysis and removal of emerging contaminants in wastewater and drinking water. TrAC Trends Anal. Chem. 22, 685–696.

Radke, C.J., Prausnitz, J.M., 1972. Thermodynamics of multi-solute adsorption from dilute liquid solutions. AIChE J. 18, 761–768. https://doi.org/10.1002/aic.690180417

Renwick, A.G., Flynn, A., Fletcher, R.J., Müller, D.J.G., Tuijtelaars, S., Verhagen, H., 2004. Risk-benefit analysis of micronutrients. Food Chem. Toxicol. 42, 1903–1922. https://doi.org/10.1016/j.fct.2004.07.013

Richardson, S.D., Kimura, S.Y., 2016. Water Analysis: Emerging Contaminants and Current Issues. Anal. Chem. 88, 546–582. https://doi.org/10.1021/acs.analchem.5b04493

Riva, F., Castiglioni, S., Fattore, E., Manenti, A., Davoli, E., Zuccato, E., 2018. International Journal of Hygiene and Monitoring emerging contaminants in the drinking water of Milan and assessment of the human risk. Int. J. Hyg. Environ. Health 0–1. https://doi.org/10.1016/j.ijheh.2018.01.008

Rodríguez-Gil, J.L., Cáceres, N., Dafouz, R., Valcárcel, Y., 2018. Caffeine and paraxanthine in aquatic systems: Global exposure distributions and probabilistic risk assessment. Sci. Total Environ. 612, 1058–1071. https://doi.org/10.1016/j.scitotenv.2017.08.066

Ryan, B.C., Vandenbergh, J.G., 2006. Developmental exposure to environmental estrogens alters anxiety and spatial memory in female mice. Horm. Behav. 50, 85–93.

https://doi.org/10.1016/j.yhbeh.2006.01.007

Schriks, M., Heringa, M.B., Kooi, M.M.E. Van Der, Voogt, P. De, Wezel, A.P. Van, 2010. Toxicological relevance of emerging contaminants for drinking water quality. Water Res. 44, 461–476. https://doi.org/10.1016/j.watres.2009.08.023

Schwarzenbach, R.P., Escher, B.I., Fenner, K., Hofstetter, T.B., Johnson, C.A., Gunten, U. von, Wehrli, B., 2006. The Challenge of Micropollutants in Aquatic Systems. Science (80-.). 313, 1072–1077. https://doi.org/10.1126/science.1127291

Senevirathna, S.T.M.L.D., Tanaka, S., Fujii, S., Kunacheva, C., Harada, H., Ariyadasa, B.H.A.K.T., Shivakoti, B.R., 2010. Adsorption of perfluorooctane sulfonate (n-PFOS) onto non ion-exchange polymers and granular activated carbon: Batch and column test. Desalination 260, 29–33. https://doi.org/10.1016/j.desal.2010.05.005

Seyoum, A.G., Tanyimboh, T.T., 2017. Integration of Hydraulic and Water Quality Modelling in Distribution Networks: EPANET-PMX. Water Resour. Manag. 31, 4485–4503. https://doi.org/10.1007/s11269-017-1760-0

Simazaki, D., Kubota, R., Suzuki, T., Akiba, M., Nishimura, T., Kunikane, S., 2015. Occurrence of selected pharmaceuticals at drinking water purification plants in Japan and implications for human health. Water Res. 76, 187–200. https://doi.org/10.1016/j.watres.2015.02.059

Singer, H.P., Wössner, A.E., McArdell, C.S., Fenner, K., 2016. Rapid Screening for Exposure to "non-Target" Pharmaceuticals from Wastewater Effluents by Combining HRMS-Based Suspect Screening and Exposure Modeling. Environ. Sci. Technol. 50, 6698–6707. https://doi.org/10.1021/acs.est.5b03332

Siriwardena, D.P., Crimi, M., Holsen, T.M., Bellona, C., Divine, C., Dickenson, E., 2019. Influence of groundwater conditions and co-contaminants on sorption of perfluoroalkyl compounds on granular activated carbon. Remediation 29, 5–15. https://doi.org/10.1002/rem.21603

Snyder, S.A., Adham, S., Redding, A.M., Cannon, F.S., DeCarolis, J., Oppenheimer, J., Wert, E.C., Yoon, Y., 2007. Role of membranes and activated carbon in the removal of endocrine disruptors and pharmaceuticals. Desalination 202, 156–181. https://doi.org/10.1016/j.desal.2005.12.052

Sotelo, J.L., Ovejero, G., Rodríguez, A., Álvarez, S., Galán, J., García, J., 2014. Competitive adsorption studies of caffeine and diclofenac aqueous solutions by activated carbon. Chem. Eng. J. 240, 443–453. https://doi.org/10.1016/j.cej.2013.11.094

Stuart, M., Lapworth, D., Crane, E., Hart, A., 2012. Review of risk from potential emerging contaminants in UK groundwater. Sci. Total Environ. 416, 1–21. https://doi.org/10.1016/j.scitotenv.2011.11.072

Tekindal, M.A., Erdoğan, B.D., Yavuz, Y., 2017. Evaluating Left-Censored Data Through Substitution, Parametric, Semi-parametric, and Nonparametric Methods: A Simulation Study. Interdiscip. Sci. Comput. Life Sci. 9, 153–172. https://doi.org/10.1007/s12539-015-0132-9

The European Parlament and the Council of the European Union, 2018a. COMMISSION IMPLEMENTING DECISION (EU) 2018/840 of 5 June 2018 2018, 5–8.

The European Parlament and the Council of the European Union, 2018b. Proposal for a DIRECTIVE OF THE EUROPEAN PARLIAMENT AND OF THE COUNCIL on the quality of water intended for human consumption (recast). Off. J. Eur. Union. 2018.

The European Parlament and the Council of the European Union, 2013. Directives of 12 August 2013 amending Directives 2000/60/EC and 2008/105/EC as regards priority substances in the field of water policy. Off. J. Eur. Union 2013, 1–17. https://doi.org/http://eur-lex.europa.eu/legal-content/EN/TXT/?uri=celex:32013L0039

Tyl, R.W., Myers, C.B., Marr, M.C., Thomas, B.F., Keimowitz, A.R., Brine, D.R., Veselica, M.M., Fail, P.A., Chang, T.Y., Seely, J.C., Joiner, R.L., Butala, J.H., Dimond, S.S., Cagen, S.Z., Shiotsuka, R.N., Stropp, G.D., Waechter, J.M., 2002. Three-generation reproductive toxicity study of dietary bisphenol A in CD Sprague-Dawley rats. Toxicol. Sci. 68, 121–146. https://doi.org/10.1093/toxsci/68.1.121

US EPA, 2010. Exposure assessment tools and models.

Valcárcel, Y., Alonso, S.G., Rodríguez-Gil, J.L., Maroto, R.R., Gil, A., Catalá, M., 2011. Analysis of the presence of cardiovascular and analgesic/anti-inflammatory/antipyretic pharmaceuticals in river- and drinking-water of the Madrid Region in Spain. Chemosphere 82, 1062–1071. https://doi.org/10.1016/j.chemosphere.2010.10.041

van Leeuwen, C.J., Vermeire, T.G., 2007. Risk Assessment of Chemicals: An Introduction. Springer.

Vulliet, E., Cren-Olivé, C., Grenier-Loustalot, M.F., 2011. Occurrence of pharmaceuticals and hormones in drinking water treated from surface waters. Environ. Chem. Lett. 9, 103–114. https://doi.org/10.1007/s10311-009-0253-7

Wang, D., Singhasemanon, N., Goh, K.S., 2016. A statistical assessment of pesticide pollution in surface waters using environmental monitoring data: Chlorpyrifos in Central Valley, California. Sci. Total Environ. 571, 332–341. https://doi.org/10.1016/j.scitotenv.2016.07.159

Westerhoff, P., Yoon, Y., Snyder, S., Wert, E., 2005. Fate of Endocrine-Disruptor, Pharmaceutical, and Personal Care Product Chemicals during Simulated Drinking Water Treatment Processes. Environ. Sci. Technol. 39, 6649–6663. https://doi.org/10.1021/es0484799

WHO-IPCS, 2018. Guidance document on evaluating and expressing uncertainty in hazard characterization– 2nd edition. WHO-IPCS harmonization project document no. 11. ISBN 978-92-4-151354-8. Licence: CC BYNC-SA 3.0 IGO., World Health Organization. https://doi.org/ISBN 978 92 4 150761 5

WHO, 2016. Quantitative Microbial Risk Assessment: Application for Water Safety Management. WHO Press 187.

WHO, 2010. WHO Human Health Risk Assessment Toolkit: Chemical Hazards.

Worch, E., 2008. Fixed-bed adsorption in drinking water treatment: a critical review on models and parameter estimation. J. Water Supply Res. Technol. 57, 171–183.

Yoon, Y., Westerhoff, P., Snyder, S.A., 2005. Adsorption of 3H-Labeled 17-β Estradiol on Powdered Activated Carbon. Water. Air. Soil Pollut. 166, 343–351. https://doi.org/10.1007/s11270-005-7274-z

Yu, J., Lv, L., Lan, P., Zhang, S., Pan, B., Zhang, W., 2012. Effect of effluent organic matter on the adsorption of perfluorinated compounds onto activated carbon. J. Hazard. Mater. 225–226, 99–106. https://doi.org/10.1016/j.jhazmat.2012.04.073

Yu, Q., Zhang, R., Deng, S., Huang, J., Yu, G., 2009. Sorption of perfluorooctane sulfonate and perfluorooctanoate on activated carbons and resin: Kinetic and isotherm study. Water Res. 43, 1150–8. https://doi.org/10.1016/j.watres.2008.12.001

Yu, Z., Peldszus, S., Huck, P.M., 2008. Adsorption characteristics of selected pharmaceuticals and an endocrine disrupting compound-Naproxen, carbamazepine and nonylphenol-on activated carbon. Water Res. 42, 2873–2882. https://doi.org/10.1016/j.watres.2008.02.020

References for graphs

Abdel daiem, M.M., Rivera-Utrilla, J., Sánchez-Polo, M., Ocampo-Pérez, R., 2015. Single, competitive, and dynamic adsorption on activated carbon of compounds used as plasticizers and herbicides. Sci. Total Environ. 537, 335–342. https://doi.org/10.1016/j.scitotenv.2015.07.131

Abtahi, S.M., Ilyas, S., Joannis Cassan, C., Albasi, C., de Vos, W.M., 2017. Micropollutants removal from secondary-treated municipal wastewater using weak polyelectrolyte multilayer based nanofiltration membranes. J. Memb. Sci. 548, 654–666. https://doi.org/10.1016/j.memsci.2017.10.045

Acero, J.L., Javier Benitez, F., Real, F.J., Teva, F., 2012. Coupling of adsorption, coagulation, and ultrafiltration processes for the removal of emerging contaminants in a secondary effluent. Chem. Eng. J. 210, 1–8. https://doi.org/10.1016/j.cej.2012.08.043

Ahmed, M.M., Chiron, S., 2014. Solar photo-Fenton like using persulphate for carbamazepine removal from domestic wastewater. Water Res. 48, 229–236. https://doi.org/10.1016/j.watres.2013.09.033

Akbari, S., Ghanbari, F., Moradi, M., 2016. Bisphenol A degradation in aqueous solutions by electrogenerated ferrous ion activated ozone, hydrogen peroxide and persulfate: Applying low current density for oxidation mechanism. Chem. Eng. J. 294, 298–307. https://doi.org/10.1016/j.cej.2016.02.106

Al-Rifai, J.H., Khabbaz, H., Schäfer, A.I., 2011. Removal of pharmaceuticals and endocrine disrupting compounds in a water recycling process using reverse osmosis systems. Sep. Purif. Technol. 77, 60–67. https://doi.org/10.1016/j.seppur.2010.11.020

Altmann, J., Bruebach, H., Sperlich, A., Jekel, M., 2014. Removal of micropollutants from treated domestic wastewater by addition of powdered activated carbon to rapid filtration. Water Pract. Technol. 9, 344–352. https://doi.org/10.2166/wpt.2014.036

Altmann, J., Ruhl, A.S., Zietzschmann, F., Jekel, M., 2014. Direct comparison of ozonation and adsorption onto powdered activated carbon for micropollutant removal in advanced wastewater treatment. Water Res. 55, 185–193. https://doi.org/10.1016/j.watres.2014.02.025

Altmann, J., Sperlich, A., Jekel, M., 2015a. Integrating organic micropollutant removal into tertiary filtration: Combining PAC adsorption with advanced phosphorus removal. Water Res. 84, 58–65. https://doi.org/10.1016/j.watres.2015.07.023

Altmann, J., Zietzschmann, F., Geiling, E.L., Ruhl, A.S., Sperlich, A., Jekel, M., 2015b. Impacts of coagulation on the adsorption of organic micropollutants onto powdered activated carbon in treated domestic wastewater. Chemosphere 125, 198–204. https://doi.org/10.1016/j.chemosphere.2014.12.061

Alturki, A.A., Tadkaew, N., McDonald, J.A., Khan, S.J., Price, W.E., Nghiem, L.D., 2010. Combining MBR and NF/RO membrane filtration for the removal of trace organics in indirect potable water reuse applications. J. Memb. Sci. 365, 206–215. https://doi.org/10.1016/j.memsci.2010.09.008

Alum, A., Yoon, Y., Westerhoff, P., Abbaszadegan, M., 2004. Oxidation of bisphenol A, 17??-estradiol, and 17??-ethynyl estradiol and byproduct estrogenicity. Environ. Toxicol. 19, 257–264. https://doi.org/10.1002/tox.20018

Andreozzi, R., Marotta, R., Pinto, G., Pollio, A., 2002. Carbamazepine in water: Persistence in the environment, ozonation treatment and preliminary assessment on algal toxicity. Water Res. 36, 2869–2877. https://doi.org/10.1016/S0043-1354(01)00500-0

Appleman, T.D., Dickenson, E.R. V, Bellona, C., Higgins, C.P., 2013. Nanofiltration and granular activated carbon treatment of perfluoroalkyl acids. J. Hazard. Mater. 260, 740–746. https://doi.org/10.1016/j.jhazmat.2013.06.033

Arampatzidou, A.C., Deliyanni, E.A., 2016. Comparison of activation media and pyrolysis temperature for activated carbons development by pyrolysis of potato peels for effective adsorption of endocrine disruptor bisphenol-A. J. Colloid Interface Sci. 466, 101–112. https://doi.org/10.1016/j.jcis.2015.12.003

Assalin, M.R., de Moraes, S.G., Queiroz, S.C.N., Ferracini, V.L., Duran, N., 2010. Studies on degradation of glyphosate by several oxidative chemical processes: Ozonation, photolysis and heterogeneous photocatalysis. J. Environ. Sci. Heal. - Part B Pestic. Food Contam. Agric. Wastes 45, 89–94. https://doi.org/10.1080/03601230903404598

Azaïs, A., Mendret, J., Gassara, S., Petit, E., Deratani, A., Brosillon, S., 2014. Nanofiltration for wastewater reuse: Counteractive effects of fouling and matrice on the rejection of pharmaceutical active compounds. Sep. Purif. Technol. 133, 313–327. https://doi.org/10.1016/j.seppur.2014.07.007

Bagal, M. V., Gogate, P.R., 2014. Degradation of diclofenac sodium using combined processes based on hydrodynamic cavitation and heterogeneous photocatalysis. Ultrason. Sonochem. 21, 1035–1043. https://doi.org/10.1016/j.ultsonch.2013.10.020

Baghdadi, M., Ghaffari, E., Aminzadeh, B., 2016. Removal of carbamazepine from municipal wastewater effluent using optimally synthesized magnetic activated carbon: Adsorption and sedimentation kinetic studies. J. Environ. Chem. Eng. 4, 3309–3321. https://doi.org/10.1016/j.jece.2016.06.034

Baig, S., Hansmann, G., Paolini, B., 2008. Ozone oxidation of oestrogenic active substances in wastewater and drinking water. Water Sci. Technol. 58, 451–458. https://doi.org/10.2166/wst.2008.665

Bautista-Toledo, I., Ferro-García, M.A., Rivera-Utrilla, J., Moreno-Castilla, C., Fernández, F.J.V., 2005. Bisphenol A removal from water by activated carbon. Effects of carbon characteristics and solution chemistry. Environ. Sci. Technol. 39, 6246–6250. https://doi.org/10.1021/es0481169

Benotti, M.J., Stanford, B.D., Wert, E.C., Snyder, S.A., 2009. Evaluation of a photocatalytic reactor membrane pilot system for the removal of pharmaceuticals and endocrine disrupting compounds from water. Water Res. 43, 1513–1522. https://doi.org/10.1016/j.watres.2008.12.049

Bertanza, G., Pedrazzani, R., Papa, M., Mazzoleni, G., Steimberg, N., Caimi, L., Montani, C., Dilorenzo, D., 2010. Removal of BPA and NPnEOs from secondary effluents of municipal WWTPs by means of ozonation. Ozone Sci. Eng. 32, 204–208. https://doi.org/10.1080/01919511003795303

Bhadra, B.N., Seo, P.W., Jhung, S.H., 2016. Adsorption of diclofenac sodium from water using oxidized activated carbon. Chem. Eng. J. 301, 27–34. https://doi.org/10.1016/j.cej.2016.04.143

Björklund, K., Li, L.Y., 2017. Adsorption of organic stormwater pollutants onto activated carbon from sewage sludge. J. Environ. Manage. 197, 490–497. https://doi.org/10.1016/j.jenvman.2017.04.011

Boleda, M.R., Galceran, M.T., Ventura, F., 2011. Behavior of pharmaceuticals and drugs of abuse in a drinking water treatment plant (DWTP) using combined conventional and ultrafiltration and reverse osmosis (UF/RO) treatments. Environ. Pollut. 159, 1584–1591. https://doi.org/10.1016/j.envpol.2011.02.051

Brienza, M., Mahdi Ahmed, M., Escande, A., Plantard, G., Scrano, L., Chiron, S., A. Bufo, S., Goetz, V., 2014. Relevance of a photo-Fenton like technology based on peroxymonosulphate for 17β-estradiol removal from wastewater. Chem. Eng. J. 257, 191–199. https://doi.org/10.1016/j.cej.2014.07.061

Broséus, R., Vincent, S., Aboulfadl, K., Daneshvar, A., Sauvé, S., Barbeau, B., Prévost, M., 2009. Ozone oxidation of pharmaceuticals, endocrine disruptors and pesticides during drinking water treatment. Water Res. 43, 4707–4717. https://doi.org/10.1016/j.watres.2009.07.031

Brugnera, M.F., Rajeshwar, K., Cardoso, J.C., Zanoni, M.V.B., 2010. Bisphenol A removal from wastewater using self-organized TIO2 nanotubular array electrodes. Chemosphere 78, 569–575. https://doi.org/10.1016/j.chemosphere.2009.10.058

Calisto, V., Ferreira, C.I.A., Oliveira, J.A.B.P., Otero, M., Esteves, V.I., 2015. Adsorptive removal of pharmaceuticals from water by commercial and waste-based carbons. J. Environ. Manage. 152, 83–90. https://doi.org/10.1016/j.jenvman.2015.01.019

Carabin, A., Drogui, P., Robert, D., 2015. Photo-degradation of carbamazepine using TiO2 suspended photocatalysts. J. Taiwan Inst. Chem. Eng. 54, 109–117. https://doi.org/10.1016/j.jtice.2015.03.006

Carter, K.E., Farrell, J., 2010. Removal of perfluorooctane and perfluorobutane sulfonate from water via carbon adsorption and ion exchange. Sep. Sci. Technol. 45, 762–767. https://doi.org/10.1080/01496391003608421

Caus, A., Vanderhaegen, S., Braeken, L., Van der Bruggen, B., 2009. Integrated nanofiltration cascades with low salt rejection for complete removal of pesticides in drinking water production. Desalination 241, 111–117. https://doi.org/10.1016/j.desal.2008.01.061

Chen, S., Liu, Y., 2007. Study on the photocatalytic degradation of glyphosate by TiO2 photocatalyst. Chemosphere 67, 1010–1017. https://doi.org/10.1016/j.chemosphere.2006.10.054

Chen, W., Zhang, X., Mamadiev, M., Wang, Z., 2017. Sorption of perfluorooctane sulfonate and perfluorooctanoate on polyacrylonitrile fiber-derived activated carbon fibers: in comparison with activated carbon. RSC Adv. 7, 927–938. https://doi.org/10.1039/C6RA25230C

Choi, K.J., Kim, S.G., Kim, C.W., Kim, S.H., 2005. Effects of activated carbon types and service life on removal of endocrine disrupting chemicals: Amitrol, nonylphenol, and bisphenol-A. Chemosphere 58, 1535–1545. https://doi.org/10.1016/j.chemosphere.2004.11.080

Chon, K., KyongShon, H., Cho, J., 2012. Membrane bioreactor and nanofiltration hybrid system for reclamation of municipal wastewater: Removal of nutrients, organic matter and micropollutants. Bioresour. Technol. 122, 181–188. https://doi.org/10.1016/j.biortech.2012.04.048

Chong, M.N., Jin, B., Laera, G., Saint, C.P., 2011. Evaluating the photodegradation of Carbamazepine in a sequential batch photoreactor system: Impacts of effluent organic matter and inorganic ions. Chem. Eng. J. 174, 595–602. https://doi.org/10.1016/j.cej.2011.09.065

Chularueangaksorn, P., Tanaka, S., Fujii, S., Kunacheva, C., 2014. Batch and column adsorption of perfluorooctane sulfonate on anion exchange resins and granular activated carbon. J. Appl. Polym. Sci. 131, 1–7. https://doi.org/10.1002/app.39782

Comerton, A.M., Andrews, R.C., Bagley, D.M., Hao, C., 2008. The rejection of endocrine disrupting and pharmaceutically active compounds by NF and RO membranes as a function of compound and water matrix properties. J. Memb. Sci. 313, 323–335. https://doi.org/10.1016/j.memsci.2008.01.021

da Silva, S.W., Klauck, C.R., Siqueira, M.A., Bernardes, A.M., 2015. Degradation of the commercial surfactant nonylphenol ethoxylate by advanced oxidation processes. J. Hazard. Mater. 282, 241–248. https://doi.org/10.1016/j.jhazmat.2014.08.014

da Silva, W.L., Lansarin, M.A., Livotto, P.R., dos Santos, J.H.Z., 2015. Photocatalytic degradation of drugs by supported titania-based catalysts produced from petrochemical plant residue. Powder Technol. 279, 166–172. https://doi.org/10.1016/j.powtec.2015.03.045

De la Cruz, N., Esquius, L., Grandjean, D., Magnet, A., Tungler, A., de Alencastro, L.F., Pulgarín, C., 2013. Degradation of emergent contaminants by UV, UV/H2O2and neutral photo-Fenton at pilot scale in a domestic wastewater treatment plant. Water Res. 47, 5836–5845. https://doi.org/10.1016/j.watres.2013.07.005

Deborde, M., Rabouan, S., Duguet, J.P., Legube, B., 2005. Kinetics of aqueous ozone-induced oxidation of some endocrine disrupters. Environ. Sci. Technol. 39, 6086–6092. https://doi.org/10.1021/es0501619

Deborde, M., Rabouan, S., Mazellier, P., Duguet, J.P., Legube, B., 2008. Oxidation of bisphenol A by ozone in aqueous solution. Water Res. 42, 4299–4308. https://doi.org/10.1016/j.watres.2008.07.015

Deng, S., Nie, Y., Du, Z., Huang, Q., Meng, P., Wang, B., Huang, J., Yu, G., 2015. Enhanced adsorption of perfluorooctane sulfonate and perfluorooctanoate by bamboo-derived granular activated carbon. J. Hazard. Mater. 282, 150–157. https://doi.org/10.1016/j.jhazmat.2014.03.045

Doll, T.E., Frimmel, F.H., 2005. Photocatalytic degradation of carbamazepine, clofibric acid and iomeprol with P25 and Hombikat UV100 in the presence of natural organic matter (NOM) and other organic water constituents. Water Res. 39, 403–411. https://doi.org/10.1016/j.watres.2004.09.016

Drewes, J.E., Bellona, C., Oedekoven, M., Xu, P., Kim, T.U., Amy, G., 2005. Rejection of wastewater-derived micropollutants in high-pressure membrane applications leading to indirect potable reuse. Environ. Prog. 24, 400–409. https://doi.org/10.1002/ep.10110

Dudziak, M., Bodzek, M., 2009. Selected factors affecting the elimination of hormones from water using nanofiltration. Desalination 240, 236–243. https://doi.org/10.1016/j.desal.0000.00.000

Dudziak, M., Burdzik, E., 2016. Oxidation of bisphenol A from simulated and real urban wastewater effluents by UV, O3and UV/O3. Desalin. Water Treat. 57, 1075–1083. https://doi.org/10.1080/19443994.2014.988409

Dulov, A., Dulova, N., Trapido, M., 2013. Photochemical degradation of nonylphenol in aqueous solution: The impact of pH and hydroxyl radical promoters. J. Environ. Sci. (China) 25, 1326–1330. https://doi.org/10.1016/S1001-0742(12)60205-8

Dzinun, H., Othman, M.H.D., Ismail, A.F., Puteh, M.H., Rahman, M.A., Jaafar, J., 2015. Photocatalytic degradation of nonylphenol by immobilized TiO2in dual layer hollow fibre membranes. Chem. Eng. J. 269, 255–261. https://doi.org/10.1016/j.cej.2015.01.114

Echavia, G.R.M., Matzusawa, F., Negishi, N., 2009. Photocatalytic degradation of organophosphate and phosphonoglycine pesticides using TiO2 immobilized on silica gel. Chemosphere 76, 595–600. https://doi.org/10.1016/j.chemosphere.2009.04.055

Escalona, I., Fortuny, A., Stüber, F., Bengoa, C., Fabregat, A., Font, J., 2014. Fenton coupled with nanofiltration for elimination of Bisphenol A. Desalination 345, 77–84. https://doi.org/10.1016/j.desal.2014.04.024

Eschauzier, C., Beerendonk, E., Scholte-Veenendaal, P., De Voogt, P., 2012. Impact of treatment processes on the removal of perfluoroalkyl acids from the drinking water production chain. Environ. Sci. Technol. 46, 1708–15. https://doi.org/10.1021/es201662b

Fallou, H., Cimetière, N., Giraudet, S., Wolbert, D., Le Cloirec, P., 2016. Adsorption of pharmaceuticals onto activated carbon fiber cloths - Modeling and extrapolation of adsorption isotherms at very low concentrations. J. Environ. Manage. 166, 544–555. https://doi.org/10.1016/j.jenvman.2015.10.056

Feng, X., Ding, S., Tu, J., Wu, F., Deng, N., 2005. Degradation of estrone in aqueous solution by photo-Fenton system. Sci. Total Environ. 345, 229–237. https://doi.org/10.1016/j.scitotenv.2004.11.008

Fernandez, R.L., Coleman, H.M., Le-Clech, P., 2014. Impact of operating conditions on the removal of endocrine disrupting chemicals by membrane photocatalytic reactor. Environ. Technol. 35, 2068–2078. https://doi.org/10.1080/09593330.2014.892539

Flores, C., Ventura, F., Martin-Alonso, J., Caixach, J., 2013a. Occurrence of perfluorooctane sulfonate (PFOS) and perfluorooctanoate (PFOA) in N.E. Spanish surface waters and their removal in a drinking water treatment plant that combines conventional and advanced treatments in parallel lines. Sci. Total Environ. 461–462, 618–626. https://doi.org/10.1016/j.scitotenv.2013.05.026

Flores, C., Ventura, F., Martin-Alonso, J., Caixach, J., 2013b. Occurrence of perfluorooctane sulfonate (PFOS) and perfluorooctanoate (PFOA) in N.E. Spanish surface waters and their removal in a drinking water treatment plant that combines conventional and advanced treatments in parallel

lines. Sci. Total Environ. 461–462, 618–626. https://doi.org/10.1016/j.scitotenv.2013.05.026

Flyborg, L., Björlenius, B., Ullner, M., Persson, K.M., 2017. A PLS model for predicting rejection of trace organic compounds by nanofiltration using treated wastewater as feed. Sep. Purif. Technol. 174, 212–221. https://doi.org/10.1016/j.seppur.2016.10.029

Frontistis, Z., Kouramanos, M., Moraitis, S., Chatzisymeon, E., Hapeshi, E., Fatta-Kassinos, D., Xekoukoulotakis, N.P., Mantzavinos, D., 2015. UV and simulated solar photodegradation of 17α-ethynylestradiol in secondary-treated wastewater by hydrogen peroxide or iron addition. Catal. Today 252, 84–92. https://doi.org/10.1016/j.cattod.2014.10.012

Frontistis, Z., Xekoukoulotakis, N.P., Hapeshi, E., Venieri, D., Fatta-Kassinos, D., Mantzavinos, D., 2011. Fast degradation of estrogen hormones in environmental matrices by photo-Fenton oxidation under simulated solar radiation. Chem. Eng. J. 178, 175–182. https://doi.org/10.1016/j.cej.2011.10.041

Fukuhara, T., Iwasaki, S., Kawashima, M., Shinohara, O., Abe, I., 2006. Adsorbability of estrone and 17β-estradiol in water onto activated carbon. Water Res. 40, 241–248. https://doi.org/10.1016/j.watres.2005.10.042

Garcia-Ivars, J., Martella, L., Massella, M., Carbonell-Alcaina, C., Alcaina-Miranda, M.I., Iborra-Clar, M.I., 2017. Nanofiltration as tertiary treatment method for removing trace pharmaceutically active compounds in wastewater from wastewater treatment plants. Water Res. 125, 360–373. https://doi.org/10.1016/j.watres.2017.08.070

Garcia, N., Moreno, J., Cartmell, E., Rodriguez-Roda, I., Judd, S., 2013. The application of microfiltration-reverse osmosis/nanofiltration to trace organics removal for municipal wastewater reuse. Environ. Technol. (United Kingdom) 34, 3183–3189. https://doi.org/10.1080/09593330.2013.808244

Garoma, T., Matsumoto, S., 2009. Ozonation of aqueous solution containing bisphenol A: Effect of operational parameters. J. Hazard. Mater. 167, 1185–1191. https://doi.org/10.1016/j.jhazmat.2009.01.133

Garoma, T., Matsumoto, S.A., Wu, Y., Klinger, R., 2010. Removal of bisphenol a and its reaction-intermediates from aqueous solution by ozonation. Ozone Sci. Eng. 32, 338–343. https://doi.org/10.1080/01919512.2010.508484

Gökçe, C.E., Arayici, S., 2016. Adsorption of 17β-estradiol and estrone by activated carbon derived from sewage sludge. Desalin. Water Treat. 57, 2503–2514. https://doi.org/10.1080/19443994.2015.1034183

Grover, D.P., Zhou, J.L., Frickers, P.E., Readman, J.W., 2011. Improved removal of estrogenic and pharmaceutical compounds in sewage effluent by full scale granular activated carbon: Impact on receiving river water. J. Hazard. Mater. 185, 1005–1011. https://doi.org/10.1016/j.jhazmat.2010.10.005

Han, J., Qiu, W., Cao, Z., Hu, J., Gao, W., 2013. Adsorption of ethinylestradiol (EE2) on polyamide 612: Molecular modeling and effects of water chemistry. Water Res. 47, 2273–2284. https://doi.org/10.1016/j.watres.2013.01.046

Hang, X., Chen, X., Luo, J., Cao, W., Wan, Y., 2015. Removal and recovery of perfluorooctanoate from wastewater by nanofiltration. Sep. Purif. Technol. 145, 120–129. https://doi.org/10.1016/j.seppur.2015.03.013

He, Y., Sutton, N.B., Rijnaarts, H.H.H., Langenhoff, A.A.M., 2016. Degradation of pharmaceuticals in wastewater using immobilized TiO2photocatalysis under simulated solar irradiation. Appl. Catal. B Environ. 182, 132–141. https://doi.org/10.1016/j.apcatb.2015.09.015

Hernández-Leal, L., Temmink, H., Zeeman, G., Buisman, C.J.N., 2011. Removal of micropollutants from aerobically treated grey water via ozone and activated carbon. Water Res. 45, 2887–2896. https://doi.org/10.1016/j.watres.2011.03.009

Hu, J.Y., Morita, T., Magara, Y., Aizawa, T., 2000. Evaluation of reactivity of pesticides with ozone in water using the energies of frontier molecular orbitals. Water Res. 34, 2215–2222. https://doi.org/10.1016/S0043-1354(99)00385-1

Huber, M.M., Canonica, S., Park, G.Y., Von Gunten, U., 2003. Oxidation of pharmaceuticals during ozonation and advanced oxidation processes. Environ. Sci. Technol. 37, 1016–1024. https://doi.org/10.1021/es025896h

Huber, M.M., Göbel, A., Joss, A., Hermann, N., Löffler, D., McArdell, C.S., Ried, A., Siegrist, H., Ternes, T.A., Von Gunten, U., 2005. Oxidation of pharmaceuticals during ozonation of municipal wastewater effluents: A pilot study. Environ. Sci. Technol. 39, 4290–4299. https://doi.org/10.1021/es048396s

Huber, M.M., Ternes, T.A., Von Gunten, U., 2004. Removal of estrogenic activity and formation of oxidation products during ozonation of 17α-ethinylestradiol. Environ. Sci. Technol. 38, 5177–5186. https://doi.org/10.1021/es035205x

Hübner, U., Seiwert, B., Reemtsma, T., Jekel, M., 2014. Ozonation products of carbamazepine and their removal from secondary effluents by soil aquifer treatment - Indications from column experiments. Water Res. 49, 34–43. https://doi.org/10.1016/j.watres.2013.11.016

Huerta-Fontela, M., Galceran, M.T., Ventura, F., 2011. Occurrence and removal of pharmaceuticals and hormones through drinking water treatment. Water Res. 45, 1432–1442. https://doi.org/10.1016/j.watres.2010.10.036

Ifelebuegu, A.O., Ukpebor, J.E., Obidiegwu, C.C., Kwofi, B.C., 2015. Comparative potential of black tea leaves waste to granular activated carbon in adsorption of endocrine disrupting compounds from aqueous solution. Glob. J. Environ. Sci. Manag. 1, 205–214. https://doi.org/10.7508/GJESM.2015.03.003

Irmak, S., Erbatur, O., Akgerman, A., 2005. Degradation of 17β-estradiol and bisphenol A in aqueous medium by using ozone and ozone/UV techniques. J. Hazard. Mater. 126, 54–62. https://doi.org/10.1016/j.jhazmat.2005.05.045

Jasim, S.Y., Irabelli, A., Yang, P., Ahmed, S., Schweitzer, L., 2006. Presence of pharmaceuticals and pesticides in Detroit River water and the effect of ozone on removal. Ozone Sci. Eng. 28, 415–423. https://doi.org/10.1080/01919510600985945

Jiang, C., Xu, Z., Guo, Q., Zhuo, Q., 2014. Degradation of bisphenol A in water by the heterogeneous photo-Fenton. Environ. Technol. (United Kingdom) 35, 966–972. https://doi.org/10.1080/09593330.2013.857699

Jodeh, S., Abdelwahab, F., Jaradat, N., Warad, I., Jodeh, W., 2016. Adsorption of diclofenac from aqueous solution using Cyclamen persicum tubers based activated carbon (CTAC). J. Assoc. Arab Univ. Basic Appl. Sci. 20, 32–38. https://doi.org/10.1016/j.jaubas.2014.11.002

Joss, A., Baenninger, C., Foa, P., Koepke, S., Krauss, M., McArdell, C.S., Rottermann, K., Wei, Y., Zapata, A., Siegrist, H., 2011. Water reuse: >90% water yield in MBR/RO through concentrate recycling and CO2 addition as scaling control. Water Res. 45, 6141–6151. https://doi.org/10.1016/j.watres.2011.09.011

Jung, Y.J., Kiso, Y., Park, H.J., Nishioka, K., Min, K.S., 2007. Rejection properties of NF membranes for alkylphenols. Desalination 202, 278–285. https://doi.org/10.1016/j.desal.2005.12.065

Justo, A., González, O., Aceña, J., Pérez, S., Barceló, D., Sans, C., Esplugas, S., 2013. Pharmaceuticals and organic pollution mitigation in reclamation osmosis brines by UV/H2O2and ozone. J. Hazard. Mater. 263, 268–274. https://doi.org/10.1016/j.jhazmat.2013.05.030

Karci, A., Arslan-Alaton, I., Bekbolet, M., Ozhan, G., Alpertunga, B., 2014. H2O2/UV-C and Photo-Fenton treatment of a nonylphenol polyethoxylate in synthetic freshwater: Follow-up of degradation products, acute toxicity and genotoxicity. Chem. Eng. J. 241, 43–51. https://doi.org/10.1016/j.cej.2013.12.022

Karpinska, A., Sokół, A., Karpinska, J., 2015. Studies on the kinetics of carbamazepine degradation in aqueous matrix in the course of modified Fenton's reactions. J. Pharm. Biomed. Anal. 106, 46–51. https://doi.org/10.1016/j.jpba.2014.06.033

Katsigiannis, A., Noutsopoulos, C., Mantziaras, J., Gioldasi, M., 2015. Removal of emerging pollutants through Granular Activated Carbon. Chem. Eng. J. 280, 49–57. https://doi.org/10.1016/j.cej.2015.05.109

Kim, I., Yamashita, N., Tanaka, H., 2009a. Photodegradation of pharmaceuticals and personal care products during UV and UV/H2O2 treatments. Chemosphere 77, 518–525. https://doi.org/10.1016/j.chemosphere.2009.07.041

Kim, I., Yamashita, N., Tanaka, H., 2009b. Performance of UV and UV/H2O2processes for the removal of pharmaceuticals detected in secondary effluent of a sewage treatment plant in Japan. J. Hazard. Mater. 166, 1134–1140. https://doi.org/10.1016/j.jhazmat.2008.12.020

Kim, J., Korshin, G. V., Velichenko, A.B., 2005. Comparative study of electrochemical degradation and

ozonation of nonylphenol. Water Res. 39, 2527–2534. https://doi.org/10.1016/j.watres.2005.04.070

Kim, S.E., Yamada, H., Tsuno, H., 2004. Evaluation of estrogenicity for 17 β-estradiol decomposition during ozonation. Ozone Sci. Eng. 26, 563–571. https://doi.org/10.1080/01919510490885370

Kim, T.-U., Drewes, J.E., Scott Summers, R., Amy, G.L., 2007. Solute transport model for trace organic neutral and charged compounds through nanofiltration and reverse osmosis membranes. Water Res. 41, 3977–3988. https://doi.org/10.1016/j.watres.2007.05.055

Kimura, K., Amy, G., Drewes, J.E., Heberer, T., Kim, T.-U., Watanabe, Y., 2003. Rejection of organic micropollutants (disinfection by-products, endocrine disrupting compounds, and pharmaceutically active compounds) by NF/RO membranes. J. Memb. Sci. 227, 113–121. https://doi.org/10.1016/j.memsci.2003.09.005

Koduru, J.R., Lingamdinne, L.P., Singh, J., Choo, K.H., 2016. Effective removal of bisphenol-A (BPA) from water using a goethite/activated carbon composite. Process Saf. Environ. Prot. 103, 87–96. https://doi.org/10.1016/j.psep.2016.06.038

Komtchou, S., Dirany, A., Drogui, P., Bermond, A., 2015. Removal of carbamazepine from spiked municipal wastewater using electro-Fenton process. Environ. Sci. Pollut. Res. 22, 11513–11525. https://doi.org/10.1007/s11356-015-4345-6

Kong, F. xin, Yang, H. wei, Wang, X. mao, Xie, Y.F., 2016. Assessment of the hindered transport model in predicting the rejection of trace organic compounds by nanofiltration. J. Memb. Sci. 498, 57–66. https://doi.org/10.1016/j.memsci.2015.09.062

Koyuncu, I., Arikan, O.A., Wiesner, M.R., Rice, C., 2008. Removal of hormones and antibiotics by nanofiltration membranes. J. Memb. Sci. 309, 94–101. https://doi.org/10.1016/j.memsci.2007.10.010

Kukurina, O., Elemesova, Z., Syskina, A., 2014. Mineralization of Organophosphorous Pesticides by Electro-generated Oxidants. Procedia Chem. 10, 209–216. https://doi.org/10.1016/j.proche.2014.10.036

Lan, H., Jiao, Z., Zhao, X., He, W., Wang, A., Liu, H., Liu, R., Qu, J., 2013. Removal of glyphosate from water by electrochemically assisted MnO2oxidation process. Sep. Purif. Technol. 117, 30–40. https://doi.org/10.1016/j.seppur.2013.04.012

Launer, M., Lyko, S., Fahlenkamp, H., Jagemann, P., Ehrhard, P., 2013. Application of CFD modelling at a full-scale ozonation plant for the removal of micropollutants from secondary effluent. Water Sci. Technol. 68, 1336–44. https://doi.org/10.2166/wst.2013.378

Lee, J., Lee, B.C., Ra, J.S., Cho, J., Kim, I.S., Chang, N.I., Kim, H.K., Kim, S.D., 2008. Comparison of the removal efficiency of endocrine disrupting compounds in pilot scale sewage treatment processes. Chemosphere 71, 1582–1592. https://doi.org/10.1016/j.chemosphere.2007.11.021

Lee, S., Lee, J.-W., Kim, S., Park, P.-K., Kim, J.-H., Lee, C.-H., 2009. Removal of 17β-estradiol by powdered activated carbon—Microfiltraion hybrid process: The effect of PAC deposition on membrane surface. J. Memb. Sci. 326, 84–91. https://doi.org/10.1016/j.memsci.2008.09.031

Lee, Y., von Gunten, U., 2010. Oxidative transformation of micropollutants during municipal wastewater treatment: Comparison of kinetic aspects of selective (chlorine, chlorine dioxide, ferrateVI, and ozone) and non-selective oxidants (hydroxyl radical). Water Res. 44, 555–566. https://doi.org/10.1016/j.watres.2009.11.045

Li, X., Hai, F.I., Nghiem, L.D., 2011. Simultaneous activated carbon adsorption within a membrane bioreactor for an enhanced micropollutant removal. Bioresour. Technol. 102, 5319–5324. https://doi.org/10.1016/j.biortech.2010.11.070

Lima, D.R.S., Baêta, B.E.L., Aquino, S.F., Libânio, M., Afonso, R.J.C.F., 2014. Removal of Pharmaceuticals and Endocrine Disruptor Compounds from Natural Waters by Clarification Associated with Powdered Activated Carbon. Water, Air, Soil Pollut. 225, 2170. https://doi.org/10.1007/s11270-014-2170-z

Lin, A.Y.C., Panchangam, S.C., Chang, C.Y., Hong, P.K.A., Hsueh, H.F., 2012. Removal of perfluorooctanoic acid and perfluorooctane sulfonate via ozonation under alkaline condition. J. Hazard. Mater. 243, 272–277. https://doi.org/10.1016/j.jhazmat.2012.10.029

Lin, Y.L., 2017. Effects of organic, biological and colloidal fouling on the removal of pharmaceuticals and personal care products by nanofiltration and reverse osmosis membranes. J. Memb. Sci. 542, 342–

351. https://doi.org/10.1016/j.memsci.2017.08.023

Liu, J., Carr, S., Rinaldi, K., Chandler, W., 2005. Screening estrogenic oxidized by-products by combining ER binding and ultrafiltration. Environ. Toxicol. Pharmacol. 20, 269–278. https://doi.org/10.1016/j.etap.2005.01.008

Löwenberg, J., Zenker, A., Baggenstos, M., Koch, G., Kazner, C., Wintgens, T., 2014. Comparison of two PAC/UF processes for the removal of micropollutants from wastewater treatment plant effluent: Process performance and removal efficiency. Water Res. 56, 26–36. https://doi.org/10.1016/j.watres.2014.02.038

Ma, X., Zhang, C., Deng, J., Song, Y., Li, Q., Guo, Y., Li, C., 2015. Simultaneous degradation of estrone, 17β-estradiol and 17α-ethinyl estradiol in an aqueous UV/H2o2system. Int. J. Environ. Res. Public Health 12, 12016–12029. https://doi.org/10.3390/ijerph121012016

Madsen, H.T., Søgaard, E.G., 2014. Applicability and modelling of nanofiltration and reverse osmosis for remediation of groundwater polluted with pesticides and pesticide transformation products. Sep. Purif. Technol. 125, 111–119. https://doi.org/10.1016/j.seppur.2014.01.038

Mailler, R., Gasperi, J., Coquet, Y., Buleté, A., Vulliet, E., Deshayes, S., Zedek, S., Mirande-Bret, C., Eudes, V., Bressy, A., Caupos, E., Moilleron, R., Chebbo, G., Rocher, V., 2016. Removal of a wide range of emerging pollutants from wastewater treatment plant discharges by micro-grain activated carbon in fluidized bed as tertiary treatment at large pilot scale. Sci. Total Environ. 542, 983–996. https://doi.org/10.1016/j.scitotenv.2015.10.153

Mailler, R., Gasperi, J., Coquet, Y., Deshayes, S., Zedek, S., Cren-Olivé, C., Cartiser, N., Eudes, V., Bressy, A., Caupos, E., Moilleron, R., Chebbo, G., Rocher, V., 2015. Study of a large scale powdered activated carbon pilot: Removals of a wide range of emerging and priority micropollutants from wastewater treatment plant effluents. Water Res. 72, 315–30. https://doi.org/10.1016/j.watres.2014.10.047

Manassero, A., Passalia, C., Negro, A.C., Cassano, A.E., Zalazar, C.S., 2010. Glyphosate degradation in water employing the H2O2/UVC process. Water Res. 44, 3875–3882. https://doi.org/10.1016/j.watres.2010.05.004

Margot, J., Kienle, C., Magnet, A., Weil, M., Rossi, L., de Alencastro, L.F., Abegglen, C., Thonney, D., Chèvre, N., Schärer, M., Barry, D.A., 2013a. Treatment of micropollutants in municipal wastewater: Ozone or powdered activated carbon? Sci. Total Environ. 461–462, 480–498. https://doi.org/10.1016/j.scitotenv.2013.05.034

Margot, J., Kienle, C., Magnet, A., Weil, M., Rossi, L., de Alencastro, L.F., Abegglen, C., Thonney, D., Chèvre, N., Schärer, M., Barry, D.A.A., 2013b. Treatment of micropollutants in municipal wastewater: ozone or powdered activated carbon? Sci. Total Environ. 461–462, 480–98. https://doi.org/10.1016/j.scitotenv.2013.05.034

Martínez, F., López-Muñoz, M.J., Aguado, J., Melero, J.A., Arsuaga, J., Sotto, A., Molina, R., Segura, Y., Pariente, M.I., Revilla, A., Cerro, L., Carenas, G., 2013. Coupling membrane separation and photocatalytic oxidation processes for the degradation of pharmaceutical pollutants. Water Res. 47, 5647–5658. https://doi.org/10.1016/j.watres.2013.06.045

McCallum, E., Hyung, H., Shah, A., Huang, C.-H., Kim, J.-H., 2005. Removal of Hormones by Nanofiltration: Effects of Hormone Concentration and Natural Organic Matter Fouling on Removal.

Mcdowell, D.C., Huber, M.M., Wagner, M., Von Gunten, U., Ternes, T.A., 2005. Ozonation of carbamazepine in drinking water: Identification and kinetic study of major oxidation products. Environ. Sci. Technol. 39, 8014–8022. https://doi.org/10.1021/es050043l

Mir, N.A., Haque, M.M., Khan, A., Muneer, M., Vijayalakshmi, S., 2014. Photocatalytic degradation of herbicide Bentazone in aqueous suspension of TiO2: Mineralization, identification of intermediates and reaction pathways. Environ. Technol. (United Kingdom) 35, 407–415. https://doi.org/10.1080/09593330.2013.829872

Miralles-Cuevas, S., Arqués, A., Maldonado, M.I., Sánchez-Pérez, J.A., Malato Rodríguez, S., 2013. Combined nanofiltration and photo-Fenton treatment of water containing micropollutants. Chem. Eng. J. 224, 89–95. https://doi.org/10.1016/j.cej.2012.09.068

Miralles-Cuevas, S., Audino, F., Oller, I., Sánchez-Moreno, R., Sánchez Pérez, J.A., Malato, S., 2014a. Pharmaceuticals removal from natural water by nanofiltration combined with advanced tertiary treatments (solar photo-Fenton, photo-Fenton-like Fe(III)–EDDS complex and ozonation). Sep. Purif. Technol. 122, 515–522. https://doi.org/10.1016/j.seppur.2013.12.006

Miralles-Cuevas, S., Oller, I., Agüera, A., Ponce-Robles, L., Pérez, J.A.S., Malato, S., 2015. Removal of microcontaminants from MWTP effluents by combination of membrane technologies and solar photo-Fenton at neutral pH. Catal. Today 252, 78–83. https://doi.org/10.1016/j.cattod.2014.11.015

Miralles-Cuevas, S., Oller, I., Pérez, J.A.S., Malato, S., 2014b. Removal of pharmaceuticals from MWTP effluent by nanofiltration and solar photo-Fenton using two different iron complexes at neutral pH. Water Res. 64, 23–31. https://doi.org/10.1016/j.watres.2014.06.032

Mo, Y., Xiao, K., Liang, P., Huang, X., 2015. Effect of nanofiltration membrane surface fouling on organic micro-pollutants rejection: The roles of aqueous transport and solid transport. Desalination 367, 103–111. https://doi.org/10.1016/j.desal.2015.03.036

Molkenthin, M., Olmez-Hanci, T., Jekel, M.R., Arslan-Alaton, I., 2013. Photo-Fenton-like treatment of BPA: Effect of UV light source and water matrix on toxicity and transformation products. Water Res. 47, 5052–5064. https://doi.org/10.1016/j.watres.2013.05.051

Monteagudo, J.M., Durán, A., González, R., Expósito, A.J., 2015. In situ chemical oxidation of carbamazepine solutions using persulfate simultaneously activated by heat energy, UV light, Fe2+ ions, and H<inf>2</inf>O<inf>2</inf>. Appl. Catal. B Environ. 176–177, 120–129. https://doi.org/10.1016/j.apcatb.2015.03.055

Muneer, M., Boxall, C., 2008. Photocatalyzed degradation of a pesticide derivative glyphosate in aqueous suspensions of titanium dioxide. Int. J. Photoenergy 2008, 27–29. https://doi.org/10.1155/2008/197346

Naddeo, V., Belgiorno, V., Ricco, D., Kassinos, D., 2009. Degradation of diclofenac during sonolysis, ozonation and their simultaneous application. Ultrason. Sonochem. 16, 790–794. https://doi.org/10.1016/j.ultsonch.2009.03.003

Nagarnaik, P.M., Boulanger, B., 2011. Advanced oxidation of alkylphenol ethoxylates in aqueous systems. Chemosphere 85, 854–860. https://doi.org/10.1016/j.chemosphere.2011.06.105

Nakonechny, M., Ikehata, K., Gamal El-Din, M., 2008. Kinetics of estrone ozone/hydrogen peroxide advanced oxidation treatment. Ozone Sci. Eng. 30, 249–255. https://doi.org/10.1080/01919510802084570

Nasseri, S., Ebrahimi, S., Abtahi, M., Saeedi, R., 2018. Synthesis and characterization of polysulfone/graphene oxide nano-composite membranes for removal of bisphenol A from water. J. Environ. Manage. 205, 174–182. https://doi.org/10.1016/j.jenvman.2017.09.074

Ng, H.Y., Elimelech, M., 2004. Influence of colloidal fouling on rejection of trace organic contaminants by reverse osmosis. J. Memb. Sci. 244, 215–226. https://doi.org/10.1016/j.memsci.2004.06.054

Nghiem, L.D., Sch??fer, A.I., Elimelech, M., 2005. Pharmaceutical retention mechanisms by nanofiltration membranes. Environ. Sci. Technol. 39, 7698–7705. https://doi.org/10.1021/es0507665

Nghiem, L.D., Schäfer, A.I., 2002. Adsorption and Transport of Trace Contaminant Estrone in NF/RO Membranes. Environ. Eng. Sci. 19, 441–451. https://doi.org/10.1089/109287502320963427

Nghiem, L.D., Schäfer, A.I., Elimelech, M., 2006. Role of electrostatic interactions in the retention of pharmaceutically active contaminants by a loose nanofiltration membrane. J. Memb. Sci. 286, 52–59. https://doi.org/10.1016/j.memsci.2006.09.011

Nielsen, L., Biggs, M.J., Skinner, W., Bandosz, T.J., 2014. The effects of activated carbon surface features on the reactive adsorption of carbamazepine and sulfamethoxazole. Carbon N. Y. 80, 419–432. https://doi.org/10.1016/j.carbon.2014.08.081

Nikfar, E., Dehghani, M.H., Mahvi, A.H., Rastkari, N., Asif, M., Tyagi, I., Agarwal, S., Gupta, V.K., 2015. Removal of Bisphenol A from aqueous solutions using ultrasonic waves and hydrogen peroxide. J. Mol. Liq. 213, 332–338. https://doi.org/10.1016/j.molliq.2015.08.053

Ning, B., Graham, N., Zhang, Y., Nakonechny, M., El-Din, M.G., 2007a. Degradation of endocrine disrupting chemicals by ozone/AOPs. Ozone Sci. Eng. 29, 153–176. https://doi.org/10.1080/01919510701200012

Ning, B., Graham, N.J.D., Zhang, Y., 2007b. Degradation of octylphenol and nonylphenol by ozone - Part II: Indirect reaction. Chemosphere 68, 1173–1179. https://doi.org/10.1016/j.chemosphere.2007.01.056

Noutsopoulos, C., Mamais, D., Mpouras, T., Kokkinidou, D., Samaras, V., Antoniou, K., Gioldasi, M., 2014. The role of activated carbon and disinfection on the removal of endocrine disrupting chemicals and

non-steroidal anti-inflammatory drugs from wastewater. Environ. Technol. (United Kingdom) 35, 698–708. https://doi.org/10.1080/09593330.2013.846923

Ochoa-Herrera, V., Sierra-Alvarez, R., 2008. Removal of perfluorinated surfactants by sorption onto granular activated carbon, zeolite and sludge. Chemosphere 72, 1588–1593. https://doi.org/10.1016/j.chemosphere.2008.04.029

Ohko, Y., Iuchi, K.I., Niwa, C., Tatsuma, T., Nakashima, T., Iguchi, T., Kubota, Y., Fujishima, A., 2002. 17β-estradiol degradation by TiO2 photocatalysis as a means of reducing estrogenic activity. Environ. Sci. Technol. 36, 4175–4181. https://doi.org/10.1021/es011500a

Olmez-Hanci, T., Dursun, D., Aydin, E., Arslan-Alaton, I., Girit, B., Mita, L., Diano, N., Mita, D.G., Guida, M., 2015. S<inf>2</inf>O<inf>8</inf>2-/UV-C and H<inf>2</inf>O<inf>2</inf>/UV-C treatment of Bisphenol A: Assessment of toxicity, estrogenic activity, degradation products and results in real water. Chemosphere 119, S115–S123. https://doi.org/10.1016/j.chemosphere.2014.06.020

Padhye, L.P., Yao, H., Kung'u, F.T., Huang, C.H., 2014. Year-long evaluation on the occurrence and fate ofpharmaceuticals, personal care products, andendocrine disrupting chemicals in an urban drinking water treatment plant. Water Res. 51, 266–276. https://doi.org/10.1016/j.watres.2013.10.070

Pan, Z., Stemmler, E.A., Cho, H.J., Fan, W., LeBlanc, L.A., Patterson, H.H., Amirbahman, A., 2014. Photocatalytic degradation of 17α-ethinylestradiol (EE2) in the presence of TiO2-doped zeolite. J. Hazard. Mater. 279, 17–25. https://doi.org/10.1016/j.jhazmat.2014.06.040

Park, H.S., Koduru, J.R., Choo, K.H., Lee, B., 2015. Activated carbons impregnated with iron oxide nanoparticles for enhanced removal of bisphenol A and natural organic matter. J. Hazard. Mater. 286, 315–324. https://doi.org/10.1016/j.jhazmat.2014.11.012

Pereira, V.J., Galinha, J., Barreto Crespo, M.T., Matos, C.T., Crespo, J.G., 2012. Integration of nanofiltration, UV photolysis, and advanced oxidation processes for the removal of hormones from surface water sources. Sep. Purif. Technol. 95, 89–96. https://doi.org/10.1016/j.seppur.2012.04.013

Pérez-Estrada, L.A., Maldonado, M.I., Gernjak, W., Agüera, A., Fernández-Alba, A.R., Ballesteros, M.M., Malato, S., 2005. Decomposition of diclofenac by solar driven photocatalysis at pilot plant scale. Catal. Today 101, 219–226. https://doi.org/10.1016/j.cattod.2005.03.013

Perisic, D.J., Gilja, V., Stankov, M.N., Katancic, Z., Kusic, H., Stangar, U.L., Dionysiou, D.D., Bozic, A.L., 2016. Removal of diclofenac from water by zeolite-assisted advanced oxidation processes. J. Photochem. Photobiol. A Chem. 321, 238–247. https://doi.org/10.1016/j.jphotochem.2016.01.030

Pešoutová, R., Stříteský, L., Hlavínek, P., 2014. A pilot scale comparison of advanced oxidation processes for estrogenic hormone removal from municipal wastewater effluent. Water Sci. Technol. 70, 70–75. https://doi.org/10.2166/wst.2014.196

Pirilä, M., Saouabe, M., Ojala, S., Rathnayake, B., Drault, F., Valtanen, A., Huuhtanen, M., Brahmi, R., Keiski, R.L., 2015. Photocatalytic Degradation of Organic Pollutants in Wastewater. Top. Catal. 58, 1085–1099. https://doi.org/10.1007/s11244-015-0477-7

Pisarenko, A.N., Stanford, B.D., Yan, D., Gerrity, D., Snyder, S.A., 2012. Effects of ozone and ozone/peroxide on trace organic contaminants and NDMA in drinking water and water reuse applications. Water Res. 46, 316–326. https://doi.org/10.1016/j.watres.2011.10.021

Pourata, R., Khataee, A.R., Aber, S., Daneshvar, N., 2009. Removal of the herbicide Bentazon from contaminated water in the presence of synthesized nanocrystalline TiO2 powders under irradiation of UV-C light. Desalination 249, 301–307. https://doi.org/10.1016/j.desal.2008.10.033

Prieto-Rodriguez, L., Miralles-Cuevas, S., Oller, I., Agüera, A., Puma, G.L., Malato, S., 2012. Treatment of emerging contaminants in wastewater treatment plants (WWTP) effluents by solar photocatalysis using low TiO2concentrations. J. Hazard. Mater. 211–212, 131–137. https://doi.org/10.1016/j.jhazmat.2011.09.008

Prieto-Rodríguez, L., Oller, I., Klamerth, N., Agüera, A., Rodríguez, E.M., Malato, S., 2013. Application of solar AOPs and ozonation for elimination of micropollutants in municipal wastewater treatment plant effluents. Water Res. 47, 1521–1528. https://doi.org/10.1016/j.watres.2012.11.002

Qian, J., Shen, M., Wang, P., Wang, C., Li, K., Liu, J., Lu, B., Tian, X., 2017. Perfluorooctane sulfonate adsorption on powder activated carbon: Effect of phosphate (P) competition, pH, and temperature. Chemosphere 182, 215–222. https://doi.org/10.1016/j.chemosphere.2017.05.033

Qu, Y., Zhang, C., Li, F., Bo, X., Liu, G., Zhou, Q., 2009. Equilibrium and kinetics study on the adsorption of

perfluorooctanoic acid from aqueous solution onto powdered activated carbon. J. Hazard. Mater. 169, 146–152. https://doi.org/10.1016/j.jhazmat.2009.03.063

Quiñones, D.H., Álvarez, P.M., Rey, A., Beltrán, F.J., 2015a. Removal of emerging contaminants from municipal WWTP secondary effluents by solar photocatalytic ozonation. A pilot-scale study. Sep. Purif. Technol. 149, 132–139. https://doi.org/10.1016/j.seppur.2015.05.033

Quiñones, D.H., Álvarez, P.M., Rey, A., Contreras, S., Beltrán, F.J., 2015b. Application of solar photocatalytic ozonation for the degradation of emerging contaminants in water in a pilot plant. Chem. Eng. J. 260, 399–410. https://doi.org/10.1016/j.cej.2014.08.067

Radjenović, J., Petrović, M., Ventura, F., Barceló, D., 2008. Rejection of pharmaceuticals in nanofiltration and reverse osmosis membrane drinking water treatment. Water Res. 42, 3601–3610. https://doi.org/10.1016/j.watres.2008.05.020

Rahman, M.F., Yanful, E.K., Jasim, S.Y., Bragg, L.M., Servos, M.R., Ndiongue, S., Borikar, D., 2010. Advanced oxidation treatment of drinking water: Part I. occurrence and removal of pharmaceuticals and endocrine-disrupting compounds from Lake Huron water. Ozone Sci. Eng. 32, 217–229. https://doi.org/10.1080/01919512.2010.489185

Ravina, M., Campanella, L., Kiwi, J., 2002. Accelerated mineralization of the drug Diclofenac via Fenton reactions in a concentric photo-reactor. Water Res. 36, 3553–3560. https://doi.org/10.1016/S0043-1354(02)00075-1

Reungoat, J., Macova, M., Escher, B.I., Carswell, S., Mueller, J.F., Keller, J., 2010. Removal of micropollutants and reduction of biological activity in a full scale reclamation plant using ozonation and activated carbon filtration. Water Res. 44, 625–637. https://doi.org/10.1016/j.watres.2009.09.048

Rigau, J., Saitua, H., 2015. Optimization and Modeling of Glyphosate Removal by Nanofiltration at a Pilot Scale, Using Response Surface Methodology. World J. Environ. Eng. 3, 126–132. https://doi.org/10.12691/wjee-3-4-4

Rigobello, E.S., Dantas, A.D.B., Di Bernardo, L., Vieira, E.M., 2013. Removal of diclofenac by conventional drinking water treatment processes and granular activated carbon filtration. Chemosphere 92, 184–191. https://doi.org/10.1016/j.chemosphere.2013.03.010

Rioja, N., Benguria, P., Peñas, F.J., Zorita, S., 2014. Competitive removal of pharmaceuticals from environmental waters by adsorption and photocatalytic degradation. Environ. Sci. Pollut. Res. 21, 11168–11177. https://doi.org/10.1007/s11356-014-2593-5

Rizzo, L., Fiorentino, A., Grassi, M., Attanasio, D., Guida, M., 2015. Advanced treatment of urban wastewater by sand filtration and graphene adsorption for wastewater reuse: Effect on a mixture of pharmaceuticals and toxicity. J. Environ. Chem. Eng. 3, 122–128. https://doi.org/10.1016/j.jece.2014.11.011

Rizzo, L., Meric, S., Kassinos, D., Guida, M., Russo, F., Belgiorno, V., 2009. Degradation of diclofenac by TiO2photocatalysis: UV absorbance kinetics and process evaluation through a set of toxicity bioassays. Water Res. 43, 979–988. https://doi.org/10.1016/j.watres.2008.11.040

Rosario-Ortiz, F.L., Wert, E.C., Snyder, S.A., 2010. Evaluation of UV/H2O2 treatment for the oxidation of pharmaceuticals in wastewater. Water Res. 44, 1440–1448. https://doi.org/10.1016/j.watres.2009.10.031

Rosenfeldt, E.J., Linden, K.G., 2004. Degradation of Endocrine Disrupting Chemicals Bisphenol A, Ethinyl Estradiol, and Estradiol during UV Photolysis and Advanced Oxidation Processes. Environ. Sci. Technol. 38, 5476–5483. https://doi.org/10.1021/es035413p

Ruhl, A.S., Altmann, J., Zietzschmann, F., Meinel, F., Sperlich, A., Jekel, M., 2014. Integrating micro-pollutant removal by powdered activated carbon into deep bed filtration. Water. Air. Soil Pollut. 225, 1–11. https://doi.org/10.1007/s11270-014-1877-1

Sadmani, A.H.M.A., Andrews, R.C., Bagley, D.M., 2014a. Impact of natural water colloids and cations on the rejection of pharmaceutically active and endocrine disrupting compounds by nanofiltration. J. Memb. Sci. 450, 272–281. https://doi.org/10.1016/j.memsci.2013.09.017

Sadmani, A.H.M.A., Andrews, R.C., Bagley, D.M., 2014b. Nanofiltration of pharmaceutically active and endocrine disrupting compounds as a function of compound interactions with DOM fractions and cations in natural water. Sep. Purif. Technol. 122, 462–471. https://doi.org/10.1016/j.seppur.2013.12.003

Saggioro, E.M., Oliveira, A.S., Pavesi, T., Tototzintle, M.J., Maldonado, M.I., Correia, F.V., Moreira, J.C., 2014. Solar CPC pilot plant photocatalytic degradation of bisphenol A in waters and wastewaters using suspended and supported-TiO2. Influence of photogenerated species. Environ. Sci. Pollut. Res. 12112–12121. https://doi.org/10.1007/s11356-014-2723-0

Saha, B., Karounou, E., Streat, M., 2010. Removal of 17β-oestradiol and 17α-ethinyl oestradiol from water by activated carbons and hypercrosslinked polymeric phases. React. Funct. Polym. 70, 531–544. https://doi.org/10.1016/j.reactfunctpolym.2010.04.004

Saitúa, H., Giannini, F., Padilla, A.P., 2012. Drinking water obtaining by nanofiltration from waters contaminated with glyphosate formulations: Process evaluation by means of toxicity tests and studies on operating parameters. J. Hazard. Mater. 227–228, 204–210. https://doi.org/10.1016/j.jhazmat.2012.05.035

Salaeh, S., Juretic Perisic, D., Biosic, M., Kusic, H., Babic, S., Lavrencic Stangar, U., Dionysiou, D.D., Loncaric Bozic, A., 2016. Diclofenac removal by simulated solar assisted photocatalysis using TiO2-based zeolite catalyst; mechanisms, pathways and environmental aspects. Chem. Eng. J. 304, 289–302. https://doi.org/10.1016/j.cej.2016.06.083

Salman, J.M., Mohammed, M.J., 2013. Batch study for herbicide bentazon adsorption onto branches of pomegranates trees activated carbon. Desalin. Water Treat. 51, 5005–5008. https://doi.org/10.1080/19443994.2013.774118

Salman, J.M., Njoku, V.O., Hameed, B.H., 2011a. Bentazon and carbofuran adsorption onto date seed activated carbon: Kinetics and equilibrium. Chem. Eng. J. 173, 361–368. https://doi.org/10.1016/j.cej.2011.07.066

Salman, J.M., Njoku, V.O., Hameed, B.H., 2011b. Adsorption of pesticides from aqueous solution onto banana stalk activated carbon. Chem. Eng. J. 174, 41–48. https://doi.org/10.1016/j.cej.2011.08.026

Sanches, S., Penetra, A., Rodrigues, A., Ferreira, E., Cardoso, V. V., Benoliel, M.J., Barreto Crespo, M.T., Pereira, V.J., Crespo, J.G., 2012. Nanofiltration of hormones and pesticides in different real drinking water sources. Sep. Purif. Technol. 94, 44–53. https://doi.org/10.1016/j.seppur.2012.04.003

Sánchez-Polo, M., Abdel daiem, M.M., Ocampo-Pérez, R., Rivera-Utrilla, J., Mota, A.J., 2013. Comparative study of the photodegradation of bisphenol A by HO, SO4-and CO3-/HCO3radicals in aqueous phase. Sci. Total Environ. 463–464, 423–431. https://doi.org/10.1016/j.scitotenv.2013.06.012

Sarasidis, V.C., Plakas, K. V., Patsios, S.I., Karabelas, A.J., 2014. Investigation of diclofenac degradation in a continuous photo-catalytic membrane reactor. Influence of operating parameters. Chem. Eng. J. 239, 299–311. https://doi.org/10.1016/j.cej.2013.11.026

Sarkar, S., Ali, S., Rehmann, L., Nakhla, G., Ray, M.B., 2014. Degradation of estrone in water and wastewater by various advanced oxidation processes. J. Hazard. Mater. 278, 16–24. https://doi.org/10.1016/j.jhazmat.2014.05.078

Schröder, H.F., José, H.J., Gebhardt, W., Moreira, R.F.P.M., Pinnekamp, J., 2010. Biological wastewater treatment followed by physicochemical treatment for the removal of fluorinated surfactants. Water Sci. Technol. 61, 3208–3215. https://doi.org/10.2166/wst.2010.917

Semião, A.J.C., Foucher, M., Schäfer, A.I., 2013. Removal of adsorbing estrogenic micropollutants by nanofiltration membranes: Part B-Modeldevelopment. J. Memb. Sci. 431, 257–266. https://doi.org/10.1016/j.memsci.2012.11.079

Semião, A.J.C., Schäfer, A.I., 2011. Estrogenic micropollutant adsorption dynamics onto nanofiltration membranes. J. Memb. Sci. 381, 132–141. https://doi.org/10.1016/j.memsci.2011.07.031

Senevirathna, S.T.M.L.D., Tanaka, S., Fujii, S., Kunacheva, C., Harada, H., Ariyadasa, B.H.A.K.T., Shivakoti, B.R., 2010. Adsorption of perfluorooctane sulfonate (n-PFOS) onto non ion-exchange polymers and granular activated carbon: Batch and column test. Desalination 260, 29–33. https://doi.org/10.1016/j.desal.2010.05.005

Shan, D., Deng, S., Zhao, T., Wang, B., Wang, Y., Huang, J., Yu, G., Winglee, J., Wiesner, M.R., 2016. Preparation of ultrafine magnetic biochar and activated carbon for pharmaceutical adsorption and subsequent degradation by ball milling. J. Hazard. Mater. 305, 156–163. https://doi.org/10.1016/j.jhazmat.2015.11.047

Sharma, J., Mishra, I.M., Kumar, V., 2016. Mechanistic study of photo-oxidation of Bisphenol-A (BPA) with hydrogen peroxide (H2O2) and sodium persulfate (SPS). J. Environ. Manage. 166, 12–22.

https://doi.org/10.1016/j.jenvman.2015.09.043

Sharma, J., Mishra, I.M., Kumar, V., 2015. Degradation and mineralization of Bisphenol A (BPA) in aqueous solution using advanced oxidation processes: UV/H<inf>2</inf>O<inf>2</inf> and UV/S2O82- oxidation systems. J. Environ. Manage. 156, 266–275. https://doi.org/10.1016/j.jenvman.2015.03.048

Simon, A., Price, W.E., Nghiem, L.D., 2013. Impact of chemical cleaning on the nanofiltration of pharmaceutically active compounds (PhACs): The role of cleaning temperature. J. Taiwan Inst. Chem. Eng. 44, 713–723. https://doi.org/10.1016/j.jtice.2013.01.030

Snyder, S.A., Adham, S., Redding, A.M., Cannon, F.S., DeCarolis, J., Oppenheimer, J., Wert, E.C., Yoon, Y., 2007. Role of membranes and activated carbon in the removal of endocrine disruptors and pharmaceuticals. Desalination 202, 156–181. https://doi.org/10.1016/j.desal.2005.12.052

Snyder, S.A., Wert, E.C., Rexing, D.J., Zegers, R.E., Drury, D.D., 2006. Ozone Oxidation of Endocrine Disruptors and Pharmaceuticals in Surface Water and Wastewater. Ozone Sci. Eng. 28, 445–460. https://doi.org/10.1080/01919510601039726

Solak, S., Vakondios, N., Tzatzimaki, I., Diamadopoulos, E., Arda, M., Kabay, N., Yüksel, M., 2014. A comparative study of removal of endocrine disrupting compounds (EDCs) from treated wastewater using highly crosslinked polymeric adsorbents and activated carbon. J. Chem. Technol. Biotechnol. 89, 819–824. https://doi.org/10.1002/jctb.4315

Solcova, O., Spacilova, L., Maleterova, Y., Morozova, M., Ezechias, M., Kresinova, Z., 2016. Photocatalytic water treatment on TiO 2 thin layers. Desalin. Water Treat. 57, 11631–11638. https://doi.org/10.1080/19443994.2015.1049964

Soni, H., Padmaja, P., 2014. Palm shell based activated carbon for removal of bisphenol A: An equilibrium, kinetic and thermodynamic study. J. Porous Mater. 21, 275–284. https://doi.org/10.1007/s10934-013-9772-5

Sotelo, J.L., Rodríguez, A., Álvarez, S., García, J., 2012. Removal of caffeine and diclofenac on activated carbon in fixed bed column. Chem. Eng. Res. Des. 90, 967–974. https://doi.org/10.1016/j.cherd.2011.10.012

Spaltro, A., Simonetti, S., Torrellas, S.A., Rodriguez, J.G., Ruiz, D., Juan, A., Allegretti, P., 2018. Adsorption of bentazon on CAT and CARBOPAL activated carbon: Experimental and computational study. Appl. Surf. Sci. 433, 487–501. https://doi.org/10.1016/j.apsusc.2017.10.011

Speth, T.F., 1993. Glyphosate Removal From Drinking Water. J. Environ. Eng. 119, 1139–1157. https://doi.org/10.1061/(ASCE)0733-9372(1993)119:6(1139)

Sudhakar, P., Mall, I.D., Srivastava, V.C., 2016. Adsorptive removal of bisphenol-A by rice husk ash and granular activated carbon—A comparative study. Desalin. Water Treat. 57, 12375–12384. https://doi.org/10.1080/19443994.2015.1050700

Takagi, S., Adachi, F., Miyano, K., Koizumi, Y., Tanaka, H., Watanabe, I., Tanabe, S., Kannan, K., 2011. Fate of Perfluorooctanesulfonate and perfluorooctanoate in drinking water treatment processes. Water Res. 45, 3925–3932. https://doi.org/10.1016/j.watres.2011.04.052

Tan, Y.H., Goh, P.S., Ismail, A.F., 2015. Development of photocatalytic coupled zinc-iron oxide nanoparticles via solution combustion for bisphenol-A removal. Int. Biodeterior. Biodegrad. 102, 346–352. https://doi.org/10.1016/j.ibiod.2015.03.010

Tang, H., Xiang, Q., Lei, M., Yan, J., Zhu, L., Zou, J., 2012. Efficient degradation of perfluorooctanoic acid by UV-Fenton process. Chem. Eng. J. 184, 156–162. https://doi.org/10.1016/j.cej.2012.01.020

Ternes, T.A., Meisenheimer, M., McDowell, D., Sacher, F., Brauch, H.J., Haist-Gulde, B., Preuss, G., Wilme, U., Zulei-Seibert, N., 2002. Removal of Pharmaceuticals during Drinking Water Treatment. Environ. Sci. Technol. 36, 3855–3863. https://doi.org/10.1021/es015757k

Ternes, T.A., Stüber, J., Herrmann, N., McDowell, D., Ried, A., Kampmann, M., Teiser, B., 2003. Ozonation: A tool for removal of pharmaceuticals, contrast media and musk fragrances from wastewater? Water Res. 37, 1976–1982. https://doi.org/10.1016/S0043-1354(02)00570-5

To, M.H., Hadi, P., Hui, C.W., Lin, C.S.K., McKay, G., 2017. Mechanistic study of atenolol, acebutolol and carbamazepine adsorption on waste biomass derived activated carbon. J. Mol. Liq. 241, 386–398. https://doi.org/10.1016/j.molliq.2017.05.037

Tokumura, M., Sugawara, A., Raknuzzaman, M., Habibullah-Al-Mamun, M., Masunaga, S., 2016. Comprehensive study on effects of water matrices on removal of pharmaceuticals by three

different kinds of advanced oxidation processes. Chemosphere 159, 317–325. https://doi.org/10.1016/j.chemosphere.2016.06.019

Torrellas, S.Á., García Lovera, R., Escalona, N., Sepúlveda, C., Sotelo, J.L., García, J., 2015. Chemical-activated carbons from peach stones for the adsorption of emerging contaminants in aqueous solutions. Chem. Eng. J. 279, 788–798. https://doi.org/10.1016/j.cej.2015.05.104

Vergili, I., 2013. Application of nanofiltration for the removal of carbamazepine, diclofenac and ibuprofen from drinking water sources. J. Environ. Manage. 127, 177–187. https://doi.org/10.1016/j.jenvman.2013.04.036

Vieno, N.M., Härkki, H., Tuhkanen, T., Kronberg, L., 2007. Occurrence of pharmaceuticals in river water and their elimination in a pilot-scale drinking water treatment plant. Environ. Sci. Technol. 41, 5077–5084. https://doi.org/10.1021/es062720x

Vogna, D., Marotta, R., Andreozzi, R., Napolitano, A., D'Ischia, M., 2004a. Kinetic and chemical assessment of the UV/H2O2treatment of antiepileptic drug carbamazepine. Chemosphere 54, 497–505. https://doi.org/10.1016/S0045-6535(03)00757-4

Vogna, D., Marotta, R., Napolitano, A., Andreozzi, R., D'Ischia, M., 2004b. Advanced oxidation of the pharmaceutical drug diclofenac with UV/H2O2and ozone. Water Res. 38, 414–422. https://doi.org/10.1016/j.watres.2003.09.028

Vona, A., di Martino, F., Garcia-Ivars, J., Picó, Y., Mendoza-Roca, J.A., Iborra-Clar, M.I., 2015. Comparison of different removal techniques for selected pharmaceuticals. J. Water Process Eng. 5, 48–57. https://doi.org/10.1016/j.jwpe.2014.12.011

Wang, S., Zhou, N., 2016. Removal of carbamazepine from aqueous solution using sono-activated persulfate process. Ultrason. Sonochem. 29, 156–162. https://doi.org/10.1016/j.ultsonch.2015.09.008

Wang, X. mao, Li, B., Zhang, T., Li, X. yan, 2015. Performance of nanofiltration membrane in rejecting trace organic compounds: Experiment and model prediction. Desalination 370, 7–16. https://doi.org/10.1016/j.desal.2015.05.010

Wang, Y., Zhang, P., Pan, G., Chen, H., 2008. Ferric ion mediated photochemical decomposition of perfluorooctanoic acid (PFOA) by 254 nm UV light. J. Hazard. Mater. 160, 181–186. https://doi.org/10.1016/j.jhazmat.2008.02.105

Westerhoff, P., Yoon, Y., Snyder, S., Wert, E., 2005. Fate of endocrine-disruptor, pharmaceutical, and personal care product chemicals during simulated drinking water treatment processes. Environ. Sci. Technol. 39, 6649–6663. https://doi.org/10.1021/es0484799

Wintgens, T., Gallenkemper, M., Melin, T., 2002. Endocrine disrupter removal from wastewater using membrane bioreactor and nanofiltration technology. Desalination 146, 387–391. https://doi.org/10.1016/S0011-9164(02)00519-2

Wirasnita, R., Hadibarata, T., Yusoff, A.R.M., Yusop, Z., 2014. Removal of Bisphenol A from Aqueous Solution by Activated Carbon Derived from Oil Palm Empty Fruit Bunch. Water, Air, Soil Pollut. 225, 2148. https://doi.org/10.1007/s11270-014-2148-x

Wols, B.A., Hofman-Caris, C.H.M., Harmsen, D.J.H., Beerendonk, E.F., 2013. Degradation of 40 selected pharmaceuticals by UV/H2O2. Water Res. 47, 5876–5888. https://doi.org/10.1016/j.watres.2013.07.008

Xie, M., Nghiem, L.D., Price, W.E., Elimelech, M., 2012. Comparison of the removal of hydrophobic trace organic contaminants by forward osmosis and reverse osmosis. Water Res. 46, 2683–2692. https://doi.org/10.1016/j.watres.2012.02.023

Xie, Y.B., Li, X.Z., 2006. Degradation of bisphenol A in aqueous solution by H2O2-assisted photoelectrocatalytic oxidation. J. Hazard. Mater. 138, 526–533. https://doi.org/10.1016/j.jhazmat.2006.05.074

Xu, P., Drewes, J.E., Bellona, C., Amy, G., Kim, T.-U., Adam, M., Heberer, T., 2005. Rejection of Emerging Organic Micropollutants in Nanofiltration–Reverse Osmosis Membrane Applications. Water Environ. Res. 77, 40–48. https://doi.org/10.2175/106143005X41609

Xue, W., Zhang, G., Xu, X., Yang, X., Liu, C., Xu, Y., 2011. Preparation of titania nanotubes doped with cerium and their photocatalytic activity for glyphosate. Chem. Eng. J. 167, 397–402. https://doi.org/10.1016/j.cej.2011.01.007

Yan, H., Cousins, I.T., Zhang, C., Zhou, Q., 2015. Perfluoroalkyl acids in municipal landfill leachates from

China: Occurrence, fate during leachate treatment and potential impact on groundwater. Sci. Total Environ. 524–525, 23–31. https://doi.org/10.1016/j.scitotenv.2015.03.111

Yan, L., Lv, D., Huang, X., Shi, H., Zhang, G., 2016. Adsorption characteristics of Bisphenol-A on tailored activated carbon in aqueous solutions. Water Sci. Technol. 74, 1744–1751. https://doi.org/10.2166/wst.2016.325

Yoon, Y., Westerhoff, P., Snyder, S.A., 2005. Adsorption of 3H-Labeled 17-β Estradiol on Powdered Activated Carbon. Water. Air. Soil Pollut. 166, 343–351. https://doi.org/10.1007/s11270-005-7274-z

Yoon, Y., Westerhoff, P., Snyder, S.A., Esparza, M., 2003. HPLC-fluorescence detection and adsorption of bisphenol A, 17β-estradiol, and 17α-ethynyl estradiol on powdered activated carbon. Water Res. 37, 3530–3537. https://doi.org/10.1016/S0043-1354(03)00239-2

Yoon, Y., Westerhoff, P., Snyder, S.A., Wert, E.C., 2006. Nanofiltration and ultrafiltration of endocrine disrupting compounds, pharmaceuticals and personal care products. J. Memb. Sci. 270, 88–100.

Yoon, Y., Westerhoff, P., Snyder, S.A., Wert, E.C., Yoon, J., 2007. Removal of endocrine disrupting compounds and pharmaceuticals by nanofiltration and ultrafiltration membranes. Desalination 202, 16–23. https://doi.org/10.1016/j.desal.2005.12.033

Yoon, Y., Westerhoff, P., Yoon, J., Snyder, S. a., 2004. Removal of 17β Estradiol and Fluoranthene by Nanofiltration and Ultrafiltration. J. Environ. Eng. 130, 1460–1467. https://doi.org/10.1061/(ASCE)0733-9372(2004)130:12(1460)

Yu, J., Hu, J., 2011. Adsorption of Perfluorinated Compounds onto Activated Carbon and Activated Sludge. J. Environ. Eng. 137, 945–951. https://doi.org/10.1061/(ASCE)EE.1943-7870.0000402

Yu, J., Lv, L., Lan, P., Zhang, S., Pan, B., Zhang, W., 2012. Effect of effluent organic matter on the adsorption of perfluorinated compounds onto activated carbon. J. Hazard. Mater. 225–226, 99–106. https://doi.org/10.1016/j.jhazmat.2012.04.073

Yu, Q., Zhang, R., Deng, S., Huang, J., Yu, G., 2009. Sorption of perfluorooctane sulfonate and perfluorooctanoate on activated carbons and resin: Kinetic and isotherm study. Water Res. 43, 1150–8. https://doi.org/10.1016/j.watres.2008.12.001

Yu, Z., Peldszus, S., Huck, P.M., 2008. Adsorption characteristics of selected pharmaceuticals and an endocrine disrupting compound-Naproxen, carbamazepine and nonylphenol-on activated carbon. Water Res. 42, 2873–2882. https://doi.org/10.1016/j.watres.2008.02.020

Yuan, S., Gou, N., Alshawabkeh, A.N., Gu, A.Z., 2013. Efficient degradation of contaminants of emerging concerns by a new electro-Fenton process with Ti/MMO cathode. Chemosphere 93, 2796–2804.

Yüksel, S., Kabay, N., Yüksel, M., 2013. Removal of bisphenol A (BPA) from water by various nanofiltration (NF) and reverse osmosis (RO) membranes. J. Hazard. Mater. 263, 307–310. https://doi.org/10.1016/j.jhazmat.2013.05.020

Zhang, A., Li, Y., 2014. Removal of phenolic endocrine disrupting compounds from waste activated sludge using UV, H2O2, and UV/H2O2oxidation processes: Effects of reaction conditions and sludge matrix. Sci. Total Environ. 493, 307–323. https://doi.org/10.1016/j.scitotenv.2014.05.149

Zhang, D., Luo, Q., Gao, B., Chiang, S.Y.D., Woodward, D., Huang, Q., 2016. Sorption of perfluorooctanoic acid, perfluorooctane sulfonate and perfluoroheptanoic acid on granular activated carbon. Chemosphere 144, 2336–2342. https://doi.org/10.1016/j.chemosphere.2015.10.124

Zhao, F.B., Tang, C.C., Liu, X.Y., Shi, F.J., Song, X.R., Tian, Y., Li, Z.S., 2015. Transportation characteristics of bisphenol A on ultrafiltration membrane with low molecule weight cut-off. Desalination 362, 18–25. https://doi.org/10.1016/j.desal.2015.01.048

Zhi, Y., Liu, J., 2015. Adsorption of perfluoroalkyl acids by carbonaceous adsorbents: Effect of carbon surface chemistry. Environ. Pollut. 202, 168–176. https://doi.org/10.1016/j.envpol.2015.03.019

Zhou, H., Liu, J., Xia, H., Zhang, Q., Ying, T., Hu, T., 2015. Removal and reduction of selected organic micro-pollutants in effluent sewage by the ozone-based oxidation processes. Chem. Eng. J. 269, 245–254. https://doi.org/10.1016/j.cej.2015.01.116

Zielińska, M., Bułkowska, K., Cydzik-Kwiatkowska, A., Bernat, K., Wojnowska-Baryła, I., 2016. Removal of bisphenol A (BPA) from biologically treated wastewater by microfiltration and nanofiltration. Int. J. Environ. Sci. Technol. 13, 2239–2248. https://doi.org/10.1007/s13762-016-1056-6

Zwiener, C., Frimmel, F.H., 2000. Oxidative treatment of pharmaceuticals in water. Water Res. 34, 1881–1885. https://doi.org/10.1016/S0043-1354(99)00338-3

DESIGN OF THE RESEARCH

Drinking water (DW) sources in industrialized areas are often contaminated by a wide variety of Contaminants of Emerging Concern (CECs). Despite they are present at low concentrations (sub-ng L^{-1} - µg L^{-1}), these contaminants may represent a health hazard, depending on their toxicity. Few CECs have been proposed for introduction in the revision of the European Directive on drinking water, while a relevant number of compounds is still unregulated or just candidate for future regulation. Moreover, the revision of the European DW Directive promoted a shift in the current paradigm, pushing the preventive estimation of human health risk, in order to identify the main risk sources and predict, prevent and minimize risks for the consumer throughout the whole supply system (from source to tap). Human health risk prediction consists of understanding if CECs exposure concentrations exceed a tolerable health-based threshold. The use of risk assessment can also be an important tool for the prioritization of the CECs to be regulated.

However, several knowledge gaps and high uncertainties on the occurrence, fate and hazard of CECs in DW inhibit this paradigm shift for CECs, due to analytical methods that should be improved to detect low concentrations of CECs in DW, limited number of monitoring and toxicity data, and lack in modeling tools able to take into account the uncertainties related to the fate of CECs in treatment plant and distribution networks. These knowledge gaps and uncertainties hinder to answer to the following questions:

- which CECs should be prioritized for inclusion in the regulations and which limits should be proposed?
- are the current DW supply systems effective and resilient in reducing the risk related to CECs in DW or additional measures should be taken to reduce the health risk?
- what should be the future focus and direction of scientific research, in order to reduce uncertainties and provide reliable tools for DW supply system management?

Scientific literature is not always exhaustive to answer these questions or to provide proper experimental and modelling tools to support answering.

The overall objective of this thesis is to provide a contribution in answering to the above questions providing tools that could support: i) decision-makers in evaluating the current human health risk and prioritizing CECs regulation, and ii) water utilities in planning affordable and effective upgrading, management and/or monitoring interventions for risk minimization throughout the whole water supply system. To fulfil this goal, the water supply system was conceptualized in 4 elements, each one contributing to CEC concentration in water delivered to consumers: (i) DW sources (e.g. groundwater, surface water), (ii) drinking water treatment plant (DWTP), (iii) drinking water distribution network (DWDN) and (iv) point of use (i.e. the consumer's tap). Experimental activity, at lab- and full-scale, advanced statistical methods and modelling techniques were combined to apportion the contribution of each element of the DW supply system in determining human health risk, in order to prioritize mitigation actions in view of an overall risk minimization.

The work was structured in five tasks, each one described in one thematic chapter, following a scientific article-based structure and published/intended for publication on an international peer-reviewed scientific journal. A schematic overview of the thesis chapters is given in Figure 1, and their content is briefly described in the following paragraphs.

- *Chapter 1*: a field monitoring campaign was designed to evaluate CECs concentrations in addition to routinely monitored parameters in groundwater (GW) and drinking water (DW) in 28 DWTPs spread in a highly urbanized area. Due to the low concentrations and the continuously refining of the

analytical methods, the monitoring database was rich in censored data (e.g. samples with concentrations below the limit of quantification, LOQ), which are traditionally eliminated or replaced with a value between 0 and LOQ, leading to erroneous estimations, but also to not fully exploit the information contained in the monitoring database. Therefore, an advanced Maximum Likelihood Estimation method for left-censored data (MLE_{LC}), that combines the values above the LOQ with the information contained in the proportion of censored data, was applied to estimate the statistical distribution of CECs concentrations and compared to the traditional methods. Competing methods were compared in three applications that are fundamental to predict the future raw water quality and to define intervention scenarios: evaluation of contaminants concentration time trend, estimation of treatment removal efficiency and risk assessment. Finally, a guideline was provided to select the data elaboration method to be preferred based on the comparison of the methods estimation errors, as a function of the percentage of censored data (from 0.3 to 99.0%) and the amplitude of concentration data range. This was made possible by the wide range of contaminants (19 parameters), the several DWTPs and the numerous sampling locations (from groundwater to drinking water) considered in this study, that result in more than 450 available datasets. The MLE_{LC} method was demonstrated to be the most accurate method in the three evaluated applications. On the other hand, traditional elimination and substitution methods can lead to erroneous conclusions under- or overestimating the human health risk, leading to potentially not precautionary or unsustainable intervention plans.

- *Chapter 2*: a new probabilistic procedure, that is the quantitative chemical risk assessment (QCRA), was developed to assess health risk, in terms of benchmark quotient, related to the occurrence of CECs in DW. Uncertainties were included in risk calculation in both exposure and hazard assessments, obtaining as output the benchmark quotient probabilistic distribution. The probabilistic distribution of CECs concentration in DW was estimated based on their concentration in source water and simulating the breakthrough curves of a granular activated carbon (GAC) treatment process, through mathematical simulations with the Ideal Adsorbed Solution Theory (IAST) model, modifying the *AquaPriori* tool to accept distributions - instead of point values - for input parameters. The uncertainties in the CECs hazard assessment were included using the APROBA-Plus tool developed by the USEPA. The model inputs and output uncertainties were evaluated by sensitivity and uncertainty analyses for each step of the risk assessment to identify the most relevant factors affecting risk estimation, that need further investigation. To stress the potential of this new QCRA approach, several case studies were considered with focus on bisphenol A as an example CEC and various GAC management options. The probabilistic risk quantified by the QCRA was compared to the deterministic risk estimated by the traditional CRA procedure, demonstrating that QCRA is more effective than deterministic CRA in evaluating the effect of each management option in risk minimization, permitting to select and prioritize the most appropriate interventions.

- *Chapters 3 and 4*: Since with the QCRA it was found that modelling of GAC breakthrough curves has a relevant role in the accuracy of risk estimation, experimental work has been performed to more accurately model GAC performance towards CECs, in particular perfluoroalkyl substances (PFAS), as reported in Chapter 3, and pharmaceutical active compounds (PhACs), described in Chapter 4. Various commercial GACs were tested by equilibrium batch experiments, providing isotherms, and rapid small-scale column tests (RSSCT), to calibrate CECs breakthrough curves. These studies were performed on 8 PFAS and 8 PhACs in 3 water matrices, which were tap water and additional two synthetic matrixes at lower dissolved organic carbon (DOC) and two levels of conductivity. As for activated carbon, 4 GACs were tested, differing for origin, micro- and mesoporous structure and surface charge, in order to evaluate the effect of GAC regeneration being a common practice in DWTPs. The resulting lab scale data were analyzed through multivariate analysis (such as factorial analysis and cluster analysis) and used to calibrate a performance predictive model able to predict the breakthrough curves parameters as a function of the CEC, carbon and water characteristics and

their interactions. Moreover, full-scale data collected through a monitoring campaign on PFAS were used for model validation. Finally, a correlation was built between the reduction of UV absorbance at 254 nm and CECs removal, in order to evaluate whether UVA_{254} can be used as a proxy variable for CECs continuous on-line monitoring. Actually, UVA_{254} is correlated to CECs removal, independently from the type of GAC and water matrix, but it depends on the test scale.

- *Chapter 5*: Potential recontamination events in the DWDN were studied with particular focus on BPA release from epoxy resins used to renovate pipelines. Lab migration tests were performed on three commercial epoxy resins, characterized by different formulations, BPA content and installation technique, put in contact with three water matrices: (i) tap water, (ii) deionized water, (iii) chlorinated tap water. The most critical resin was selected for a second set of experiments designed with the Design of Experiments (DoE) method, in order to build a BPA release model as a function of two water characteristics that were varied in a realistic range: (i) chlorine concentration, from 0 to 0.4 $mgCl_2\ L^{-1}$, (ii) water stability, described by the aggressivity index varying from 11.5 to 13.5. The calibrated release model was positively validated based on literature data. Then, to evaluate the fate of BPA in the DWDN, the validated BPA release model was combined with the hydraulic model of a highly urbanized area where two epoxy resins are installed, through EPANET MSX software. A field monitoring campaign was also designed in the same area of the DWDN to measure BPA concentrations in locations nearby pipelines renovated with epoxy resins. The model was successfully validated on full-scale monitoring data, demonstrating the occurrence of BPA leaching and the potential risk for consumers, especially if appropriate re-opening procedures are not adopted.

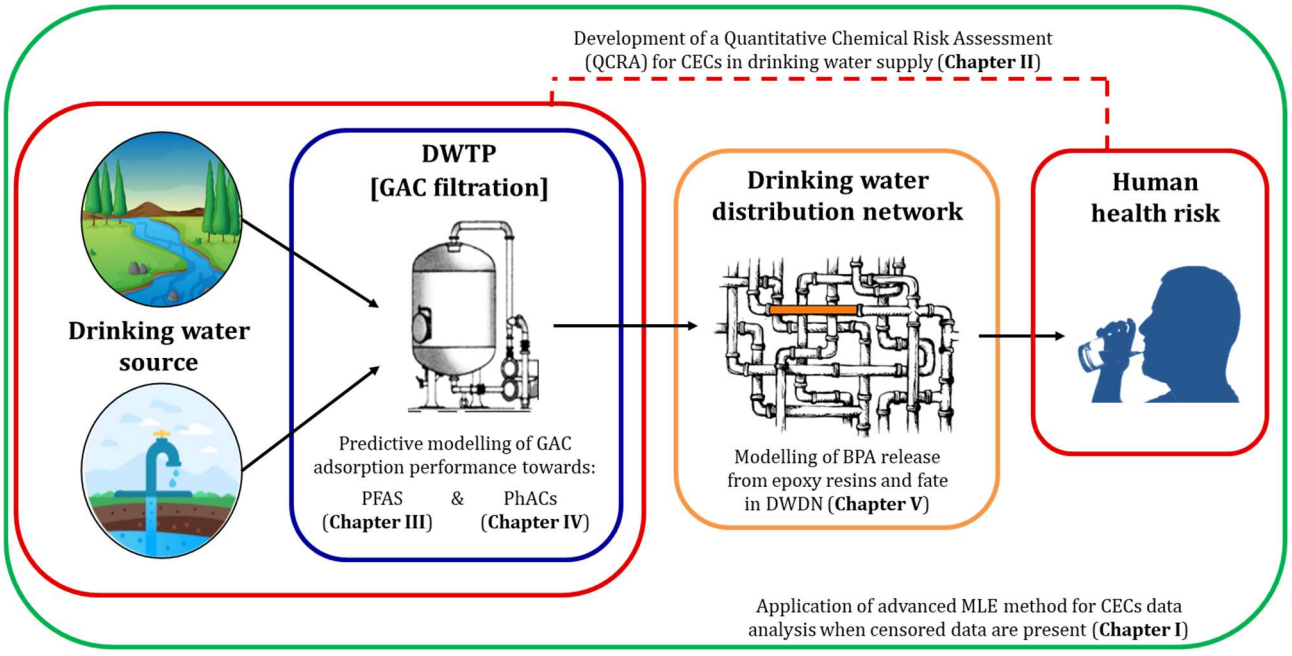

Figure 1. Schematic overview of the thesis chapters and their focus on each part of the drinking water supply system.

CHAPTER 1

A statistical assessment of micropollutants occurrence, time trend, fate and human health risk using left-censored water quality data

Abstract: In recent years, the presence of micropollutants in drinking water has become an issue of growing global concern. Due to their low concentrations, monitoring databases are usually rich in censored data (e.g. samples with concentrations reported below the limit of quantification, LOQ) which are typically eliminated or replaced with a value arbitrarily chosen between 0 and LOQ. These conventional methods have some limitations and can lead to erroneous conclusions on: presence of micropollutants in the source water, treatment efficiencies, produced water quality and associated human health risk. In this work, an advanced approach, based on Maximum Likelihood Estimation method for left-censored data (MLE_{LC}), was applied on monitoring data of 19 contaminants (metals, volatile organic compounds, pesticides and perfluorinated compounds) in 5,362 groundwater (GW) and 12,344 drinking water (DW) samples, collected from 2012 to 2017 in 28 drinking water treatment plants in an urbanized area. This study demonstrates the benefits of MLE_{LC} method, especially for high percentages of censored data. Data are used to build statistical distributions which can be effectively used for several applications, such as the time trend evaluation of GW micropollutant concentrations and the estimation of treatment removal efficiency, highlighting the adequacy or the need for an upgrade. Moreover, the MLE_{LC} method has been applied to assess the human health risk associated with micropollutants, indicating the high discrepancy in the estimations obtained with conventional methods, whose results do not follow precautionary or sustainability criteria.

Keywords: Censored data monitoring; Drinking water supply; Probabilistic risk assessment; Stochastic methods.

The research work presented in this chapter was carried out with the valuable support of Prof. Ilenia Epifani (Department of Mathematics, Politecnico di Milano) and Riccardo Delli Compagni (Department of civil and environmental engineering, Politecnico di Milano).

This chapter has been published in "Chemosphere[1]".

[1] Cantoni B., Delli Compagni R., Turolla A., Epifani I., & Antonelli M. (2020). A statistical assessment of micropollutants occurrence, time trend, fate and human health risk using left-censored water quality data. Chemosphere, 257, 127095. https://doi.org/10.1016/j.chemosphere.2020.127095

List of symbols and abbreviations

DW	Drinking Water
DWTP	Drinking Water Treatment Plant
GW	Groundwater
LOQ	Limits of quantification
MLE_{LC}	Maximum Likelihood Estimation method for left-censored data
PFAS	Perfluoroalkyl substances
THMs	Trihalomethanes
VOC	Volatile Organic Chemicals
WHO	World Health Organization

1. Introduction

Water utilities have a large quantity of water quality monitoring data, collected at several locations along drinking water supply systems, from the source to the tap, for conventional and emerging contaminants which are inserted in the revision of the drinking water European Directive 98/83/EC (The European Parlament and the Council of the European Union, 2018). Besides, the growing adoption of online monitoring devices leads to a dramatic increase of available databases. The analysis of the resulting databases is crucial to define the status of drinking water (DW) source quality, its trend over time, the effectiveness of drinking water treatment plants (DWTPs) towards specific contaminants and the related human health risk. However, the direct use of monitoring data in this analysis is undermined by uncertainty, since water quality databases have high percentages of left-censored data, that are values lower than the limit of quantification (LOQ) of the adopted analytical methods, for which a value cannot be quantified by the instrument and, thus, are present in the database as "< LOQ" (Baccarelli et al., 2005). When practitioners deal with censored datasets, where the piece of information hidden in censored data is missed, they should adopt the most effective method to elaborate data, to approach the most accurate answer, assuring an adequate safety factor in the elaboration outputs, for an optimized design and management of drinking water treatment systems.

Conventionally, censored data are treated through their elimination or substitution with specific values, arbitrarily selected in the range between zero and LOQ (typically, zero, half the LOQ or the LOQ). However, these methods lead to neglect, in case of elimination, or modify, in case of substitution, the information coming from the original dataset (Tekindal et al., 2017). In fact, several previous research studies have shown that these conventional methods generate poor estimates of statistics, and commonly hides patterns and trends in the data. Water utility operators or decision makers using censored data elimination or substitution may conclude that significant differences, correlations, and regression relationships do not exist, when in fact they do, and vice versa. To overcome this constrain, several researchers have proposed the application of an advanced Maximum Likelihood Estimation for left-censored data (MLE_{LC}) which is a parametric technique, based on the principles of the survival analysis, relying on knowledge of the statistical distribution underlying the data (Gilliom and Helsel, 1986). In this method, the uncensored data, the censoring limit and the percentage of censored ones are used to estimate the parameters which lead to the best fit of the distribution to the data (Antweiler and Taylor, 2008). Therefore, with this method the information coming from the censored data is also included and the estimated distribution is descriptive of the complete dataset (Gilliom and Helsel, 1986). Previous works compared the precision of conventional (elimination and substitution) and MLE_{LC} methods in computing summary statistics (mean, standard deviation, median, and interquartile range) of computer-generated censored datasets (Gilliom and Helsel, 1986; Helsel, 2006; Hewett and Ganser, 2007; She, 1997; Shoari et al., 2016) or actual water concentration data of nutrients (Helsel, 1986), metals (Antweiler, 2015), viruses (Canales et al., 2018) and pesticides (Chen et al., 2013). These studies

highlighted the better performance of the MLE_{LC} method in estimating concentrations summary statistics compared to the conventional ones, especially for high percentages of censored data (Antweiler, 2015). In recent years, few studies have applied the MLE_{LC} method in the analysis of contaminants time trend, estimation of removal efficiency or for risk assessment related to micropollutants in aquatic systems, but without comparing the results to the ones that could be obtained with conventional methods (Kleywegt et al., 2011; Rodríguez-Gil et al., 2018; Wang et al., 2016). Only Hansen et al. (2015) (Hansen et al., 2015) compared the MLE_{LC} and the elimination method on time trend estimation of the concentrations of two herbicides in groundwater: the two methods led to different conclusions in the time trend of bentazone, while they both demonstrated the increasing trend of glyphosate concentration. Therefore, no clear general conclusions can be drawn from (Hansen et al., 2015) about the comparability of results obtained with the two methods. This could be due to the limited number of available datasets, additionally characterized by similar features, in terms of number of data (12˙316 for bentazone and 9˙446 for glyphosate), censored percentage (97.2% for bentazone and 98.8% for glyphosate) and amplitude of the concentration data range (for both the compounds, median concentrations over the years was at maximum 10 times higher than the LOQ).
To the best of authors' knowledge, there are no research studies comparing the results obtained by all conventional and MLE_{LC} methods in the following applications: (i) analysis of contaminants time trend, (ii) estimation of the treatment removal efficiency and (iii) risk assessment related to micropollutants in drinking water. Since these three analyses are fundamental to predict the future quality of the source water and to define intervention scenarios for risk preventive control, it is crucial to evaluate the performances of all the methods in these applications and compare them in order to support the choice of the most effective method to be used (MLE_{LC} or conventional ones) in data processing. Thus, this study presents the differences in the results obtained by all the competing methods in those three applications and provides a guideline to select the data elaboration method to be preferred. The choice is based on the comparison of the estimation errors of the methods, as a function of the percentage of censored data and the amplitude of concentration data range. This is made possible by the wide range of contaminants, the several DWTPs and the numerous sampling locations (from groundwater to drinking water) considered in this study that result in more than 450 available datasets.

2. Materials and methods

Two sets of water quality databases were derived from routinely monitoring of groundwater (GW) and drinking water (DW) in 28 DWTPs spread in a highly urbanized area. Samples were collected from 2012 to 2018 and were analyzed for all the compounds defining drinking water quality according to European regulations. In this study, only 19 contaminants were considered, among metals, volatile organic compounds (VOCs), including trihalomethanes (THMs), pesticides and perfluoroalkyl substances (PFAS). Each dataset was created collecting separately the concentration data of each of the 19 contaminants in each of the 28 DWTPs, distinguishing between influent (GW) and effluent (DW) of the DWTP. Over the 532 datasets created for GW and DW, 213 GW and 394 DW datasets were eliminated, because of a percentage of censored data higher than 99.0%. The remaining 319 GW and 138 DW datasets were elaborated separately. Each compound was characterized by two censoring levels based on two different criteria: (i) for some contaminants (i.e. chromium and PFAS), samples were analyzed by two analytical methods, with two different LOQs; (ii) for compounds with only one censoring level, a random computer-generated LOQ was generated from a uniform distribution between the analytical LOQ and the maximum detected data. For each contaminant Table 1 reports the available analytical methods LOQs, the number of available datasets corresponding to the DWTPs with censored percentages lower than 99% for which the data analysis was possible, the ranges of samples size and the censoring percentages detected in the different datasets for GW and DW. For PFAS, the available

data from the 28 DWTPs were collected together in order to have one database large enough for the applications and in order to have an idea of occurrence, time trend, fate and risk related to the whole urbanized area.

Table 1. Occurrence of compounds analyzed in GW and DW, with LOQs, number of datasets available, range of number of samples per dataset and range of censored data percentages.

Compound	LOQs (µg/L)	Groundwater			Drinking water		
		# datasets	# samples per data set	Censored percentages (%)	# datasets	# samples per data set	Censored percentages (%)
Chromium VI	1.0; 2.0	17	71 - 224	1.4 - 66.8	14	51 - 120	1.3 - 93.9
Trichloroethylene	0.25	25	63 - 445	1.1 - 66.7	25	221 - 403	1.0 - 96.1
Tetrachloroethylene	0.25	16	90 - 445	0.6 - 29.2	13	290 - 403	0.3 - 85.5
Chloroform	0.25	21	72 - 445	0.6 - 67.8	18	290 - 403	0.3 - 36.7
2,6 dichlorobenzammide	0.1	26	64 - 225	0.8 - 57.1	15	46 - 127	4.8 - 72.9
Atrazine	0.1	25	78 - 227	7.7 - 59.4	9	66 - 126	1.7 - 84.3
Atrazine-desetil	0.1	26	64 - 226	2.5 - 60.4	6	65 - 126	10.8 - 59.5
Bromacil	0.1	17	77 - 211	30 - 88.2	1	81	82.7
Hexazinone	0.1	15	64 - 212	22.4 - 70.4	0	-	-
Metolaclor	0.1	5	129 - 211	36.0 - 54.3	0	-	-
Prometrine	0.1	8	125 - 214	16 - 99.0	0	-	-
Propazine	0.1	18	64 - 212	22.1 - 84.4	0	-	-
Simazine	0.1	18	64 - 224	15.2 - 68.8	1	80	16.3
Terbutilazine	0.1	14	112 - 230	7.5 - 52.6	2	81 - 85	16.5 - 17.3
Terbutilazine-desentil	0.1	25	64 - 230	3.0 - 70.3	3	66 - 126	7.6 - 37.3
3,6 Diclhoropiridazine	0.1	19	102 - 226	0.6 - 61.7	17	70 - 122	1.2 - 82.9
Tris (2-chloroethyl) phosphate	0.1	22	78 - 229	5.2 - 69.2	12	65 - 128	3.6 - 82.6
PFOA	0.002; 0.01	1	92	4.3	1	96	43.8
PFOS	0.002; 0.01	1	92	34.8	1	96	80.2
TOTAL		**319**	**63 - 445**	**0.6 - 99.0**	**138**	**46 - 403**	**0.3 - 96.1**

2.1. Data distribution fitting

For each dataset the two LOQs were used to define a "censored dataset", where concentration data above the higher LOQ are taken as exact data and all the data below the higher LOQ are taken as censored data, and a "reference dataset", where all the data above the lower LOQ are taken as exact. Therefore, data between the two LOQs are considered censored in the "censored dataset" while they are considered exact in the "reference dataset". To deal with censored data, the following methods were applied: (a) elimination of censored data (Elim); replacement methods in which censored data are replaced with (b) zero (Zero), (c) half the LOQ (LOQ/2), (d) the LOQ (LOQ) and (e) MLE_{LC} method. For conventional methods (a-d), in the "censored dataset", censored data were eliminated or replaced according to the higher LOQ. The "censored dataset" was used to estimate data statistical distribution with all conventional and MLE_{LC} methods. For each method, fits to the lognormal, normal, Weibull, gamma and logistic statistical distributions were tested. The data fitting to specific distributions were performed with the `fitdist` function for Elim, Zero, LOQ, LOQ/2 and `fitdistrcens` function for MLE_{LC} in the R `fitdistrplus` package (Delignette-Muller et al., 2010). The model selection was based on the log-likelihood criterion; the method and distribution with the maximum log-likelihood were chosen as the

most appropriate method and the best fitting for the "reference dataset" (Myung, 2004). 95-percent confidence intervals for the distribution parameters and summary statistics were calculated via non-parametric bootstrapping (1000 iterations) with the `bootdiscens` function in the R `fitdistrplus` package (Rodríguez-Gil et al., 2018). To evaluate and compare the goodness of the results provided by each method in time trend, removal efficiency and risk assessment, the fractional error percentage (e) was estimated as follows:

$$e_j\ [\%] = \left[\frac{\theta cens,j - \theta_{ref}}{\theta_{ref}}\right] \cdot 100 \qquad \text{(Eq. 1)}$$

where $\theta_{cens,j}$ is the analysis parameter calculated by method j on the "censored dataset", while θ_{ref} is the analysis parameter calculated on the "reference dataset". The selected parameters for each application are reported in the following sections.

2.2. Time trend in contaminants concentration in GW

Linear time trend of contaminant concentrations in GW was assessed by parametric MLE regression likelihood-ratio test for both conventional and MLE_{LC} methods, using `cenreg` function in the `R NADA` package (Helsel, 2012). Data were assumed to follow the parametric distribution established in the previous step. The assumption on the time trend linearity was based on prior statistical evaluations that showed that more than 96.5% of the analysed datasets were best fitted by linear trends compared to second and third degree polynomial regression models. The time trend was considered significant for p-values < 0.05. Finally, the robustness of the results obtained on the time trend were positively verified by the non-parametric Akritas–Theil–Sen test, using `cenken` function in the `R NADA` package. Each conventional method was compared to the MLE_{LC} one, computing the trend error, i.e. the percentage of cases where the former provides an estimate of the time slope (positive, null or negative) different from the latter. The fractional error percentage et was calculated according to Eq. 1, where θ is fixed to the compound median concentration estimated by the trend over 10 years.

2.3. Treatment removal efficiency estimation

For all conventional and MLE_{LC} methods, the "censored datasets" of each compound were used to estimate the median concentrations in GW and DW, that in turn were used to estimate the median removal efficiency for each contaminant. The "reference dataset" was used to estimate the actual median removal efficiency. The estimates were compared to the actual efficiency through the fractional error percentage (e_η), calculated according to Eq. 1, considering θ equal to the removal efficiencies of the parameters.

2.4. Probabilistic human health risk

The exceedance of the concentration limit set by the drinking water regulation is seen as a hazardous event for citizen health (WHO, 2009). The potential and residual risks were estimated looking at the probability of exceedance of the regulatory limit for each selected compound in GW and DW concentration, respectively. For each method, the exceedance probability was estimated from the "censored dataset" fitted distribution, as the area underlying the probability density curve of the compound for concentrations above the regulatory limit, set in the revision of the drinking water European Directive (The European Parlament and the Council of the European Union, 2018). The different estimates of the exceedance probability were compared to the "reference" one through the fractional error percentage (e_L), calculated as in Eq. 1.

3. Results and discussion

As reported in Table 1, a total of 319 and 138 datasets were analyzed for GW and DW, respectively. This high number of datasets enabled to test conventional and MLE_{LC} methods on a wide variety of concentration ranges and distributions, with dataset numerosity varying from 46 to 445 samples and censoring percentages from 0.3% to 99.0%.

3.1. Evaluation of data distribution fitting

When the goal is the assessment of compounds occurrence in water, their fate and related human health risk, an accurate estimation of the statistical distribution for concentration data is the first crucial step (Leith et al., 2010). In fact, compared to data summary statistics (mean, standard deviation, median, and interquartile range), estimating the distribution allows to incorporate and get the whole information from the data. Therefore, the first step of this study is to understand which method leads to the best fit of the data distribution in presence of censored data. As an example, GW chromium VI concentration in one of the 28 DWTPs is shown in Figure 1: the parametric distribution functions selected as the best estimated by each method are reported, together with the empirical distribution function of the measured data. Table S1, in the supplementary material, reports the log-likelihood values for each method and parametric distribution (the log-likelihood criterion was used for selecting both best distribution and method).

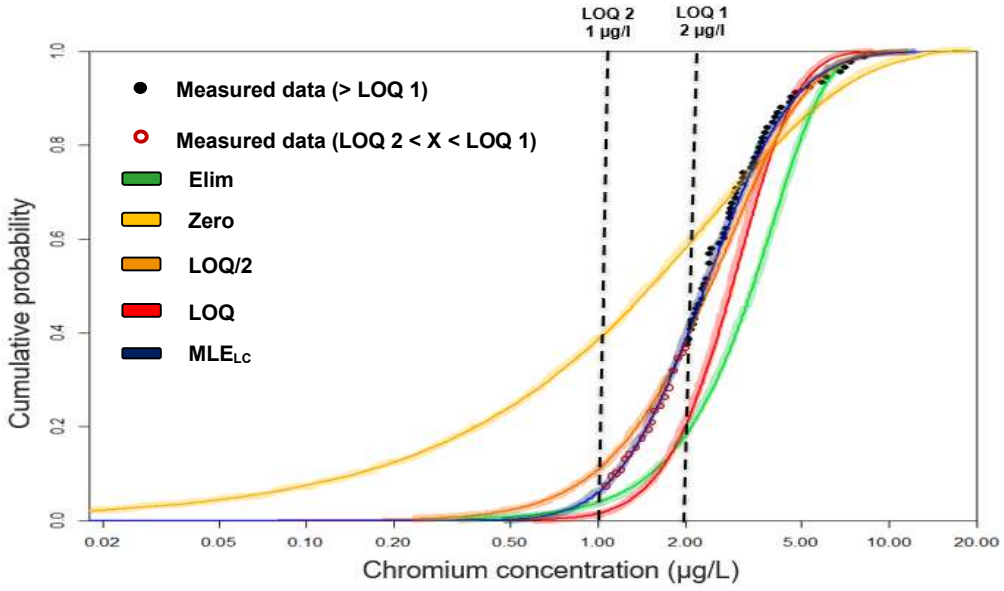

Figure 1. Example of fitting of GW chromium VI concentration data in one of the 28 DWTPs with the parametric distribution functions estimated by each method. "Censored dataset" (black dots) and "uncensored data" (red empty dots) are the results of two different analytical methods LOQs.

As reported in Figure 1 and Table S1, the best method selected in this case is the MLE_{LC} method. In this example, chromium VI GW concentration data were found to follow a lognormal distribution, which in turn was then confirmed by the Anderson-Darling test (p-value=0.23). To analyze the effect of censored data percentages on the goodness of each estimation method, censored percentages were summarized by the corresponding 5^{th}, 10^{th}, 25^{th}, 50^{th}, 75^{th}, 90^{th} and 95^{th} quantiles, that represent the extreme and central cases of the population from a statistical perspective. Table 2 shows the percentage of datasets found to be fitted at best by each method, as a function of the percentage of censored data in the dataset.

Table 2. Percentage of datasets better fitted by each method as a function of the censored percentage in GW and DW datasets. The number of datasets available for each group is reported.

Groundwater							Drinking water						
Censored percentage	**# GW Datasets**	**Elim**	**Zero**	**LOQ/2**	**LOQ**	**MLE_{LC}**	**Censored percentage**	**# DW Datasets**	**Elim**	**Zero**	**LOQ/2**	**LOQ**	**MLE_{LC}**
< 1	16	13	6.3	6.3	6.3	68.5	**< 1**	8	12.5	12.5	0.0	0.0	75.0
1 - 3	17	5.9	5.9	5.9	0.0	82.3	**1 - 3**	9	11.1	0.0	11.1	0.0	77.8
3 - 10	48	4.2	0.0	4.2	0.0	91.6	**3 - 6**	21	9.5	0.0	4.8	0.0	85.7
10 - 15	83	0.0	0.0	2.4	0.0	97.6	**6 - 25**	37	0.0	0.0	2.6	0.0	97.4
15 - 40	80	0.0	0.0	1.3	0.0	98.7	**25 - 60**	34	0.0	0.0	2.9	0.0	97.1
40 - 60	41	0.0	0.0	0.0	0.0	100	**60 - 80**	17	0.0	0.0	0.0	0.0	100
60 - 75	18	0.0	0.0	0.0	0.0	100	**80 - 85**	7	0.0	0.0	0.0	0.0	100
75 - 99	16	0.0	0.0	0.0	0.0	100	**85 -99**	5	0.0	0.0	0.0	0.0	100

It can be stated that, regardless the percentage of censored data, most of the datasets are better fitted by a probability density estimated through the MLE_{LC} method. It is remarkable to note that the Elim method displays better results than the substitution methods (Zero, LOQ/2, LOQ), which appear to be inadequate for any value of the percentage of censored data. The percentage of datasets better fitted by the MLE_{LC} method increases with the percentage of the censored data. For censored percentages higher than 40% and 60%, the MLE_{LC} method is preferred over all the others, for all the analyzed GW and DW datasets, respectively. This observation is particularly worth when dealing with emerging contaminants or high-efficiency treatments, both characterized by a high number of data below the LOQ, which reduces the number of exact data, undermining the general validity of the related elaborations. The adoption of the MLE_{LC} method helps to overcome this constrain.
As for the probabilistic distribution of the compounds in GW and DW, 67.5% of the compounds datasets are well fitted with the lognormal distribution, followed by the Weibull (17.7%) and normal (4.5%) distributions.

3.2. Time trend estimation of GW compounds concentrations

Predicting the future quality of the water supply source is fundamental for estimating the related potential risk and the requested interventions to minimize the residual health risk for citizens (Ferrier et al., 2001). To achieve this goal, the estimation of the time trend of contaminants concentration in GW is an important aspect (Hansen et al., 2015). For this reason, to compare each method predictions of the future quality of GW, we used the compounds concentration, the time trend slope and the median concentration predicted to occur in 10 years. A 10-year interval is the usual time-frame given by European regulations in case of reduction of a contaminant limit, as for chromium VI and lead in the revision of the drinking water European Directive 98/83/EC (The European Parlament and the Council of the European Union, 2018). Since the MLE_{LC} method has been demonstrated to be accurate in estimating the data distribution for the analyzed datasets and several literature studies stressed that conventional methods lead to biased estimations of compounds time trends (Helsel, 2011; Hansen et al., 2015; Wang et al., 2016), it was interesting to compare the conventional methods results to the ones obtained by the MLE_{LC} method, using the parametric MLE regression likelihood-ratio test as reference. In fact, this comparison can highlight the extent of the estimation error, quantifying the bias associated to conventional methods, which could lead to misleading outputs. Table 3 reports the comparison between the conventional and the MLE_{LC} methods in the time trend analysis, as a function of the censored data censored percentage.

Table 3. Comparison of conventional and MLE_{LC} methods in the estimated time trend of contaminants concentration in GW and ranges of fractional error percentage (e_t).

Censored Percentage	Elim		Zero		LOQ/2		LOQ	
	Trend error	e_t	Trend error	e_t	Trend error	e_t	Trend error	e_t
[%]	[%]	[%]	[%]	[%]	[%]	[%]	[%]	[%]
< 1	16.3	[-3.6 ÷ 34.2]	25.7	[-4.5 ÷ -2.1]	8.8	[-1.5 ÷ 2.6]	26.1	[0.6 ÷ 3.2]
1 - 3	46.2	[1.6 ÷ 36.8]	21.2	[-6.5 ÷ -2.7]	13.2	[-3.5 ÷ 4.8]	22.4	[1.6 ÷ 3.9]
3 - 10	56.3	[6.2 ÷ 38.5]	33.3	[-7.2 ÷ -3.1]	14.0	[-4.5 ÷ 4.1]	23.2	[2.8 ÷ 5.2]
10 - 15	56.8	[10.1 ÷ 39.5]	37.1	[-6.8 ÷ -3.2]	33.3	[-3.1 ÷ 5.2]	36.8	[4.0 ÷ 5.7]
15 - 40	100.0	[15.7 ÷ 31.3]	27.5	[-9.4 ÷ -6.5]	37.5	[-9.0 ÷ 7.5]	30.6	[5.7 ÷ 9.1]
40 - 60	50.0	[29.3 ÷ 75.3]	40.3	[-10.9 ÷ -5.3]	0.0	[-3.9 ÷ 8.5]	47.9	[6.2 ÷ 10.3]
60 - 75	20.0	[43.3 ÷ 65.4]	29.7	[-12.2 ÷ -10.1]	0.0	[-10.0 ÷ 9.1]	31.2	[5.3 ÷ 13.4]
75 - 99	100.0	[75.2 ÷ 82.2]	35.1	[-14.3 ÷ -10.3]	25.0	[-12.8 ÷ 10.8]	37.0	[8.6 ÷ 15.2]

Looking at the trend errors, it can be noticed that the estimated time trend provided by the Elim method results in a higher probability of erroneous conclusions (from 16.3% to 100% of the cases) compared to the one obtained by substitution methods (from 0% to 47.9% of the cases). Elim method highly overestimates the median concentration expected in 10 years, as can be noticed by the high (until 82.2%) fractional error percentages (e_t). Figure 2 shows an example of wrong estimation of the time trend in 3,6-dichloropiridazine concentration in GW in one DWTP. It can be observed that, the Elim method estimates a decreasing time trend of 3,6-dichloropiridazine in GW, whereas the MLE_{LC} method estimates that the actual time trend of this pesticide in GW is stable. Therefore, in this case, applying the Elim method, an improvement in the 3,6-dichloropiridazine concentration in GW would be expected and, it can be concluded that there is no need for further specific management or upgrade actions on the treatment processes for this specific contaminant. On the other hand, applying the MLE_{LC} method, a stable concentration is estimated, implying the need for keeping under control the performance of the current treatments.

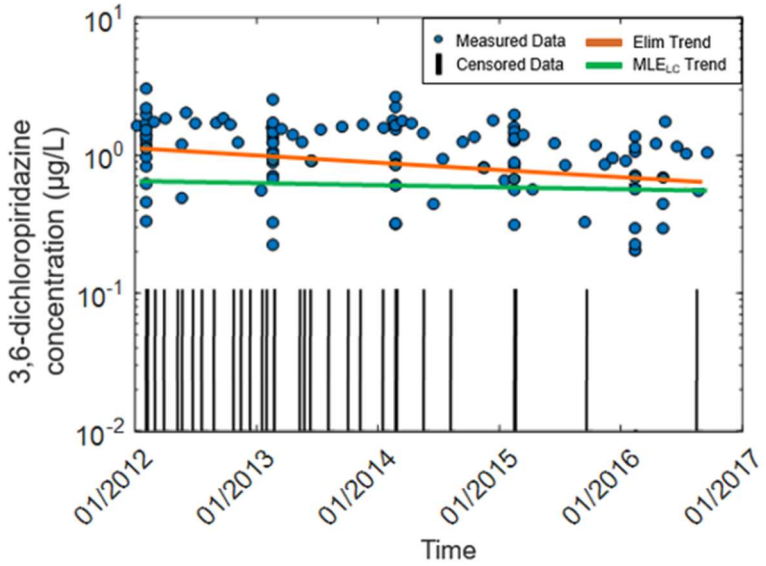

Figure 2. Example of estimate of the time trend of 3,6-dichloropiridazine in GW obtained through Elim and MLE_{LC} methods.

Looking at the substitution methods, they result in a limited error in the prevision of the compounds median concentration over 10 years: the Zero method leads to a maximum underestimate of 14.3%, the overestimate under the LOQ method achieves 15.2%, while the LOQ/2 absolute fractional error is never higher than 13.0%. In particular, the use of substitution methods for time trend analysis of datasets with censored percentages lower than 40% provides acceptable estimates of the future median concentration (fractional error always lower than 10%).

3.3. Estimated compounds removal in the DWTPs

The DWTPs differ for the treatment processes adopted for micropollutant removal, namely granular activated carbon (GAC) adsorption, air-stripping and reverse osmosis (RO). The value of the median removal efficiency, estimated by the median GW and DW concentrations, is useful to understand the performance of the removal process, providing useful inputs for an optimization analysis. The median removal efficiency was estimated with all the methods on each "censored" dataset and compared with the median removal efficiency evaluated on the "reference" one. Table S2 shows, for each method, the percentage of datasets for which each method was the best in estimating the median removal efficiency and the average absolute value of the fractional error percentage (e_η) as a function of the censored percentage. MLE_{LC} turns out to be the best method to estimate the median removal efficiency in most of the cases, regardless the censored data percentage. Increasing the percentage of censored data, the cases for which the MLE_{LC} method provides the best estimate rise from 66.7%, for censored percentages below 5%, to 93.8%, for censored percentages above 80%. Moreover, the average absolute value of the fractional error percentage (e_η) is always lower for the MLE_{LC} method (from 5.8 to 13.4) compared to the others (from 18.4 to 923.8). Furthermore, it was evaluated how the removal efficiency prediction is affected by the amplitude of the concentration range of each dataset. In particular, the distance between the censored data and the maximum level reached by the uncensored data was estimated as the ratio between the LOQ and the 95th empirical quantile ($R_{LOQ\text{-}95th}$). Figure 3 reports a contour plot of the fractional error percentages for the estimated removal efficiency (e_η) as a function of both the percentage of the censored data and the above defined ratio, $R_{LOQ\text{-}95th}$, for all the methods.

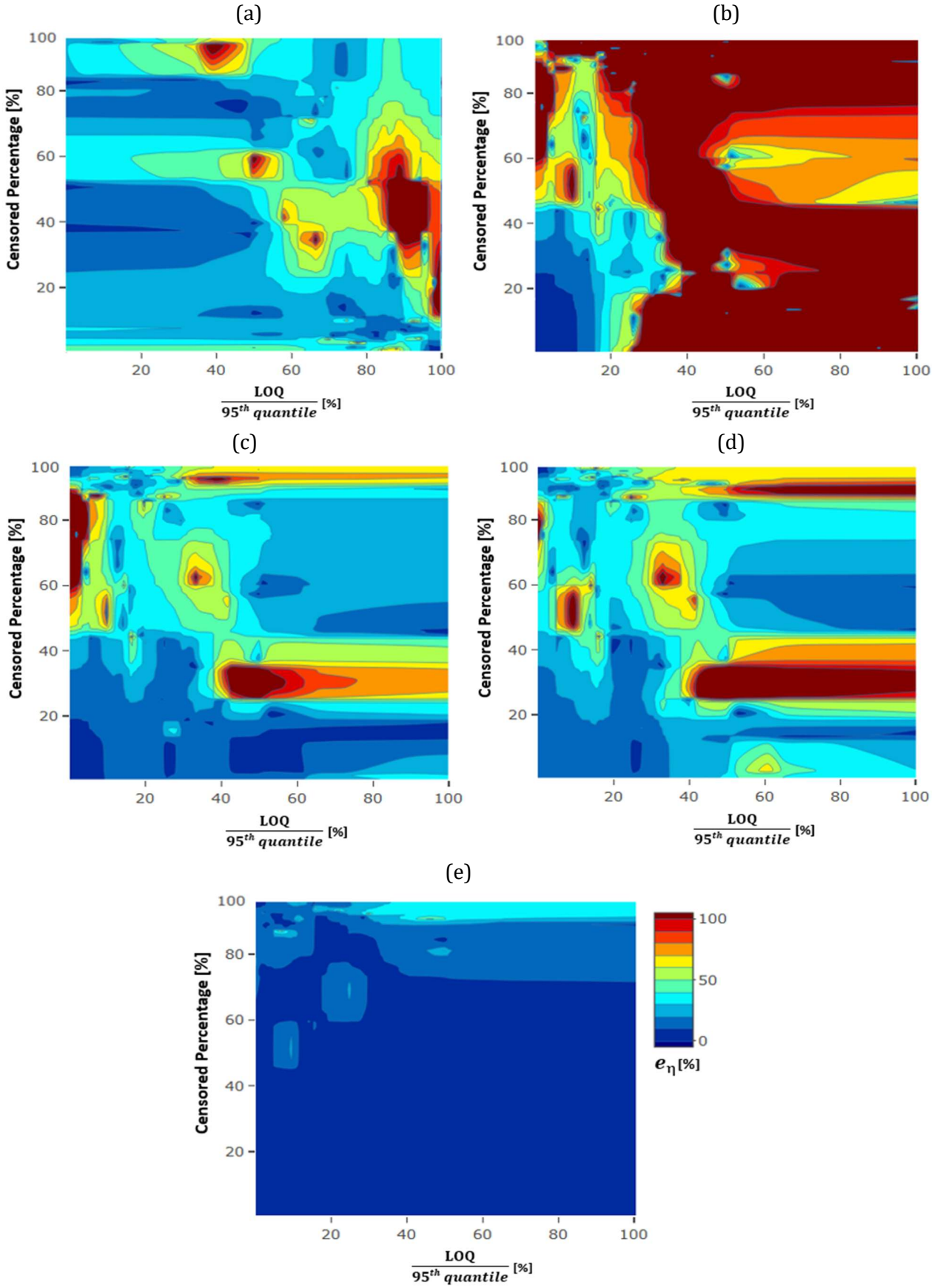

Figure 3. Contour plot of the fractional error percentages for estimated removal efficiency (e_η) as a function of the percentage of censored data and the ratio $R_{LOQ\text{-}95th}$ for (a) Elim, (b) Zero, (c) LOQ/2, (d) LOQ, (e) MLE_{LC} methods.

The e_η contour plots provide a clear indication of the goodness of the adopted data elaboration method, being the red color an indicator of high errors. The worst method for removal efficiency estimation is the Zero method, with an under- or overestimation of the removal efficiency of more than 50% of the "reference" estimation in almost all the datasets. However, it shows a good estimation (fractional error below 10%) of the removal efficiency for the cases with censored percentage below 20% and high data range amplitude (with LOQ below 10% of the 95th quantile). The estimated errors, under Elim, LOQ/2 and LOQ methods, range from around 10% to more than 100%, as a function of the percentage of the censored data and concentration range amplitude; it is better for low censored percentages and low LOQ values compared to the 95th quantile. Therefore, these methods can provide good estimates for conventional contaminants with a considerable contamination, compared to the analytical method sensitivity. However, they are not accurate in estimating removal efficiencies for micropollutants or emerging contaminants, that are characterized by high censored percentages, low concentrations and high LOQs. Finally, the MLE_{LC} method is the best in estimating the median removal efficiency of a DWTP towards micropollutants: the fractional errors are always lower than 10% for censored percentage below 75%, it increases to 20% for censored percentage from 75% to 90%. Such low estimation errors underline that the MLELC method, not only is better than the conventional ones in estimating the pollutants removal efficiency, but also that provides accurate estimations in this application even for datasets characterized by censored percentages until 90%. For higher censoring percentages the fractional error depends on the amplitude of concentration data range: it reaches 40% in cases of LOQ higher than 30% of the 95th quantile.

Analyzing micropollutants fate through a DW treatment train, it is important not only to estimate the median removal efficiencies, but also to look at the probability distribution of the compound concentration along the treatment train. An application of all conventional and MLE_{LC} methods to the evaluation of compounds fate during treatment is reported in Figure 4 with the cumulative distributions for PFOA concentration data collected in several points throughout the DWTPs trains where only GAC is present.

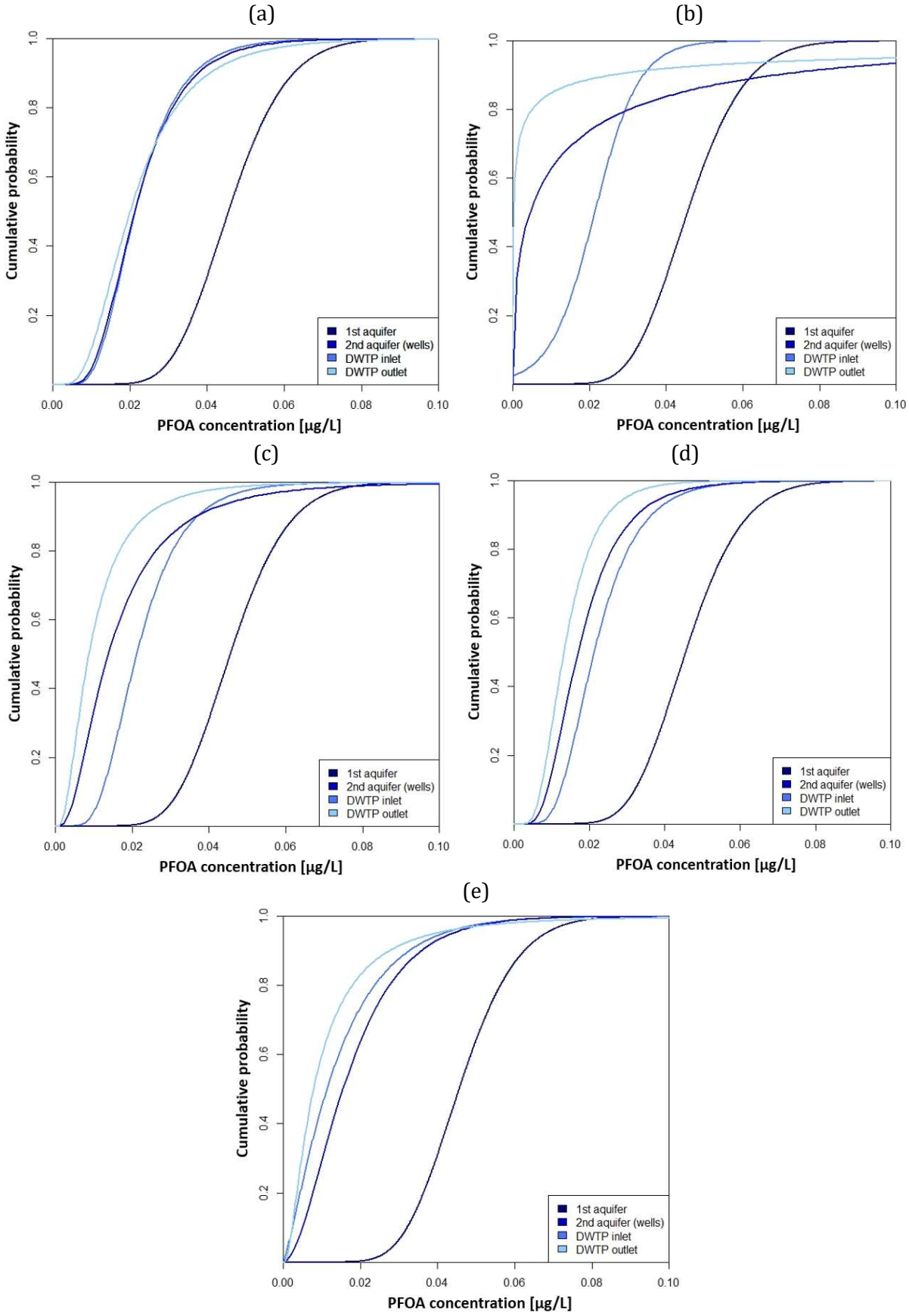

Figure 4. Example of fitting of PFOA concentration data throughout the treatment train of DWTPs constituted by GAC process with the parametric distribution functions estimated by the (a) Elim, (b) Zero, (c) LOQ/2, (d) LOQ, (e) MLE_{LC} methods.

This tool can be useful to support decisions on the DW source to be preferred, and to optimize and upgrade the current DWTP process design and management. However, comparing the graphs in Figure 4, it is important to notice that the choice of the method to handle censored data affects the estimated concentration data distributions and, as a consequence, the optimization strategies. In this case study, the GW is extracted from the second aquifer through multiple wells, feeding the DWTP. Therefore, it is important to optimize the combination of flowrates extracted by each well in order to feed GW at low contaminants concentration. Looking at Figure 4, it is possible to compare PFOA concentration distribution in the single wells in the second aquifer and at the inlet to the DWTPs, to verify the correct management of the extraction wells. Applying the MLE_{LC} method, it is possible to notice a reduction in PFOA concentration from the single wells to the DWTP inlet. This means that the combination of wells currently used to extract GW is correctly managed to extract higher flowrates from wells less contaminated by PFOA. Applying the conventional methods, the conclusion would have been different. In particular, no significant reduction in PFOA concentration would have been noticed with the Elim method, while applying the substitution methods, a worsening in PFOA concentration from the wells to the DWTP inlet would have been identified. Therefore, possible interventions would have been applied to improve the management of the extraction wells that, instead, is currently well designed, as demonstrated by the MLE_{LC} method. Moreover, it is possible to verify the GAC efficiency towards PFOA, comparing the concentration distributions at the DWTP inlet and outlet. While the application of the Elim method results in no significant GAC removal of PFOA instead, both the substitution and the MLE_{LC} methods observe a reduction in PFOA concentration from the inlet to the outlet, highlighting the GAC efficacy towards this compound. However, all substitution methods overestimate GAC removal efficiency towards PFOA. In particular, the median removal efficiency estimated by the MLE_{LC} method as 31.3% is overestimated by the LOQ (37.8%), LOQ/2 (58.7%) and Zero (98.9%) methods.

3.4. Probabilistic health risk assessment

In recent years, World Health Organization (WHO) promoted the adoption of a health risk-based approach to achieve an integrated preventive management and to control the hazardous events through the whole DW supply chain (WHO, 2011). Therefore, the application of a quantitative health risk assessment on monitoring data collected in the whole DW supply chain is crucial. Assessing the health potential risk due to a residual contaminant in water asks for the estimation of the probability of exceeding the regulatory limit (WHO, 2009). When looking at the source water (GW), the extent of the probability of exceedance defines the need for a specific treatment and the requested removal efficiency to reduce the risk to an acceptable value; if the focus is the produced drinking water, the probability of exceedance can address optimization actions in the normally management of the DWTP. Therefore, both an underestimation or an overestimation of the exceedance probability could have important drawbacks in terms of underestimation of the risk or overestimation of the intervention needed, and the related costs, to minimize the risk. The exceedance probability was estimated by all the methods on each dataset and compared to the "reference" one by the fractional error percentage (e_L). The evaluation of the exceedance probability of the chromium VI concentration in GW, used as source water for one of the DWTPs, according to conventional and MLE_{LC} methods, is reported in Figure 5, as an example.

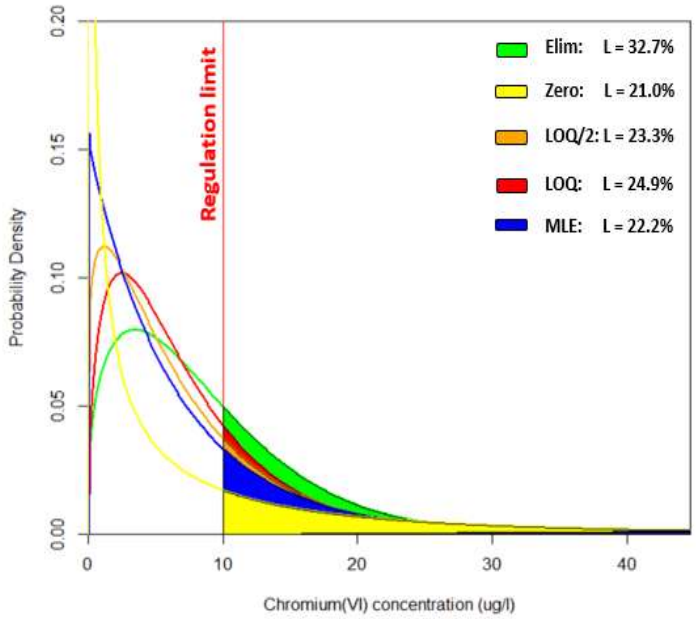

Figure 5. Example of GW chromium VI concentration exceedance probability for one of the 28 DWTPs with the parametric distribution functions estimated by Elim, Zero, LOQ/2, LOQ, MLE_{LC} methods. The limit considered in the analysis is defined in the proposed revision (DM 14 November 2016) of the Italian legislation for drinking water quality (D. Lgs. 31/2001).

One can notice how the differences in probability densities estimation result in discrepancies in the health risk assessment: the MLE_{LC} method exceedance probability (22.2%) is underestimated by the Zero method (21.0%) and overestimated by the Elim (32.7%), LOQ (23.3%) and LOQ/2 (24.9%) methods. These results have in turn a significant implication on the design and management of the DWTPs. In fact, using the Zero method, the potential risk due to chromium VI occurrence in GW would be underestimated and, consequently, this could result in designing an inadequate treatment or monitoring plan. On the other side, using the other conventional methods would overestimate the potential health risk, consequently leading to an oversizing of the needed interventions and related capital and operating costs. Table S3 reports for each method the percentage of datasets for which that method was the best in estimating the exceedance probability and the average absolute value of e_L as a function of the percentage of censored data. It turns out that MLE_{LC} is the best method to estimate the exceedance probability in most of the cases, regardless the dataset censored percentage. In particular, in 78.9% of the cases with censored percentages below 5% the MLE_{LC} method provides the best estimate, rising to 100% of the cases for dataset censored percentages above 60%. This is of particular interest for emerging contaminants, often characterized by high censored percentages but with severe effects on human health also at very low concentrations. An accurate estimation of their risk is necessary to correctly plan the upgrading interventions of the current treatment processes in order to meet the new regulatory limits proposed worldwide for emerging contaminants. Moreover, the average absolute value of the fractional error percentage (e_L) is always lower for the MLE_{LC} method (from 0.6 to 38.4) compared to the conventional ones (from 29.9 to 346.4). Furthermore, it was evaluated if the amplitude of the concentration range of the dataset affects the performance of the exceedance probability prediction. In Figure 6, a contour plot for e_L is reported as a function of both the percentage of the censored data and the ratio $R_{LOQ\text{-}95th}$, for the various methods.

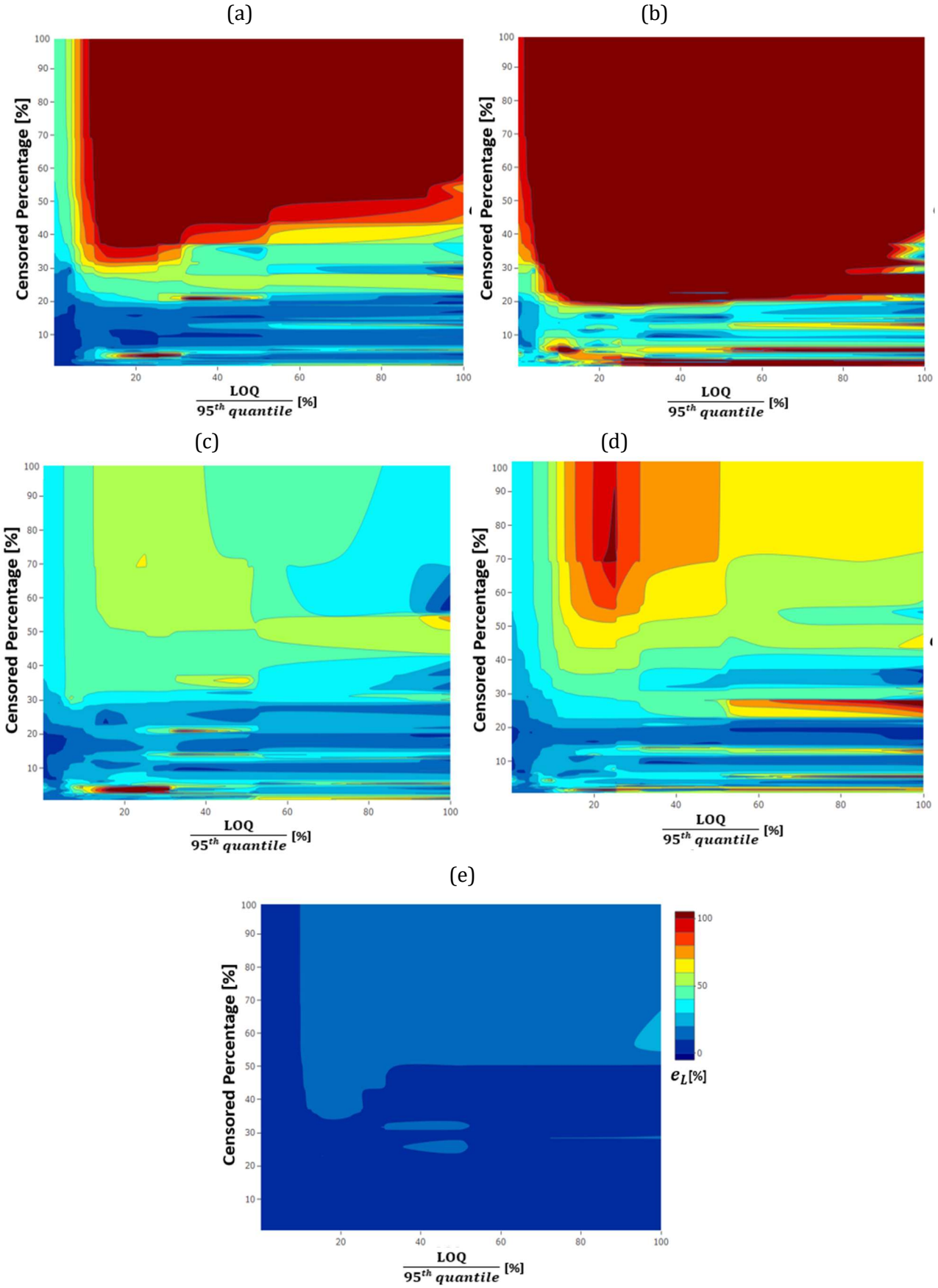

Figure 6. Contour plot for the fractional error percentages for exceedance limit estimation (e_L) as a function of the percentage of censored data and the ratio $R_{LOQ\text{-}95th}$ for (a) Elim, (b) Zero, (c) LOQ/2, (d) LOQ, (e) MLE_{LC} methods.

Once again, the MLE_{LC} method appears to be accurate and better than the conventional ones in estimating micropollutant concentration limit exceedance with fractional errors always lower than 30%: it is lower than 10% for percentages of censored data lower than 37%, and for LOQ below 10% of the 95th quantile. Again, the substitution with zero turns out to be the worst method, with an under- or overestimation of the limit exceedance of more than 100% with respect to the "reference" estimate, in almost all the datasets with percentages of censored data over 20%. The Elim method results in an estimated error below 10% for low censored percentages (below 15%) and wide concentration ranges (with the LOQ below 5% of the data 95th quantile). The Elim fractional error is over 100% for all the cases with more than 50% of censored data and LOQ higher than 10% of the 95th quantile. The estimated error of LOQ/2 and LOQ methods ranges from 10% to more than 100% as a function of the percentage of censored data and the concentration range amplitude, with better performance of LOQ/2 method in almost all the cases. Regardless the method applied, the fractional error rises with increasing censored percentage and LOQ/95th quantile ratio.

4. Conclusions

The application of conventional (elimination and substitution) and MLE_{LC} methods to a wide variety of datasets of monitoring data of micropollutants in water demonstrated that, in the presence of left-censored data, the estimation of the concentration distribution function is affected by the method applied to handle censored data. In particular, the advanced MLE_{LC} method provides a more accurate probability density estimation, compared to the conventional ones. As a consequence, it provides consistenly better results (with fractional error in most cases lower than 10% and rarely above 30%) in the application to typical water quality analyses such as source water concentrations time trend, treatment removal efficiency towards micropollutants and health risk assessment generated by the exceedance of the regulatory limit. In particular, for the estimation of the concentration time trend, it is suggested to use parametric MLE regression likelihood-ratio test, especially for high censored data percentages (higher than 40%). Elim method should be avoided since it results in a systematic overestimation of the compounds median concentration expected over 10 years, with high (from 9.6% to 82.2%) fractional error (e_t). In treatment removal efficiency and health risk estimations, the MLE_{LC} method has to be preferred, while among the conventional methods the best is the LOQ/2 method. In case of treatment removal efficiency analysis, the estimated errors under conventional methods, ranging from below 10% to above 100%, worsen at censored percentages higher than 20% and for LOQ/95th quantile ratio higher than 10%. Therefore, the analytical methods should be improved in order to reduce the instrumental LOQ at levels lower than 10% of the concentration measured 95th quantile, simultaneously reducing the censored percentages. Finally, conventional methods can lead to erroneous conclusions, highly under- or overestimating the health risk due to exceedance of regulatory limit. Therefore, applying conventional methods can have important implications, in case of needed intervention plans, leading to potentially not precautionary or unsustainable criteria.

References

Antweiler, R.C., 2015. Evaluation of Statistical Treatments of Left-Censored Environmental Data Using Coincident Uncensored Data Sets. II. Group Comparisons. Environ. Sci. Technol. 49, 13439–13446. https://doi.org/10.1021/acs.est.5b02385

Antweiler, R.C., Taylor, H., 2008. Evaluation of Statistical Treatments of Left-Censored Environmental Data using Coincident Uncensored Data Sets : I . Summary Statistics. Environ. Sci. Technol. 42, 3732–3738. https://doi.org/10.1021/es071301c

Baccarelli, A., Pfeiffer, R., Consonni, D., Pesatori, A.C., Bonzini, M., Patterson, D.G., Bertazzi, P.A., Landi,

M.T., 2005. Handling of dioxin measurement data in the presence of non-detectable values: Overview of available methods and their application in the Seveso chloracne study. Chemosphere 60, 898–906. https://doi.org/10.1016/j.chemosphere.2005.01.055

Canales, R.A., Wilson, A.M., Pearce-Walker, J.I., Verhougstraete, M.P., Reynolds, K.A., 2018. Methods for handling left-censored data in quantitative microbial risk assessment. Appl. Environ. Microbiol. 84, 1–10. https://doi.org/10.1128/AEM.01203-18

Chen, H., Quandt, S.A., Grzywacz, J.G., Arcury, T.A., 2013. A Bayesian multiple imputation method for handling longitudinal pesticide data with values below the limit of detection. Environmetrics 24, 132–142. https://doi.org/10.1002/env.2193

Delignette-Muller, M.-L., Dutang, C., Pouillot, R., Denis, J.-B., Siberchicot, A., 2010. Package ' fitdistrplus ': Help to Fit of a Parametric Distribution to Non-Censored or Censored Data Version, Journal of Statistical Software, 64(4), 1-34.

Ferrier, R.C., Edwards, A.C., Hirst, D., Littlewood, I.G., Watts, C.D., Morris, R., 2001. Water quality of Scottish rivers: spatial and temporal trends. Sci. Total Environ. 265, 327–342. https://doi.org/10.1016/S0048-9697(00)00674-4

Gilliom, R.J., Helsel, D.R., 1986. Censored Trace Level Water Quality Data 1 . Estimation Techniques. Water Resour. Res. 22, 135–146. https://doi.org/10.1029/WR022i002p00135.

Hansen, C.T., Ritz, C., Gerhard, D., Jensen, J.E., Streibig, J.C., 2015. Re-evaluation of groundwater monitoring data for glyphosate and bentazone by taking detection limits into account. Sci. Total Environ. 536, 68–71. https://doi.org/10.1016/j.scitotenv.2015.07.047

Helsel, D.R., 2012. Statistics for Censored Environmental Data using Minitab and R (Volume 77), John Wiley & Sons. (2011).

Helsel, D.R., 2006. Fabricating data: How substituting values for nondetects can ruin results, and what can be done about it. Chemosphere 65, 2434–2439. https://doi.org/10.1016/j.chemosphere.2006.04.051

Helsel, D.R., 1986. Estimation of distributional parameters for censored water quality data. Dev. Water Sci. 27, 137–157. https://doi.org/10.1016/S0167-5648(08)70789-5

Hewett, P., Ganser, G.H., 2007. A comparison of several methods for analyzing censored data. Ann. Occup. Hyg. 51, 611–632. https://doi.org/10.1093/annhyg/mem045

Kleywegt, S., Pileggi, V., Yang, P., Hao, C., Zhao, X., Rocks, C., Thach, S., Cheung, P., Whitehead, B., 2011. Pharmaceuticals, hormones and bisphenol A in untreated source and finished drinking water in Ontario, Canada - Occurrence and treatment efficiency. Sci. Total Environ. 409, 1481–1488. https://doi.org/10.1016/j.scitotenv.2011.01.010

Leith, K.F., Bowerman, W.W., Wierda, M.R., Best, D.A., Grubb, T.G., Sikarske, J.G., 2010. A comparison of techniques for assessing central tendency in left-censored data using PCB and p,p′DDE contaminant concentrations from Michigan's Bald Eagle Biosentinel Program. Chemosphere 80, 7–12. https://doi.org/10.1016/j.chemosphere.2010.03.056

Myung, I.J., 2004. Computational Approaches to Model Evaluation. Int. Encycl. Soc. Behav. Sci. 339, 2453–2457. https://doi.org/10.1016/b0-08-043076-7/00589-1

Rodríguez-Gil, J.L., Cáceres, N., Dafouz, R., Valcárcel, Y., 2018. Caffeine and paraxanthine in aquatic systems: Global exposure distributions and probabilistic risk assessment. Sci. Total Environ. 612, 1058–1071. https://doi.org/10.1016/j.scitotenv.2017.08.066

She, N., 1997. Analyzing censored water quality data. J. Am. Water Resour. Assoc. 33, 615–624. https://doi.org/10.1111/j.1752-1688.1997.tb03536.x

Shoari, N., Dubé, J.S., Chenouri, S., 2016. On the use of the substitution method in left-censored environmental data. Hum. Ecol. Risk Assess. 22, 435–446. https://doi.org/10.1080/10807039.2015.1079481

Tekindal, M.A., Erdoğan, B.D., Yavuz, Y., 2017. Evaluating Left-Censored Data Through Substitution, Parametric, Semi-parametric, and Nonparametric Methods: A Simulation Study. Interdiscip. Sci. Comput. Life Sci. 9, 153–172. https://doi.org/10.1007/s12539-015-0132-9

The European Parlament and the Council of the European Union, 2018. Proposal for a directive of the European Parliament and of the Council on the quality of water intended for human consumption (recast). Off. J. Eur. Union. 2018.

Wang, D., Singhasemanon, N., Goh, K.S., 2016. A statistical assessment of pesticide pollution in surface waters using environmental monitoring data: Chlorpyrifos in Central Valley, California. Sci. Total Environ. 571, 332–341. https://doi.org/10.1016/j.scitotenv.2016.07.159

WHO, 2011. Water quality for drinking: WHO Guidelines, Springer Reference. https://doi.org/10.1007/springerreference_30502

WHO, 2009. Overview Case Studies Examples and Tools Water Safety Plan Manual Step-by-step risk management for drinking-water suppliers.

Supporting material

Table S1. Log-likelihood values for each distribution and method for the statistical distribution of GW chromium VI concentration data in one of the 28 DWTPs. Bold values identify the best distribution for each method; the red value identifies the best method and distribution.

Method	Distributions				
	Lognormal	Weibull	Gamma	Logistic	Normal
Elim	**-193.9**	-204.8	-297.9	-204.9	-209.0
Zero	-244.7	-229.7	**-209.2**	-378.5	-378.8
LOQ/2	-164.6	-170.5	**-158.2**	-188.4	-188.8
LOQ	-179.0	-187.8	**-176.5**	-196.8	-197.4
MLE_{LC}	**-144.1**	-146.7	-145.3	-147.5	-151.0

Table S2. Percentage of datasets with best removal efficiency estimation and mean absolute fractional error percentage (e_η) for each method as a function of the censored percentages.

Censored percentage (%)	Percentage as best method					Mean $\lvert e_\eta \rvert$				
	Elim	Zero	LOQ/2	LOQ	MLE_{LC}	Elim	Zero	LOQ/2	LOQ	MLE_{LC}
< 1	14.3	0.0	14.3	4.7	66.7	47.4	43.0	45.9	45.6	13.4
1 - 3	3.8	11.5	7.7	7.7	69.3	48.7	51.5	28.4	29.6	10.4
3 - 10	5.9	5.9	11.7	5.9	70.4	43.2	45.9	35.7	32.8	8.6
10 - 15	6.3	2.1	8.4	0.0	83.2	38.7	83.1	56.0	45.9	12.4
15 - 40	6.7	11.7	0.0	0.0	81.6	18.4	140.2	35.3	50.5	5.8
40 - 60	0.0	8.3	8.7	8.7	74.3	51.2	41.1	39.4	45.6	6.2
60 - 75	4.6	3.1	3.1	5.5	83.7	37.3	104.3	97.1	42.7	10.3
75 - 99	3.7	0.0	0.0	2.5	93.8	27.2	923.8	28.2	29.4	28.3

Table S3. Percentage of datasets with best exceedance probability estimation and mean absolute fractional error percentage (e_L) for each method as a function of the datasets censored percentages.

Censored percentage [%]	Percentage as best method					Mean $\lvert e_L \rvert$				
	Elim	Zero	LOQ/2	LOQ	MLE_{LC}	Elim	Zero	LOQ/2	LOQ	MLE_{LC}
< 1	10.5	5.4	2.6	2.6	78.9	23.0	68.8	39.8	41.8	0.6
1 - 3	5.5	2.4	4.9	4.9	82.3	31.8	57.1	29.9	38.3	3.2
3 - 10	0.0	0.0	11.7	5.9	82.4	41.2	68.2	52.1	43.9	5.4
10 - 15	4.2	0.0	6.3	2.1	87.4	61.9	123.2	60.8	47.2	6.0
15 - 40	3.5	0.0	7.4	7.4	81.7	33.4	155.1	31.6	35.3	6.3
40 - 60	3.7	0.0	0.0	6.7	89.6	80.2	240.8	67.3	54.7	13.9
60 - 75	0.0	0.0	0.0	0.0	100.0	257.7	346.4	136.5	90.8	11.3
75 - 99	0.0	0.0	0.0	0.0	100.0	89.5	79.6	96.7	99.4	18.4

CHAPTER 2

Development of a quantitative chemical risk assessment (QCRA) procedure for contaminants of emerging concern in drinking water supply

Abstract: The uncertainties on the occurrence, fate and hazard of Contaminants of Emerging Concern (CECs) increasingly challenge drinking water (DW) utilities whether additional measures should be taken to reduce the health risk. This has led to the development and evaluation of risk-based approaches by the scientific community. DW guideline values are commonly derived based on deterministic chemical risk assessment (CRA). Here, we propose a new probabilistic procedure, that is a quantitative chemical risk assessment (QCRA), to assess potential health risk related to the occurrence of CECs in DW. The QCRA includes uncertainties in risk calculation in both exposure and hazard assessments. To quantify the health risk in terms of the benchmark quotient probabilistic distribution, the QCRA estimates the probabilistic distribution of CECs concentration in DW based on their concentration in source water and simulating the breakthrough curves of a granular activated carbon (GAC) treatment process. The model inputs and output uncertainties were evaluated by sensitivity and uncertainty analyses for each step of the risk assessment to identify the most relevant factors affecting risk estimation. Dominant factors resulted to be the concentration of CECs in source waters, GAC isotherm parameters and toxicological data. To stress the potential of this new QCRA approach, several case studies are considered with focus on bisphenol A as an example CEC and various GAC management options. QCRA quantifies the probabilistic risk, providing more insight compared to CRA. QCRA proved to be more effective in supporting the intervention prioritization for treatment optimization to pursue health risk minimization.

Keywords: Activated carbon adsorption; Contaminants of Emerging Concern; Drinking water treatment; Quantitative Chemical Risk Assessment; Stochastic modeling.

The research work presented in this chapter was carried out during a research stay period of 1 months at the KWR Watercycle Research Institute (Nieuwegein, The Netherlands). The research work was carried out with the valuable supervision of Dr. Patrick W. M. H. Smeets (KWR), in collaboration with Dr. Dirk Vries (KWR), Dr. Milou M.L. Dingemans (KWR), Dr. Bas G. H. Bokkers (Dutch National Institute for Public Health and the Environment (RIVM)), and the support of one MSc student, Luca Penserini.

This chapter has been published in "Water Research[2]".

[2] Cantoni, B., Penserini, L., Vries, D., Dingemans, M.M., Bokkers, B.G., Turolla, A., Smeets P.W.M.H., & Antonelli, M. (2021). Development of a quantitative chemical risk assessment (QCRA) procedure for contaminants of emerging concern in drinking water supply. Water Research, 116911. https://doi.org/10.1016/j.watres.2021.116911

List of symbols and abbreviations

1/n	Freundlich exponent	EBCT	Empty Bed Contact Time
AAT	All-[factors]-At-a-Time	EFSA	European Food Safety Authority
ADI	Acceptable daily intake	GAC	Granular Activated Carbon
AIC	Akaike information criterion	HED	Human equivalent dose
$BMDL_{10}$	Benchmark dose lower confidence limit	I	Incidence
$BMDU_{10}$	Benchmark dose upper confidence limit	IAST	Ideal Adsorbed Solution Theory
BPA	Bisphenol A	K_F	Freundlich adsorption constant
BQ	Benchmark Quotient	M	Magnitude
BQ_{DET}	Deterministic Benchmark Quotient	NOM	Natural organic matter
$BQ_{PROB,MAX}$	Maximum probabilistic BQ	P	Allocation factor
BV	Bed Volume	P(BQ>1)	Probability of BQ value above 1
BV_{REG}	Regeneration time as Bed Volumes	PoD	Point of Departure
$C_{98\%}$	Outlet concentration 98th percentile	QCRA	Quantitative Chemical Risk Assessment
$C_{IN,MAX}$	Maximum inlet concentration	QSAR	Quantitative Structure-Activity Relationship
CECs	Contaminants of emerging concern	RfD	Reference Dose
CRA	Chemical Risk Assessment	S_I	Sensitivity Index
DW	Drinking Water	TDI	Tolerable Daily Intake
DWTL	Drinking Water Target Level	WCS	Worst Case Scenario
DWTP	Drinking Water Treatment Plant	WIR	Water Intake Rate

1. Introduction

Over the last years, research on drinking water (DW) has drawn attention towards the occurrence, fate and potentially harmful impact on human health of a variety of recently identified compounds of anthropogenic origin, often labelled Contaminants of Emerging Concern (CECs), e.g., perfluorinated compounds, alkylphenols, pharmaceuticals, pesticides (Baken et al., 2018). In particular, differences in human health risks and the large number of different compounds created a need for prioritization and regulation of CECs in DW based on the risk level. This is complicated by knowledge gaps that result in uncertainties for both exposure and hazard assessment steps of the procedure (WHO-IPCS, 2018).
As for the exposure assessment, despite several studies reporting trace levels of CECs in the aquatic environment (Staples et al., 2018), CEC concentrations in DW are sometimes poorly known. As a consequence, the evaluation of this uncertainty is necessary for prioritization in the definition of DW standards (Lapworth et al., 2012). It is therefore important to fill existing knowledge gaps on fate of CECs throughout treatment processes currently applied in drinking water treatment plants (DWTPs). To mitigate potential health risks, it is important to assess whether DWTPs, as currently designed, are able to sufficiently remove CECs, and, if not, which additional treatment is the most suitable to be integrated to improve CECs removal. Among the available treatment processes, adsorption onto granular activated carbon (GAC) was so far identified as the best available technology for the removal of many CECs (Westerhoff et al., 2005). GAC removal efficiency depends on the system operating conditions and decreases over time due to GAC saturation with organic matter and CECs. Breakthrough curves are typically used to describe the GAC treatment performance regarding a specific contaminant over time, since they define the time trend of the outlet contaminant concentration during filter operation (Piazzoli and Antonelli, 2018). The GAC performance model, and thus the breakthrough curve, can be built through numerical simulations based on isotherm and kinetics data collected from batch adsorption tests (Patterson et al., 2019). Furthermore, mathematical modeling allows a less costly assessment of several non-tested operating conditions of the GAC treatment and permits the

propagation of the uncertainties related to input data resulting in a comprehensive tool able to predict the GAC treatment performance (Athanasaki et al., 2015).
For the hazard assessment, DW regulatory standards are conventionally set based on toxicological data and used for risk characterization. Not for every CEC a regulatory standard is yet derived to manage risks associated with DW (Baken et al., 2018). Moreover, toxicological studies on CECs are in some cases confidential, and they might be incomplete or contradictory (Schriks et al., 2010).
In current chemical risk assessment (CRA) in DW applications, uncertainties are taken into account by selecting conservative point values, such as a high exposure concentration, or a lower bound estimate of the health-based guideline level (Bokkers et al., 2017). Then, the ratio between the exposure concentration and the health-based guideline level point values is calculated as the deterministic benchmark quotient (BQ) that provides an indication of the risk level (Baken et al., 2018). However, replacing the point values by their uncertainty distributions in a quantitative risk assessment, would make it possible to evaluate the level of conservatism in the estimated risk and the main sources of uncertainty in the whole procedure (WHO-IPCS, 2018). Few case studies are reported in literature that provide a probabilistic quantification of the risk. Still, these applications include the uncertainty analysis just either on the exposure assessment (Kavcar et al., 2009; Thomaidi et al., 2020) or in the hazard assessment (Renwick et al., 2004), resulting in a risk estimation that is not completely representative of the uncertainties in both aspects (exposure and hazard) of the risk assessment. Van Der Voet and Slob (2007) proposed an integrated probabilistic procedure to include both variability and uncertainty in the risk assessment, but this approach is relatively time-consuming for both the data collection and the distinction of the variability and uncertainty within the assessment. Another method focusing on the uncertainty of both the exposure and hazard assessment is the APROBA-Plus tool (Bokkers et al., 2017), which applies lognormal uncertainty distributions to the hazard assessment parameters, resulting in a confidence interval for the human dose associated with specified protection goals. Furthermore, the tool includes the option to insert an estimation of the exposure uncertainty. This method is not a stand-alone tool, but it requires to be integrated in a broader assessment framework to get case-specific inputs from exposure and dose-response analyses, which also contain uncertainty (Lapworth et al., 2012).
To the best of the authors' knowledge, there are no research studies applying a quantitative chemical risk assessment (QCRA) in the field of DW production and consumption. We have developed a comprehensive procedure to implement a QCRA, that includes DW treatment performance modeling and propagation of uncertainties related to the calculation of CEC removal efficiencies. QCRA results were compared with the conventional CRA approach, illustrated by bisphenol A (BPA) as CEC and on GAC treatment process for BPA removal, to underline the benefits of QCRA in providing more insights and precise indications with respect to the CRA. Sensitivity and uncertainty analyses have been used to rank the parameters which mainly contribute to the risk assessment uncertainty and may need further investigation. Moreover, some case studies have been explored with respect to BPA concentration in source water and GAC management options, to highlight the potential of QCRA as supporting tool for the optimization of the interventions in the whole DW supply system.

2. Materials and methods

2.1. Quantitative Chemical Risk Assessment (QCRA) procedure

A probabilistic modeling framework was defined for the development of QCRA procedure (Figure 1). In particular, the developed procedure is applied for one of the CECs introduced in the revision of the European Drinking Water Directive, namely BPA (EU Parliament, 2020).

2.1.1. Exposure assessment: source water quality and treatment efficacy

GAC filtration performance has been modeled through AquaPriori, a Python based treatment simulation tool developed by KWR Water Research Institute, that provides, amongst others, breakthrough curves of GAC filters (Vries et al., 2017). Solutes adsorption on GAC is modeled using the Ideal Adsorbed Solution Theory (IAST) in its simplified version, where the competition of the CECs with natural organic matter (NOM) is considered as dominant, while competition with other micropollutants is neglected (Qi et al., 2007). The AquaPriori tool was modified to allow simulating with a statistical distribution of input parameters rather than a point value. The IAST model input parameters are: (i) CEC inlet concentration, (ii) GAC filter operating conditions (Empty Bed Contact Time, EBCT, regeneration time as Bed Volumes, BV_{REG}, GAC particle size and bed porosity), and (iii) Freundlich isotherm parameters (K_F and 1/n) for the selected CEC. Input data were collected both from literature and 17 full-scale DWTPs in an urbanized area in northern Italy. For each input parameter, the number of available data and their ranges are reported in Table 1, while detailed values are shown in Table S1-S4 and Figure S1 in Supplementary Materials (SM).

Table 1: Input parameters for GAC system performance prediction: number of available data, range and source.

Model analyzed parameters	Unit	# available data	Range	Source of data
Source water concentration	µg/L	235	0.0012 – 43	Literature
Empty Bed Contact Time	min	79	8 – 20	Literature, field data
Time of regeneration	$BV \times 10^3$	79	20 – 80	Literature, field data
GAC particle size	mm	22	0.45 – 2.4	Literature, field data
Bed porosity	-	9	0.4 – 0.8	Literature
Freundlich constant parameter, K_F	$(mg/g)/(mg/L)^{1/n}$	75	0.62 – 255	Literature
Freundlich exponent parameter, 1/n	-	75	0.1 – 1.15	Literature

Collected data were used to estimate the statistical distribution for each input parameter, according to the procedure explained in paragraph 2.2.1. The estimated statistical distributions were used to sample 1,000 data for each input parameter, whose combination resulted in 1,000 simulated breakthrough curves. Under the assumption that the CEC concentration in the GAC effluent is equal to the CEC concentration in DW, for each breakthrough curve, the quantile corresponding to the 98th percentile of the outlet concentration distribution ($C_{98\%}$) was selected as indicator of a realistic maximum CEC concentration in DW. The resulting 1,000 values for $C_{98\%}$ were used to estimate the statistical uncertainty distribution of the maximum CEC concentration.

2.1.2. Hazard assessment

The hazard assessment was aimed at estimating a health-based value, namely the Drinking Water Target Level (DWTL), which represents the concentration of a compound that does not result in the exceedance of the tolerable exposure (i.e. a health based guidance level like TDI, ADI, RfD) of a consumer over lifetime (WHO, 2006). DWTL [mg L^{-1}] was calculated by Eq. 1 (Baken et al., 2018):

$$\mathrm{DWTL} = \frac{\mathrm{RfD} \times \mathrm{P}}{\mathrm{WIR}} \qquad \text{(Eq. 1)}$$

where RfD [mg kg^{-1} day^{-1}] is the reference dose; P [%] is the allocation factor, that is the percentage of risk maximally associated to DW consumption compared to the overall exposure pathways, considered as constant and equal to 20% (Baken et al., 2018); WIR is the Water Intake Rate [L kg^{-1} day^{-1}], which is the ratio between the daily water consumption and the body weight. The DWTL should be sufficiently low to allow safe, long-term consumption of 2L of tap water for adults of 60 kg, i.e. the WIR value was assumed a fixed value of 0.033 L kg^{-1} day^{-1} (Baken et al., 2018).
For the RfD estimation, toxicological data were collected from international statutory guidelines and toxicological studies. In particular, only guidelines mentioning a toxicological reference study and providing all the specific inputs for the assessment have been considered, according to the procedure explained in Section S1 in Supplementary Materials. The most recent scientific opinion published by the European Food Safety Authority (EFSA) in 2015 on BPA has been selected as reference for the hazard assessment (EFSA, 2015). EFSA identified the mean relative kidney weight from the F1 males in a two-generation toxicity study in mice (Tyl et al., 2008) as the critical effect of BPA. The point of departure (PoD) was the lower confidence limit of the benchmark dose ($BMDL_{10}$) provided by EFSA, as 8.96 mg $kg^{-1}day^{-1}$ while the upper confidence limit of the benchmark dose ($BMDU_{10}$) was 108.9 mg $kg^{-1}day^{-1}$. In the EFSA assessment, uncertainty factors of 14.7, 2.5 and 10 were applied for interspecies toxicokinetics (i.e. calculation of the human equivalent dose (HED)), interspecies toxicodynamics and intraspecies differences, respectively; in addition, an extra factor of 6 was included to take into account the limitations of the data available on BPA toxicity for mammary gland, reproductive, neuro-behavioural, immune and metabolic systems. EFSA reports a deterministic RfD for external oral exposure to BPA in humans of 4.0 μg $kg^{-1}day^{-1}$. Finally, differently from what reported by EFSA, a duration extrapolation factor was applied for subchronic-to-chronic conversion. The critical effect in the toxicity study (Tyl et al., 2008) is not a developmental or reprotoxic effect, but a general toxicity effect (on kidney) assumed to occur after continuous, repeated exposure. Since the F1 males were exposed up to the age of 14 weeks a factor for duration is considered necessary. In the deterministic approach a factor of 2 was used as a default value proposed by the EFSA (EFSA, 2012). To derive the uncertainty distribution of the RfD and evaluate which factors are more relevant in the final RfD uncertainty, the APROBA-Plus tool was used, as described by Bokkers et al. (2017). The protection goals, namely the effect magnitude (M) and the population incidence (I), were set to 10% and 1%, respectively. Therefore, the output reference dose is the dose at which 1% of the population would be subject to an effect of 10% (or more) reduction in mean relative kidney weight. For the uncertainty factors inputs to the APROBA-Plus tool, interspecies, intraspecies and duration extrapolation data-based default uncertainty distributions provided by the software were applied. For the limited data available on BPA toxicity for mammary gland, reproductive, neuro-behavioural, immune and metabolic systems the EFSA assessment factor of 6, was considered here as the upper (95%) confidence limit. The possibility that actual additional data on these endpoints would not change the PoD is reflected by setting the lower (5%) confidence limit of this assessment factor distribution to 1. Details on the inputs to the APROBA-Plus tool based on the critical endpoint established by EFSA are reported in Table S7 and S8 in Supplementary Materials.
The estimated RfD statistical distribution, WIR and allocation factor (P) were used to calculate 1,000 values of DWTL, used to fit its statistical distribution.

2.1.3. Risk characterization

For the risk characterization step, once that both the statistical distributions of $C_{98\%}$ and DWTL were obtained, they were used to sample 1,000 data each, from which it has been possible to compute 1,000 BQ values, according to Eq. 2:

$$BQ = \frac{C_{98\%}}{DWTL} \quad \text{(Eq. 2)}$$

These values were used to estimate the BQ statistical distribution (see paragraph 2.2.1). The BQ statistical distribution was employed to extrapolate two different data: (i) the maximum probabilistic BQ ($BQ_{PROB,MAX}$), corresponding to the maximum BQ value resulting from the quantitative simulation; (ii) the probability of BQ above the health risk threshold value equal to 1 (P(BQ>1)), resulting from the BQ estimation uncertainties. P(BQ>1) represents the percentage of the total area underlying the BQ probability density curve that is above the BQ value of 1.
Moreover, the deterministic BQ (BQ_{DET}) was estimated as the ratio between the deterministic $C_{98\%}$ and the deterministic DWTL calculated from the EFSA values, according to the conventional CRA.

2.2. Stochastic simulations

2.2.1. Definition of input and output data distributions

Collected inputs and estimated outputs data were used to fit their statistical distribution. For each parameter, fits to the lognormal, Weibull, gamma, beta, Rayleigh, uniform, triangular and logistic statistical distributions were tested. Data fitting to specific distributions were performed with the fit function in the Python scipy.stats package, which applies a Maximum Likelihood Estimation method. Then, the statistical distribution having the minimum Akaike information criterion (AIC) was selected.
Because the Freundlich isotherm model parameters (K_F and 1/n) are bivariate correlated, a multivariate statistical distribution method was applied. The Gaussian Anamorphosis function method with inverse anamorphosis function, a linear transformation and the anamorphosis function was used in order to describe the joint probability distribution (Santoro et al., 2015).

2.2.2. Sensitivity analysis

Sensitivity analyses were performed on $C_{98\%}$, DWTL and BQ variables. A global sensitivity analysis approach was applied. A variance-based, quantitative and All-[factors]-At-a-Time (AAT) method was preferred to local sensitivity analysis to describe the whole inputs space dimensionality including interactions among inputs (Saltelli and Annoni, 2010). It is based on the first order effect index, S_I, in which output variations are induced by varying all the input factors simultaneously. Therefore, the sensitivity to each factor considers the direct influence of that factor, as well as the joint influence due to interactions (Saltelli and Annoni, 2010). S_I value identifies the most relevant input factors by assessing their contribution to the model output variance as defined in Eq. 3:

$$S_{I,i} = \frac{V_i(E_{-i}(Y|X_i))}{V(Y)} \quad \text{(Eq. 3)}$$

where: X_i is the *i-th* evaluated input; Y is the evaluated output; *-i* represents all the input factors except the *i-th*. For each *i-th* evaluated input, a series of *n* values was generated as uniformly distributed between the minimum and the maximum of the collected input data ranges. Then, for each of the evaluated input *n* values, 1,000 combinations of values of all the other input factors (*-ith*) were sampled from their estimated statistical distributions, resulting in 1,000 values of the assessed output Y. All the inputs were assumed to be independent, except for the Freundlich isotherm parameters that were jointly sampled from their multivariate statistical distribution. Similar to the other input parameters, all Freundlich parameter couples as found in literature were evaluated as the *i-th* input to yield a series of *n* values.

2.2.3. Uncertainty analysis

Uncertainty analysis of the BQ output was performed. A Monte Carlo simulation method was applied, which allowed for the simultaneous forward propagation of all the inputs uncertainties into the output distribution (Saltelli and Annoni, 2010). All the inputs found to be relevant in the sensitivity analysis were simultaneously sampled from their estimated statistical distributions and randomly combined, for a total of 1,000 simulations for each endpoint, resulting in 1,000 values of BQ per endpoint, whose statistical distribution has been fitted. To check whether 1,000 simulations were enough to get stable outputs, the whole procedure was repeated four times. Then, pairwise comparisons were performed with the Kolmogorov-Smirnov test, to test whether the four resulting BQ samples were drawn from the same continuous distribution. Moreover, it was checked that the standard errors for several percentiles (Table S13) of the BQ distributions were below 10%.

2.3. QCRA application for systems management and optimization

The developed QCRA procedure has been applied to three different case studies. In the first two case studies, it has been assumed to have a DW source contaminated with BPA having the maximum concentration measured, $C_{IN,MAX}$, and distributed according to the literature data (see Table S10 and Table S1); two cases have been simulated: (i) DW-NO_GAC, in which there is not a GAC process in the DWTP and, thus, no CECs removal is assumed to occur; (ii) DW-GAC, in which a GAC process is present, but it is managed aiming at the removal of conventional pollutants, implying a high regeneration time (BV_{REG} = 80,000 BV). In the third case study, the worst-case scenario with GAC treatment (WCS-GAC) has been assessed, assuming the highest BPA concentration in source water found in literature, namely 43 µg/L, constantly entering the DWTP in which there is a GAC process managed for conventional pollutants removal (BV_{REG} = 80,000 BV).

In addition, other two intervention scenarios derived from WCS-GAC were simulated for exploring the potential of QCRA for the optimization of the GAC process. Specifically, the first intervention scenario is an upgrading scenario (WCS-GAC_Up), in which the GAC process is upgraded by increasing the number of GAC filters in parallel up to an optimal value, being the EBCT the input parameter to be optimized. While, the second intervention scenario simulates an optimal management scenario (WCS-GAC_Manag), in which the regeneration frequency of the GAC filters was managed with reference to BPA, being the BV_{REG} the optimization parameter.

As for the exposure assessment step of the QCRA procedure, the Freundlich isotherm parameter pairs found in literature were reduced exclusively to those estimated through GAC tests with real DW matrices ("DW" as water matrix in Table S4). Values and assumptions for inputs variables are summarized in Table S9 for all the case studies.

For each case study, both the traditional CRA and the developed QCRA procedures have been performed: the CRA output, namely the BQ_{DET}, was compared to the two QCRA indexes, $BQ_{PROB,MAX}$=1 and P(BQ>1)=0 (defined in paragraph 2.1.3). In particular, for the two intervention scenarios (WCS-GAC_Up and WCS-GAC_Manag), the optimal values of the considered input parameter were obtained at BQ_{DET}=1 for the CRA, while both conditions of $BQ_{PROB,MAX}$=1 and P(BQ>1)=0 were evaluated for the QCRA.

3. Results and discussion

The QCRA procedure development, as reported in Figure 1, has been performed firstly identifying the statistical distribution of each input parameter that was fed to exposure assessment, hazard assessment and risk characterization models, to estimate the outputs distributions. The resulting statistical distributions, their parameters and the AIC numbers obtained for each fitted statistical distribution are reported in Table S10. Results of the sensitivity and uncertainty analyses, as well as the application of the developed procedure to the representative case studies is here reported to show how decision-makers, water utilities and scientific community may benefit from including the uncertainties within risk assessment rather than selecting deterministic point values.

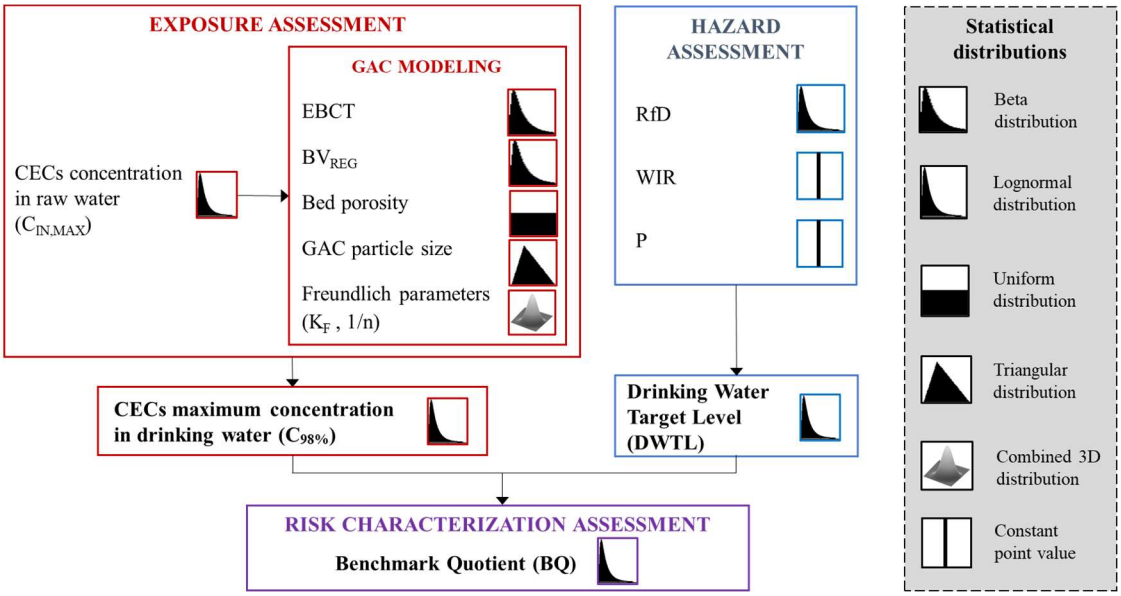

Figure 1. Schematic overview of the framework for QCRA implementation: modeling steps, input and output variables, and their statistical distributions.

3.1. Sensitivity analysis

One of the main benefits of applying a quantitative risk assessment procedure, including the related uncertainties, is that the output can highlight which aspects display the main contribution to the overall uncertainty and, therefore, what type of additional information should be collected to increase the accuracy in the modeling process, reducing the assessment uncertainty (Bokkers et al., 2017). In particular, this was achieved through two sensitivity analyses to identify which inputs, among the set required for exposure and hazard assessment steps, affect mostly $C_{98\%}$ and DWTL outputs, respectively. Then, limiting the analysis to these dominant inputs, a sensitivity analysis has been performed to evaluate which inputs are more influencing on the BQ estimation accuracy.

As for the exposure assessment, the shapes of the modeled breakthrough curves provide qualitative information about the influence of each input parameter on the $C_{98\%}$ output. In particular, a substantial difference in breakthrough curves between the minimum and maximum value of the analyzed input parameter indicates that this input has a relevant influence on the $C_{98\%}$ output. Examples of breakthrough curves obtained varying EBCT and couples of Freundlich isotherm parameters are reported in Figure 2, while graphs for the other input parameters are shown in Figure S3.

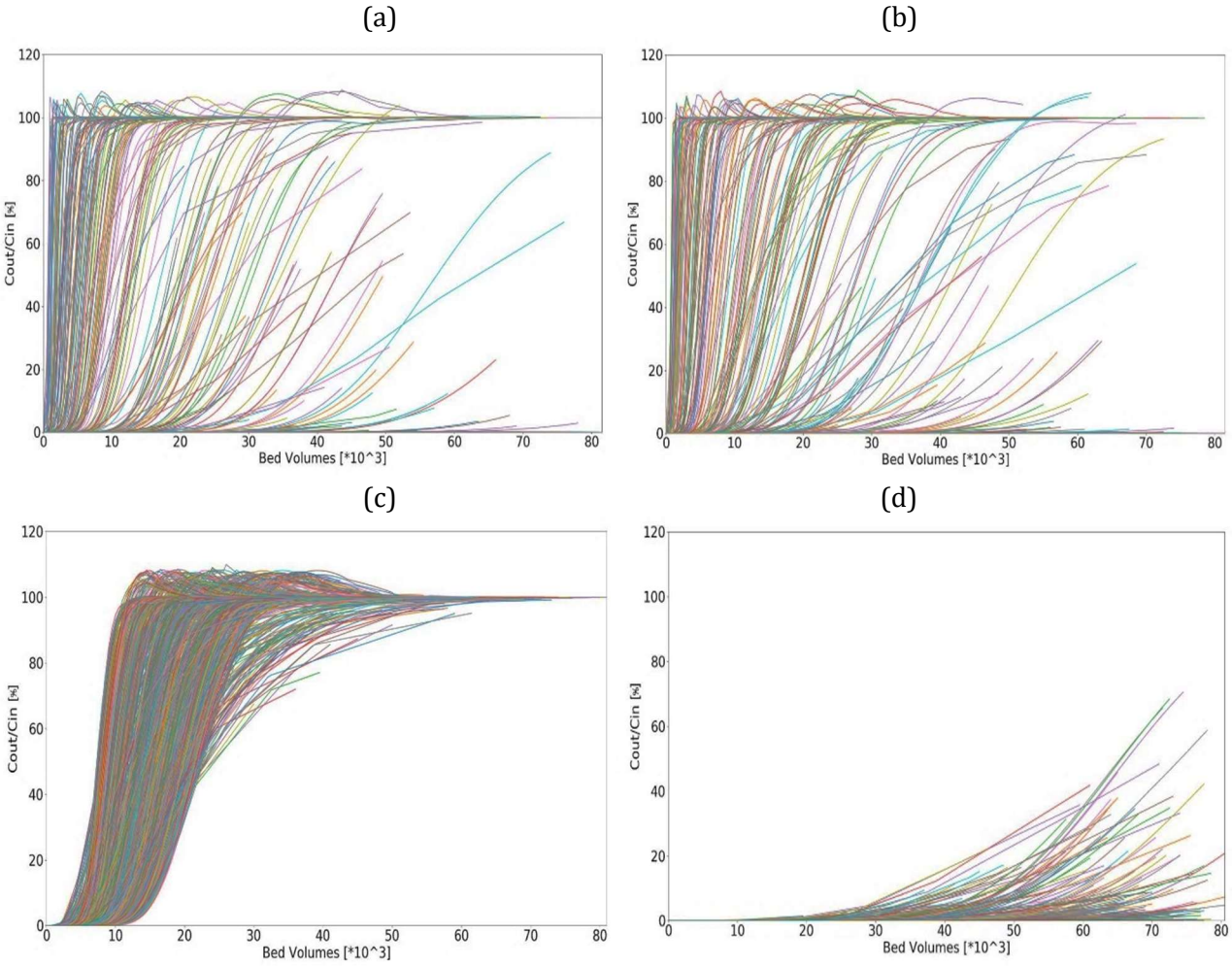

Figure 2. BPA breakthrough curves resulting from the sensitivity analysis. For each chart, 1,000 curves were simulated sampling 1,000 values from each input distributions, while fixing the evaluated input. Constant values of the evaluated input are: (a) EBCT=8 min; (b) EBCT=20 min; (c) K_F=10.55 (mg/g)(mg/L)$^{-1/n}$, 1/n=0.27; (d) K_F=28.61 (mg/g)(mg/L)$^{-1/n}$, 1/n=0.39.

The EBCT parameter seems not to have relevant influence on the breakthrough curves shape in the analyzed range, i.e. differences in breakthrough curves are graphically almost indistinguishable between minimum and maximum EBCT values (Figure 2a and 2b). Instead, it is evident that a variation in Freundlich parameter values imply a substantial variation in the resulting breakthrough curves and, consequently, have an effect on the $C_{98\%}$. It is important to notice that some curves exceed more than a 100% breakthrough ratio. Without extensive analysis, we postulate that competitive effects of NOM cause these overshoots, as NOM was included as a (possibly competing) substance in the simulation of BPA sorption and breakthrough. Due to competition with NOM, desorption and subsequent release of adsorbed CEC (BPA in this case) would lead to elution with non-adsorbed CEC (Hand et al., 1997). In addition to visual inspection of the breakthrough curves, the S_I values were calculated for each input in order to quantitatively identify and rank the most relevant input factors affecting the $C_{98\%}$ output. Recall that a higher S_I implies a higher influence of the input parameter on the output. Results are reported in Table 2.

Table 2. Sensitivity Indexes (S_I) referred to $C_{98\%}$ (exposure) and BQ (risk characterization), depending on the input parameters. S_I of the relevant parameters, further analyzed in the uncertainty analysis, are highlighted in bold.

SA Output	Exposure						Hazard
	Particle Size	Bed porosity	EBCT	BV_{REG}	C_{IN}	Freundlich parameters	RfD
C_{98}	0.0015	0.0010	0.0009	0.0018	**0.0507**	**0.0780**	
BQ	-	-	-	-	**0.0117**	**0.0229**	**0.0210**

It emerges that for each operating condition (EBCT, BV_{REG}, bed porosity and particle size), the S_I values are at least one order of magnitude lower than the one for Freundlich isotherm parameters and inlet BPA concentration. Therefore, operating conditions turned out not to have significant effects on the variability of the $C_{98\%}$ output for the studied CEC, or, at least, to be less relevant compared to Freundlich isotherm parameters and inlet BPA concentration. Consequently, only the uncertainties related to Freundlich parameters and inlet BPA concentration were considered in the BQ sensitivity analysis.
As for the hazard assessment step, the APROBA-Plus tool provides analyses on which of the assessment uncertainty factors reported by EFSA have the main contribution to the overall RfD uncertainty (see Table S11). The greatest contributor to the RfD uncertainty is the assessment factor accounting for the intraspecies differences, with 28% contribution, followed by the duration extrapolation factor (25% contribution), the uncertainty on the PoD value (20%), and the interspecies factor (17%). Finally, 10% of the RfD uncertainty is due to the EFSA assessment factor taking into account the limitations of the data available on BPA toxicity for mammary gland, reproductive, neuro-behavioural, immune and metabolic systems.
For the risk characterization assessment step, the sensitivity analysis was performed on the BQ output to prioritize those QCRA inputs that were found to be the dominant factors in the previous steps. From results in Table 2, it is possible to note that S_I indexes for the three inputs are all in the same order of magnitude and, therefore, both parameters describing the GAC process and toxicological data have a significant influence on the estimated BQ. This suggests that, when predicting the GAC performance towards BPA, it is important to precisely estimate the source water concentration and to test the selected GAC performance with the real source water through batch experiments, in order to evaluate the case-specific Freundlich isotherm parameters. Actually, these considerations can apply also to CECs other than BPA. Moreover, more toxicological data on BPA hazard on several specific endpoints (e.g. mammary gland, reproductive, neuro-behavioural, immune and metabolic systems) will make the assessment factor for the incomplete toxicity information redundant. EFSA is currently re-evaluating BPA. In case additional toxicity data does not warrant the choice of another PoD (due to a more sensitive endpoint), the uncertainty in the RfD can be reduced by eliminating the assessment factor accounting for the limited available data. Consequently, the uncertainty in the DWTL and final BQ is also reduced.

3.2. Uncertainty analysis

The main advantage of a probabilistic framework for risk assessment is the possibility to reproduce the observed variability of source water quality and CECs affinity towards GAC, and the uncertainties related to CECs toxicity. In contrast to a deterministic procedure where a single expected BQ is estimated, the probabilistic framework can provide its whole probability distribution and, therefore, more insight about its accuracy and reliability. In addition, this approach permits to relate the design of a GAC process to health risk probability, highlighting the effective benefits of a specific design assumption. In order to

highlight more clearly such benefits, the probabilistic QCRA output was compared to the results obtained by the deterministic CRA. In the QCRA uncertainty analysis, 1,000 Monte Carlo simulations were performed sampling simultaneously, from their distributions, all the relevant inputs, while keeping constant the GAC process operating conditions, not being relevant. The procedure was repeated four times and 1,000 Monte Carlo simulations were confirmed to be enough to get stable outputs. In fact, the standard errors for the main percentiles of the four BQ distributions were below 10% (Table S12). Moreover, pairwise comparisons of the four BQ outputs with Kolmogorov-Smirnov tests resulted in all p-values above the significance level α=0.05 (Table S13), meaning that the four BQ outputs can be assumed to follow the same distribution.

Starting from the exposure assessment, the probabilistic QCRA procedure shows the wide range of breakthrough curves (Figure S4) which are calculated by sampling from the whole model inputs uncertainty distributions, compared to the single GAC breakthrough curve obtained with the deterministic CRA, assuming the maximum $C_{IN,MAX}$ and the QSAR (Quantitative Structure-Activity Relationship) predicted parameters of Freundlich isotherm, set as default in the AquaPriori tool.

For the hazard assessment, the deterministic DWTL is equal to 12.0 µg/L, estimated from the EFSA RfD (4.0 µg kg^{-1} day^{-1}), the duration extrapolation factor of 2 and assuming standard daily water consumption (2 L) and body weight (60 kg) (Baken et al., 2018). The APROBA-Plus provides an approximate probabilistic RfD, defined as the 5% percentile of the target human dose (HD^1_{10}), equal to 3.69 µg kg^{-1} day^{-1} that is slightly lower than the EFSA RfD, although different assumptions and probabilistic uncertainty factors have been considered (Table S14). Considering the whole RfD distribution provided by the APROBA-Plus, the QCRA output provides a statistical distribution for the DWTL (Figure 3a), well described by a lognormal distribution with mean=5.93 µg/L and standard deviation=1.725. Both the deterministic DWTL and most of the probabilistic DWTL distribution exceed the parametric value for BPA in the revised European Drinking Water Directive (2.5 µg/L) (EU Parliament, 2020), indicating that this can be considered sufficiently protective.

Lastly, according to the conventional deterministic CRA, the BQ_{DET} is equal to 0.004, indicating that there is no human health risk linked to BPA in treated DW. As for the probabilistic QCRA, considering only a central statistic of the BQ statistical distribution, like the average, that is equal to 0.01, leads to a result in agreement with the one obtained by the deterministic approach. However, with the QCRA the maximum BQ can be calculated reflecting a conservative estimate of the risk for individuals who are highly exposed and sensitive (to the effects of BPA). This analysis suggests that, when consuming 2L of tap water, a potential health risk cannot be excluded in specific cases, since the maximum probabilistic BQ, that is the 99% percentile of the BQ distribution, is equal to 1.15, and the probability of exceeding the BQ threshold value of 1 is equal to 0.2%.

Another benefit of the probabilistic approach is that it provides two different parameters that relate to two different features of the human health risk. In fact, exposure to chemicals can have acute or chronic effects on human health, depending on their severity and duration. Acute effects usually occur rapidly as a result of short-term exposures to high pollutants concentrations (uncommon for CECs in water), while chronic effects can generally occur as a result of long-term exposure to lower concentrations (Schultz et al., 2003). Therefore, when the analyzed hazard is likely to have an acute effect on human health, the maximum probabilistic BQ should be the most important parameter to be assessed and reduced, describing the most critical situation that could happen, even with low probability. On the other hand, when the analyzed hazard is likely to have a chronic effect on human health, as it can be the case of DW pollution with CECs, the probability of BQ values exceeding the threshold value (BQ=1) should be the most important parameter to be reduced, considering not only the most critical concentration at which the consumer could be in contact but also all the concentrations higher than the threshold value and the probability that the consumer would drink contaminated water.

3.3. QCRA application to case studies

Definition of interventions based only on the compliance with quality standards can be unfeasible or ineffective due to the multiplicity of CECs which are or might be present in a water supply source, as well as the differentiated efficiency of GAC process. Instead, it is proposed here that prioritization of interventions to reduce concentrations of CECs should be based on the avoided health risk. Three case studies were identified (DW-NO_GAC, DW-GAC, WCS-GAC) to explore the potential of the developed QCRA procedure in providing a valid support to tune monitoring campaigns and design/management measures to minimize health risk due to BPA and CECs. In the first two case studies, a DW source is polluted by BPA with a maximum concentration, $C_{IN,MAX}$, distributed according to literature data (see Table S10 and Table S1). In the case study DW-NO_GAC, since supplied water does not undergo a GAC process, maximum BPA concentration, $C_{98\%}$, in DW is distributed as the maximum source water BPA concentration, $C_{IN,MAX}$. While in the DW-GAC case, the DW source undergoes a GAC treatment throughout the DWTP; therefore, $C_{98\%}$ was estimated through the breakthrough curves estimation, with the AquaPriori Tool. In the third case study, WCS-GAC, a DW source polluted by the highest BPA maximum concentration, $C_{IN,MAX}$, found in literature, namely 43 µg/L, was assumed. In case studies comprising a GAC process, it was assumed that GAC process was managed looking at the breakthrough of regulated and routinely monitored micropollutants; thus, no specific measures are taken to address CECs removal. The simulated breakthrough curves for the DW-GAC and WCS-GAC case studies are reported in Figure S5 and the distributions of the estimated $C_{98\%}$, DWTL and corresponding BQ, are reported in Figure 3 for the three cases. The deterministic CRA and probabilistic QCRA outputs are reported in Table 3.

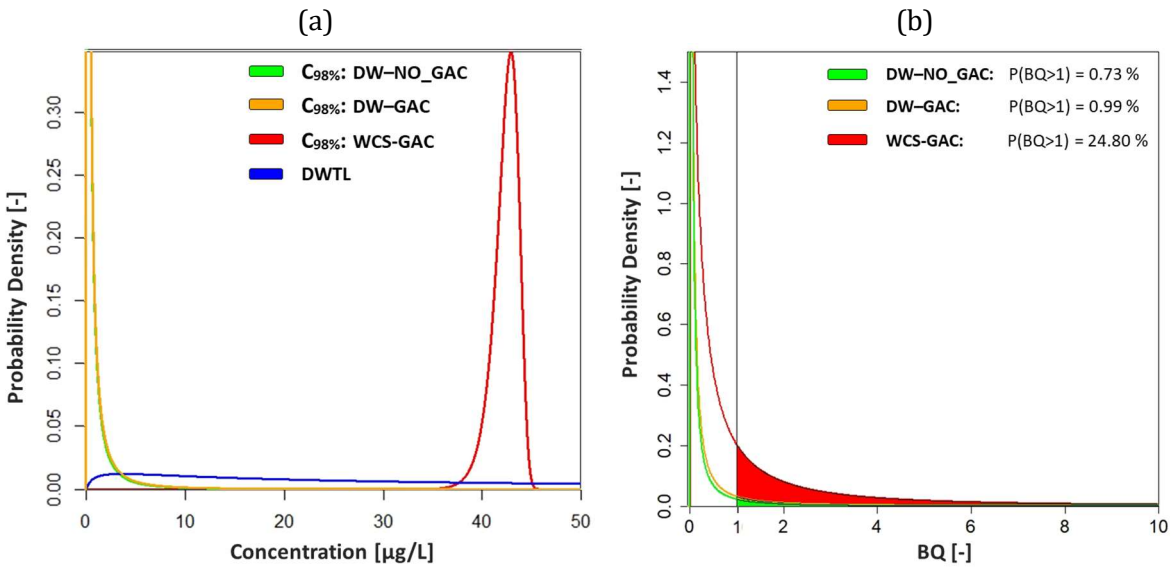

Figure 3. Probability density for: (a) estimated $C_{98\%}$ and DWTL, (b) quantitative BQ for the three cases.

Table 3. Deterministic $C_{98\%}$, DWTL and BQ, statistical distributions of probabilistic $C_{98\%}$ and BQ (distribution parameters reported in brackets), maximum quantitative BQ and probability of quantitative BQ exceeding the threshold value (BQ=1) for the three simulated case studies.

	Deterministic CRA			Probabilistic QCRA			
Case Study	$C_{98\%,DET}$ [µg/L]	$DWTL_{DET}$ [µg/L]	BQ_{DET} [-]	$C_{98\%,PROB}$ [µg/L]	BQ [-]	$BQ_{PROB,MAX}$ [-]	P(BQ>1) [%]
DW-NO_GAC	0.564	12.0	0.04	lognorm(-2.0, 1.726)	lognorm(-5.93, 2.429)	1.55	0.73
DW-GAC	0.558	12.0	0.04	lognorm(-1.9, 1.733)	lognorm(-5.87, 2.517)	1.62	0.99
WCS-GAC	42.90	12.0	3.58	Weibull(440.8, 43.0)	lognorm(-1.17, 1.726)	17.11	24.80

Both DW- case studies show that no human health risks is identified based on the deterministic approach revealing a no-risk situation (BQ_{DET}=0.04). On the other hand, the application of the probabilistic QCRA allows to highlight that, in both cases there is a potential risk in specific cases, being the P(BQ>1) greater than zero, with maximum probabilistic BQ of 1.55 and 1.62, in absence and in presence of a GAC process, respectively. Comparing the BQ parameters found in the two DW- case studies, without a specific treatment and with GAC process managed for conventional pollutants, it is clear that BQ values in both deterministic CRA and probabilistic QCRA are very similar. This finding highlights that, if the GAC process present in a DWTP is managed looking only at regulated and routinely monitored micropollutants, BPA approaches the complete breakthrough during the GAC filter functioning (see Figure S5a), making the adsorption process no longer effective in reducing BPA outlet concentration. As a parameter for BPA has been included in the revision of the European Drinking Water Directive (EU Parliament, 2020), it is important to design and manage the GAC process accordingly; in addition, the probabilistic quantitative approach, contrarily to the deterministic one, can be useful to select the more appropriate operating conditions to minimize the actual health risk, based on the joint analyses of $BQ_{PROB,MAX}$ and P(BQ>1) deriving from each operating conditions evaluated. Moreover, it can be observed that the P(BQ>1) in case of presence of the GAC process is slightly higher than the one in the case without GAC process. This could be due to the breakthrough curves shapes that show effluent concentrations exceeding the influent concentration for a while during filter functioning (Hand et al., 1997). It is essential to consider this aspect, since there could be situations in which the outlet maximum concentration, $C_{98\%}$, is higher than the concentration in DW source. This finding points out that monitoring CEC concentration only in the DW source could lead to a risk underestimation, and that coupling the monitoring with the modeling of the GAC process performance is beneficial for a more accurate risk assessment.
For the WCS-GAC case study, the high regeneration time leads to the complete BPA breakthrough and a probability of 33.58% of exceeding the BQ threshold value. In this case, also the deterministic approach would have revealed a risk (with the BQ higher than 1), but again the probabilistic maximum BQ is one order of magnitude higher than the deterministic one.

3.4. Intervention scenarios optimization for risk minimization

Both the deterministic CRA and probabilistic QCRA procedures, applied to the WCS-GAC scenario, highlighted that the GAC process designed and managed for conventional pollutants resulted to be ineffective to prevent human health risk in case of high BPA inlet concentration. Thus, the QCRA procedure was applied to evaluate the efficiency of GAC process optimization interventions in minimizing the health risk. As benchmark, the conventional deterministic CRA was used.
The first simulated intervention scenario (WCS-GAC-Up) is a typical intervention applied by the water utilities managers, that is the GAC process upgrade with an increase in the number of parallel filters treating the supplied water. In fact, the flowrate per filter would decrease by increasing the filters number, raising the EBCT and determining a reduction of the maximum outlet concentration, which means a lower BQ value and a lower probability to exceed BQ value equal to 1. In particular, it should be possible to estimate the number of filters reducing the probability to virtually 0 (if smaller than 1e-5 it is considered zero) which represents the optimal number of filters. In practice, the EBCT was the parameter to be optimized, since it was one of the AquaPriori inputs and it can be easily related to the filters number. As it was in the input of the sensitivity analysis, the EBCT has been varied between 8 and 20 minutes since operating at higher EBCT is proven not to improve the GAC filter performance, in terms of the total water volume treated between two regenerations (Crittenden et al., 2012). Figure S6 shows the breakthrough curves and the BQ values statistical distribution obtained at the minimum (8 minutes) and maximum (20 minutes) EBCT values.

The second simulated scenario (WCS-GAC-Manag) is related to a management intervention, where the GAC regeneration frequency is the parameter to be optimized. In fact, by reducing the time between two GAC filter regenerations, the breakthrough curve is interrupted in advance, resulting in a lower CEC maximum outlet concentration, and thus a lower BQ value. Consequently, the probability of exceeding BQ value equal to 1 will be lower. Therefore, in the present optimization, the goal is to determine the time of regeneration (BV_{REG}) that makes that probability to virtually 0. In this case, while the currently applied regeneration time ranges between 20,000 and 80,000 BVs (Table 1), the BV_{REG} range for the optimization based on BPA was tested between 0 and 80,000 BVs. Although more frequent regenerations compared to conventional operation would imply higher operating and environmental costs, it is an effective solution to mitigate health risks due to the occurrence of BPA in DW. In Figure S7, the breakthrough curves and the $C_{98\%}$, DWTL, and BQ statistical distribution obtained at regeneration with 11,000, 25,000 and 80,000 BVs are shown.
Finally, the two intervention scenarios were combined to evaluate the effect of concurrent changes in the EBCT and regeneration time (BV_{REG}). Figure 4 reports the three parameters used to evaluate the human health risk and optimize the GAC process, namely BQ_{DET}, $BQ_{PROB,MAX}$ and P(BQ>1), as a function of the EBCT and the BV_{REG} parameters.

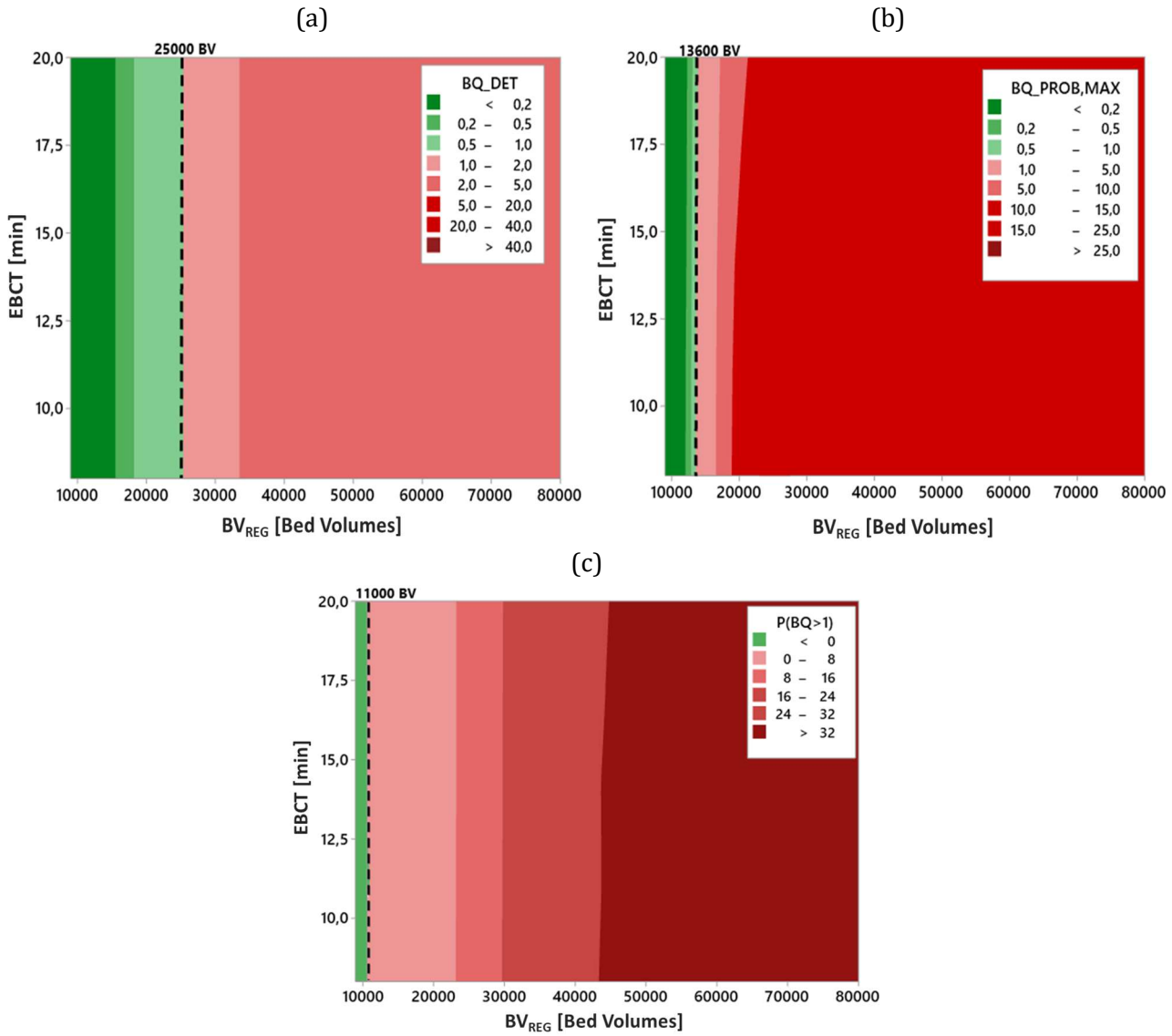

Figure 4. Trend of the optimization parameters: (a) BQ_{DET}, (b) $BQ_{PROB,MAX}$ and (c) P(BQ>1) as a function of the regeneration time, BV_{REG}, and the empty bed contact time (EBCT).

It can be seen that the EBCT has a negligible influence on all the three optimizing parameters, compared to the regeneration time. Therefore, the EBCT seems not to be a relevant parameter through which optimize BPA removal by GAC process, as it was expected from the sensitivity analysis results. Both the deterministic BQ and probabilistic maximum BQ decrease with the reduction of the regeneration time, as well as the probability of exceedance BQ equal to 1.
Using the deterministic approach (looking at the deterministic BQ), a regeneration time equal to 25,000 BV would be selected as the optimal value under which there is no significant risk (BQ_{DET}=1), while with the quantitative approach it comes out that there is still a 12.0% probability of exceeding BQ value equal to 1. Therefore, the deterministic BQ value provides the less precautionary approach, which does not identify residual human health risk in specific cases.
With the probabilistic approach, an optimal regeneration time of 13,600 BV has been obtained for the case in which the optimization goal is the maximum probabilistic BQ value equal to 1. Instead, an optimal regeneration time of 11,000 BV would result in a virtual 0% probability of exceedance of BQ value equal to 1. Since these two probabilistic risk parameters decrease with different trends with the change in the regeneration time, it is important to select the proper optimization parameter according to the evaluated risk, whether it is an acute or chronic effect. Moreover, a full optimization procedure could include the environmental and economic intervention costs, together with the QCRA output.

4. Conclusions

In the present work a QCRA procedure has been successfully developed highlighting the advantages of a stochastic approach in the assessment of a potential human health risk associated to CECs in drinking water. This has been quantitatively estimated performing a characterization of uncertainty for each phase of the risk assessment, usually neglected in the conventional deterministic approach.
Compared to conventional deterministic CRA where conservative point values are selected, the probabilistic QCRA procedure exhibits a precautionary approach since it includes uncertainties. Since for all the analyzed case studies, the probabilistic maximum BQ value was higher than the deterministic BQ value, it turned out that the output uncertainty cannot be neglected. Furthermore, the probabilistic QCRA provides additional information, i.e. the probability of exceeding the BQ threshold value (BQ=1), which is not considered in the conventional deterministic approach. By providing these two different kinds of information, the probabilistic QCRA procedure shows its adaptive nature, and it can be tailored to different contaminants and their potential health effects.
The probabilistic QCRA framework was used for a global sensitivity analysis aimed at identifying the most relevant factors affecting the risk BQ output, which thus require highest attention in the modeling process. The results showed that both the exposure inputs, excluded the GAC operating conditions, and toxicological data have relevant influence on the estimated BQ values. Hence, the developed procedure may be also used to address the future research efforts in narrowing the most relevant uncertainties.
The probabilistic QCRA is fit to be used as a decision support tool for water utilities, because its results allow to support and quantitatively justify allocation of resources in health risk management measures or control strategies. Moreover, it will be beneficial to apply the developed QCRA to different CECs for assessing health effects and DW treatment process configurations in order to provide a comprehensive evaluation and support the prioritization of CECs with regard to treatment and measures to prevent contamination of source waters and supply.

References

Athanasaki, G., Sherrill, L., Hristovski, K.D., 2015. The pore surface diffusion model as a tool for rapid screening of novel nanomaterial-enhanced hybrid ion-exchange media. Environ. Sci. Water Res. Technol. 1, 448–456. https://doi.org/10.1039/c5ew00108k

Baken, K.A., Sjerps, R.M.A., Schriks, M., Wezel, A.P. Van, 2018. Toxicological risk assessment and prioritization of drinking water relevant contaminants of emerging concern. Environ. Int. 118, 293–303. https://doi.org/10.1016/j.envint.2018.05.006

Bokkers, B.G.H., Mengelers, M.J., Bakker, M.I., Chiu, W.A., Slob, W., 2017. APROBA-Plus: A probabilistic tool to evaluate and express uncertainty in hazard characterization and exposure assessment of substances. Food Chem. Toxicol. 110, 408–417. https://doi.org/10.1016/j.fct.2017.10.038

Crittenden, J.C., Trussell, R.R., Hand, D.W., Howe, K.J., Tchobanoglous, G., 2012. MWH's water treatment: principles and design. John Wiley & Sons.

EFSA, 2015. Scientific Opinion on the risks to public health related to the presence of bisphenol A (BPA) in foodstuffs. EFSA J. 13. https://doi.org/10.2903/j.efsa.2015.3978

EFSA, 2012. Guidance on selected default values to be used by the EFSA Scientific Committee, Scientific Panels and Units in the absence of actual measured data. EFSA J. 10, 1–32. https://doi.org/10.2903/j.efsa.2012.2579

EU Parliament, 2020. Directive of the European Parliament and of the Council on the quality of water intended for human consumption, in: Off. J. Eur. Union. 2020. https://doi.org/10.1017/CBO9781107415324.004

Hand, D.W., Crittenden, J.C., Hokanson, D.R., Bulloch, J.L., 1997. Predicting the performance of fixed-bed granular activated carbon adsorbers. Water Sci. Technol. 35, 235–241. https://doi.org/10.1016/S0273-1223(97)00136-4

Kavcar, P., Sofuoglu, A., Sofuoglu, S.C., 2009. A health risk assessment for exposure to trace metals via drinking water ingestion pathway 212, 216–227. https://doi.org/10.1016/j.ijheh.2008.05.002

Lapworth, D.J., Baran, N., Stuart, M.E., Ward, R.S., 2012. Emerging organic contaminants in groundwater: a review of sources, fate and occurrence. Environ. Pollut. 163, 287–303.

Patterson, C., Burkhardt, J., Schupp, D., Krishnan, E.R., Dyment, S., Merritt, S., Zintek, L., Kleinmaier, D., 2019. Effectiveness of point-of-use/point-of-entry systems to remove per- and polyfluoroalkyl substances from drinking water. AWWA Water Sci. 1, e1131. https://doi.org/10.1002/aws2.1131

Piazzoli, A., Antonelli, M., 2018. Application of the Homogeneous Surface Diffusion Model for the prediction of the breakthrough in full-scale GAC filters fed on groundwater. Process Saf. Environ. Prot. 117, 286–295. https://doi.org/10.1016/j.psep.2018.04.027

Qi, S., Schideman, L., Mariñas, B.J., Snoeyink, V.L., Campos, C., 2007. Simplification of the IAST for activated carbon adsorption of trace organic compounds from natural water. Water Res. 41, 440–448. https://doi.org/10.1016/j.watres.2006.10.018

Renwick, A.G., Flynn, A., Fletcher, R.J., Müller, D.J.G., Tuijtelaars, S., Verhagen, H., 2004. Risk-benefit analysis of micronutrients. Food Chem. Toxicol. 42, 1903–1922. https://doi.org/10.1016/j.fct.2004.07.013

Saltelli, A., Annoni, P., 2010. How to avoid a perfunctory sensitivity analysis. Environ. Model. Softw. 25, 1508–1517. https://doi.org/10.1016/j.envsoft.2010.04.012

Santoro, D., Crapulli, F., Raisee, M., Raspa, G., Haas, C.N., 2015. Nondeterministic Computational Fluid Dynamics Modeling of Escherichia coli Inactivation by Peracetic Acid in Municipal Wastewater Contact Tanks. Environ. Sci. Technol. 49, 7265–7275. https://doi.org/10.1021/es5059742

Schriks, M., Heringa, M.B., Kooi, M.M.E. Van Der, Voogt, P. De, Wezel, A.P. Van, 2010. Toxicological relevance of emerging contaminants for drinking water quality. Water Res. 44, 461–476. https://doi.org/10.1016/j.watres.2009.08.023

Schultz, M., Strauch, U.G., Linde, H.-J., Watzl, S., Obermeier, F., Go¨ttl, C., Dunger, N., Grunwald, N., Scho¨lmerich, J., Rath, H.C., 2003. Preventive effects of Escherichia coli strain Nissle 1917 with different courses and different doses on intestinal inflammation in murine model of colitis. Inflamm. Res. 63, 873–883. https://doi.org/10.1007/s00011-014-0761-1

Staples, C., van der Hoeven, N., Clark, K., Mihaich, E., Woelz, J., Hentges, S., 2018. Distributions of concentrations of bisphenol A in North American and European surface waters and sediments determined from 19 years of monitoring data. Chemosphere 201, 448–458. https://doi.org/10.1016/j.chemosphere.2018.02.175

Thomaidi, V.S., Tsahouridou, A., Matsoukas, C., Stasinakis, A.S., Petreas, M., Kalantzi, O.I., 2020. Risk assessment of PFASs in drinking water using a probabilistic risk quotient methodology. Sci. Total Environ. 712, 136485. https://doi.org/10.1016/j.scitotenv.2019.136485

Tyl, R.W., Myers, C.B., Marr, M.C., Sloan, C.S., Castillo, N.P., Veselica, M.M., Seely, J.C., Dimond, S.S., Van Miller, J.P., Shiotsuka, R.N., Beyer, D., Hentges, S.G., Waechter, J.M., 2008. Two-generation reproductive toxicity study of dietary bisphenol A in CD-1 (swiss) mice. Toxicol. Sci. 104, 362–384. https://doi.org/10.1093/toxsci/kfn084

Van Der Voet, H., Slob, W., 2007. Integration of probabilistic exposure assessment and probabilistic hazard characterization. Risk Anal. 27, 351–371. https://doi.org/10.1111/j.1539-6924.2007.00887.x

Vries, D., Wols, B., Korevaar, M., Vonk, E., 2017. AquaPriori : a priori het verwijderingsrendement bepalen. https://library.kwrwater.nl/publication/55134952/

Westerhoff, P., Yoon, Y., Snyder, S., Wert, E., 2005. Fate of Endocrine-Disruptor, Pharmaceutical, and Personal Care Product Chemicals during Simulated Drinking Water Treatment Processes. Environ. Sci. Technol. 39, 6649–6663. https://doi.org/10.1021/es0484799

WHO-IPCS, 2018. Guidance document on evaluating and expressing uncertainty in hazard characterization– 2nd edition. WHO-IPCS harmonization project document no. 11. ISBN 978-92-4-151354-8. Licence: CC BYNC-SA 3.0 IGO., World Health Organization. https://doi.org/ISBN 978 92 4 150761 5

WHO, 2006. WHO guidelines for drinking-water quality. Water Supply 11, 1–16.

Supporting material

Table S1. BPA $C_{IN,MAX}$ data, associated with the water matrix (DW = Drinking Water, GW = Groundwater, RW = Raw Water, SW = Surface Water) and the relative reference.

Water matrix	$C_{IN,MAX}$ [µg/L]	Reference
RW	0.26	Gogoi et al., 2018
SW	0.23	
GW	1.41	
RW	0.04	
SW	0.49	Meffe, 2014
DW	0.68	Riva et al., 2018
SW	0.11	RIWA, 2016
SW	0.06	RIWA, 2017
SW	0.02	
SW	0.06	RIWA, 2018
SW	0.02	
RW	1.42	Sousa et al., 2018
SW	0.17	
SW	0.19	
RW	0.31	
RW	0.52	
RW	0.33	
SW	0.13	
RW	4.13	
RW	3.61	
RW	1.34	
RW	0.56	
SW	0.04	
RW	0.69	
RW	0.17	
RW	1.04	
SW	0.18	
SW	2.90	
RW	0.03	
SW	8.00	Staples et al., 2000
SW	0.25	Staples et al., 2018
SW	0.60	
SW	0.08	
SW	0.06	
SW	0.17	
SW	0.58	
SW	0.22	
SW	0.32	
SW	0.08	
SW	0.04	
SW	0.11	
SW	1.29	
SW	0.44	
SW	0.05	
SW	0.16	
SW	0.15	
SW	0.13	
SW	1.28	
SW	0.03	
SW	0.64	
SW	0.06	
SW	0.73	Staples et al., 2018
SW	0.02	
SW	0.01	
SW	0.00	
SW	1.53	
SW	0.09	
SW	0.01	
SW	0.14	
SW	0.08	
SW	0.20	
SW	0.04	
SW	0.08	
SW	0.11	
SW	0.30	
SW	0.06	
SW	0.12	
SW	0.01	
SW	0.02	
SW	0.02	
SW	0.05	
SW	0.04	
SW	0.08	
SW	0.07	
SW	0.02	
SW	0.04	
SW	0.45	
SW	0.90	
SW	0.02	
SW	0.05	
SW	0.02	
SW	0.61	
SW	0.01	
SW	0.16	
SW	0.05	
SW	0.24	
SW	1.90	
SW	0.14	
SW	0.05	
SW	0.93	
SW	0.12	
SW	0.32	
SW	0.74	
SW	12.00	
SW	0.19	
SW	1.50	
SW	2.76	
SW	3.20	
SW	0.07	
SW	2.00	
SW	0.02	
SW	0.28	
RW	0.02	Staples et al., 2018
RW	0.33	
RW	0.03	
RW	0.01	
RW	0.07	
RW	0.38	
RW	0.02	
RW	0.88	
RW	0.25	
RW	10.70	
RW	0.06	
RW	0.06	
RW	0.04	
RW	0.10	
RW	0.52	
RW	0.07	
RW	0.31	
RW	0.04	
RW	0.19	
RW	0.19	
RW	0.46	
RW	0.90	
RW	0.02	
RW	0.13	
RW	0.04	
RW	0.15	
RW	0.04	
RW	0.06	
RW	0.35	
SW	0.02	
SW	0.10	
SW	0.33	
SW	2.97	
SW	0.13	
SW	0.06	
SW	0.06	
SW	0.65	
SW	0.10	
SW	0.12	
RW	0.34	
RW	0.02	
RW	0.07	
RW	0.01	
RW	0.00	
RW	0.06	
RW	0.02	
RW	0.03	
RW	0.02	
SW	0.03	
SW	0.04	
SW	0.18	

SW	0.79	Staples et al., 2018
SW	0.08	
SW	0.08	
SW	0.78	
SW	0.09	
SW	0.90	
SW	0.68	
SW	0.01	
SW	0.05	
SW	0.42	
SW	5.84	
SW	0.09	
SW	1.92	
SW	0.10	
SW	6.00	
SW	0.75	
SW	0.04	
SW	0.08	
SW	1.00	
SW	0.07	
SW	0.49	
SW	0.14	
SW	0.46	
SW	0.06	
SW	0.85	
SW	0.16	
SW	0.01	
SW	0.12	

SW	0.06	Staples et al., 2018
SW	0.24	
SW	0.30	
SW	0.19	
SW	0.07	
SW	0.40	
SW	0.36	
SW	8.00	
SW	0.76	
SW	0.04	
SW	0.06	
SW	0.81	
SW	1.90	
SW	0.04	
SW	0.21	
SW	0.15	
RW	0.02	
RW	0.01	
RW	0.01	
RW	0.02	
RW	0.00	
RW	0.02	
RW	0.06	
RW	0.05	
RW	0.02	
RW	0.08	
RW	0.15	
RW	0.07	

SW	0.00	Staples et al., 2018
SW	0.07	
SW	0.14	
SW	0.49	
SW	0.03	
SW	0.17	
SW	0.28	
SW	0.16	
SW	1.00	
SW	0.01	
SW	0.00	
SW	0.04	
SW	43.00	
SW	0.01	
SW	4.00	
SW	0.01	
SW	0.68	
SW	7.60	
SW	0.06	
SW	0.05	
SW	0.01	
SW	0.03	
SW	4.80	
SW	0.11	
SW	0.12	
SW	0.00	

Table S2. GAC particle size data, carbon origin (coal or vegetal) and literature reference. For the particle size range, minimum and maximum or the mean value is reported. "Confidential" refers to data coming from the full-scale DWTPs in an urbanized area in northern Italy.

Carbon origin	**GAC particle size [mm]**			**Reference**
	Min	**Max**	**Mean**	
Coal	0.45	1	n.a.	Abdel daiem et al., 2015
Vegetal	n.a.	n.a.	1.36	Bablon et al., 1988
n.a.	n.a.	n.a.	1.2	Bablon et al., 1988
n.a.	0.5	2	n.a.	Confidential
Coal	0.6	2	n.a.	Frank et al., 2015
Coal	n.a.	n.a.	0.55	Katsigiannis et al., 2015
n.a.	0.92	1.29	n.a.	Kennedy et al., 2017
Vegetal	0.72	1.24	n.a.	Knappe et al., 1999
Vegetal	0.79	1.18	n.a.	Knappe et al., 1999
n.a.	1.005	1.413	n.a.	Park et al., 2020
Coal	0.6	2.4	n.a.	Ruhl et al., 2015
Coal	0.6	1.7	n.a.	Ruhl et al., 2015
n.a.	n.a.	n.a.	2	Worch, 2008

Table S3. Bed porosity data, carbon origin (coal or vegetal) and literature reference. For the bed porosity range, minimum and maximum or the mean value is reported.

Carbon origin	Bed porosity [-]			Reference
	Min	Max	Mean	
Coal	0.45	1	n.a.	Abdel daiem et al., 2015
Vegetal	n.a.	n.a.	0.45	Bablon et al., 1988
n.a.	n.a.	n.a.	0.45	Bablon et al., 1988
n.a.	n.a.	n.a.	n.a.	Kennedy et al., 2017
Vegetal	0.59	0.6	n.a.	Knappe et al., 1999
Vegetal	0.58	0.6	n.a.	Knappe et al., 1999
Coal	n.a.	n.a.	0.79	Piazzoli & Antonelli, 2018
Vegetal	n.a.	n.a.	0.78	Piazzoli & Antonelli, 2018
n.a.	n.a.	n.a.	0.4	Worch, 2008

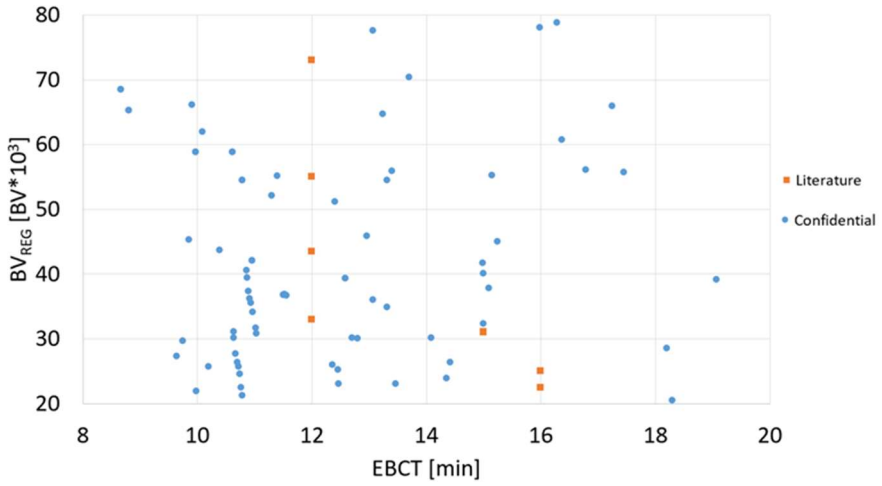

Figure S1. Distribution of the BV_{REG} and EBCT value related data. Data collected from literature (orange dots) and data from confidential data collected from different DWTPs in an urbanised area in northern Italy (blue dots).

Table S4. BPA Freundlich parameters data (K_F and 1/n) found in literature. Each couple of parameters was obtained from a batch adsorption test, where also information about the water matrix (DW = Drinking Water, GW = Groundwater, RW = Raw Water, SM = Synthetic Matrix, SW = Surface Water, TWW = Treated Wastewater), the carbon origin (coal or vegetal), and type of activation (commercial or experimental) were reported.

Water matrix	Activated Carbon		Freundlich parameters		Reference
	Origin	Activation	K_F (mg/g)/(mg/L)$^{1/n}$	1/n [-]	
SM	Vegetal	Commercial	80.82	0.15	Abdel daiem et al., 2015
SM	Vegetal	Commercial	92.17	0.30	Abdel daiem et al., 2015
SM	Vegetal	Experimental	5.48	0.34	Antero et al., 2019
SM	Vegetal	Experimental	67.24	0.36	Arampatzidou & Deliyanni, 2016
SM	Vegetal	Experimental	49.43	0.34	Arampatzidou & Deliyanni, 2016
SM	Vegetal	Experimental	41.13	0.29	Arampatzidou & Deliyanni, 2016
SM	Vegetal	Experimental	28.61	0.39	Arampatzidou & Deliyanni, 2016
SM	Vegetal	Experimental	19.45	0.41	Arampatzidou & Deliyanni, 2016
SM	Vegetal	Experimental	8.66	0.51	Arampatzidou & Deliyanni, 2016
SM	Vegetal	Commercial	153.82	0.34	Arampatzidou et al., 2018
SM	Vegetal	Commercial	86.68	0.45	Arampatzidou et al., 2018
SM	Vegetal	Commercial	126.47	0.39	Arampatzidou et al., 2018
SM	Vegetal	Commercial	63.58	0.38	Arampatzidou et al., 2018

Water matrix	Activated Carbon		Freundlich parameters		Reference
	Origin	Activation	K_F (mg/g)/(mg/L)$^{1/n}$	1/n [-]	
SM	Vegetal	Commercial	54.06	0.40	Arampatzidou et al., 2018
SM	Vegetal	Commercial	41.46	0.42	Arampatzidou et al., 2018
SM	Coal	Commercial	44.85	0.27	Bautista-Toledo et al., 2005
SM	Coal	Commercial	79.84	0.38	Bautista-Toledo et al., 2005
SM	Vegetal	Experimental	46.08	0.38	Bautista-Toledo et al., 2005
SM	Coal	Commercial	16.35	0.46	Bhadra et al., 2018
SM	n.a.	Experimental	63.02	0.37	Bhadra et al., 2018
SM	n.a.	Experimental	100.04	0.44	Bhadra et al., 2018
SM	n.a.	Experimental	75.98	0.42	Bhadra et al., 2018
TWW	Coal	Commercial	184.00	0.10	Choi et al., 2005
TWW	Coal	Commercial	119.00	0.11	Choi et al., 2005
TWW	Coal	Commercial	67.00	1.15	Choi et al., 2005
TWW	Vegetal	Commercial	115.00	0.11	Choi et al., 2005
TWW	Vegetal	Commercial	68.00	1.00	Choi et al., 2005
TWW	Vegetal	Commercial	68.00	0.20	Choi et al., 2005
TWW	Vegetal	Commercial	144.00	0.32	Choi et al., 2005
SM	Vegetal	Commercial	88.10	0.34	Choong et al., 2018
SM	Vegetal	Commercial	55.10	0.26	Choong et al., 2018
SM	Coal	Commercial	10.549	0.271	Ifelebuegu et al., 2015
SM	Coal	Commercial	145.00	0.18	Javed et al., 2018
DW	n.a.	Experimental	88.47	0.27	Liu et al., 2017
DW	n.a.	Experimental	71.42	0.30	Liu et al., 2017
DW	n.a.	Experimental	53.41	0.36	Liu et al., 2017
DW	n.a.	Experimental	39.62	0.36	Liu et al., 2017
DW	n.a.	Experimental	33.19	0.37	Liu et al., 2017
DW	n.a.	Experimental	23.93	0.43	Liu et al., 2017
DW	n.a.	Commercial	42.99	0.30	Liu et al., 2017
DW	n.a.	Commercial	49.77	0.23	Liu et al., 2017
DW	n.a.	Commercial	41.89	0.25	Liu et al., 2017
SM	Vegetal	Commercial	190.55	0.25	Liu et al., 2017
SM	Vegetal	Commercial	157.67	0.28	Liu et al., 2017
SM	Vegetal	Commercial	134.56	0.31	Liu et al., 2017
SM	Vegetal	Commercial	124.34	0.30	Liu et al., 2017
SM	Vegetal	Commercial	255.26	0.20	Liu et al., 2017
SM	Vegetal	Commercial	223.77	0.24	Liu et al., 2017
SM	Vegetal	Commercial	211.14	0.24	Liu et al., 2017
SM	Vegetal	Commercial	208.95	0.23	Liu et al., 2017
SM	Coal	Commercial	96.04	0.43	López-Ramón et al., 2019
SM	Coal	Commercial	55.50	0.38	López-Ramón et al., 2019
SM	Coal	Commercial	81.49	0.17	Ndagijimana et al., 2019
SM	Coal	Commercial	66.80	0.20	Ndagijimana et al., 2019
SM	Coal	Commercial	62.54	0.17	Ndagijimana et al., 2019
SM	Coal	Commercial	98.95	0.10	Ndagijimana et al., 2019
SM	Coal	Commercial	110.00	0.10	Ndagijimana et al., 2019
SM	Coal	Commercial	120.99	0.11	Ndagijimana et al., 2019
TWW	n.a.	Commercial	62.15	0.95	Noutsopoulos et al., 2014
DW	Vegetal	Experimental	26.61	0.52	Soni & Padmaja, 2014
SM	Coal	Commercial	30.75	0.13	Wang & Harrison, 2018
SM	Vegetal	Experimental	20.66	0.18	Wirasnita et al., 2014
DW	Vegetal	Commercial	27.07	0.55	Yan et al., 2016
DW	Coal	Commercial	101.56	0.19	Yan et al., 2016
SM	Vegetal	Experimental	185.84	0.53	Zbair et al., 2018
SM	Vegetal	Experimental	190.55	0.39	Zbair et al., 2018

Section S1

In this section the databases of all the factors on which the health effects assessment step of the developed QCRA procedure is based are reported. Firstly, the procedure that has been applied to each guideline or documentation containing toxicological information about the CECs of interest is reported. In particular, the methodology through which the data have been identified and, then, kept or discarded, is reported. The list of all the Guidelines processed and analysed for the BPA toxicological characterization is reported in the Table S5, while the collected toxicological data are reported in Table S6 for BPA. In Figure S2 a scheme of the procedure through which all these guidelines were processed for the BPA case is illustrated.

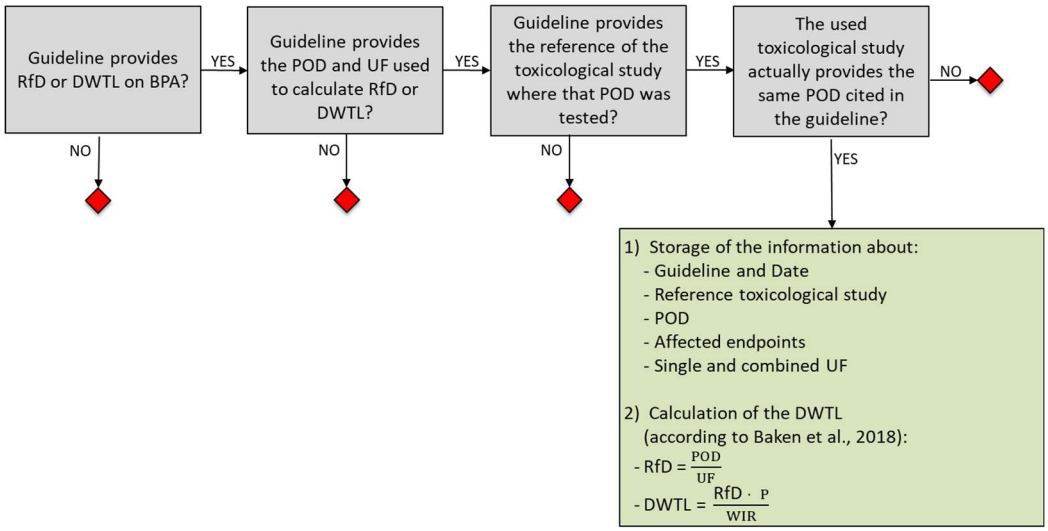

Figure S2. Schematic overview of the guidelines processing procedure for the BPA case.

This procedure can be summarized in the following steps:

1) The guideline has been read through looking for RfD or DWTL. If no data were found on the considered CEC, the guideline has been excluded, otherwise the procedure was brought forward;
2) Once one of the afore-mentioned data has been found, information about the Point of Departure (PoD) and UF used for the calculation of RfD or DWTL have been looked for. If no data were found, the guidelinehas been excluded, otherwise the procedure was brought forward;
3) Once that PoD data has been found, it was checked if it was reported the toxicological study where that specific PoD was measured. If no reference on the toxicological study was reported, the guideline has been excluded, otherwise the procedure was brought forward;
4) Once that the toxicological study was found, it was checked whether the used toxicological study actually provides the same PoD cited in the guideline. If no correspondence was found, the guideline/documentation has been excluded, otherwise the procedure was brought forward;
5) In the final database a new row for that guideline was inserted and information were stored about:
   - Reference toxicological study;
   - PoD given by the toxicological study;
   - Combined UF, associated to the PoD, defined in the guideline;
   - Affected endpoints given by the toxicological study;
6) Once that all the required values were found, the DWTL has been computed according to the relations reported by Baken et al. (2018):
   - $\text{RfD} = \frac{\text{PoD}}{\text{UF}}$
   - $\text{DWTL} = \frac{\text{RfD} \cdot \text{P}}{\text{WIR}}$

Table S5: List of processed guidelines and their compliance to requirements.

Guideline	RfD or DWTL provided?	PoD and UF used to calculate RfD or DWTL provided?	Toxicological study actually provides the same PoD cited in the guideline?
Drinkwaterbesluit	NO		
Drinkwaterregeling	NO		
Regeling materialen en chemicaliën drink- en warm tapwatervoorziening	NO		
Rijksinstituut voor Volksgezondheid en Milieu (RIVM)	NO		
US E.P.A. National Primary DW Standards and Regulations	NO		
US E.P.A. DW Contaminant Candidate List (CCL4)	NO		
Public Health Goals OEHHA California	NO		
Australian DW Guidelines	NO		
Guidelines for Canadian DW Quality	NO		
U.S. Geological Survey (USGS) Health-based Screening Levels	YES	NO	
WHO Guidelines for DW quality	YES	NO	
EU DW Directive	YES	NO	
U.S. EPA Human Health Benchmarks for Pesticides	YES	NO	
Pesticide Properties DataBase (PPDB)	YES	NO	
EC Scientific Committees	YES	NO	
European Chemicals Agency (ECHA)/CSTEE	YES	NO	
CSTEE	YES	NO	
National Toxicology Program - Center for the Evaluation of Risks to Human Reproduction (NTP-CERHR)	YES	NO	
WHO International Programme on Chemical Safety (IPCS)	YES	NO	
U.S. EPA (Chemistry Dashboard)	YES	NO	
Australian Pesticides and Veterinary Medicines Authority	YES	NO	
TOXNET	YES	NO	
Agency for Toxic Substances and Disease Registry (ATSDR)	YES	NO	
Danish EPA (2014)	YES	YES	YES
DTU - National Food Institute (2015)	YES	YES	YES
Minnesota Department of Health (MDH) (2015)	YES	YES	YES
European Food Safety Authority (EFSA) CEF (2015)	YES	YES	YES
NSF (2008)	YES	YES	YES
European Food Safety Authority (EFSA) AFC (2007)	YES	YES	YES
European Food Safety Authority (EFSA) (2010)	YES	YES	YES
American Water Works Association (AWWA) 2008	YES	YES	YES
IRIS (2011)	YES	YES	YES
WHO OECD eChemPortal (1998)	YES	YES	YES

Table S6. Collected BPA toxicological data (RfD), toxicological parameters, endpoints affected (DEV = developmental, END = endocrine, HEP = hepatic, NEUR = neurological, REN = renal, IMM = immune, REPR = reproductive), the guideline from which the RfD has been collected and the reference study from which the NOAEL has been collected.

RfD [mg/(kg day)]	DWTL [μg/L]	Endpoints affected	Guideline	Reference study
0.05	350.00	DEV	AWWA, 2008	Tyl et al., 2002
0.046	322.00	HEP	AWWA, 2008	National Toxicology Program, 1982
0.00005	0.35	REPR	Danish EPA, 2014	Jones et al., 2011
0.0004	2.67	DEV, END	Danish EPA, 2014	Ryan & Vandenbergh, 2006
0.00095	6.67	DEV	Danish EPA, 2014	Xu et al., 2010
0.0018	12.80	DEV, NEUR	Danish EPA, 2014	Viberg et al., 2011
0.007	5.04	END	DTU National Food Institute, 2015	Delclos et al., 2014
0.01	70.00	END, HEP, NEUR, REN	EFSA, 2010	Tyl et al., 2002
0.05	350.00	END, HEP, NEUR, REN	EFSA, 2010	Tyl et al., 2002
0.004	28.43	DEV, END, NEUR, REPR	EFSA, 2015	Tyl et al., 2008
0.16	1096.2	DEV, END, HEP, REPR, REN	MDH, 2014	Delclos et al., 2014
0.0065	45.50	HEP, REN	MDH, 2014	Tyl et al., 2008
0.017	116.67	END, HEP, NEUR, REN	NSF, 2008	Tyl et al., 2002, 2008
0.05	350.0	DEV	US EPA, 2010	National Toxicology Program, 1982
0.25	1750.0	REPR	WHO OECD ILSI/HESI, 2011	Tyl et al., 2002
0.016	112.0	DEV, REPR	Willhite et al., 2008	Tyl et al., 2002, 2008

Table S7. APROBA-Plus inputs related to study, endpoint and protection goals of the hazard characterization of BPA.

INPUTS RELATED TO STUDY, END-POINT AND PROTECTION GOALS		
DESCRIPTION	**INPUTS**	**COMMON VALUE(S)**
End-point	Mean relative kidney weight	Case-specific
Data type	Continuous	Case-specific
Data route	Oral	Case-specific
Study type	Subchronic	Case-specific
Test species	Mouse	Case-specific
Body weight test species (kg)	0.020	0.02
Human median body weight (kg)	60	60
Target BMR (= *M* , user input for BMDLs only)	10%	5%
Population incidence goal (= *I*)	1%	5%, 1%, 0.1%, 0.01%
Probabilistic coverage goal	95%	95%
PoD type	BMDL	Case-specific
PoD value	8.96	Case-specific
BMDU (User input for BMDL PoDs)	108.9	Case-specific
PoD units	mg/kg body weight per day	mg/kg body weight per day
Deterministic overall AF	2205	Case-specific
Deterministic RfD	0.00406	Calculated
Exposure estimate (optional)		User supplied

Table S8. APROBA-Plus inputs related to adjustment, variability and uncertainty of the hazard characterization of BPA.

INPUTS RELATED TO ADJUSTMENT, VARIABILITY AND UNCERTAINTY			
HAZARD CHARACTERIZATION ASPECT		**INPUTS**	**PROVISIONAL VALUE(S)**
PoD	LCL	8.96	Calculated from inputs
(Modelled BMD uncertainty)	UCL	108.90	Calculated from inputs
NOAEL to BMD	LCL	1.00	1.00
(NOAEL or LOAEL only)	UCL	1.00	1.00
Interspecies scaling	LCL	8.02	8.02
(Allometric for oral)	UCL	15.21	15.21
Interspecies TK/TD	LCL	0.33	0.33
(Remaining TK & TD)	UCL	3.00	3.00
Duration extrapolation	LCL	0.50	0.50
	UCL	8.00	8.00
Intraspecies	LCL	2.24	2.24
	UCL	41.88	41.88
Other aspect #1	LCL	1.00	1.00
Limited toxicity data	UCL	6.00	1.00
Other aspect #2	LCL	1.00	1.00
(Description here)	UCL	1.00	1.00
Other aspect #3	LCL	1.00	1.00
(Description here)	UCL	1.00	1.00

Table S9. Summary of the case studies conditions and assumed input values.

Case study	**DW-NO_GAC**	**DW-GAC**	**WCS-GAC**	**WCS-GAC_Up**	**WCS-GAC_Manag**
Maximum inlet concentration	0.0012 – 43 µg/L	0.0012 – 43 µg/L	43 µg/L	43 µg/L	43 µg/L
GAC process	Absent	Managed for regulated and routinely monitored micropollutants	Managed for regulated and routinely monitored micropollutants	Optimally managed for CECs	Optimally managed for CECs
Freundlich parameters	NA	Literature on real DW sources tests	Literature on real DW sources tests	Literature on real DW sources tests	Literature on real DW sources tests
EBCT	NA	12 min	12 min	8 – 20 min	12 min
Time of GAC regeneration	NA	80,000 BV	80,000 BV	80,000 BV	0 – 80,000 BV

Table S10. Summary of the obtained statistical distributions of input parameters and AIC values. For the lognormal distribution *a* corresponds to µ and *b* to σ on a $\log_{10}$-scale; for the beta distribution *a* corresponds to α and *b* to β; for the triangular distribution *a*, *b* and *c* correspond respectively to minimum, maximum and mode; while for the uniform distribution *a* and *b* correspond to minimum and maximum.

Model input parameter	**Best fitting distribution**	**Distribution parameters**			**AIC value**
		a	*b*	*c*	
$C_{IN,MAX}$	lognormal	-2.04	1.81		628.28
EBCT	beta	1.04	1.86		530.36
BV_{REG}	beta	0.94	1.58		655.61
GAC particle size	triangular	0.45	2.4	1.2	597.33
Bed porosity	uniform	0.4	0.8		501.12

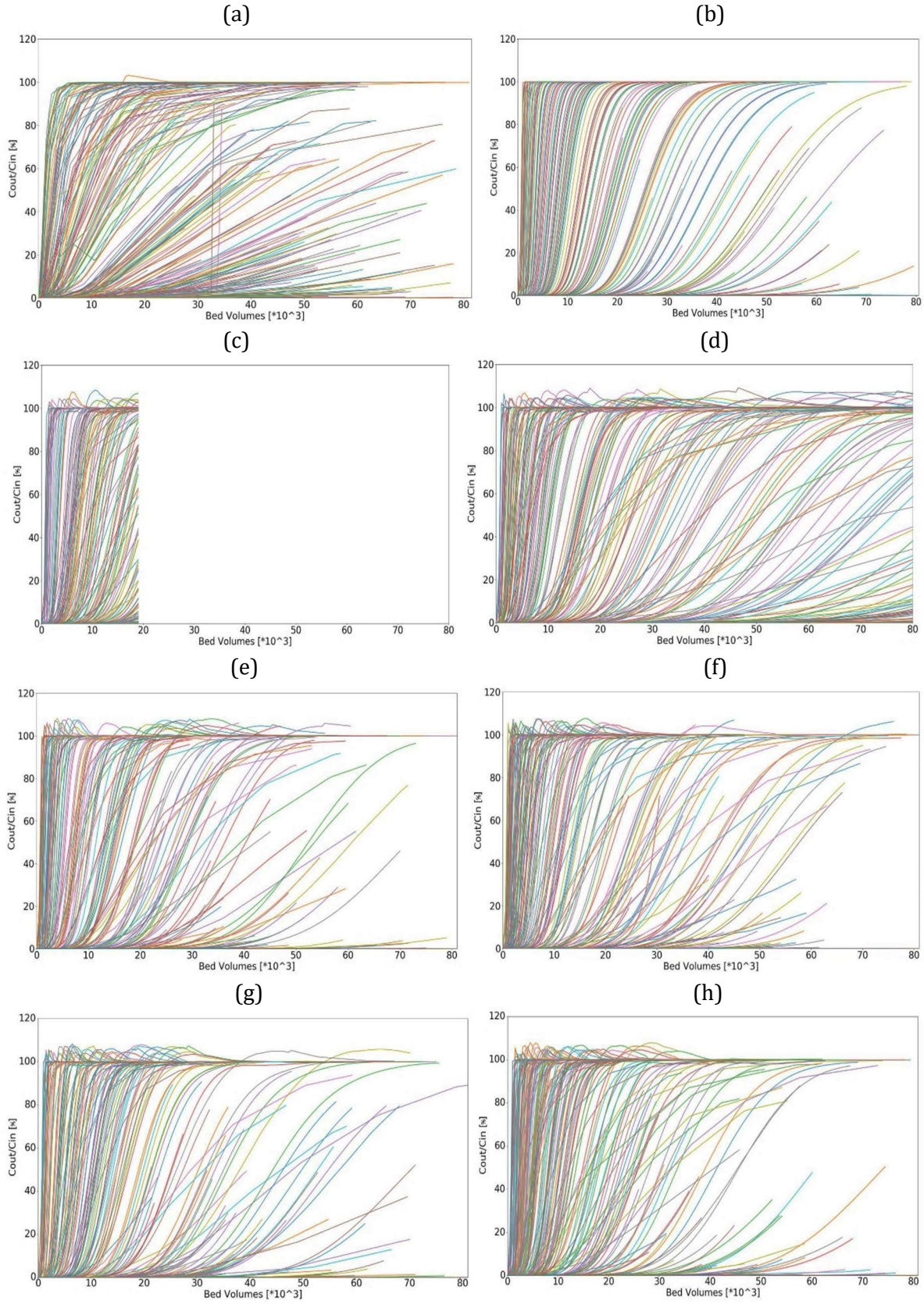

Figure S3. Breakthrough curves resulting from the sensitivity analysis of inputs. For each chart, the evaluated input was kept constant at the value reported below, while all the other factors were varied. The constant values of the evaluated input in each graph are reported here: (a) $C_{IN,MAX}$ = 0.0012 µg/L; (b) $C_{IN,MAX}$ = 43 µg/L; (c) BV_{REG} = 19000 BV; (d) BV_{REG} = 80000 BV; (e) GAC particle size = 0.45 mm; (f) GAC particle size = 2.4 mm; (g) bed porosity = 0.4; (h) bed porosity = 0.8.

Table S11. APROBA-Plus output for RfD uncertainty contribution evaluation.

INTERMEDIATE CALCULATIONS FOR UNCERTAINTY ANALYSES				**% contribution**
ASPECT			**[log(P95/P50)]^2**	**to overall uncertainty**
PoD	**P50**	31.24		20%
	P95/P50	3.49	0.294	
NOAEL to BMD	**P50**	1.00		--
	P95/P50	1.00	0.000	
Interspecies scaling	**P50**	11.04		1%
	P95/P50	1.38	0.019	
Interspecies TK/TD	**P50**	1.00		16%
	P95/P50	3.00	0.228	
Duration extrapolation	**P50**	2.00		25%
	P95/P50	4.00	0.362	
Intraspecies	**P50**	9.69		28%
	P95/P50	4.32	0.404	
Other aspect #1	**P50**	2.45		10%
Limited toxicity data	**P95/P50**	2.45	0.151	
Other aspect #2	**P50**	1.00		--
(Description here)	**P95/P50**	1.00	0.000	
Other aspect #3	**P50**	1.00		--
(Description here)	**P95/P50**	1.00	0.000	
		Non-Prob.	**Approx. Prob.**	**Greatest contributor**
Target Human Dose (HD_M^I)	**P50**	**0.060**	**0.060**	**to overall uncertainty**
	UCL/P50	**610.376**	**16.145**	**Intraspecies**

Table S12. Percentiles of the BQ distributions resulting from the four repetition of 1000 Monte Carlo simulations with mean, standard deviation, and standard error.

Repetition	**Percentiles**										
	1%	**5%**	**10%**	**25%**	**50%**	**75%**	**90%**	**95%**	**98%**	**99%**	**99.9%**
1	0.00038	0.00040	0.00045	0.00066	0.0016	0.0063	0.0348	0.115	0.479	1.210	8.892
2	0.00043	0.00045	0.00051	0.00075	0.0017	0.0069	0.0375	0.123	0.502	1.256	9.039
3	0.00037	0.00040	0.00043	0.00061	0.0015	0.0058	0.0335	0.114	0.488	1.250	9.353
4	0.00041	0.00042	0.00048	0.00070	0.0016	0.0065	0.0356	0.117	0.482	1.213	8.841
Mean	0.0004	0.00042	0.00047	0.00068	0.0016	0.0063	0.0354	0.117	0.488	1.232	9.031
Dev.st	2.6E-05	2.5E-05	3.3E-05	5.7E-05	0.0001	0.0005	0.0017	0.004	0.010	0.024	0.230
Err.st	6.65	6.02	7.06	8.41	6.88	7.30	4.72	3.22	2.09	1.97	2.55

Table S13. Results of the pairwise comparison of the BQ output of the four simulations through a two-sample Kolmogorov-Smirnov test with two-sided alternative hypothesis and significance level α=0.05: test statistic D and p-values for each couple of simulations.

Coupled Simulations	1-2	1-3	1-4	2-3	2-4	3-4
Statistic D	0.027	0.04	0.021	0.032	0.038	0.049
p-value	0.8593	0.4005	0.9802	0.6852	0.4658	0.1811

Table S14. APROBA-Plus output for approximate probabilistic RfD.

APPROXIMATE PROBABILISTIC ANALYSIS OUTPUTS			
Standard Confidence Interval			
Target Human Dose (HD_M^I)	**LCL (P05)**	**0.0036918**	**mg/kg body weight per day**
	UCL (P95)	**0.9623248**	**mg/kg body weight per day**
Degree of Uncertainty (Fold Range)			**261**
Estimated "Coverage" of Deterministic RfD			**94.4%**
Probabilistic RfD	= Approximate probabilistic HD_M^I at specified % confidence		
0.0036918	= Estimate of dose (mg/kg body weight per day) at which, with		
	95% confidence		
	1% of the population will have		**Mean relative kidney weight**
	of magnitude ≥		**10%**

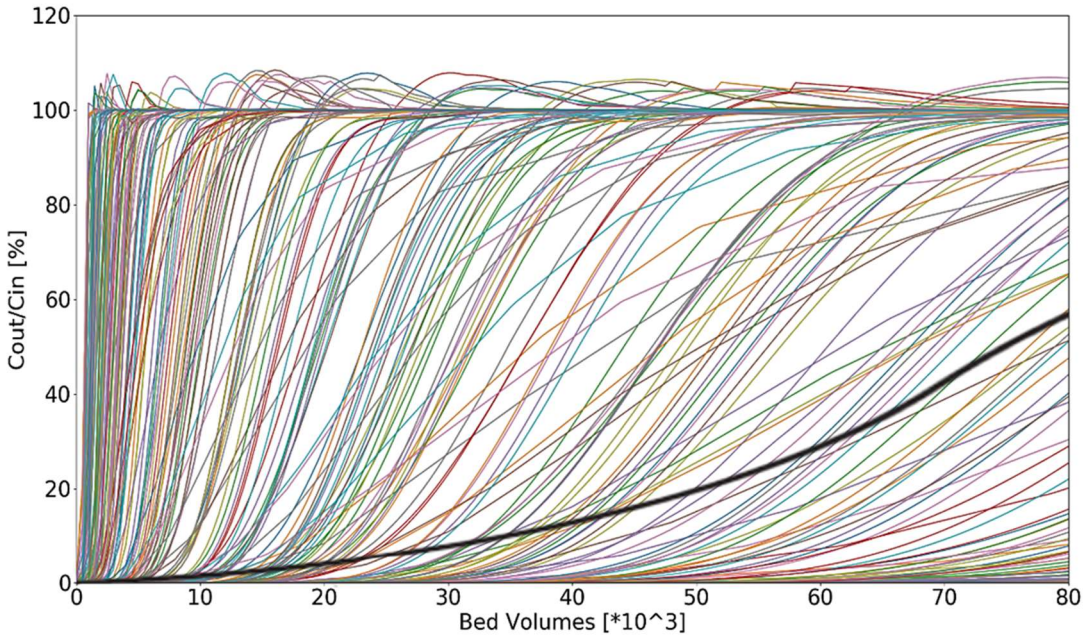

Figure S4. Breakthrough curves resulting from the uncertainty analysis: coloured curves are the output of 1000 Monte Carlo simulations, while the black curve is the deterministic breakthrough curve.

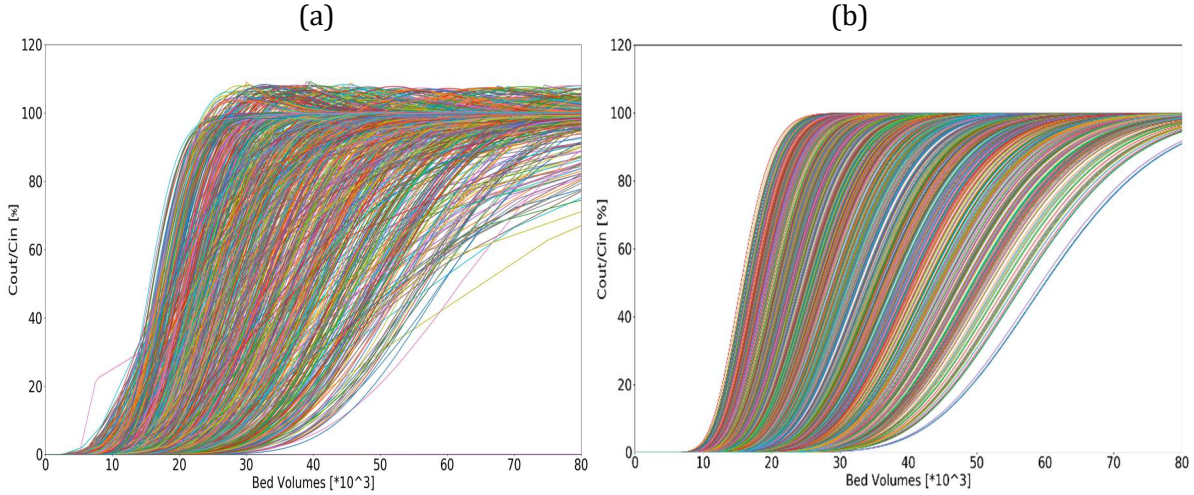

Figure S5 Simulated BPA breakthrough curves for: (a) DW-GAC case study, (b) WCS-GAC case study.

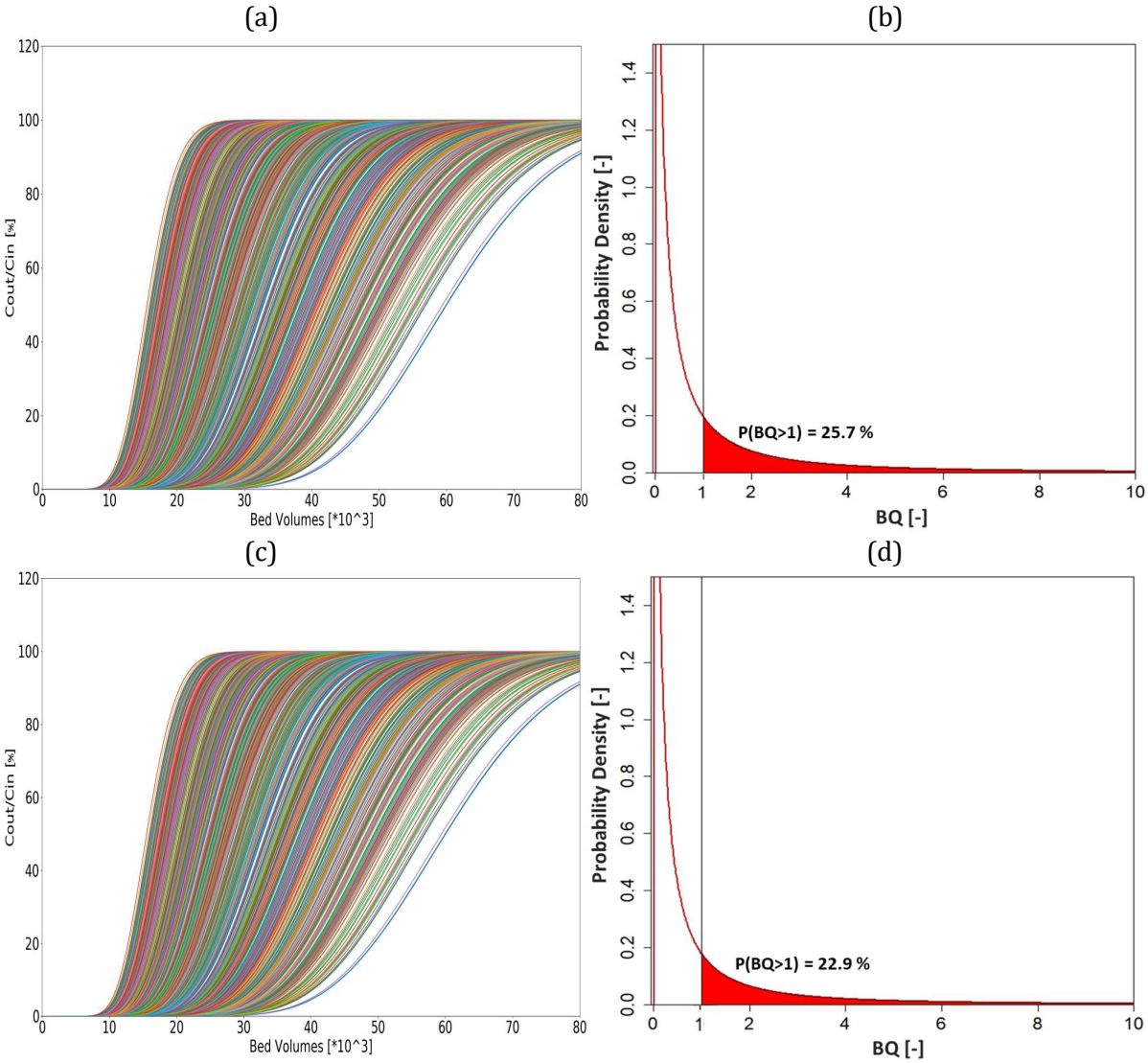

Figure S6. Results from the WCS-GAC_Up case where the EBCT is the optimized parameter. Charts (a) and (b) show respectively the breakthrough curves and the BQ distribution obtained for the minimum EBCT (8 min); while charts (c) and (d) show the same outputs for the maximum EBCT (20 min).

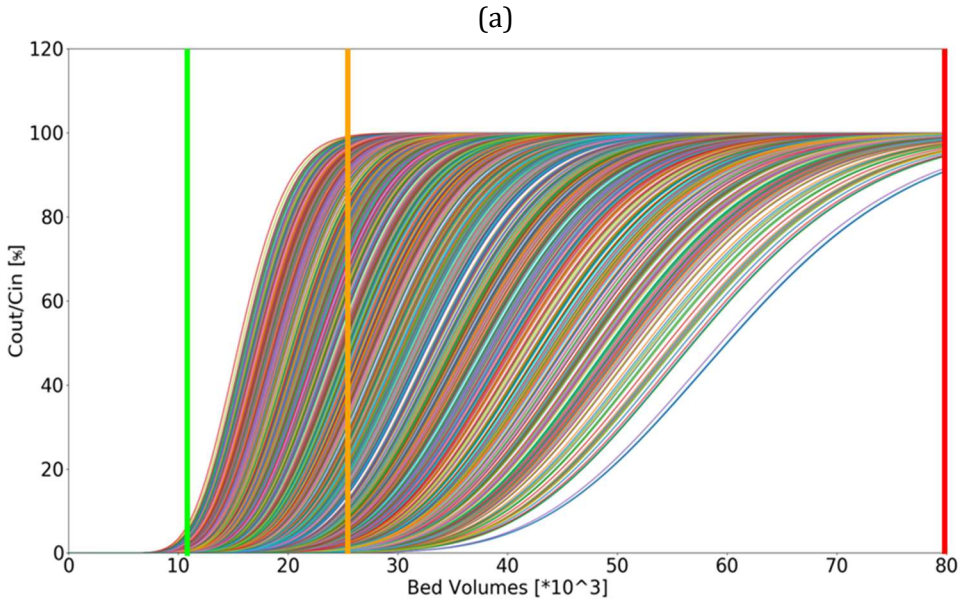

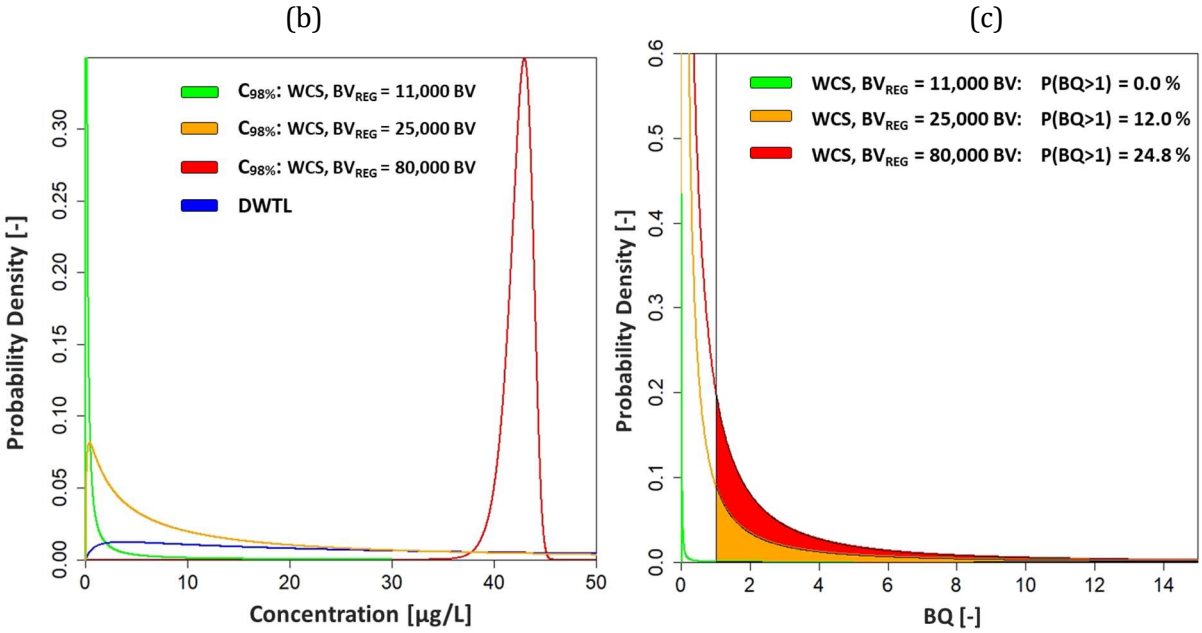

Figure S7. Optimization output: (a) breakthrough curves, probability density for (b) $C_{98\%}$ and DWTL, (c) quantitative BQ for the WCS-GAC_Manag scenario at three simulated regeneration times (BV_{REG}).

Supporting material - References

Abdel daiem, M. M., Rivera-Utrilla, J., Sánchez-Polo, M., & Ocampo-Pérez, R. (2015). Single, competitive, and dynamic adsorption on activated carbon of compounds used as plasticizers and herbicides. *Science of the Total Environment*, *537*, 335–342. https://doi.org/10.1016/j.scitotenv.2015.07.131

Antero, R. V. P., Alves, A. C. F., Ferreira Sales, P. de T., de Oliveira, S. B., Ojala, S. A., & Brum, S. S. (2019). A new approach to obtain mesoporous-activated carbon via hydrothermal carbonization of Brazilian Cerrado biomass combined with physical activation for bisphenol-A removal. *Chemical Engineering Communications*, *206*(11), 1509–1525. https://doi.org/10.1080/00986445.2019.1601625

Arampatzidou, A. C., & Deliyanni, E. A. (2016). Comparison of activation media and pyrolysis temperature for activated carbons development by pyrolysis of potato peels for effective adsorption of endocrine disruptor bisphenol-A. *Journal of Colloid and Interface Science*, *466*, 101–112. https://doi.org/10.1016/j.jcis.2015.12.003

Arampatzidou, A. C., Voutsa, D., Deliyanni, E. A., & Matis, K. A. (2017). Adsorption of endocrine disruptor bisphenol A by carbonaceous materials: Influence of their porosity and specific surface area. *Desalination and Water Treatment*, *76*, 232–240. https://doi.org/10.5004/dwt.2017.20706

Arampatzidou, A., Voutsa, D., & Deliyanni, E. (2018). Removal of bisphenol A by Fe-impregnated activated carbons. *Environmental Science and Pollution Research*, *25*(26), 25869–25879. https://doi.org/10.1007/s11356-018-2652-4

AWWA. (2008). Toxicological Relevance of EDCs and Pharmaceuticals in Drinking Water. In *WateReuse*.

Bablon, G. P., Ventresque, C., & Ben Aim, R. (1988). Developing a sand-GAC filter to achieve high-rate biological filtration. *Journal / American Water Works Association*, *80*(12), 47–53. https://doi.org/10.1002/j.1551-8833.1988.tb03149.x

Baken, K. A., Sjerps, R. M. A., Schriks, M., & Wezel, A. P. Van. (2018). Toxicological risk assessment and prioritization of drinking water relevant contaminants of emerging concern. *Environment International*, *118*(May), 293–303. https://doi.org/10.1016/j.envint.2018.05.006

Bautista-Toledo, I., Ferro-García, M. A., Rivera-Utrilla, J., Moreno-Castilla, C., & Fernández, F. J. V. (2005). Bisphenol A removal from water by activated carbon. Effects of carbon characteristics and solution chemistry. *Environmental Science and Technology*, *39*(16), 6246–6250. https://doi.org/10.1021/es0481169

Bhadra, B. N., Lee, J. K., Cho, C. W., & Jhung, S. H. (2018). Remarkably efficient adsorbent for the removal of bisphenol A from water: Bio-MOF-1-derived porous carbon. *Chemical Engineering Journal*,

343(February), 225–234. https://doi.org/10.1016/j.cej.2018.03.004

Choi, K. J., Kim, S. G., Kim, C. W., & Kim, S. H. (2005). Effects of activated carbon types and service life on removal of endocrine disrupting chemicals: Amitrol, nonylphenol, and bisphenol-A. *Chemosphere*, *58*(11), 1535–1545. https://doi.org/10.1016/j.chemosphere.2004.11.080

Choong, C. E., Ibrahim, S., Yoon, Y., & Jang, M. (2018). Removal of lead and bisphenol A using magnesium silicate impregnated palm-shell waste powdered activated carbon: Comparative studies on single and binary pollutant adsorption. *Ecotoxicology and Environmental Safety*, *148*(October 2017), 142–151. https://doi.org/10.1016/j.ecoenv.2017.10.025

Danish EPA. (2014). *Background for national legislation on bisphenol A (BPA) in EU and EFTA countries* (Issue 1552).

Delclos, K. B., Camacho, L., Lewis, S. M., Vanlandingham, M. M., Latendresse, J. R., Olson, G. R., Davis, K. J., Patton, R. E., Da costa, G. G., Woodling, K. A., Bryant, M. S., Chidambaram, M., Trbojevich, R., Juliar, B. E., Felton, R. P., & Thorn, B. T. (2014). Toxicity evaluation of bisphenol a administered by gavage to sprague dawley rats from gestation day 6 through postnatal day 90. *Toxicological Sciences*, *139*(1), 174–197. https://doi.org/10.1093/toxsci/kfu022

DTU National Food Institute. (2015). Evaluation of EFSA ' s new Scientific Opinion on Bisphenol A. *National Food Institute*, *February*, 1–9.

EFSA. (2010). Scientific Opinion on Bisphenol A: evaluation of a study investigating its neurodevelopmental toxicity, review of recent scientific literature on its toxicity and advice on the Danish risk assessment of Bisphenol A. *EFSA Journal*, *8*(9). https://doi.org/10.2903/j.efsa.2010.1829

EFSA. (2015). Scientific Opinion on the risks to public health related to the presence of bisphenol A (BPA) in foodstuffs. *EFSA Journal*, *13*(1). https://doi.org/10.2903/j.efsa.2015.3978

Frank, J., Ruhl, A. S., & Jekel, M. (2015). Impacts of backwashing on granular activated carbon filters for advanced wastewater treatment. *Water Research*, *87*, 166–174. https://doi.org/10.1016/j.watres.2015.09.020

Gogoi, A., Mazumder, P., Tyagi, V. K., Tushara Chaminda, G. G., An, A. K., & Kumar, M. (2018). Occurrence and fate of emerging contaminants in water environment: A review. *Groundwater for Sustainable Development*, *6*(December 2017), 169–180. https://doi.org/10.1016/j.gsd.2017.12.009

Ifelebuegu, A. O., Ukpebor, J. E., Obidiegwu, C. C., & Kwofi, B. C. (2015). Comparative potential of black tea leaves waste to granular activated carbon in adsorption of endocrine disrupting compounds from aqueous solution. *Global Journal of Environmental Science and Management*, *1*(3), 205–214. https://doi.org/10.7508/GJESM.2015.03.003

Javed, H., Luong, D. X., Lee, C. G., Zhang, D., Tour, J. M., & Alvarez, P. J. J. (2018). Efficient removal of bisphenol-A by ultra-high surface area porous activated carbon derived from asphalt. *Carbon*, *140*, 441–448. https://doi.org/10.1016/j.carbon.2018.08.038

Jones, B. A., Shimell, J. J., & Watson, N. V. (2011). Pre- and postnatal bisphenol A treatment results in persistent deficits in the sexual behavior of male rats, but not female rats, in adulthood. *Hormones and Behavior*, *59*(2), 246–251. https://doi.org/10.1016/j.yhbeh.2010.12.006

Kennedy, A. M., Reinert, A. M., Knappe, D. R. U., & Summers, R. S. (2017). Prediction of Full-Scale GAC Adsorption of Organic Micropollutants. *Environmental Engineering Science*, *34*(7), 496–507. https://doi.org/10.1089/ees.2016.0525

Knappe, D. R. U., Snoeyink, V. L., Röche, P., Prados, M. J., & Bourbigot, M. M. (1999). Atrazine removal by preloaded GAG. *Journal / American Water Works Association*, *91*(10), 97–109. https://doi.org/10.1002/j.1551-8833.1999.tb08719.x

Liu, G., Li, X., & Campos, L. C. (2017). Role of the functional groups in the adsorption of bisphenol A onto activated carbon: Thermal modification and mechanism. *Journal of Water Supply: Research and Technology - AQUA*, *66*(2), 105–115. https://doi.org/10.2166/aqua.2017.047

López-Ramón, M. V., Ocampo-Pérez, R., Bautista-Toledo, M. I., Rivera-Utrilla, J., Moreno-Castilla, C., & Sánchez-Polo, M. (2019). Removal of bisphenols A and S by adsorption on activated carbon clothes enhanced by the presence of bacteria. *Science of the Total Environment*, *669*, 767–776. https://doi.org/10.1016/j.scitotenv.2019.03.125

MDH. (2014). *Toxicological Summary for: Bisphenol A*. *July*, 1–19.

Meffe, R., & de Bustamante, I. (2014). Emerging organic contaminants in surface water and

groundwater: A first overview of the situation in Italy. *Science of the Total Environment*, *481*(1), 280–295. https://doi.org/10.1016/j.scitotenv.2014.02.053

National Toxicology Program. (1982). Carcinogenesis Bioassay of Bisphenol A (CAS No. 80-05-7) in F344 Rats and B6C3F1 Mice (Feed Study). *National Toxicology Program Technical Report Series*, *215*(80), 1–116.

Ndagijimana, P., Liu, X., Li, Z., Yu, G., & Wang, Y. (2019). Optimized synthesis of a core-shell structure activated carbon and its adsorption performance for Bisphenol A. *Science of the Total Environment*, *689*, 457–468. https://doi.org/10.1016/j.scitotenv.2019.06.235

Noutsopoulos, C., Mamais, D., Mpouras, T., Kokkinidou, D., Samaras, V., Antoniou, K., & Gioldasi, M. (2014). The role of activated carbon and disinfection on the removal of endocrine disrupting chemicals and non-steroidal anti-inflammatory drugs from wastewater. *Environmental Technology (United Kingdom)*, *35*(6), 698–708. https://doi.org/10.1080/09593330.2013.846923

Park, M., Wu, S., Lopez, I. J., Chang, J. Y., Karanfil, T., & Snyder, S. A. (2020). Adsorption of perfluoroalkyl substances (PFAS) in groundwater by granular activated carbons: Roles of hydrophobicity of PFAS and carbon characteristics. *Water Research*, *170*. https://doi.org/10.1016/j.watres.2019.115364

Piazzoli, A., & Antonelli, M. (2018). Application of the Homogeneous Surface Diffusion Model for the prediction of the breakthrough in full-scale GAC filters fed on groundwater. *Process Safety and Environmental Protection*, *117*, 286–295. https://doi.org/10.1016/j.psep.2018.04.027

Riva, F., Castiglioni, S., Fattore, E., Manenti, A., Davoli, E., & Zuccato, E. (2018). International Journal of Hygiene and Monitoring emerging contaminants in the drinking water of Milan and assessment of the human risk. *International Journal of Hygiene and Environmental Health*, *September 2017*, 0–1. https://doi.org/10.1016/j.ijheh.2018.01.008

RIWA. (2016). *Jaarrapport 2016 De Rijn Inhoud*.

RIWA. (2017). *Jaarrapport 2017 De Rijn Inhoud Inleiding*.

RIWA. (2018). *Jaarrapport 2018 De Rijn Inhoud*.

Ruhl, A. S., Zietzschmann, F., Altmann, J., Meinel, F., Sperlich, A., & Jekel, M. (2015). Stratification of Granular Activated Carbon Filters for Advanced Wastewater Treatment. *Water, Air, and Soil Pollution*, *226*(11). https://doi.org/10.1007/s11270-015-2655-4

Ryan, B. C., & Vandenbergh, J. G. (2006). Developmental exposure to environmental estrogens alters anxiety and spatial memory in female mice. *Hormones and Behavior*, *50*(1), 85–93. https://doi.org/10.1016/j.yhbeh.2006.01.007

Soni, H., & Padmaja, P. (2014). Palm shell based activated carbon for removal of bisphenol A: An equilibrium, kinetic and thermodynamic study. *Journal of Porous Materials*, *21*(3), 275–284. https://doi.org/10.1007/s10934-013-9772-5

Sousa, J. C. G., Ribeiro, A. R., Barbosa, M. O., Pereira, M. F. R., & Silva, A. M. T. (2018). A review on environmental monitoring of water organic pollutants identified by EU guidelines. *Journal of Hazardous Materials*, *344*, 146–162. https://doi.org/10.1016/j.jhazmat.2017.09.058

Staples, C. A., Dorn, P. B., Klecka, G. M., O'Block, S. T., Branson, D. R., & Harris, L. R. (2000). Bisphenol A concentrations in receiving waters near US manufacturing and processing facilities. *Chemosphere*, *40*(5), 521–525. https://doi.org/10.1016/S0045-6535(99)00288-X

Staples, C., van der Hoeven, N., Clark, K., Mihaich, E., Woelz, J., & Hentges, S. (2018). Distributions of concentrations of bisphenol A in North American and European surface waters and sediments determined from 19 years of monitoring data. *Chemosphere*, *201*, 448–458. https://doi.org/10.1016/j.chemosphere.2018.02.175

Tyl, R. W., Myers, C. B., Marr, M. C., Thomas, B. F., Keimowitz, A. R., Brine, D. R., Veselica, M. M., Fail, P. A., Chang, T. Y., Seely, J. C., Joiner, R. L., Butala, J. H., Dimond, S. S., Cagen, S. Z., Shiotsuka, R. N., Stropp, G. D., & Waechter, J. M. (2002). Three-generation reproductive toxicity study of dietary bisphenol A in CD Sprague-Dawley rats. *Toxicological Sciences*, *68*(1), 121–146. https://doi.org/10.1093/toxsci/68.1.121

Tyl, Rochelle W., Myers, C. B., Marr, M. C., Sloan, C. S., Castillo, N. P., Veselica, M. M., Seely, J. C., Dimond, S. S., Van Miller, J. P., Shiotsuka, R. N., Beyer, D., Hentges, S. G., & Waechter, J. M. (2008). Two-generation reproductive toxicity study of dietary bisphenol A in CD-1 (swiss) mice. *Toxicological Sciences*, *104*(2), 362–384. https://doi.org/10.1093/toxsci/kfn084

US EPA. (2010). Bisphenol A Action Plan (CASRN 80-05-7) [CA Index Name: Phenol, 4,4'-(1-

methylethylidene)bis-]. *Environmental Health*, 22.

Viberg, H., Fredriksson, A., Buratovic, S., & Eriksson, P. (2011). Dose-dependent behavioral disturbances after a single neonatal Bisphenol A dose. *Toxicology*, *290*(2–3), 187–194. https://doi.org/10.1016/j.tox.2011.09.006

Wang, J., & Harrison, M. (2018). Removal of organic micro-pollutants from water by β-cyclodextrin triazine polymers. *Journal of Inclusion Phenomena and Macrocyclic Chemistry*, *92*(3–4), 347–356. https://doi.org/10.1007/s10847-018-0851-8

Willhite, C. C., Ball, G. L., & McLellan, C. J. (2008). Derivation of a bisphenol a oral reference dose (RfD) and drinking-water equivalent concentration. *Journal of Toxicology and Environmental Health - Part B: Critical Reviews*, *11*(2), 69–146. https://doi.org/10.1080/10937400701724303

Wirasnita, R., Hadibarata, T., Yusoff, A. R. M., & Yusop, Z. (2014). Removal of Bisphenol A from Aqueous Solution by Activated Carbon Derived from Oil Palm Empty Fruit Bunch. *Water, Air, & Soil Pollution*, *225*(10), 2148. https://doi.org/10.1007/s11270-014-2148-x

Worch, E. (2008). Fixed-bed adsorption in drinking water treatment: a critical review on models and parameter estimation. *Journal of Water Supply: Research and Technology-Aqua*, *57*(3), 171–183.

Xu, X. hong, Zhang, J., Wang, Y. min, Ye, Y. ping, & Luo, Q. qing. (2010). Perinatal exposure to bisphenol-A impairs learning-memory by concomitant down-regulation of N-methyl-d-aspartate receptors of hippocampus in male offspring mice. *Hormones and Behavior*, *58*(2), 326–333. https://doi.org/10.1016/j.yhbeh.2010.02.012

Yan, L., Lv, D., Huang, X., Shi, H., & Zhang, G. (2016). Adsorption characteristics of Bisphenol-A on tailored activated carbon in aqueous solutions. *Water Science and Technology*, *74*(7), 1744–1751. https://doi.org/10.2166/wst.2016.325

Zbair, M., Ainassaari, K., Drif, A., Ojala, S., Bottlinger, M., Pirilä, M., Keiski, R. L., Bensitel, M., & Brahmi, R. (2018). Toward new benchmark adsorbents: preparation and characterization of activated carbon from argan nut shell for bisphenol A removal. *Environmental Science and Pollution Research*, *25*(2), 1869–1882. https://doi.org/10.1007/s11356-017-0634-6

CHAPTER 3

Perfluoroalkyl substances (PFAS) adsorption in drinking water by granular activated carbon: influence of activated carbon and PFAS characteristics

Abstract: The presence of perfluoroalkyl substances (PFAS) in drinking water is of high concern due to their persistence in the environment and the related potential human health risk. Adsorption onto activated carbon (AC) has been identified as an effective technique to remove PFAS. Adsorption isotherms and breakthrough curves, determined by rapid small-scale column tests (RSSCTs), were studied for eight PFAS and four granular ACs, characterized by different origins, porosity and number of reactivation cycles. Both batch and RSSCT results highlighted the strong interaction of AC and PFAS characteristics in determining adsorption capacity. The most important factor affecting AC performance is the surface charge: the positively-charged AC showed higher adsorption capacities with greater Freundlich constant (KF) and later 50% breakthrough compared to the AC with neutral surface. Among the positively-charged ACs, the microporous AC demonstrated higher adsorption capacities for hydrophilic and marginally hydrophobic PFAS, while the mesoporous AC performed better for more hydrophobic PFAS, possibly due to lower pore blockage by organic matter. These results were confirmed at full-scale through a one-year monitoring campaign, in which samples were collected at the inlets and outlets of GAC systems in 17 drinking water treatment plants spread in a wide urban area, where the four analyzed ACs are used.

Keywords: Breakthrough prediction; Full-scale validation; Granular Activated Carbon; PFAS; RSSCT; Surface water.

The research work presented in this chapter was carried out during a research stay period of 3 months at the German Environmental Protection Agency (Umwelt Bundesamt – UBA), in collaboration with the Technical University of Berlin. The research work was carried out with the valuable supervision of Dr. Aki Sebastian Ruhl (UBA). PFAS and adsorbable organic fluorine (AOF) analyses described in this chapter were carried out with the helpful collaboration of Jörg Wellmitz (UBA), the staff of Metropolitana Milanese Spa, Ronny Wischer (UBA) and Jennifer Bartz (UBA).

This chapter will be submitted soon for publication to "Chemical Engineering Journal"[3].

[3] Beatrice Cantoni[1], Andrea Turolla[1], Jörg Wellmitz[2], Aki S. Ruhl[3], Manuela Antonelli[1]

[1] Politecnico Milano, Department of Civil and Environmental Engineering (DICA) - Environmental Section, Piazza Leonardo da Vinci 32, 20133 Milano, Italy
[2] German Environment Agency (UBA), Section II 2.5, Bismarckplatz 1, Berlin, Germany
[3] German Environment Agency (UBA), Section II 3.1, Schichauweg 58, Berlin, Germany

List of symbols and abbreviations

1/n	Freundlich exponent
AC	Activated Carbon
ANOVA	Analysis of variance
AOF	Adsorbable Organic Fluorine
BV	Bed Volume
BV_{50}	Bed Volume of half saturation
C_e	Equilibrium concentration in solution
C_{IN}	RSSCT column inlet concentration
C_{OUT}	RSSCT column outlet concentration
D	Diffusivity
DOC	Dissolved Organic Carbon
DOM	Dissolved Organic Matter
D_{ow}	Octanol-water partition coefficient
dp	Particle Diameter
DWTP	Drinking Water Treatment Plants
EBCT	Empty Bed Contact Time
FS	Full scale
GAC	Granular Activated Carbon
HPLC-MS	High Performance Liquid Chromatography Mass Spectrophotometry

k_C	RSSCT column constant
K_F	Freundlich adsorption constant
K_{ow}	Octanol-water partition coefficient
LOQ	Limit Of Quantification
PAC	Powdered Activated Carbon
pH_{PZC}	pH of the Point of Zero Charge
pKa	acid dissociation constant
PSDM	Pore Surface Diffusion Model
PFAS	Per- and poly-fluoroalkyl substances
q_e	Equilibrium concentration on solid phase
rb-AC	Reactivated bituminous AC
rc-AC	Reactivated coconut-based AC
RSSCT	Rapid Small-Scale Column Test
$SUVA_{254}$	Specific UV Absorbance at 254 nm
US EPA	U.S. Environmental Protection Agency
UVA_{254}	Specific UV Absorbance at 254 nm
vb-AC	Virgin bituminous AC
vc-AC	Virgin coconut-based AC

1. Introduction

Per- and poly-fluoroalkyl substances (PFAS) are a class of aliphatic compounds in which hydrogen atoms are either partially or fully substituted by fluorine atoms (Renner, 2001). PFAS have been widely applied in industry as surfactants, especially in the areas of polymer synthesis, semiconductors, photolithography, fire retardants, and paper protection (Takagi et al., 2008). As PFAS usage is increasing and due to their bio-accumulative and persistent properties (Fuertes et al., 2017), they can now be detected in drinking waters all over the world (Castiglioni et al., 2015; Fujii et al., 2007). For what concerns their human health effects, these compounds have been identified as probable carcinogens and toxic for the reproductive and immune systems (Lindh et al., 2012; Panaretakis et al., 2001). The U.S. Environmental Protection Agency (US EPA) set a health advisory level of 70 ng/L, individually or as sum concentration, for perfluorooctanesulfonate (PFOS) and perfluorooctanoate (PFOA), which are comparably well studied. The new European drinking water directive contains a limit value of 0.1 µg/L for the individual PFAS concentrations and as sum concentration of 20 PFAS (i.e., PFBA, PFPeA, PFHxA, PFHpA, PFOA, PFNA, PFDA, PFUnDA, PFDoDA, PFTrDA, PFBS, PFHxS, PFHpS, PFOS, PFNS, PFDS), whose names and abbreviations are reported in Table S1 in the Supplementary Material (The European Parlament and the Council of the European Union, 2018).

To minimize PFAS contamination in the aquatic environment, effective removal techniques are needed, being adsorption onto activated carbon (AC) one of the most successful processes, particularly for long-chain PFAS (Appleman et al., 2014). The majority of the available studies focuses only on PFOA and PFOS (Ochoa-Herrera and Sierra-Alvarez, 2008; Qian et al., 2017; Qu et al., 2009; Yu and Hu, 2011; Zhi and Liu, 2016), likely because: i) these were mainly produced until they were phased out, and ii) in the past, regulatory limits have always been proposed only for these two PFAS. However, the introduction of new PFAS in the current revision of the EU drinking water directive stresses the need for a better understanding of AC performance and removal mechanisms for a wider range of PFAS, having different physical-chemical characteristics. Moreover, few works are available on PFAS transport phenomena in a fixed-bed adsorber (Carter and Farrell, 2010; Hansen et al., 2010; Senevirathna et al., 2010; Yu et al., 2012), although it is the most commonly used operation mode in the drinking water treatment

applications (Chowdhury et al., 2013), while literature studies mainly focus on isotherm evaluations (Zhang et al., 2016). Ideally, micropollutants fate in a full-scale fixed-bed adsorber can be represented at best by pilot-testing (Corwin and Summers, 2011). Recently, a couple of studies were performed to assess realistic breakthrough curves of various PFAS in groundwater at pilot-scale (Liu et al., 2019; McCleaf et al., 2017), but pilot-testing is highly time consuming especially when the goal is to generate long-chain PFAS full breakthrough curve (Park et al., 2020). Although their lower precision, two more practical and feasible methods are: i) numerical simulations based on dependable isotherm data, or ii) rapid small-scale column tests (RSSCTs) based on a similitude approach (Crittenden et al., 1987). Numerical simulations, such as the Pore Surface Diffusion Model (PSDM), have been already applied to predict PFAS breakthrough curves in full-scale treatment systems (Patterson et al., 2019; Xiao et al., 2017), but uncertainty is inevitably associated to kinetic parameters estimation which negatively affect predictive capabilities (Athanasaki et al., 2015). The experimental RSSCT approach is widely implemented to derive breakthrough curves of target compounds, since it allows convenient testing of various operating conditions of full-scale adsorbers in a short time, requiring small water volume, without the need for isotherm or kinetic data and complex modeling (Crittenden et al., 1987). This approach has been recently adopted by Park et al., for assessing the breakthrough of 9 PFAS, spiked in groundwater, having a low organic content (<1 mg/L DOC, Dissolved Organic Carbon), comparing four bituminous ACs (Park et al., 2020). A correlation between physical-chemical properties of PFAS and AC characteristics was derived from different breakthrough profiles. Park et al. recommended a comprehensive study with DOM (Dissolved Organic Matter) rich water to confirm their results, considering the potential competition by DOM for active sites.

Another important issue is related to reactivation of exhausted AC, which is a common practice for full-scale fixed-bed granular activated carbon (GAC) adsorbers, since it has lower environmental and economic impacts compared to the substitution of exhausted AC with virgin one (Shah et al., 2013). Few studies have evaluated the efficacy of several reactivation processes, such as high-temperature incineration and solvent washing, in desorbing PFAS from exhausted ACs (Chen et al., 2017; Chularueangaksorn et al., 2014; Deng et al., 2015; Senevirathna et al., 2010). However, to the best of authors' knowledge, there are no available studies analyzing the influence of reactivation on reactivated ACs adsorption performance towards PFAS.

Finally, for AC adsorption in lab-scale experiments, previous studies have reported good correlations between organic micropollutants removal and corresponding removal of UV absorbance at 254 nm (UVA_{254}), that proves the latter to be a good surrogate variable for AC efficiency towards micropollutants (Altmann et al., 2016; Zietzschmann et al., 2014). Few studies highlighted that the correlation between PFAS removal and UVA_{254} removal is dependent on the tested water matrix (synthetic and real surface water and wastewater) (Anumol et al., 2015; Sgroi et al., 2018), but no studies evaluate whether this correlation is also influenced by the AC characteristics. Besides, to the best of authors' knowledge, there are no available studies about the transferability of this correlation among different scales, from batch to pilot and full scale.

Our study is aimed at evaluating the influence of AC characteristics and reactivation on PFAS adsorption capacity in the presence of DOM. To this end, tap water spiked with eight PFAS, having various physical-chemical properties, at individual concentration of about 1,000 ng/L was tested, both in isotherm experiments and RSSCTs, comparing four ACs differing in origin and activation state. The adsorption performance was evaluated to highlight the main affecting factors among AC characteristics, taking into account PFAS properties and the interactions between AC and PFAS characteristics. Moreover, we investigated the applicability of UVA_{254} as a surrogate parameter for PFAS removal in fixed-bed GAC applications. Obtained results were successfully validated based on PFAS monitoring data derived from full-scale GAC adsorbers, from which AC were collected for the lab experiments. To the best of the

authors' knowledge, this is the first study in which results from batch experiments and RSSCTs about PFAS removal performances are directly correlated to full-scale evidences.

2. Materials and methods

2.1. Activated carbons and reagents

All the experiments were performed using four GAC collected in full-scale adsorbers, whose characteristics are described in section 2.5, located in various drinking water treatment plants (DWTP) in a highly urbanized area in Italy. The ACs differ for: i) origin (two derive from coconut (Acticarbone NCL 1240, Arkema Group), two from bituminous coal (Cecarbon Gac 1240, Arkema Group)); ii) activation state (two are virgin, two are reactivated ACs). The adsorption capacities of the reactivated ACs have been restored through a steam-activation process to remove previously adsorbed pollutants. Abbreviations used to indicate the tested AC samples are summarized in Table 1, where their main characteristics are also reported: iodine number, BET (Brunauer–Emmett–Teller) specific surface area, micropore volume fraction and pH at point of zero charge (pH_{PZC}). Both for isotherm experiments and RSSCTs, AC samples were preliminarily milled: for isotherms, a powdered activated carbon (PAC) was obtained (44-53 μm particle size range), while for RSSCTs the fine fraction of 90-125 μm particle size range was separated by sieving. PAC stock suspensions (2 g/L) were prepared for each AC in ultra-pure water and stored overnight for full wetting.

Table 1. Abbreviations (vc-AC for virgin coconut-based AC, rc-AC for reactivated coconut-based AC, vb-AC for virgin bituminous AC and rb-AC for reactivated bituminous AC) and main characteristics of the tested ACs.

Activated carbon	Activation state	Origin	Porosity status	Bulk density	Iodine number	BET specific surface area	Micropore volume fraction	pH_{PZC}
	-	-	-	mg/mL	mg/g	m^2/g	%	-
vc-AC	Activated	Coconut	Microporous	423.3	1072	1001.9	53.3	7.8
vb-AC	Activated	Bituminous coal	Microporous	451.0	1020	992.4	58.1	9.7
rc-AC	Reactivated	Coconut	Mesoporous	395.2	820	839.7	40.6	9.7
rb-AC	Reactivated	Bituminous coal	Mesoporous	370.0	871	897.3	35.0	9.8

As for PFAS, the reference standards were obtained from Sigma-Aldrich (Sweden): PFBA (purity 98%), PFBS (98%), PFPeA (97%), PFHxA (97%), PFHpA (99%), PFOA (96%) PFHxS (98%) and PFOS (98%). The main chemical characteristics of the studied PFAS are reported in Table 2. All the reagents used for PFAS analysis and AC characterization (as described in section 2.6) were analytical grade.

Table 2. Structure and physical-chemical properties of the eight studied PFAS: octanol-water partition coefficient at pH 7.0 (log D_{ow}), octanol-water partition coefficient (log K_{ow}), acid dissociation constant (pK_a) and bulk diffusivity (D).

Structure and characteristic		Short-chain hydrophilic and marginally hydrophobic PFAS (group 1)				Medium-chain hydrophobic PFAS (group 2)			PFOS
		PFBA	**PFPeA**	**PFBS**	**PFHxA**	**PFHpA**	**PFHxS**	**PFOA**	**PFOS**
Structure	Molecular weight [g/mol]	214	264	300	314	364	400	414	500
	Chain length	4	5	4	6	7	6	8	8
	Number of fluorinated carbons	3	4	4	5	6	6	7	8
	Carboxylate group (c), sulfonate group (s)	c	c	s	c	c	s	c	s
Characteristics	log D_{ow} at pH 7.0 [α]	-1.22	-0.52	0.25	0.18	0.88	1.65	1.58	3.05
	log K_{ow} [α]	2.31	3.01	2.63	3.71	4.41	4.03	5.11	5.43
	pK_a [α]	1.07	0.20	-3.31	-0.78	-1.36	-3.32	-4.20	-3.32
	D ($cm^2/s \times 10^{-6}$) [β]	7.89	7.19	7.15	6.58	6.06	5.32	5.63	5.21
	Minimal projection diameter (nm) [α]	0.64	0.66	0.70	0.72	0.82	0.68	0.78	0.80
	Maximal projection diameter (nm) [α]	0.92	1.00	1.00	1.10	1.20	1.41	1.30	1.30

[α] Data estimated through MarvinSketch 18.11.0 (ChemAxon Ltd., http://www.chemaxon.com/).
[β] Estimated values using SPARC (ARChem, http://www.archemcalc.com/).

2.2. Test solution

Tap water derived from surface source water was used both for isotherm experiments and RSSCTs. Tested tap water is characterized by an organic content of 5.0±0.07 mg/L DOC, conductivity of 736±17.2 μS/cm, pH of 7.5±0.16, alkalinity of 91.5 mg/L, nitrate at 12.4 mg/L NO_3, sulfate at 192 mg/L SO_4, a specific UV absorbance at 254 nm ($SUVA_{254}$) value equal to 2.1 L mg^{-1} m^{-1}. Tap water was spiked with a stock solution containing eight PFAS (PFBA, PFBS, PFPeA, PFHxA, PFHpA, PFHxS, PFOA, PFOS), at 10 mg/L each one, to adjust single PFAS concentration at 1 μg/L in the test solutions for both isotherm experiments and RSSCTs.

2.3. Batch isotherm experiments

Isotherm experiments were performed with PFAS-spiked tap water (characteristics reported in section 2.2) and varying PAC doses (5, 10, 20, 50, 100, 200 mg/L): specifically, different volumes of the PAC stock suspensions (homogenized by stirring) were pipetted into 100 mL of the PFAS-spiked tap water, never exceeding a 10% maximum dilution. Flasks were then closed and agitated on a horizontal shaker allowing for continuous and full mixture of the test suspensions for 48 hours at room temperature, whereupon PAC was separated with a membrane in a syringe filter (0.45 μm pore size regenerated cellulose membrane, PP-housing, Sartorius Stedim Lab Ltd., Minisart RC 4, Ref.No. 17821-K). An additional flask only with PFAS-spiked tap water was used as reference. Filtrated samples were analyzed for PFAS concentration, UVA_{254} and pH.

2.4. Rapid small-scale column tests (RSSCTs)

RSSCTs were carried out with PFAS-spiked tap water (characteristics reported in section 2.2) and the four ACs in cylindrical borings in an acrylic glass block with an inner diameter and cross-sectional area of 7 mm and $3.85 \cdot 10^{-5}$ m^2, respectively. Each column was filled with 190 mg AC on supporting glass beads to prevent the grains from being washed out and AC was rinsed for 2 hours with deionized water prior to RSSCT experiments. Since previous studies demonstrated that PFAS intra-particle diffusion is independent from adsorbent size (Park et al., 2020), the downscaling Eq. (1) for the case of constant diffusivity (Crittenden et al., 1991) was adopted for determining the empty bed contact time (EBCT) to be applied:

$$\frac{\mathrm{EBCT}_{RSSCT}}{EBCT_{FS}} = \left[\frac{\mathrm{d}_{p,RSSCT}}{d_{p,FS}}\right]^2 \qquad \text{(Eq. 1)}$$

where $EBCT_{RSSCT}$ and $EBCT_{FS}$ represent the EBCT values of the RSSCT and the full-scale adsorber. $EBCT_{FS}$ was set to 11 min, calculated as the average EBCT of fixed-bed GAC adsorbers located in 17 DWTPs in an urbanized area were the GAC samples were collected (see Figure S1 in the Supplementary Material). The RSSCT mean particle diameter ($d_{p,RSSCT}$) was assumed 110 μm (as the mean value of the opening sizes of the two sieves), while the full-scale mean particle diameter ($d_{p,FS}$) is 1.2 mm. Therefore, the $EBCT_{RSSCT}$ was set to 5.5 s. Since each AC has a different bulk density (see Table 1), the volume of the AC bed in each column was different. Consequently, in order to guarantee the same $EBCT_{RSSCT}$, different flowrates were set for columns containing vc-AC, vb-AC, rc-AC and rb-AC corresponding to 0.29, 0.28, 0.31 and 0.34 L/h, respectively. RSSCTs column set-up details are reported in Table S3. The columns were operated in up-flow for seven days. The complete effluent volumes were separately collected in order to quantify and control the amount of water fed on each column. The influent to each column was sampled every two days, while effluent sampling was performed every three hours by an automatic sampler. Collected samples were used for PFAS, UVA_{254} and pH determination. Furthermore, the flowrate and the pressure drop for each column were registered daily.

2.5. Full-scale GAC adsorber monitoring

In order to monitor PFAS concentrations, from January 2019 to January 2020, water samples were monthly collected at the inlet and outlet of groups of full-scale GAC adsorbers (where AC were sampled). The adsorbers are located in 17 DWTPs with vc-AC used in three, vb-AC in three, rc-AC in two and rb-AC in nine of them. The studied GAC systems are all constituted by several GAC adsorbers operating in parallel configuration: they differ for adsorber number (from 7 to 22) and volume (from 10 to 18 m^3) as well as for the flowrate treated by each adsorber (from 11 to 30 L/s). Hourly flowrate data were registered during the monitoring campaign allowing the estimation of the mean EBCT for each GAC adsorber group, ranging from 5.5 to 25.4 min. Water composition at the inlet and outlet of the full-scale GAC adsorbers is provided in Figure S2 and S3 in the Supplementary Material.

2.6. Analytical methods

Iodine number was determined according to the standard ASTM4604. The pH_{PZC} was determined by the pH drift method (Lopez-Ramon et al., 1999): 0.3 g of carbon were added in 100 mL of 0.01 mol/L NaCl solution, after pH adjustment by means of 0.1 mol/L HCl or NaOH solutions; for each AC, 6 initial pH values were evaluated (in duplicate), measuring the final pH of the solution after 48 h of mixing on a magnetic stirrer; pH_{PZC} was determined by plotting initial vs. final pH values. Carbon surface area was determined according to the BET method (Brunauer et al., 1938), specific area and volume of

micropores were determined by the t-Plot method (Barrett et al., 1951), pore size distribution was determined by the BJH method (Horvath and Kawazoe, 1983).
UV absorption was measured at 254 nm wavelength (1 cm optical path) with a Smartline UV Detector 200 (Knauer, Germany).
For PFAS analyses, samples were filtered using a 0.45 μm pore size syringe filter. Afterwards, 100 μL of the samples were spiked in a plastic vial with 90 μL of methanol and 10 μL of a C13-labelled internal standard mixture (MPFAC-24ES from Wellington, c = 20 μg/L in methanol). PFAS were analyzed using high performance liquid chromatography mass spectrometry (HPLC-MS/MS, 1290 Infinity II HPLC from Agilent with ZORBAX Eclipse XDB-C18 150 mm x 2.1 mm column from Agilent and QTRAP 6500+ MS/MS from SCIEX) and evaluated by linear calibration with ten calibration points in the range of 0.02 to 5.0 μg/L (PFAC-24PAR mixture from Wellington) and correlation coefficients for all the analytes greater than 0.98. The mobile phases were (A) water with 5 mmol/L ammonium acetate and (B) methanol with 0.05% acetic acid with a flow of 0.35 mL/min at 40 °C. The separation started with 40% (B), changed to 95% (B) in 15 min and was kept constant for another 5 min. Quantification was conducted using precursor-product ion multiple reaction monitoring (MRM) transitions. For all precursor compounds an additional product ion was recorded for confirmation, where possible (see Table S2). Limits of quantification (LOQ) were verified prior to the analysis by multiple measurement of spiked water samples at the concentration levels of LOQ according to ISO/TS 13530 Annex A. The analytical method LOQ was equal to 0.01 μg/L for all the PFAS except for PFBA (0.1 μg/L), PFPeA (0.02 μg/L) and PFOS (0.02 μg/L). For concentrations lower than LOQ, the value was set to half the LOQ. Information about ion transitions in multiple reaction monitoring for the measured analytes are reported in Table S2.
The adsorbable organic fluorine (AOF) measurement was determined using combustion ion chromatography (CIC): 0.2 g of AC samples before the tests were placed on a quartz boat and combusted, in a combustion unit AQF-2100H from EnviroTech (Germany) in the furnace at 1000–1050°C to convert organo-fuorine into mainly HF, which was trapped in an aqueous solution. The resulting fluoride is then quantified by ion chromatography, with a Dionex ICS-2100 system from Thermo Fisher Scientific (USA).

3. Results and discussion

The eight analyzed PFAS were selected because of their different structure and chemical characteristics (Table 2) for which they can be classified in three different groups: i) short-chain hydrophilic (Log D_{ow} lower than 0) or marginally hydrophobic (Log D_{ow} between 0 and 1) PFAS, with a low number of fluorine carbon atoms (group 1: PFBA, PFPeA, PFBS, PFHxA), ii) medium-chain and hydrophobic (Log D_{ow} close to and higher than 1) PFAS, with an intermediate number of fluorinated atoms (group 2: PFHpA, PFOA, PFHxS), and iii) PFOS, which is the most hydrophobic one. Indeed, the length of the PFAS chain is strictly related to their physical-chemical properties: PFAS with a longer chain possess greater hydrophobicity than shorter ones, underlined by the higher log D_{ow} values (Liu et al., 2019). Moreover, the eight analyzed PFAS can be classified into two groups based on their functional groups: i) carboxylate PFAS (PFBA, PFPeA, PFHxA, PFHpA and PFOA) and ii) sulfonate PFAS (PFBS, PFHxS, PFOS). Finally, due to their low pK_a values (Table 2), PFAS are negatively-charged for a wide range of pH, including the pH of the tested tap water. This might lead to electrostatic attraction of PFAS towards positively-charged AC, expecting stronger adsorption in comparison to the AC characterized by a neutral surface (Xiao et al., 2011).
The AC samples were selected for studying the influence of AC reactivation on PFAS adsorption kinetics and capacity, since it modifies their physical-chemical properties (Table 1). In detail, the two virgin ACs (vc-AC and vb-AC) are microporous carbons, having high BET surface and micropore volume fractions of 53.3% and 58.1%, respectively. ACs reactivation showed to influence the pore size distribution (Table

1 and Figure S4), transforming microporous ACs in mesoporous ACs. In fact, evaluating the effect of the reactivation by comparing the characteristics of the couple virgin/reactivated ACs, reactivation reduced both the BET surface and the micropore volume fraction of 16.2% and 23.8% for coconut-based AC and of 9.6% and 39.8% for bituminous-based AC. Consequently, virgin carbons (vc-AC and vb-AC) should display a higher affinity towards small compounds, considering that the adsorption is favored when the sizes of pore and solute are similar (Newcombe et al., 1997). Additionally, vc-AC is characterized by a neutral surface, differently from the other ACs, which have a positively-charged surface. In fact, only vc-AC has a pH_{PZC} similar to the pH of the tested tap water, while the other three ACs have similar pH_{PZC}, lying in the pH range 9.7 and 9.8, thus resulting in a positive surface charge for all of them at the tap water pH of 7.8.
In addition, to evaluate the effectiveness of ACs reactivation in desorbing PFAS, the adsorbable organic fluorine (AOF), being a proxy variable of total adsorbed PFAS content, has been analyzed in the tested ACs. The AOF content in virgin ACs was equal to 33.6 μgAOF/g for vc-AC and 20.9 μgAOF/g for vb-AC, while the AOF content in reactivated ACs was higher, equal to 58.7 μgAOF/g for rc-AC and 73.3 μgAOF/g for rb-AC. This evidence highlights that the ACs reactivation does not permit the complete desorption of the total amount of PFAS adsorbed during adsorbers' operation, especially for bituminous-based AC, for which the increase of AOF is about 250% with respect to an increase of about 75% for the coconut-based AC.

3.1. Isotherm tests and RSSCT modeling

Isotherms data fitted best to the Freundlich model, which is an empirical relationship widely used to describe the adsorption process for many compounds in diluted solutions, assuming multiple adsorption sites working in parallel with different free energies (Schwarzenbach et al., 2003). The Freundlich equation is defined by:

$$q_e = K_F C_e^{\frac{1}{n}} \qquad \text{(Eq. 2)}$$

where q_e (ng/mg) is the equilibrium concentration of the target compound on the solid phase (or loading), C_e (ng/L) is the equilibrium concentration in solution, K_F [(ng/mg)(ng/L)$^{-1/n}$] is the Freundlich adsorption coefficient or capacity factor and 1/n [-] is the Freundlich exponent which provides a measure for the sorption intensity (Ochoa-Herrera and Sierra-Alvarez, 2008). The coefficients estimated for each AC and PFAS according to the Freundlich equation are reported in Table 3. Isotherm data and related interpolation lines are reported in Figure 1 for PFPeA, PFOA and PFOS, each representing one of the PFAS groups previously identified (for the other PFAS, see Figure S5). Determination coefficients R^2 vary from 0.82 to 0.99, with an average of 0.93. All isotherms are non-linear as the values of 1/n are in the range from 0.18 to 0.94. Instead, the isotherms would have been linear for 1/n equal to 1, meaning that the partition between the solid and liquid phases is not linearly dependent from the concentration. Sorption site heterogeneity and sorbate-sorbate interactions are reported to be possible causes for isotherms non-linearity (Cheung et al., 2001).

Table 3. Freundlich isotherm constants (6 data for each fitting) and parameters of the RSSCT breakthrough model (15 data for each fitting) according to Lin and Huang model (Lin and Huang, 1999), estimated for each combination of PFAS and AC.

Test	Activated carbon	Models Coefficients	PFBA	PFPeA	PFBS	PFHxA	PFHpA	PFHxS	PFOA	PFOS
Isotherms	vc-AC	K_F [(ng/mg)(ng/L)$^{-1/n}$]	2.44×10^{-32}	0.01	0.60	0.87	2.09	1.74	2.20	2.43
		1/n [-]	11.01	0.94	0.54	0.43	0.30	0.45	0.33	0.23
		R^2	0.82	0.96	0.92	0.94	0.99	0.98	0.97	0.94
	vb-AC	K_F [(ng/mg)(ng/L)$^{-1/n}$]	3.12×10^{-7}	0.82	2.21	2.3	4.43	4.91	5.40	5.95
		1/n [-]	2.55	0.44	0.41	0.41	0.32	0.40	0.28	0.27
		R^2	0.94	0.97	0.92	0.97	0.94	0.95	0.92	0.86
	rc-AC	K_F [(ng/mg)(ng/L)$^{-1/n}$]	3.13×10^{-17}	0.05	1.16	1.7	2.86	2.14	3.43	3.66
		1/n [-]	5.95	0.77	0.48	0.36	0.31	0.48	0.29	0.18
		R^2	0.84	0.93	0.93	0.85	0.95	0.99	0.97	0.93
	rb-AC	K_F [(ng/mg)(ng/L)$^{-1/n}$]	2.07×10^{-9}	0.62	1.90	2.06	3.02	3.13	4.02	4.48
		1/n [-]	3.30	0.45	0.41	0.35	0.34	0.44	0.31	0.21
		R^2	0.95	0.98	0.95	0.83	0.97	0.98	0.94	0.85
RSSCT	vc-AC	BV_{50} [BV×10^3]	0.92	0.97	2.66	1.45	2.01	3.36	2.24	4.77
		k_c [(BV×10^3)$^{-1}$]	10.83	9.70	0.61	1.28	0.90	0.44	0.78	0.55
		R^2	0.95	0.97	0.87	0.92	0.92	0.86	0.87	0.93
	vb-AC	BV_{50} [BV×10^3]	1.53	3.00	8.57	5.80	7.00	11.79	8.36	15.35
		k_c [(BV×10^3)$^{-1}$]	1.15	0.42	0.14	0.17	0.15	0.09	0.12	0.17
		R^2	0.89	0.88	0.92	0.90	0.91	0.81	0.84	0.82
	rc-AC	BV_{50} [BV×10^3]	0.98	2.35	6.54	4.20	6.34	11.41	8.20	11.20
		k_c [(BV×10^3)$^{-1}$]	9.22	0.93	0.28	0.45	0.28	0.16	0.19	0.33
		R^2	0.90	0.89	0.96	0.94	0.95	0.94	0.95	0.81
	rb-AC	BV_{50} [BV×10^3]	1.03	2.60	6.58	4.54	7.27	14.78	11.90	22.81
		k_c [(BV×10^3)$^{-1}$]	8.44	1.16	0.48	0.58	0.28	0.14	0.15	0.11
		R^2	0.84	0.85	0.98	0.87	0.88	0.90	0.86	0.82

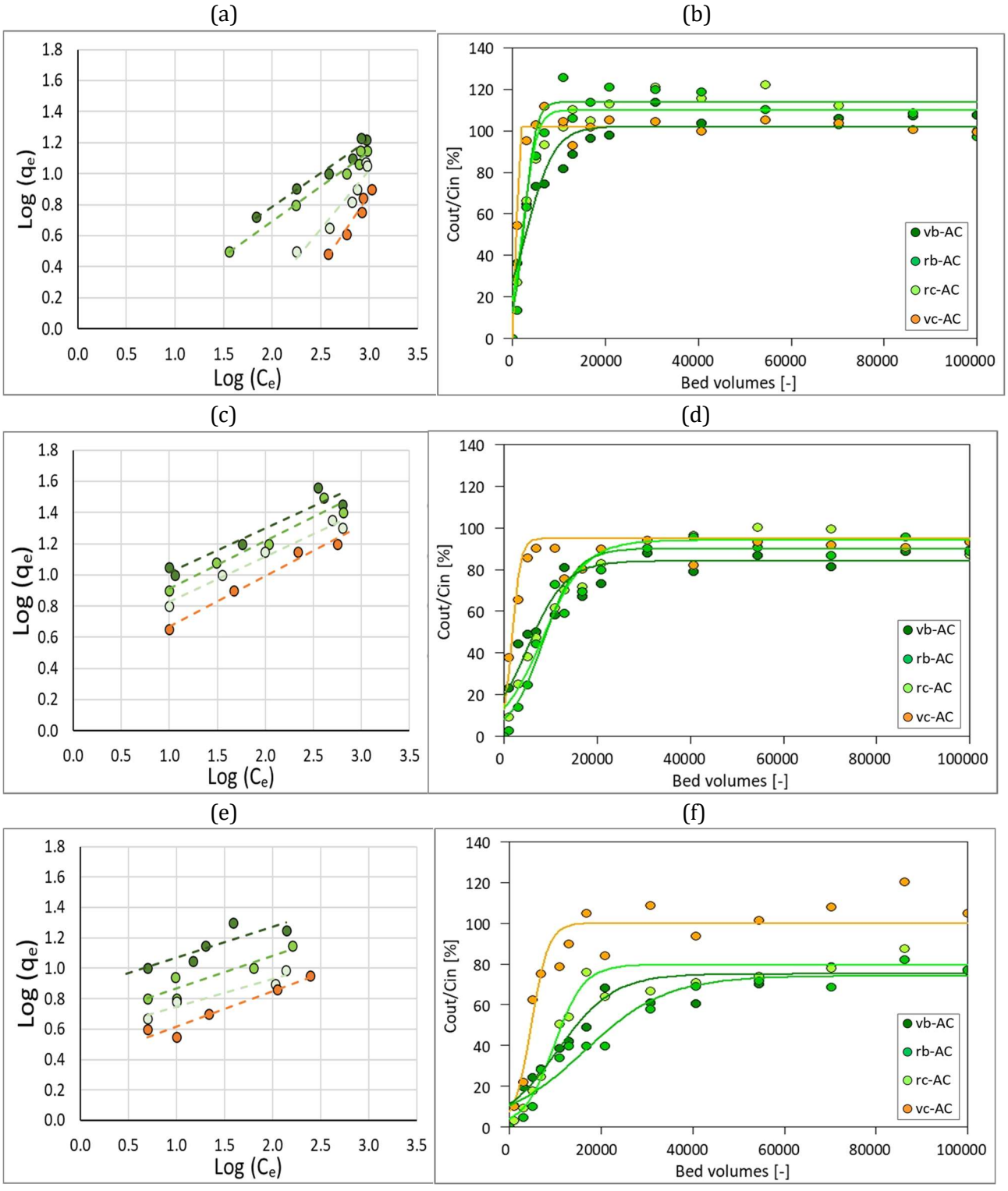

Figure 1. Isotherms (a, c, e) and breakthrough curves (b, d, f) for PFPeA (a, b), PFOA (c, d) and PFOS (e, f) for the four tested ACs.

For RSSCT, the experimental breakthrough for PFPeA, PFOA and PFOS are shown in Figure 1 (for the other PFAS, see Figure S5). The breakthrough curves for all the PFAS as a function of their log D_{ow} are reported in Figure S6 for each tested AC. The theoretical model proposed by Lin and Huang (Lin and Huang, 1999) to describe the breakthrough of a sorbate in a column (Eq. 3) was selected to interpolate the RSSCT results:

$$t = BV_{50} + \frac{1}{k_C} ln\left[\frac{Cout\,(t)}{Cin - Cout\,(t)}\right] \quad \text{(Eq. 3)}$$

where c_{in} and c_{out} are the concentrations of the individual PFAS, respectively, in the column influent and effluent at time t, here expressed in thousand bed volumes [BV×10³], namely the treated water volume normalized with respect to the volume of the AC bed. According to Eq. 3, k_C is a column constant that is related to the slope of the breakthrough curve, while BV_{50} corresponds to the throughput in BV at which c_{out} reaches 50% of c_{in}. BV_{50} was chosen as an indicator of adsorption capacity, to which it is proportional if the concentrations of target compounds are low enough (in the range of µg/L or below) and DOM is present (Corwin and Summers, 2011). Table 3 summarizes the estimated BV_{50} and k_c for each combination of PFAS and AC. The performances of the columns were well explained by the Lin and Huang model, being the R^2 values between 0.81 and 0.98, with an average value of 0.89.
AC performance is directly correlated to K_F and BV_{50} values: higher K_F and BV_{50} values indicate greater adsorption capacity of the adsorbent. To verify whether the batch and RSSCT results are in agreement, a bubble chart was used and shown in Figure 2. While bubble centers are located in the graph according to PFAS log D_{ow} and the RSSCT BV_{50}, bubbles diameters are proportional to the isotherm K_F value. Bubble colors depend on AC type: vc-AC is reported in orange as it is the only AC characterized by neutral surface charge. The other three positively-charged ACs are shown in green with darkness being proportional to the BET specific surface area (Table 1).

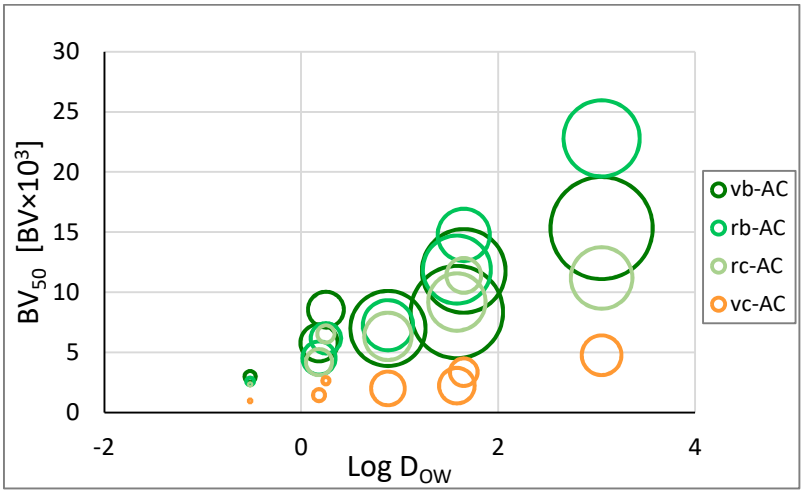

Figure 2. Bubble chart with bubble centers located according to log D_{ow} of the respective PFAS and the RSSCT BV_{50}. Bubble diameters are proportional to the isotherm K_F values.

In general, there is a good agreement among RSSCT breakthrough and isotherm results. In detail, for the majority of the analyzed PFAS, both K_F and BV_{50} increase from short-chain hydrophilic and marginally hydrophobic PFAS (group 1) to medium-chain and hydrophobic PFAS (group 2), to PFOS.
Analyzing the role of the AC type, vb-AC generally showed the highest BV_{50} and the highest K_F, followed by rb-AC and rc-AC. However, longer BV_{50} are found for rb-AC compared to vb-AC for hydrophobic PFAS, although higher K_F values were found for the latter in batch experiments. This discrepancy between batch and RSSCT is mainly dependent on the method by which the adsorbent is put in contact with water. In fact, in batch isotherm tests the contact is kept until the equilibrium and PFAS have the time to diffuse through the liquid film and the AC pores, even in case of microporous ACs. While, for continuous flow systems, such as RSSCTs, the particle diffusion is limiting (Xie et al., 2011). This can explain the lower adsorption shown in the RSSCTs for hydrophobic PFAS, having lower diffusivity coefficients D (Table 2), in microporous virgin ACs compared to mesoporous reactivated ACs. These

results reveals that adsorption kinetics should also be considered, since PFAS effluent concentration in RSSCT is influenced not only by the amount of AC vacant sites, that are evaluated through isotherm experiments, but also by the time required to establish the sorbate-sorbent bond (Senevirathna et al., 2010).

3.2. Influence of AC characteristics on adsorption performance as a function of PFAS properties

It is important to understand the role of AC characteristics in determining PFAS removal performance, since they affect the choice of the best AC to be selected and, as a consequence, the need for ACs reactivation or substitution with virgin ones, and the expected effectiveness of the adsorption process depending on the PFAS mixture present in the water to be treated.

To make evident the different affinities among PFAS and AC, reflecting in various shapes of isotherms and breakthrough curves (as shown in Figure 1 and Figure S5 and S6), an analysis of variance (ANOVA, significance level α=0.05) was performed to test the influence on K_F and BV_{50} values of AC characteristics (BET specific surface and pH_{PZC}), in relation to two PFAS properties (log D_{ow} and functional groups) and their interactions. To assess which of the PFAS properties listed in Table 2 mainly influence their adsorption onto AC, all of them were firstly included as predictors in the ANOVA (as reported in the Supplementary Materials, Section S5) and only the significant ones (being log D_{ow} and functional groups) were considered for further analyses. This two characteristics measure PFAS hydrophobicity and are correlated to most of the other characteristics, such as PFAS molecular weight, chain length, log K_{ow}, diffusivity D, and projection diameters. The ANOVA results are summarized in the Pareto charts (Figure 3) showing the standardized effects, that are indicators of the influence of AC characteristics, PFAS properties and their interactions on the ACs adsorption capacity, represented by the two responses, K_F and BV_{50}. Detailed ANOVA results and residual plots are reported in Table S5 and Figure S8.

The AC characteristics, PFAS properties and their interaction were found to have a significant influence on PFAS adsorption capacity, even if in a different extent, when considering batch and RSSCT results and all the ACs or only the positively-charged ACs, as explained in the following paragraphs.

Looking at the standardized effects for the ANOVA including all four ACs (Figure 3a and 3c), it can be stated that the main influencing factor (highest standardized effect) for both K_F and BV_{50} is the interaction between the AC surface charge (pH_{PZC}) and PFAS hydrophobicity (log D_{ow}). This reflects in significantly different breakthrough curve for vc-AC compared to the other ACs (Figure 1 and Figure S5), as supported by the outputs of Kruskal-Wallis test on PFAS BV_{50} medians, reported in Section S6 in the Supplementary Materials. In detail, for all the PFAS the breakthrough was achieved earlier (lower BV_{50}) for vc-AC that is the only AC characterized by a neutral surface, while the three positively-charged ACs, regardless their porosity, displayed better performance (later breakthrough being higher the BV_{50}) in adsorbing the negatively-charged PFAS. This observation suggests that surface charge plays a dominant role in all PFAS adsorption, compared to other AC characteristics, such as the pore size distribution, which is more commonly addressed when selecting an AC.

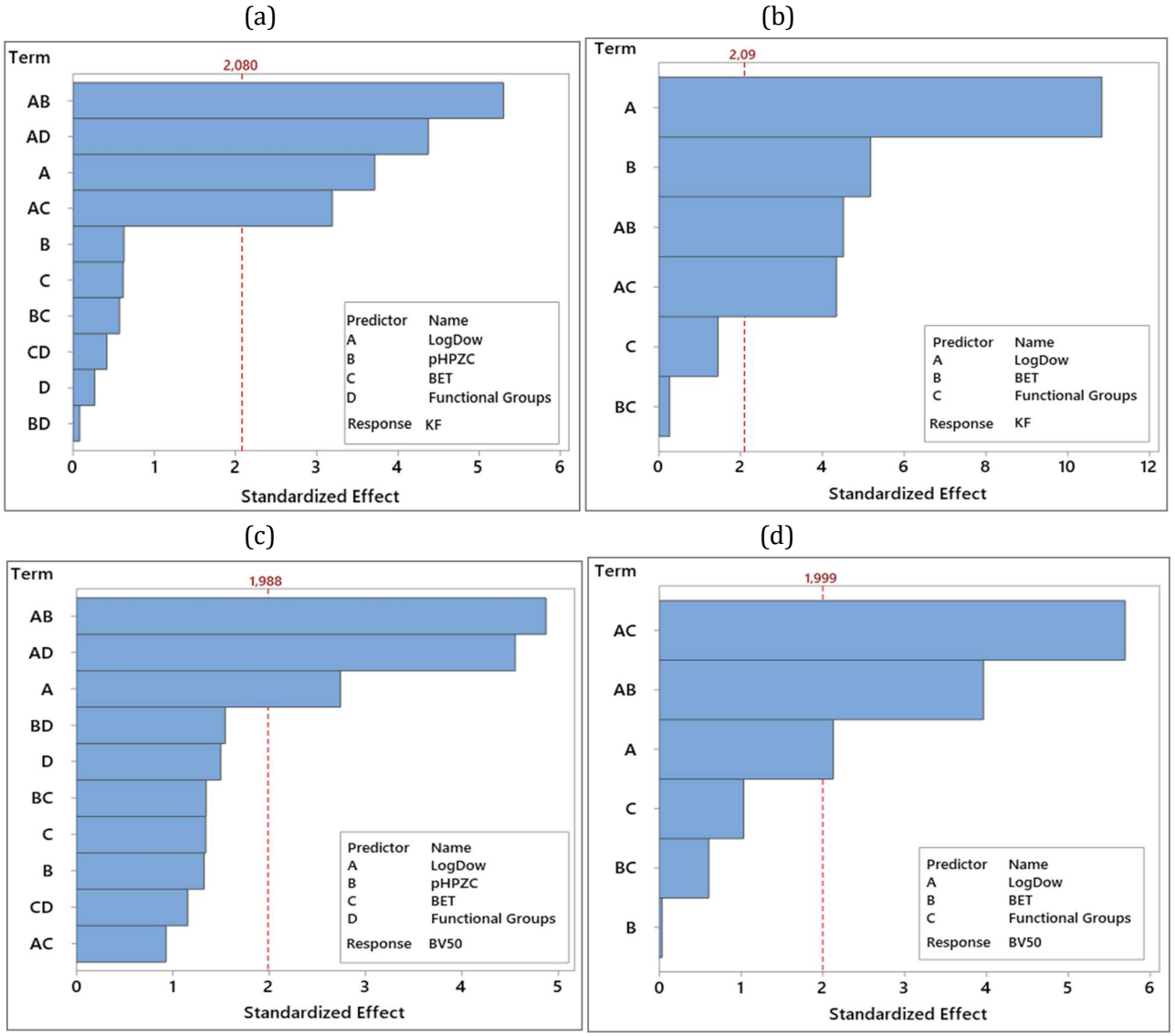

Figure 3. Pareto charts showing factors standardized effects on responses: K_F (a, b) and BV_{50} (c, d) when analyzing results of all the four tested ACs (a, c) or only the three positively-charged ACs (b, d): the red dashed line represents the significance threshold at α=0.05.

Based on ANOVA results on the three positively-charged ACs (Figure 3b and 3d), PFAS hydrophobicity (log D_{ow}) and functional groups and their interaction have a greater influence (higher standardized effect) on PFAS BV_{50} compared to the AC characteristics, in agreement with data in Figure 2. Actually, hydrophobic interactions relate primarily to the compatibility between sorbates and water: hydrophobic compounds dislike aqueous phase and therefore they are more likely to partition to the solid phase (Park et al., 2020). This observation agrees with other studies that assessed PFAS adsorption on AC in batch experiments (Hansen et al., 2010; Ochoa-Herrera and Sierra-Alvarez, 2008) or in RSSCT and pilot-scale columns (Liu et al., 2019; McCleaf et al., 2017; Park et al., 2020). In particular, an increase in adsorption capacity and later breakthroughs were observed with increasing PFAS log D_{ow} in the corresponding functional groups, independently from the studied AC, as shown in Section S7 in Supplementary Material. In detail, adsorption capacity in batch tests was evaluated in terms of removal efficiency for each PFAS at an AC dose of 20 mg/L (Figure S11a and Table S7), highlighting the relation with the number of fluorinated carbons in the molecule for both carboxylate and sulfonate PFAS. The AC dose of 20 mg/L was selected because it is the dose at which a good removal of hydrophilic PFAS was

observed and, at the same time, all hydrophobic PFAS equilibrium concentrations were still higher than the analytical method LOQ. As for RSSCT, the correlation between BV_{50} values for each PFAS and the corresponding log D_{ow} is shown in Figure S11b and Table S7. In both batch tests and RSSCTs, good linear correlation between removal efficiency and BV_{50} values with parameters describing PFAS hydrophobicity were always found, with R^2 values varying from 0.84 to 0.99, with an average of 0.94±0.05.

When comparing the two acidic functional groups, sulfonate PFAS, which have a greater hydrophobicity (higher log D_{ow}) than carboxylate ones at an equal number of fluorinated carbons, demonstrated better adsorption capacity in batch experiments and later 50%-breakthrough (Figure S11). This confirms results reported in previous works on PFAS removal by AC in drinking water (Hansen et al., 2010; Ochoa-Herrera and Sierra-Alvarez, 2008).

Given that PFAS characterized by different hydrophobicity and/or functional groups have different affinities with ACs, it is important to evaluate what is the influence of AC porosity distribution on the adsorption performance of the different groups of PFAS. According to the ANOVA results, BET specific surface area was found to be a significant affecting factor, as both single factor (on K_F) and interaction with PFAS log D_{ow} (on K_F and BV_{50}) (Figure 3b and 3d). The significant influence of the interaction between ACs BET and PFAS log D_{ow} means that the pore size distribution of an AC has a different influence on PFAS adsorption as a function of PFAS hydrophobicity, as shown in Figure 4, where BV_{50} values are reported as a function of AC type and PFAS.

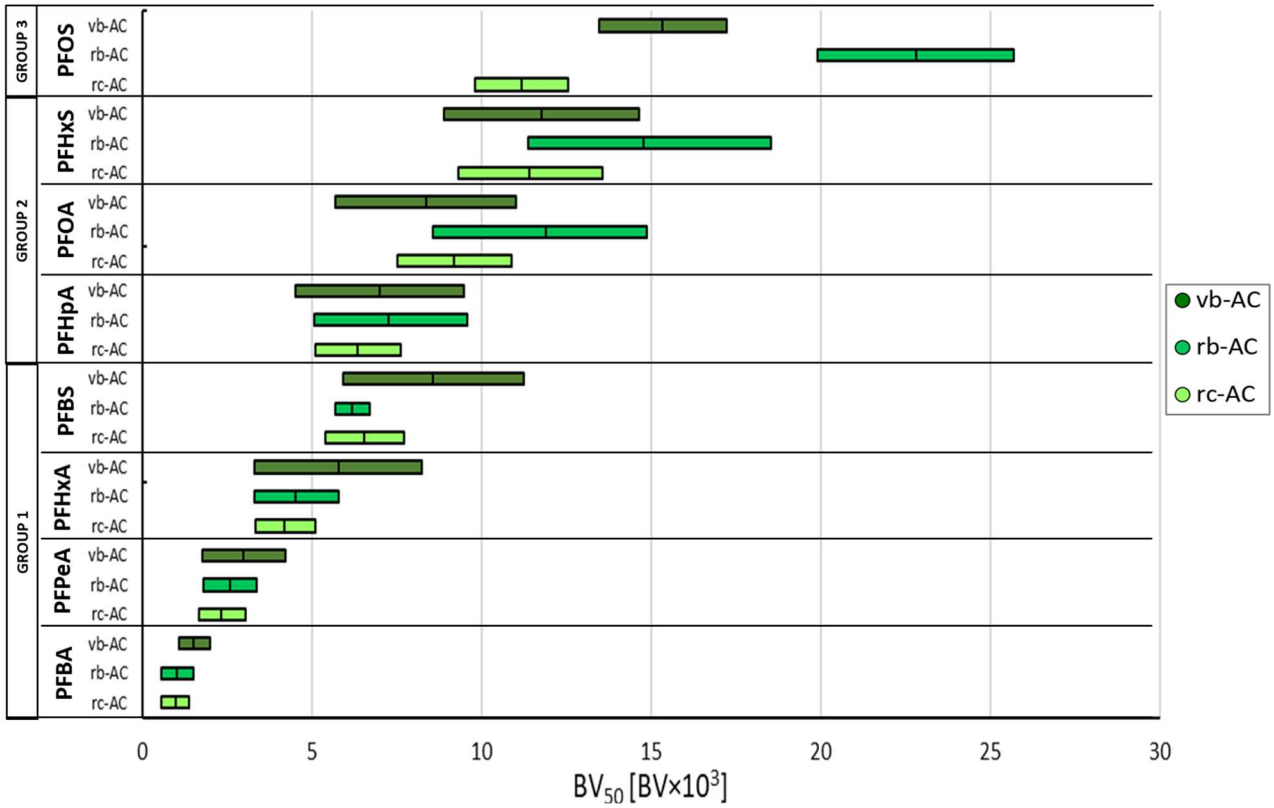

Figure 4. Estimated BV_{50}, with the related 90% confidence interval, for the three positively-charged AC and the eight PFAS.

The micropore surface area is fundamental in determining adsorption phenomena for hydrophilic and marginally hydrophobic short-chain PFAS (group 1), which have later 50% breakthrough for microporous vb-AC compared to the mesoporous ones; this observation is supported by data in Figure S12a, where the estimated BV_{50} of these PFAS is linearly correlated to the ACs BET specific surface area.

Moreover, for a given compound, the positively-charged ACs showed similar specific BV_{50} values (Figure S12b), that are the BV_{50} values divided by the micropore surface area, used as an indicator of the adsorption capacity per unit surface area of micropores (Piazzoli and Antonelli, 2018). This evidence indicates that a similar amount of short-chain PFAS was adsorbed onto the unit micropore surface area of the three ACs. Therefore, knowing the decrease in micropore surface area to be expected during ACs reactivation, it is possible to estimate the BV_{50} of the hydrophilic and marginally hydrophobic short-chain PFAS in the next AC reactivation cycle and decide whether it is more convenient to reactivate the AC or to substitute it with virgin microporous one. On the other hand, hydrophobic and long-chain PFAS (group 2 and PFOS) have later 50% breakthrough for mesoporous rb-AC compared to microporous vb-AC. This evidence highlights that mesopore surface area and DOM competition are fundamental in determining adsorption phenomena for these PFAS, as stressed in section 3.3 on competition phenomena.
However, it can be noted that for the majority of hydrophilic and hydrophobic PFAS, for breakthrough higher than 80%, vb-AC displayed a greater additional adsorption capacity compared to rb-AC, except for PFOS (Figure 1 and Figure S5). In fact, it is important to evaluate, not only the BV_{50} value, but also the PFAS solid phase loading ($\mu g_{PFAS}/g_{AC}$) at the complete exhaustion of the AC, that is higher for vb-AC compared to rb-AC for all PFAS, except for PFOS being equal to 74.8 and 82.6 $\mu g_{PFOS}/g_{AC}$ for vb-AC and rb-AC, respectively. Calculations, as integral area under the estimated breakthrough curves, are reported in Table S8.

3.3 Effect of competition phenomena on PFAS adsorption as a function of AC

When looking at the more hydrophobic PFAS, adsorption capacity is enhanced by mesopore surface area, resulting in better performances for reactivated mesoporous ACs compared to virgin microporous ones. Since UVA_{254}, that is a proxy variable for DOM water content, reaches the breakthrough in vb-AC before than in rb-AC, as shown in Figure S13, DOM competition was assumed to be fundamental in influencing adsorption. In fact, this likely causes pore blocking prior to the long-chain PFAS accessing the micropores of vb-AC. It has been widely accepted that mesoporous ACs, such as rb-AC, suffer from less pore blocking (Li et al., 2003) and facilitate hydrophobic PFAS accessing the micropores. Furthermore, micropores narrowed by pore blockage likely excluded larger PFAS more effectively than smaller ones, due to a larger minimal projected diameter, a metric that indicates molecular accessibility into pores (Table 2) (Pan et al., 2017). Therefore, it can be concluded that micropore surface area is imperative to improve the removal of short-chain PFAS, whereas the role of mesopores become increasingly more important for more hydrophobic PFAS eluted at a larger throughput, accordingly to Park et al. observations (Park et al., 2020).
Moreover, to evaluate DOM competing effect on PFAS adsorption, the breakthrough curves found in this study were compared to the ones reported by Park et al. (2020) in RSSCTs performed on three positively-charged ACs, with full-scale $EBCT_{FS}$ of 10 minutes, that is comparable to the one adopted in this study. Comparing the results, regardless the AC type, lower BV_{50} values as a function of PFAS log D_{ow} were found in our study, ranging from 2.5% to 8% of the values found by Park et al. (2020). This result is likely due to DOM competition, being DOC nine times higher in our study. Another possible explanation is related to the higher single PFAS initial concentration in our study compared to the one tested by Park et al. (2020) (350 ± 75 ng/L). In fact, being the difference in solute concentration between liquid and solid phase the driving force for solute diffusion up to adsorption sites, higher influent concentration results in faster adsorption kinetics and corresponding faster breakthrough (Yu et al., 2005). However, the relatively small difference in influent concentrations, that in this study is almost three times higher than the one tested by Park et al. (2020), cannot explain alone such anticipation in PFAS breakthrough. Therefore, DOM competition is believed to be the main affecting factor.

Looking at RSSCT breakthrough curves (Figure 1 and Figure S5), a chromatographic effect (Hand et al., 1997) is evident: the breakthrough curves for short chain PFAS showed effluent concentrations exceeding the influent concentration for a while, being more relevant the competitive effects with other sorbing species, such as more hydrophobic PFAS and/or DOM. This competition leads to desorption and release of sorbed short-chain PFAS that are eluted together with non-adsorbed ones (Appleman et al., 2013). The extent of the release was higher for shorter chain PFAS, with a pick in the PFBA and PFPeA breakthrough achieving C_{out}/C_{in} values over 120% at almost 11˙000 BVs, and gradually reduced and shifted at increasing log D_{ow}, with a breakthrough pick for PFHpA reaching C_{out}/C_{in} values of 110% at almost 31˙000 BVs. The chromatographic effect displays differently depending on AC type. In fact, for vb-AC only PFBA and PFPeA showed displacement phenomena, while for rb-AC all the short-chain PFAS exceeded their influent concentration. Since vb-AC suffers less of DOM competition, the main cause of displacement is probably due to the competition with longer chain PFAS. Therefore, being PFBA and PFPeA the most weakly adsorbing compounds (lowest log D_{ow}) and the most mobile (highest molecular and surface diffusivity), they are expected to travel faster than the other tested PFAS. Instead, for rb-AC, that has later UVA_{254} breakthrough compared to vb-AC one, DOM competition can be seen as the main responsible of the release (Scheurer et al., 2010).

3.4 AC selection and fixed-bed adsorber design and management

All the evidences reported on the combined influence of PFAS, AC characteristics and DOM competition have important implications in the design and management of GAC adsorbers. First of all, since this study showed that surface charge plays a dominant role in PFAS adsorption, compared to AC pore size distribution, it is suggested to test AC's surface charge prior to the selection and, considering the pH of the water to be treated, to opt for positively-charged AC rather than negatively-charged or neutral AC, to fully exploit electrostatic attraction towards negatively-charged PFAS (Xiao et al., 2011).

Moreover, it was demonstrated that the AC characteristics to be preferred in each case study depend by the PFAS mixture in the source water to be treated. In detail, when the source water contains higher hydrophilic PFAS concentrations compared to hydrophobic ones, that is highly probable in the future due to the strong limitations on the industrial use of long-chain PFAS, microporous AC have to be preferred; therefore, it would be preferably renovating exhausted AC with virgin ones, since the reactivation process leads to a decrease of AC micropores and increasing mesopores (see Table 1) (Molina-Sabio et al., 1996). Instead, for source water with high PFOS concentration, mesoporous AC should be preferred. Finally, for source water where hydrophobic PFAS (Group 2) concentrations are of higher concern compared to hydrophilic PFAS concentrations, the AC choice should be optimized based on the ratio between PFAS influent concentration and the regulatory limits, which set the BV corresponding to the maximum admissible concentration in the effluent. Actually, for stringent limits, mesoporous AC should be preferred due to later breakthroughs of the contaminants; conversely, when the above ratio is higher than 80%, microporous AC could be more beneficial for their ability to better adsorb hydrophobic PFAS at higher throughput. However, the optimal choice should be supported by an economic assessment minimizing the operating costs as a function of the different costs of virgin and reactivated AC and the required substitution frequencies.

Finally, in case of source water with high DOC content, if both short-chain and long-chain PFAS can likely exceed legislation limits, a GAC lead-lag configuration could be beneficial to minimize human health risk. In fact, a mesoporous AC could be used as the lead adsorber to remove long-chain PFAS and DOM, and a microporous AC could be selected for the lag adsorber to remove short-chain PFAS, having already reduced through the lead adsorber the possible competition with more hydrophobic PFAS and DOM.

3.5. UVA_{254} as surrogate parameter for PFAS removal monitoring

As UVA_{254} is usually easy to measure and monitor, it appears interesting to evaluate whether it is possible to monitor and predict PFAS removal in GAC adsorber applications using UVA_{254} measurements and the batch test correlations (Altmann et al., 2014). The overall PFAS removal and the corresponding UVA_{254} decrease found in the isotherm tests are shown in Figure 5a as a function of the tested AC: the relationship between PFAS removal and UVA_{254} removal assumes a saturation trend, with the plateau approached for UVA_{254} removal higher than 80%.

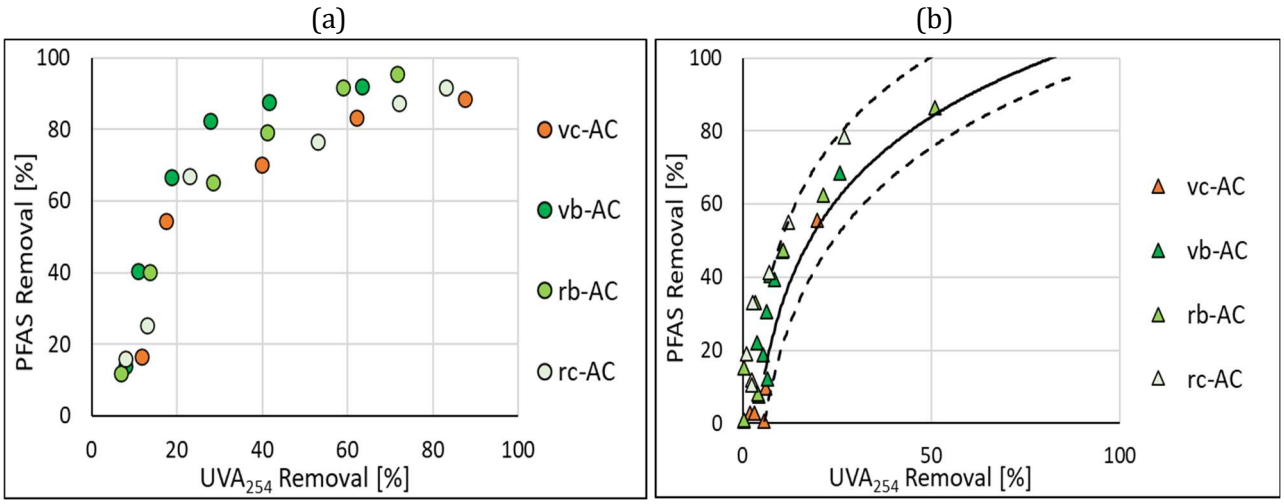

Figure 5. Correlations between overall PFAS removal and UVA_{254} removal as a function of the four tested ACs: (a) data from isotherm experiments and (b) data from RSSCTs. Solid line indicates the correlation estimated from isotherm data, dashed lines represent the model 95% confidence intervals.

Based on a two-ways ANOVA outputs (significance level: α=0.05), this correlation is not influenced by the AC type (p-value equal to 0.78), permitting to group together and fit all the isotherms data by a lognormal regression. The fitted line ($y=32.7 \cdot \ln(x) - 43.9$) and its 95% confidence interval are plotted in Figure 5b, having a satisfactory R^2 (0.91). Then, experimental data from RSSCTs were compared to the fitting line (Figure 5b), to verify that the correlation found in batch experiments can be used to predict PFAS breakthrough. RSSCTs data followed the trend of the fitting line estimated on data from batch experiments, being positioned within the 95% confidential interval. This brings to the positive conclusion that UVA_{254} removal can be considered a useful surrogate parameter for overall PFAS removal, with an important practical implication for the monitoring plan of GAC adsorbers systems. In fact, PFAS-UVA_{254} correlation can be easily build with batch experiments on one AC, regardless its activation state, to be used in combination with UVA_{254} on-line monitoring data to predict the overall PFAS breakthrough. This is an important tool to promptly identify possible system failures, which may result in human health risk, and apply rapidly mitigation measures.

3.6. PFAS removals in full-scale GAC adsorbers

About the full-scale PFAS monitoring, monthly GAC adsorber inlet and outlet concentration data were used to calculate punctual removal efficiency. Figure 6a reports the boxplot for calculated removal efficiencies as a function of AC type and PFAS group, while in Figure S2, an example of the boxplots for PFOA and PFOS as a function of AC type is reported.

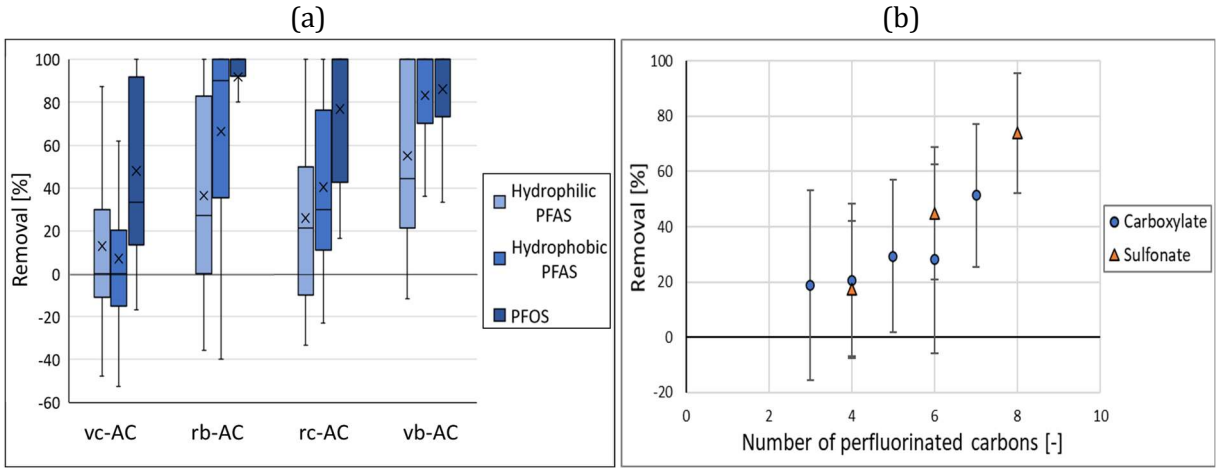

Figure 6. Full-scale PFAS removal as a function of: (a) AC type and PFAS group, (b) number of fluorinated carbons in each compound and functional group in the PFAS molecule.

Wide ranges of removal efficiencies have been observed during the monitoring campaign. Multiple reasons can explain this phenomenon. The main reason is that the plotted removal efficiencies, coming from the one-year monitoring, covered the whole breakthrough curves for almost all the PFAS. Additional reasons for variability can derive from the different water quality characteristics (i.e., PFAS inlet concentrations, conventional micro-pollutants competition effects) and operating conditions (i.e., EBCT, surface velocity) of the full-scale adsorbers.

Despite this variability, the main RSSCT findings on the effect of AC characteristics on PFAS breakthrough are confirmed: in fact, regardless the PFAS group, vc-AC showed the worst performance, with median removal efficiency more than 20% lower compared to the other ACs. As for the other three ACs, looking at the hydrophilic and marginally hydrophobic PFAS, median removal efficiency follows the order vb-AC > rb-AC > rc-AC, and it increases with AC microporous surface area. Moreover, hydrophobic PFAS were better removed by vb-AC, while PFOS was better removed by rb-AC. These results are in agreement with the overall solid phase loading estimated for each PFAS through RSSCT (Table S8).

PFAS hydrophobicity effect found through RSSCT had a correspondence with full-scale data. In fact, hydrophilic or marginally hydrophobic PFAS showed lower median removal efficiencies compared to hydrophobic PFAS, and PFOS removal efficiency was significantly higher than the one of the other compounds, as clearly highlighted by data in Figure 6b, where the removal efficiency achieved for each PFAS, regardless the AC type, is reported as a function of the number of fluorinated carbons in the molecule for both carboxylate and sulfonate PFAS.

Finally, it can be stated that the chromatographic effect found in RSSCT was experienced also at full-scale (see Figure 6a). In fact, negative removal efficiencies have been calculated for hydrophilic and marginally hydrophobic PFAS, demonstrating that their outlet concentration exceeded the inlet one. For rb-AC this phenomenon occurred at a greater extent compared to vb-AC, in agreement with the RSSCT breakthrough curves shown in Figure S6.

4. Conclusions

The adsorption behaviour of eight PFAS in tap water was studied by batch tests and RSSCT with four ACs. Full-scale monitoring data were collected to validate experimental findings.

As for the AC characteristics, the main factor influencing PFAS removal was found to be the AC surface charge, pointing out electrostatic interactions to be fundamental for PFAS removal. In particular, the worst performance was found for a neutral AC compared to positively-charged ACs. Among the

positively-charged ACs, the pore size distribution showed crucial influence on PFAS adsorption capacity depending on their hydrophobicity. In particular, the micropore surface area, more developed in virgin ACs, was important for determining the RSSCT BV_{50} and full-scale median removal for hydrophilic and marginally hydrophobic PFAS. Instead, the role of mesopores, highly present in reactivated ACs, became increasingly more important for more hydrophobic PFAS eluted at a later throughput. This was explained by the lower DOM competition that caused less pore blocking in case of mesoporous ACs compared to microporous ones. A chromatographic effect was observed in both RSSCT and at full-scale, with hydrophilic PFAS effluent concentrations exceeding the influent ones due to their displacement for competition with hydrophobic PFAS and DOM.

Moreover, UVA_{254} measurements are suitable to effectively monitor PFAS removals in GAC systems, since correlations determined in lab-scale batch adsorption tests are suitable to predict PFAS removals in column tests samples with adequate accuracy.

Finally, full-scale monitoring data demonstrated general agreement with the mechanisms found with the laboratory scale experiments.

References

Altmann, J., Massa, L., Sperlich, A., Gnirss, R., Jekel, M., 2016. UV254 absorbance as real-time monitoring and control parameter for micropollutant removal in advanced wastewater treatment with powdered activated carbon. Water Res. 94, 240–245. https://doi.org/10.1016/j.watres.2016.03.001

Anumol, T., Sgroi, M., Park, M., Roccaro, P., Snyder, S.A., 2015. Predicting trace organic compound breakthrough in granular activated carbon using fluorescence and UV absorbance as surrogates. Water Res. 76, 76–87. https://doi.org/10.1016/j.watres.2015.02.019

Appleman, T.D., Dickenson, E.R. V, Bellona, C., Higgins, C.P., 2013. Nanofiltration and granular activated carbon treatment of perfluoroalkyl acids. J. Hazard. Mater. 260, 740–746. https://doi.org/10.1016/j.jhazmat.2013.06.033

Appleman, T.D., Higgins, C.P., Quiñones, O., Vanderford, B.J., Kolstad, C., Zeigler-Holady, J.C., Dickenson, E.R.V., 2014. Treatment of poly- and perfluoroalkyl substances in U.S. full-scale water treatment systems. Water Res. 51, 246–255. https://doi.org/10.1016/j.watres.2013.10.067

Athanasaki, G., Sherrill, L., Hristovski, K.D., 2015. The pore surface diffusion model as a tool for rapid screening of novel nanomaterial-enhanced hybrid ion-exchange media. Environ. Sci. Water Res. Technol. 1, 448–456. https://doi.org/10.1039/c5ew00108k

Barrett, E.P., Joyner, L.G., Skold, R., 1951. The Determination of Pore Volume and Area Distributions in Porous Substances. II. Comparison between Nitrogen Isotherm and Mercury Porosimeter Methods. J. Am. Chem. Soc. 73, 3155–3158. https://doi.org/10.1021/ja01151a046

Brunauer, S., Emmett, P.H., Teller, E., 1938. Adsorption of gases in multimolecular layers. J. Am. Chem. Soc. 60, 309–319.

Carter, K.E., Farrell, J., 2010. Removal of perfluorooctane and perfluorobutane sulfonate from water via carbon adsorption and ion exchange. Sep. Sci. Technol. 45, 762–767. https://doi.org/10.1080/01496391003608421

Castiglioni, S., Valsecchi, S., Polesello, S., Rusconi, M., Melis, M., Palmiotto, M., Manenti, A., Davoli, E., Zuccato, E., 2015. Sources and fate of perfluorinated compounds in the aqueous environment and in drinking water of a highly urbanized and industrialized area in Italy. J. Hazard. Mater. 282, 51–60. https://doi.org/10.1016/j.jhazmat.2014.06.007

Chen, W., Zhang, X., Mamadiev, M., Wang, Z., 2017. Sorption of perfluorooctane sulfonate and perfluorooctanoate on polyacrylonitrile fiber-derived activated carbon fibers: in comparison with activated carbon. RSC Adv. 7, 927–938. https://doi.org/10.1039/C6RA25230C

Cheung, C.W., Porter, J.F., Mckay, G., 2001. Sorption kinetic analysis for the removal of cadmium ions from effluents using bone char. Water Res. 35, 605–612. https://doi.org/10.1016/S0043-1354(00)00306-7

Chowdhury, Z.Z., Zain, S.M., Rashid, A.K., Rafique, R.F., Khalid, K., 2013. Breakthrough curve analysis for column dynamics sorption of Mn(II) ions from wastewater by using Mangostana garcinia peel-based granular-activated carbon. J. Chem. https://doi.org/10.1155/2013/959761

Chularueangaksorn, P., Tanaka, S., Fujii, S., Kunacheva, C., 2014. Batch and column adsorption of perfluorooctane sulfonate on anion exchange resins and granular activated carbon. J. Appl. Polym. Sci. 131, 1–7. https://doi.org/10.1002/app.39782

Corwin, C.J., Summers, R.S., 2011. Adsorption and desorption of trace organic contaminants from granular activated carbon adsorbers after intermittent loading and throughout backwash cycles. Water Res. 45, 417–426. https://doi.org/10.1016/j.watres.2010.08.039

Crittenden, J.C., Berrigan, J.K., Hand, D.W., Lykins, B., 1987. Design of rapid fixed-bed adsorption tests for nonconstant diffusivities. J. Environ. Eng. (United States) 113, 243–259. https://doi.org/10.1061/(ASCE)0733-9372(1987)113:2(243)

Deng, S., Nie, Y., Du, Z., Huang, Q., Meng, P., Wang, B., Huang, J., Yu, G., 2015. Enhanced adsorption of perfluorooctane sulfonate and perfluorooctanoate by bamboo-derived granular activated carbon. J. Hazard. Mater. 282, 150–157. https://doi.org/10.1016/j.jhazmat.2014.03.045

Fuertes, I., Gómez-Lavín, S., Elizalde, M.P., Urtiaga, A., 2017. Perfluorinated alkyl substances (PFASs) in northern Spain municipal solid waste landfill leachates. Chemosphere 168, 399–407. https://doi.org/10.1016/j.chemosphere.2016.10.072

Fujii, S., Polprasert, C., Tanaka, S., Lien, N.P.H., Qiu, Y., 2007. New POPs in the water environment: Distribution, bioaccumulation and treatment of perfluorinated compounds - A review paper. J. Water Supply Res. Technol. - AQUA 56, 313–326. https://doi.org/10.2166/aqua.2007.005

Hand, D.W., Crittenden, J.C., Hokanson, D.R., Bulloch, J.L., 1997. Predicting the performance of fixed-bed granular activated carbon adsorbers. Water Sci. Technol. 35, 235–241. https://doi.org/10.1016/S0273-1223(97)00136-4

Hansen, M.C., Børresen, M.H., Schlabach, M., Cornelissen, G., 2010. Sorption of perfluorinated compounds from contaminated water to activated carbon. J. Soils Sediments 10, 179–185. https://doi.org/10.1007/s11368-009-0172-z

Horvath, G. and Kawazoe, K., 1983. Method for calclualtion effective pore size distribution in molecular sieve carbon. J. Chem. Eng. Japan 16, 470.

Karanfil, T., Kilduff, J.E., 1999. Role of granular activated carbon surface chemistry on the adsorption of organic compounds. 1. Priority pollutants. Environ. Sci. Technol. 33, 3217–3224. https://doi.org/10.1021/es981016g

Li, Q., Snoeyink, V.L., Mariãas, B.J., Campos, C., 2003. Elucidating competitive adsorption mechanisms of atrazine and NOM using model compounds. Water Res. 37, 773–784. https://doi.org/10.1016/S0043-1354(02)00390-1

Lin, S.H., Huang, C.Y., 1999. Adsorption of BTEX from aqueous solution by macroreticular resins. J. Hazard. Mater. 70, 21–37. https://doi.org/10.1016/S0304-3894(99)00148-X

Lindh, C.H., Rylander, L., Toft, G., Axmon, A., Rignell-Hydbom, A., Giwercman, A., Pedersen, H.S., Góalczyk, K., Ludwicki, J.K., Zvyezday, V., Vermeulen, R., Lenters, V., Heederik, D., Bonde, J.P., Jönsson, B.A.G., 2012. Blood serum concentrations of perfluorinated compounds in men from Greenlandic Inuit and European populations. Chemosphere 88, 1269–1275. https://doi.org/10.1016/j.chemosphere.2012.03.049

Liu, C.J., Werner, D., Bellona, C., 2019. Removal of per- And polyfluoroalkyl substances (PFASs) from contaminated groundwater using granular activated carbon: A pilot-scale study with breakthrough

modeling. Environ. Sci. Water Res. Technol. 5, 1844–1853. https://doi.org/10.1039/c9ew00349e

Lopez-Ramon, M. V., Stoeckli, F., Moreno-Castilla, C., Carrasco-Marin, F., 1999. On the characterization of acidic and basic surface sites on carbons by various techniques. Carbon N. Y. 37, 1215–1221. https://doi.org/10.1016/S0008-6223(98)00317-0

McCleaf, P., Englund, S., Östlund, A., Lindegren, K., Wiberg, K., Ahrens, L., 2017. Removal efficiency of multiple poly- and perfluoroalkyl substances (PFASs) in drinking water using granular activated carbon (GAC) and anion exchange (AE) column tests. Water Res. 120, 77–87. https://doi.org/10.1016/j.watres.2017.04.057

Molina-Sabio, M., González, M.T., Rodriguez-Reinoso, F., Sepúlveda-Escribano, A., 1996. Effect of steam and carbon dioxide activation in the micropore size distribution of activated carbon. Carbon N. Y. 34, 505–509. https://doi.org/10.1016/0008-6223(96)00006-1

Newcombe, G., Drikas, M., Hayes, R., 1997. Influence of characterised natural organic material on activated carbon adsorption: II. Effect on pore volume distribution and adsorption of 2-methylisoborneol. Water Res. 31, 1065–1073. https://doi.org/10.1016/S0043-1354(96)00325-9

Ochoa-Herrera, V., Sierra-Alvarez, R., 2008. Removal of perfluorinated surfactants by sorption onto granular activated carbon, zeolite and sludge. Chemosphere 72, 1588–1593. https://doi.org/10.1016/j.chemosphere.2008.04.029

Pan, L., Takagi, Y., Matsui, Y., Matsushita, T., Shirasaki, N., 2017. Micro-milling of spent granular activated carbon for its possible reuse as an adsorbent: Remaining capacity and characteristics. Water Res. 114, 50–58. https://doi.org/10.1016/j.watres.2017.02.028

Panaretakis, T., Shabalina, I.G., Grandér, D., Shoshan, M.C., Depierre, J.W., 2001. Reactive oxygen species and mitochondria mediate the induction of apoptosis in human hepatoma HepG2 cells by the rodent peroxisome proliferator and hepatocarcinogen, perfluorooctanoic acid. Toxicol. Appl. Pharmacol. 173, 56–64. https://doi.org/10.1006/taap.2001.9159

Park, M., Wu, S., Lopez, I.J., Chang, J.Y., Karanfil, T., Snyder, S.A., 2020. Adsorption of perfluoroalkyl substances (PFAS) in groundwater by granular activated carbons: Roles of hydrophobicity of PFAS and carbon characteristics. Water Res. 170. https://doi.org/10.1016/j.watres.2019.115364

Patterson, C., Burkhardt, J., Schupp, D., Krishnan, E.R., Dyment, S., Merritt, S., Zintek, L., Kleinmaier, D., 2019. Effectiveness of point-of-use/point-of-entry systems to remove per- and polyfluoroalkyl substances from drinking water. AWWA Water Sci. 1, e1131. https://doi.org/10.1002/aws2.1131

Piazzoli, A., Antonelli, M., 2018. Feasibility Assessment of Chromium Removal from Groundwater for Drinking Purposes by Sorption on Granular Activated Carbon and Strong Base Anion Exchange. Water. Air. Soil Pollut. 229. https://doi.org/10.1007/s11270-018-3842-x

Qian, J., Shen, M., Wang, P., Wang, C., Li, K., Liu, J., Lu, B., Tian, X., 2017. Perfluorooctane sulfonate adsorption on powder activated carbon: Effect of phosphate (P) competition, pH, and temperature. Chemosphere 182, 215–222. https://doi.org/10.1016/j.chemosphere.2017.05.033

Qu, Y., Zhang, C., Li, F., Bo, X., Liu, G., Zhou, Q., 2009. Equilibrium and kinetics study on the adsorption of perfluorooctanoic acid from aqueous solution onto powdered activated carbon. J. Hazard. Mater. 169, 146–152. https://doi.org/10.1016/j.jhazmat.2009.03.063

Renner, R., 2001. Growing concern over perfluorinated chemicals. Environ. Sci. Technol. 35. https://doi.org/10.1021/es012317k

Scheurer, M., Storck, F.R., Brauch, H.J., Lange, F.T., 2010. Performance of conventional multi-barrier drinking water treatment plants for the removal of four artificial sweeteners. Water Res. 44, 3573–3584. https://doi.org/10.1016/j.watres.2010.04.005

Schwarzenbach, R., Gschwend, P., Imboden, D., 2003. Environmental organic chemistry, 2nd Ed. ed. Wiley-Interscience, Hoboken.

Senevirathna, S.T.M.L.D., Tanaka, S., Fujii, S., Kunacheva, C., Harada, H., Ariyadasa, B.H.A.K.T., Shivakoti,

B.R., 2010. Adsorption of perfluorooctane sulfonate (n-PFOS) onto non ion-exchange polymers and granular activated carbon: Batch and column test. Desalination 260, 29–33. https://doi.org/10.1016/j.desal.2010.05.005

Sgroi, M., Anumol, T., Roccaro, P., Vagliasindi, F.G.A., Snyder, S.A., 2018. Modeling emerging contaminants breakthrough in packed bed adsorption columns by UV absorbance and fluorescing components of dissolved organic matter. Water Res. 145, 667–677. https://doi.org/10.1016/j.watres.2018.09.018

Shah, I.K., Pre, P., Alappat, B.J., 2013. Steam Regeneration of Adsorbents: An Experimental and Technical Review. Chem. Sci. Trans. 2, 1078–1088. https://doi.org/10.7598/cst2013.545

Takagi, S., Adachi, F., Miyano, K., Koizumi, Y., Tanaka, H., Mimura, M., Watanabe, I., Tanabe, S., Kannan, K., 2008. Perfluorooctanesulfonate and perfluorooctanoate in raw and treated tap water from Osaka, Japan. Chemosphere 72, 1409–1412. https://doi.org/10.1016/j.chemosphere.2008.05.034

The European Parlament and the Council of the European Union, 2018. COMMISSION IMPLEMENTING DECISION (EU) 2018/840 of 5 June 2018 2018, 5–8.

Xiao, F., Zhang, X., Penn, L., Gulliver, J.S., Simcik, M.F., 2011. Effects of monovalent cations on the competitive adsorption of perfluoroalkyl acids by kaolinite: Experimental studies and modeling. Environ. Sci. Technol. 45, 10028–10035. https://doi.org/10.1021/es202524y

Xiao, X., Ulrich, B.A., Chen, B., Higgins, C.P., 2017. Sorption of Poly- and Perfluoroalkyl Substances (PFASs) Relevant to Aqueous Film-Forming Foam (AFFF)-Impacted Groundwater by Biochars and Activated Carbon. Environ. Sci. Technol. 51, 6342–6351. https://doi.org/10.1021/acs.est.7b00970

Yu, J., Hu, J., 2011. Adsorption of Perfluorinated Compounds onto Activated Carbon and Activated Sludge. J. Environ. Eng. 137, 945–951. https://doi.org/10.1061/(ASCE)EE.1943-7870.0000402

Yu, J., Lv, L., Lan, P., Zhang, S., Pan, B., Zhang, W., 2012. Effect of effluent organic matter on the adsorption of perfluorinated compounds onto activated carbon. J. Hazard. Mater. 225–226, 99–106. https://doi.org/10.1016/j.jhazmat.2012.04.073

Zhang, D., Luo, Q., Gao, B., Chiang, S.Y.D., Woodward, D., Huang, Q., 2016. Sorption of perfluorooctanoic acid, perfluorooctane sulfonate and perfluoroheptanoic acid on granular activated carbon. Chemosphere 144, 2336–2342. https://doi.org/10.1016/j.chemosphere.2015.10.124

Zhi, Y., Liu, J., 2016. Surface modification of activated carbon for enhanced adsorption of perfluoroalkyl acids from aqueous solutions. Chemosphere 144, 1224–32. https://doi.org/10.1016/j.chemosphere.2015.09.097

Zietzschmann, F., Altmann, J., Ruhl, A.S., Dünnbier, U., Dommisch, I., Sperlich, A., Meinel, F., Jekel, M., 2014. Estimating organic micro-pollutant removal potential of activated carbons using UV absorption and carbon characteristics. Water Res. 56, 48–55. https://doi.org/10.1016/j.watres.2014.02.044

Supporting material

Section S1: Tested PFAS

Table S1. Names and abbreviations of the cited PFAS.

Abbreviation	Name
PFBA	Perfluorobutanoic acid
PFPeA	Perfluoropentanoic acid
PFHxA	Perfluorohexanoic acid
PFHpA	Perfluoheptanoic acid
PFOA	Perfluorooctanoic acid
PFNA	Perfluorononanoic acid
PFDA	Perfluorodecanoic acid
PFUnDA	Perfluoroundecanoic acid
PFDoDA	Perfluorododecanoic acid
PFTrDA	Perfluorotridecanoic acid
PFBS	Perfluorobutanesulfonic acid
PFHxS	Perfluorohexanesulfonic acid
PFHpS	Perfluoroheptanesulfonic acid
PFOS	Perfluorooctanesulfonoic acid
PFNS	Perfluorononanesulfonic acid
PFDS	Perfluorodecanesulfonic acid

Table S2. Ion transitions in multiple reaction monitoring (MRM) for the measured analytes.

Analyte	Precursor ion (m/z)	1st Product ion (quantifier)	2nd Product ion (qualifier)
PFBA	213	169	--
PFPeA	263	219	--
PFBS	299	80	99
PFHxA	313	269	119
PFHpA	363	319	169
PFHxS	399	80	99
PFOA	413	369	169
PFOS	499	80	99

Section S2: RSSCTs columns set-up details

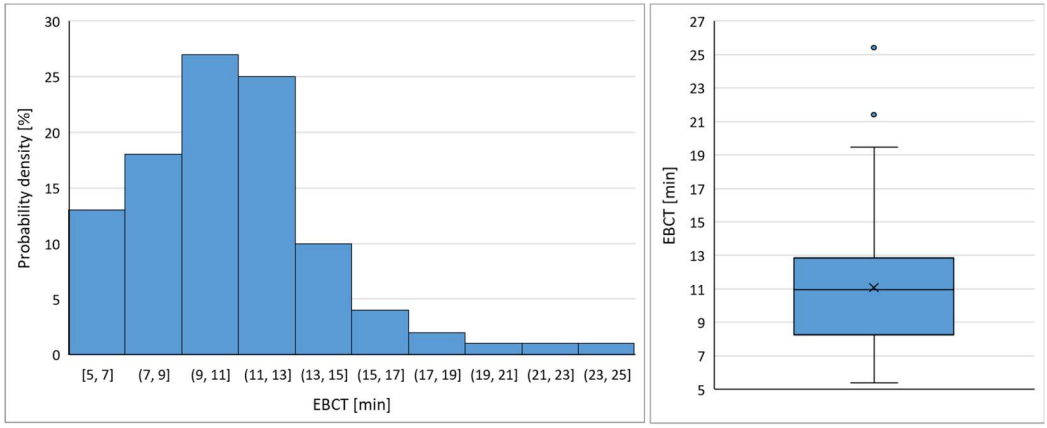

Figure S1. Distribution and boxplot of the EBCT values measured in all 17 full-scale drinking water treatment plants (DWTPs) monitored over 1 year. Data were collected to calculate the average $EBCT_{FS}$, used for RSSCT design.

Table S3. RSSCTs columns set-up details for the different ACs: full-scale EBCT ($EBCT_{FS}$) and mean AC particle diameter ($d_{p,FS}$), RSSCT mean AC particle diameter ($d_{p,RSSCT}$) and calculated EBCT ($EBCT_{RSSCT}$), ACs bulk density, column volume and calculated flowrate.

Activated carbon	$EBCT_{FS}$	$d_{p,FS}$	$d_{p,RSSCT}$	$EBCT_{RSSCT}$	Bulk density	AC column volume	Flowrate
	min	mm	µm	sec	mg/mL	mL	L/h
vc-AC	11	1.2	110	5.5	423.3	0.448	0.29
vb-AC	11	1.2	110	5.5	451.0	0.421	0.28
rc-AC	11	1.2	110	5.5	395.2	0.481	0.31
rb-AC	11	1.2	110	5.5	370.0	0.514	0.34

Section S3: Full scale GAC adsorbers inlet and outlet water composition

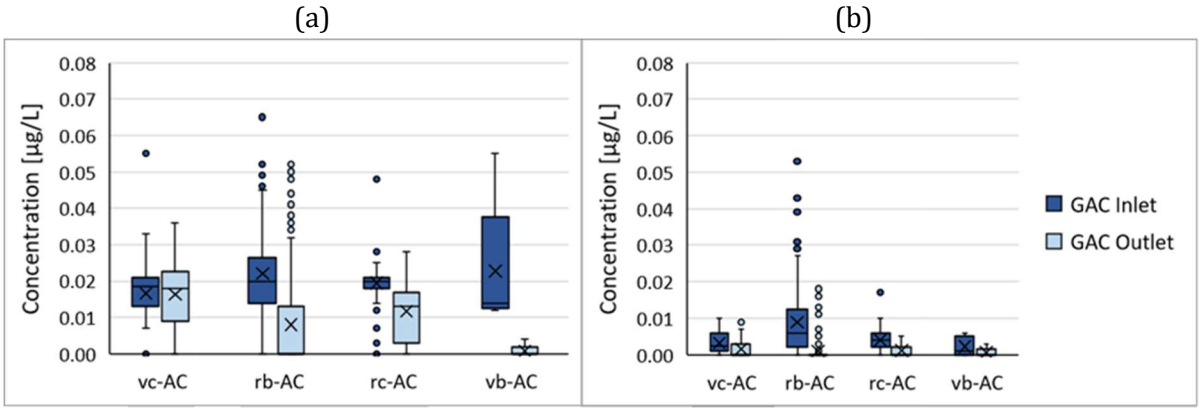

Figure S2. Boxplots for the measured inlet and outlet concentration data used for removal efficiency calculation for (a) PFOA and (b) PFOS as a function of AC type.

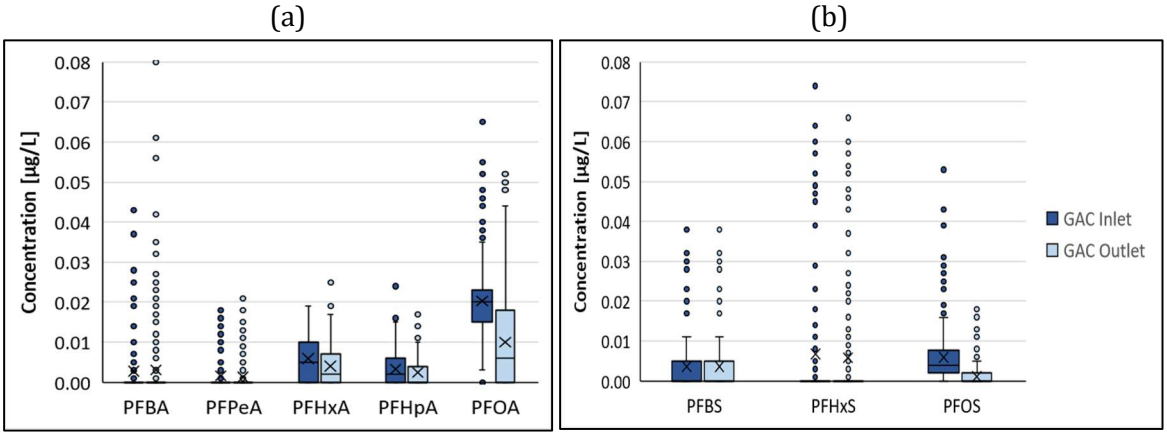

Figure S3. Boxplots for the measured inlet and outlet concentration data used for removal efficiency calculation for (a) carboxylate and (b) sulfonate PFAS.

Section S5: Tested ACs porosity

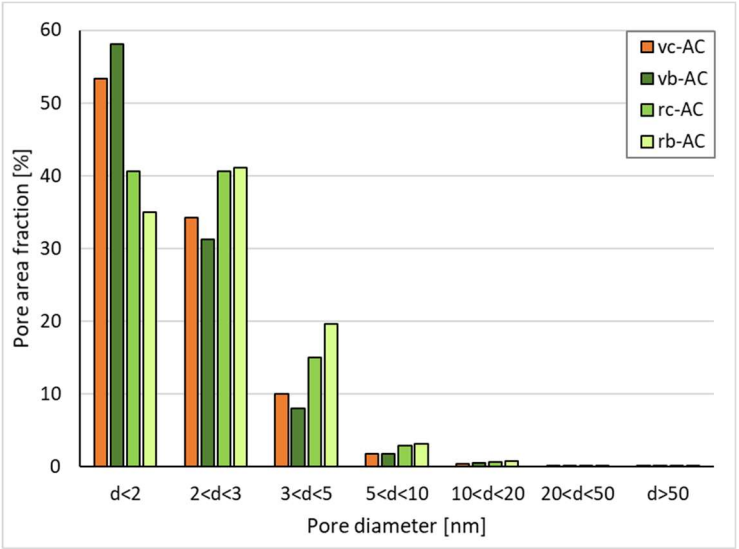

Figure S4. Pore size distribution of the four tested ACs.

Section S6: Batch isotherms and RSSCT breakthrough curves for tested PFAS

(a)

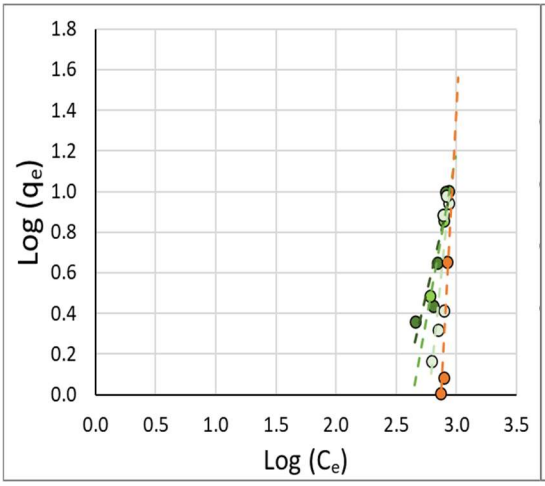

(b)

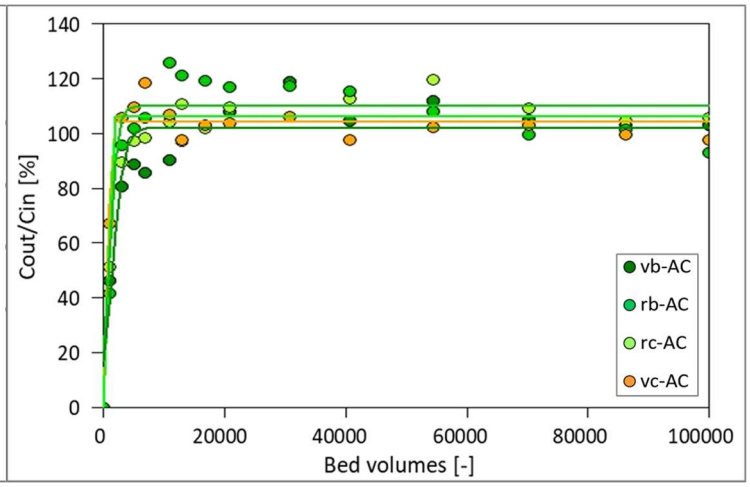

(c)

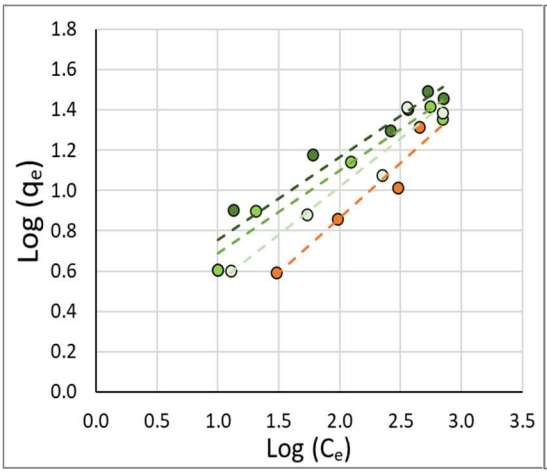

(d)

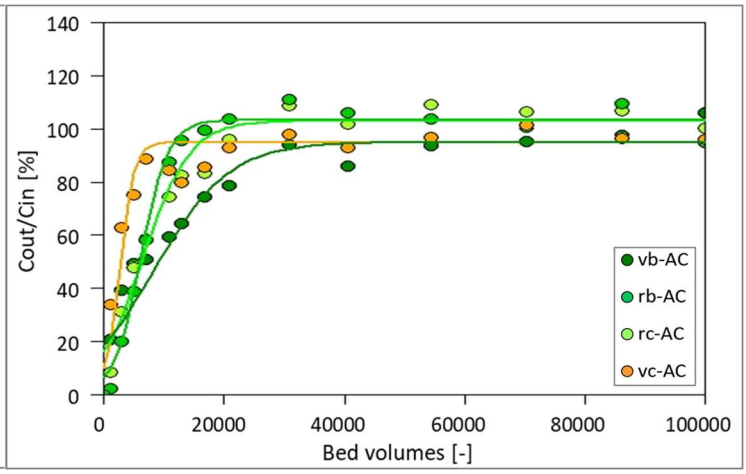

(e)

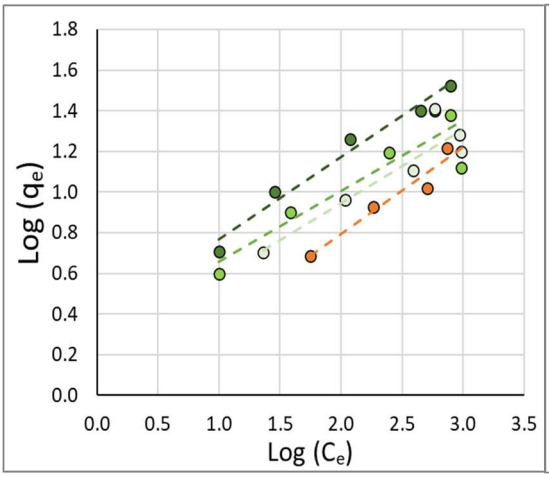

(f)

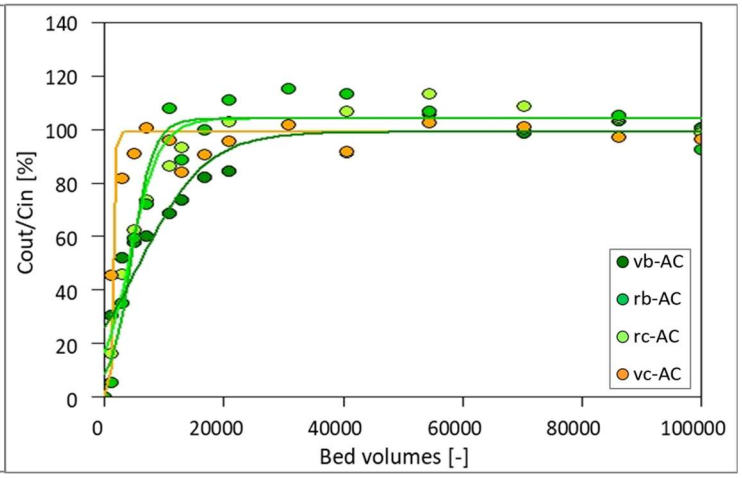

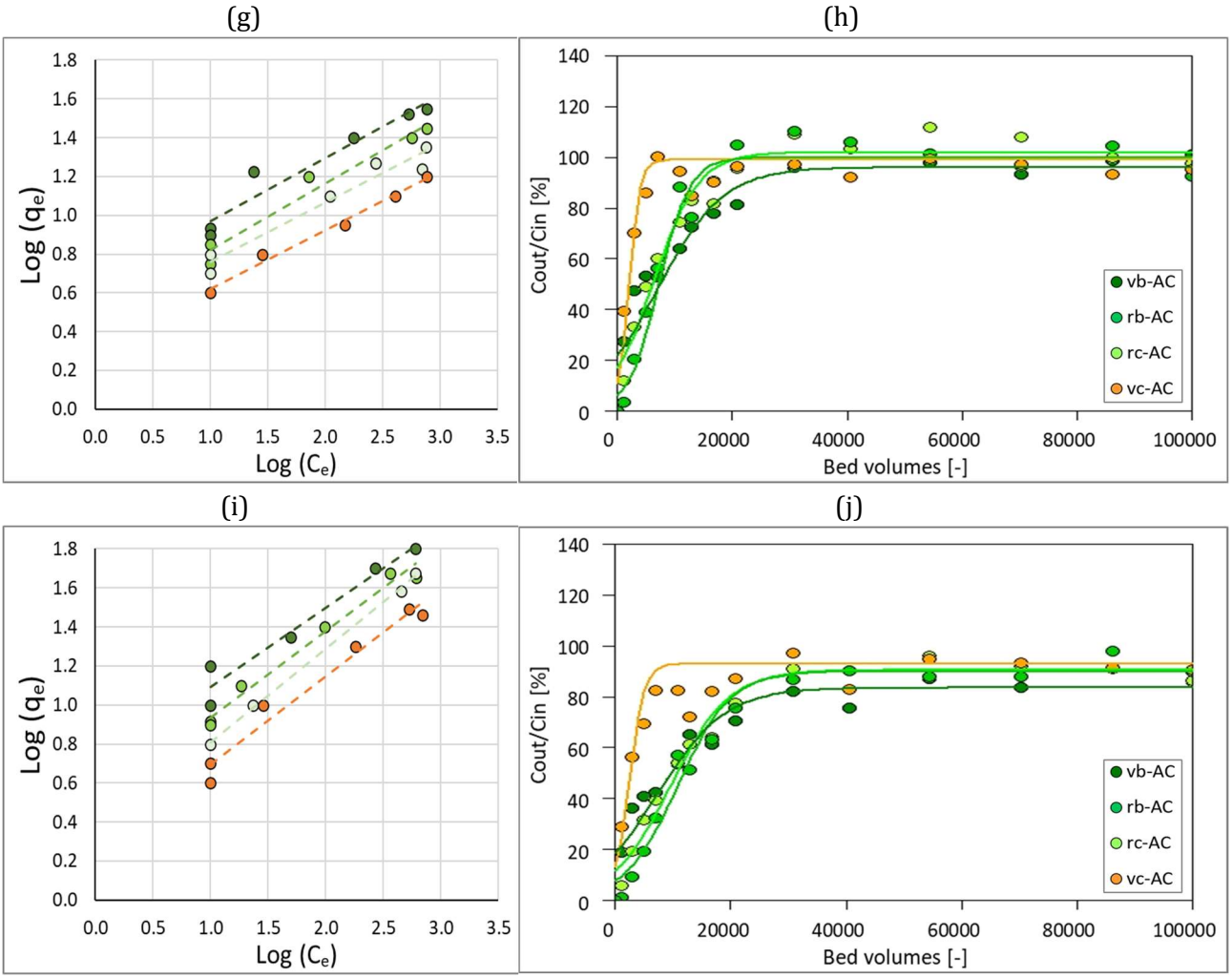

Figure S5. Isotherm curves (a, c, e, g, i) and breakthrough profiles (b, d, f, h, j) for PFBA (a, b), PFBS (c, d), PFHxA (e, f), PFHpA (g, h) and PFHxS (i, j) as a function of the tested AC type.

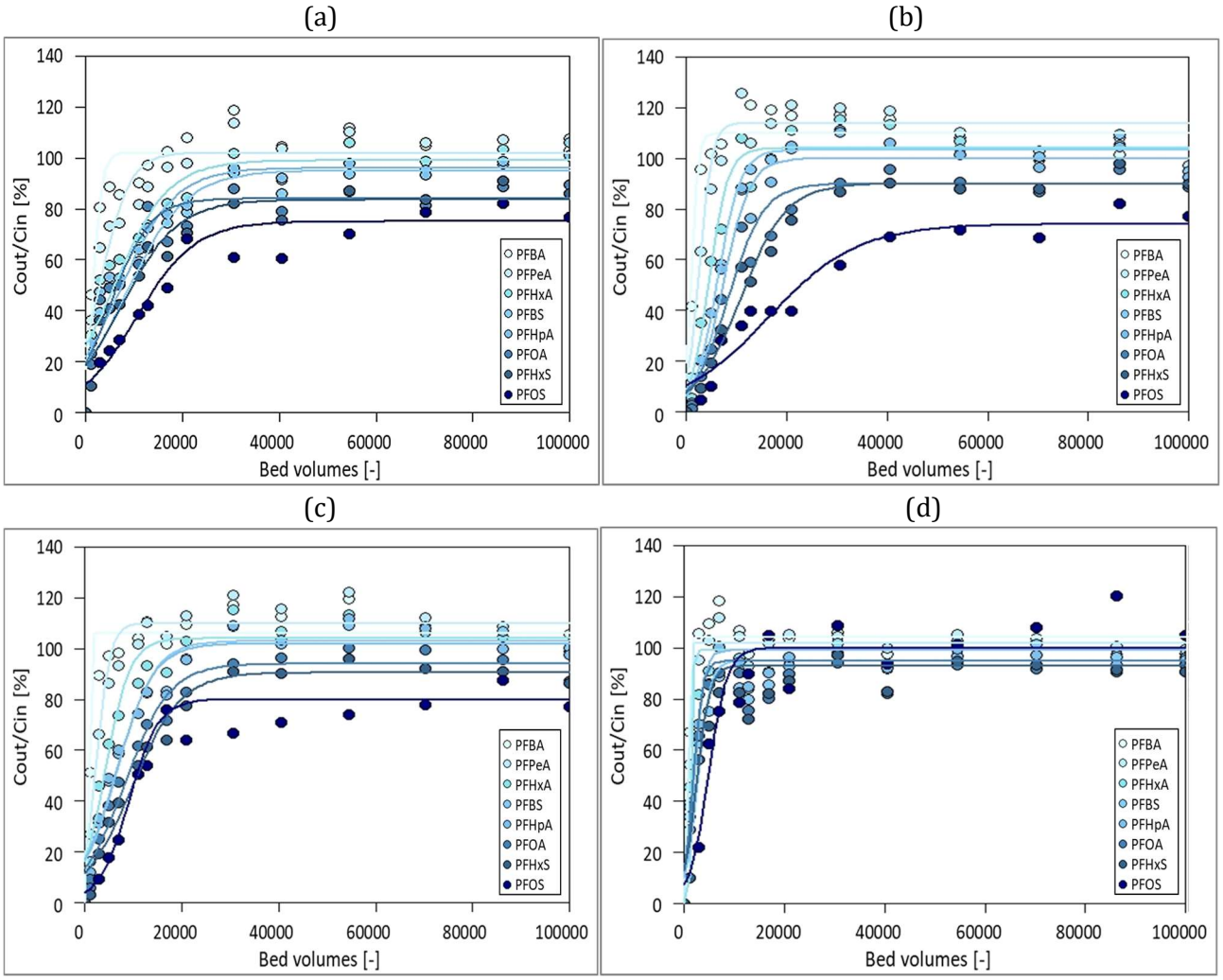

Figure S6. Breakthrough curves for all tested PFAS for (a) vb-AC and (b) rb-AC (c) rc-AC and (d) vc-AC. Line colors were selected as a function of PFAS Log D_{OW} values (Table 2) being lighter the PFAS with lower Log D_{OW} values.

Section S6: ANOVA results

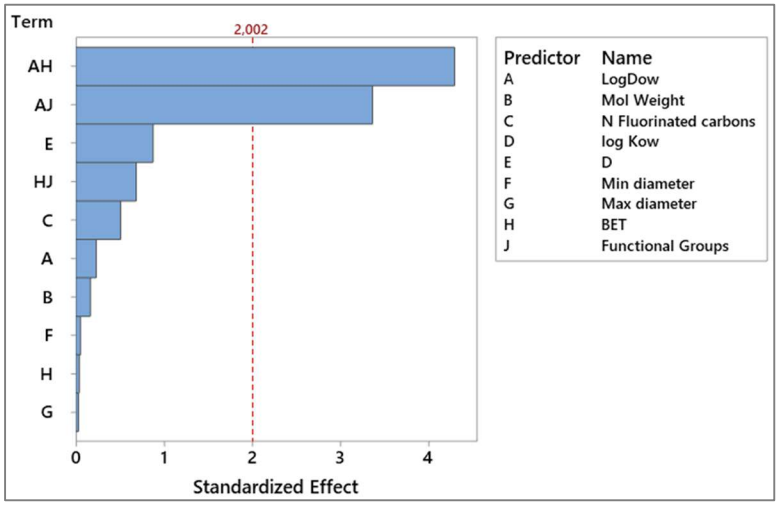

Figure S7. Pareto charts showing all PFAS and ACs factors standardized effects on responses BV_{50} when analyzing results of the three positively-charged ACs: the red dashed line represents the significance threshold at α=0.05.

Table S4. Correlation table for factors related to PFAS structure. Correlation coefficients for the correlated coupled parameters are reported in bold.

	LogDow	Functional Groups	Mol Weight	N Fluorinated carbons	log Kow	D	Min diameter	Max diameter
Functional Groups	0.561							
Mol Weight	**0.997**	0.527						
N Fluorinated carbons	**0.964**	0.471	**0.981**					
log Kow	**0.908**	0.409	**0.936**	**0.986**				
D	**-0.951**	-0.571	**-0.956**	**-0.950**	**-0.917**			
Min diameter	**0.714**	0.102	**0.750**	**0.811**	**0.840**	**-0.677**		
Max diameter	**0.880**	0.549	**0.883**	**0.874**	**0.841**	**-0.975**	**0.554**	
BV_{50}	**0.711**	**0.719**	**0.701**	**0.663**	**0.611**	**-0.627**	0.440	0.554

As can be seen from Figure S7, the only two PFAS characteristics that have a significant effect in the prediction of PFAS BV_{50} are log D_{ow} and functional groups (having standardized effects higher than the significance threshold level, reported as the dashed red line). The other PFAS characteristics are correlated to PFAS log D_{ow} (see Table S4) and therefore their effect on PFAS BV50 is already included when analyzing log D_{ow}. This is confirmed by the R^2-adjusted of the prediction models correlating the factors to the BV_{50}: the simple model, including only PFAS log D_{ow} and functional groups, explains 87.24% of the variability (R^2-adjusted= 0.8724), while the complete model, including all the PFAS characteristics reported in Table 2, explains 88.93% of the output variability (R^2-adjusted= 0.8893). This means that the inclusion of the additional 6 PFAS characteristics does not have a significant improvement in the model prediction performance, since their information is already included in the log D_{ow} that is well correlated to all of them.

Table S5. ANOVA results (significance level α=0.05) for the influence of PFAS properties (log D_{ow} and functional groups), AC characteristics (BET specific surface area and pH_{PZC}) and their interactions on K_F and BV_{50} values considering: all the four tested ACs and only the three positively-charged ACs. p-value of the significant parameters are reported in bold.

		All four AC						Three positively charged AC					
K_F	**Source**	**DF**	**Adj SS**	**Adj MS**	**F-value**	**p-value**	**Standard Effect**	**DF**	**Adj SS**	**Adj MS**	**F-value**	**p-value**	**Standard Effect**
	Regression	10	87.2	8.72	65.6	0.000		9	71.8	8.0	66.4	0.000	
	log D_{ow}	1	1.9	1.9	14.2	**0.001**	**3.67**	1	14.2	14.2	118.0	**0.000**	**10.86**
	BET	1	0.1	0.1	0.9	0.350	0.96	2	2.0	1.0	8.1	**0.005**	**3.38**
	Func gr	1	0.00	0.0	0.00	0.958	0.05	1	0.2	0.2	1.4	0.257	1.18
	log D_{ow} · BET	1	1.4	1.4	10.7	**0.004**	**3.27**	2	1.7	0.9	7.1	**0.007**	**3.14**
	logD_{ow}· Func gr	1	2.4	2.4	17.8	**0.000**	**4.22**	1	2.3	2.3	19.1	**0.001**	**4.37**
	BET · Func gr	1	0.01	0.00	0.02	0.887	0.14	2	0.09	0.04	0.4	0.668	0.44
	pH_{PZC}	1	0.1	0.1	1.0	0.337	0.98						
	pH_{PZC} · log D_{ow}	1	3.4	3.4	25.7	**0.000**	**5.07**						
	BET · pH_{PZC}	1	0.1	0.1	0.9	0.366	0.92						
	pH_{PZC} · Func gr	1	0.01	0.01	0.1	0.761	0.31						
	Error	21	2.8	0.13				14	1.68	0.12			
	Total	31	90.0					23	73.48				
BV_{50}	**Source**	**DF**	**Adj SS**	**Adj MS**	**F-value**	**p-value**	**Standard Effect**	**DF**	**Adj SS**	**Adj MS**	**F-value**	**p-value**	**Standard Effect**
	Regression	10	4691.5	469.1	40.1	0.000		9	4307.9	478.7	54.9	0.000	
	log D_{ow}	1	93.1	93.1	8.0	**0.006**	**2.82**	1	39.6	39.6	4.5	**0.037**	**2.13**
	BET	1	28.0	28.0	2.4	0.125	1.55	2	0.5	0.2	0.03	0.971	0.04
	Func gr	1	30.2	30.2	2.6	0.112	1.61	1	9.4	9.3	1.1	0.304	1.04
	log D_{ow} · BET	1	0.3	0.2	0.02	0.883	0.15	2	171.9	85.9	9.9	**0.000**	**3.97**
	logD_{ow}· Func gr	1	230.5	230.5	19.7	**0.000**	**4.44**	1	283.1	283.1	32.5	**0.000**	**5.70**
	BET · Func gr	1	16.6	16.6	1.4	0.237	1.19	2	10.7	5.3	0.6	0.544	0.61
	pH_{PZC}	1	27.2	27.2	2.3	0.131	1.52						
	pH_{PZC} · log D_{ow}	1	267.5	267.5	22.9	**0.000**	**4.78**						
	BET · pH_{PZC}	1	28.1	28.1	2.4	0.125	1.55						
	pH_{PZC} · Func gr	1	25.5	25.5	2.2	0.143	1.48						
	Error	85	994.7	11.7				62	540.3	8.7			
	Lack-of-Fit	21	746.3	35.5	9.2	0.000		14	300.7	21.5	4.3	0.000	
	Pure Error	64	248.4	3.9				48	239.6	4.99			
	Total	95	5686.2					71	4848.2				

(a)

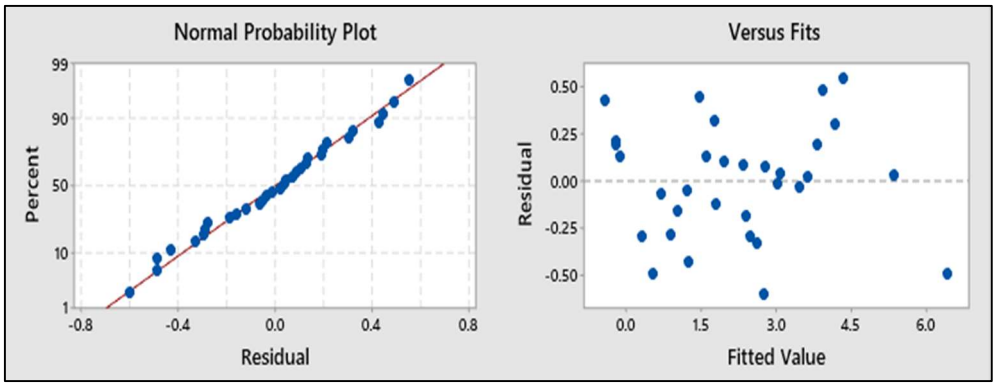

(b)

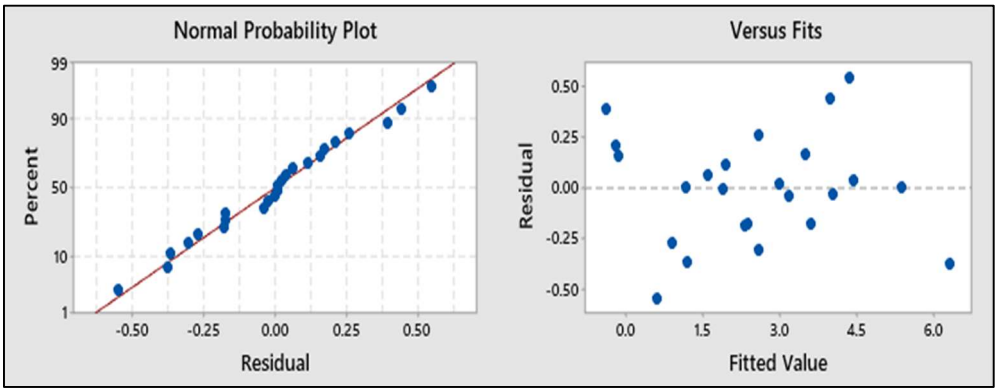

(c)

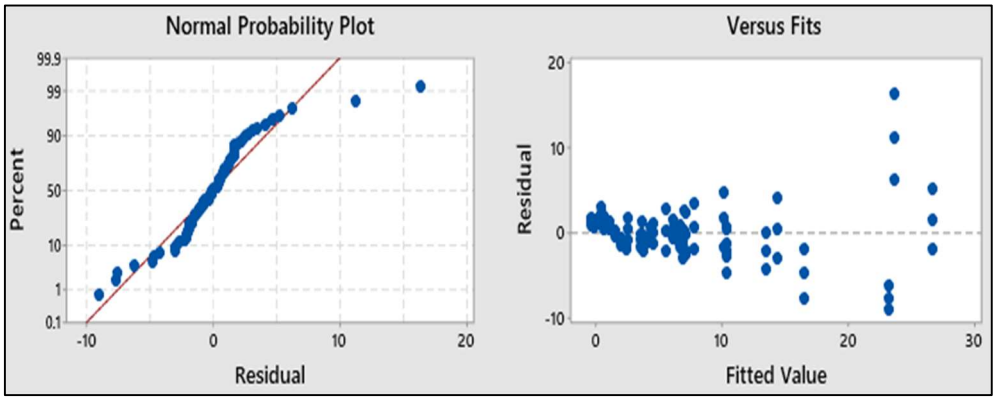

(d)

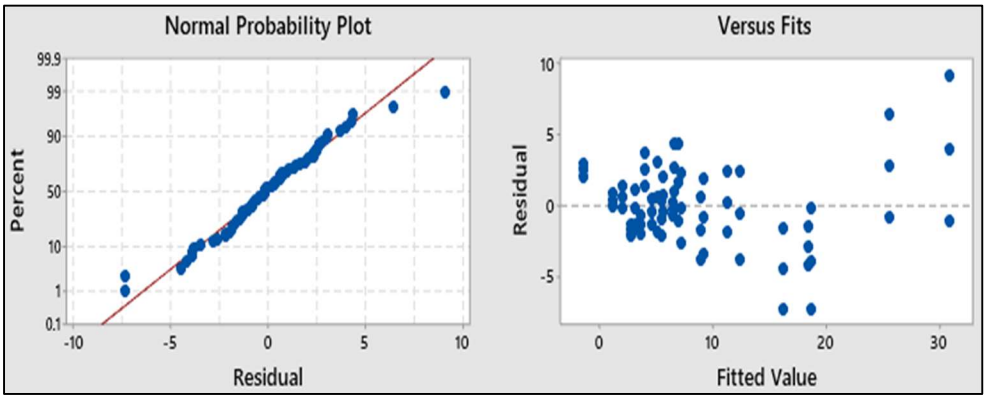

Figure S8. ANOVA residual plots for K_F (a, b) and BV_{50} (c, d) considering: all the four tested ACs (a, c) and only the three positively-charged ACs (b, d).

Section S7: ACs adsorption performance

A Kruskal-Wallis test (significance level, α=0.05) was performed to test whether PFAS BV_{50} medians for the ACs are significantly different. The test was firstly applied considering all four ACs (Fig. S4), with the null hypothesis (H_0) that BV_{50} medians for the four ACs are equal and the alternative one (H_1) that at least one BV_{50} median is different. The null hypothesis was rejected (p-value < 0,05).

AC	N	Median	Mean Rank	Z-Value
rb-AC	24	6,44174	58,0	1,92
rc-AC	24	6,44239	53,8	1,07
vb-AC	24	7,62990	58,3	1,99
vc-AC	24	1,89249	24,0	-4,98
Overall	96		48,5	

Null hypothesis H_0: All medians are equal
Alternative hypothesis H_1: At least one median is different

DF	H-Value	P-Value
3	25,15	0,000

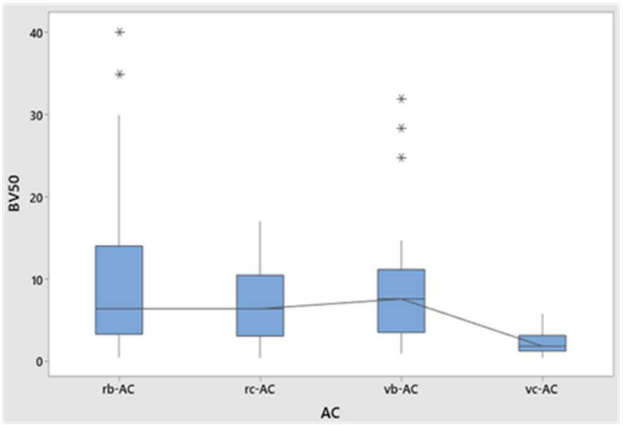

Figure S9. Kruskal-Wallis results on PFAS median BV_{50} of the four tested ACs.

The Kruskal-Wallis test was then performed on the BV_{50} medians of three out of four ACs (rb-AC, rc-AC and vb-AC), to test whether their medians are the same. Results are reported in Figure S5. The null hypothesis was accepted (p-value > 0.05).

AC	N	Median	Mean Rank	Z-Value
rb-AC	24	6,44174	37,9	0,41
rc-AC	24	6,44239	34,0	-0,72
vb-AC	24	7,62990	37,6	0,31
Overall	72		36,5	

Null hypothesis H_0: All medians are equal
Alternative hypothesis H_1: At least one median is different

DF	H-Value	P-Value
2	0,52	0,772

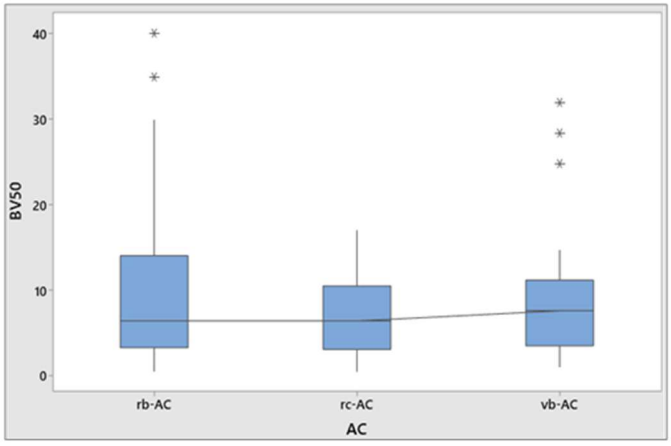

Figure S10. Kruskal-Wallis results on PFAS median BV_{50} of the three positively-charged ACs.

To double check that the surface charge has more influence than the pore size distribution on the BV_{50} the Pearson correlation was firstly evaluated. Results are summarized in Table S6: correlation between BV_{50} and BET is not significant, while the BV_{50} is significantly influenced by the AC surface charge (pH_{PZC}).

Table S6. Pairwise Pearson correlations (significance level, α=0.05) for the influence of AC characteristics (BET specific surface area and pH_{PZC}) on PFAS BV_{50} values considering all four tested ACs. p-value of the significant correlations are reported in bold.

Factor 1	Factor 2	Correlation (ρ)	95% CI for ρ	p-Value
pH_{PZC}	**BET**	-0.590	(-0.778; -0.303)	**0.000**
BV_{50}	**BET**	-0.156	(-0.478; 0.204)	0.395
BV_{50}	**pH_{PZC}**	0.375	(0.030; 0.640)	**0.034**

Section S8: Effect of PFAS hydrophobicity

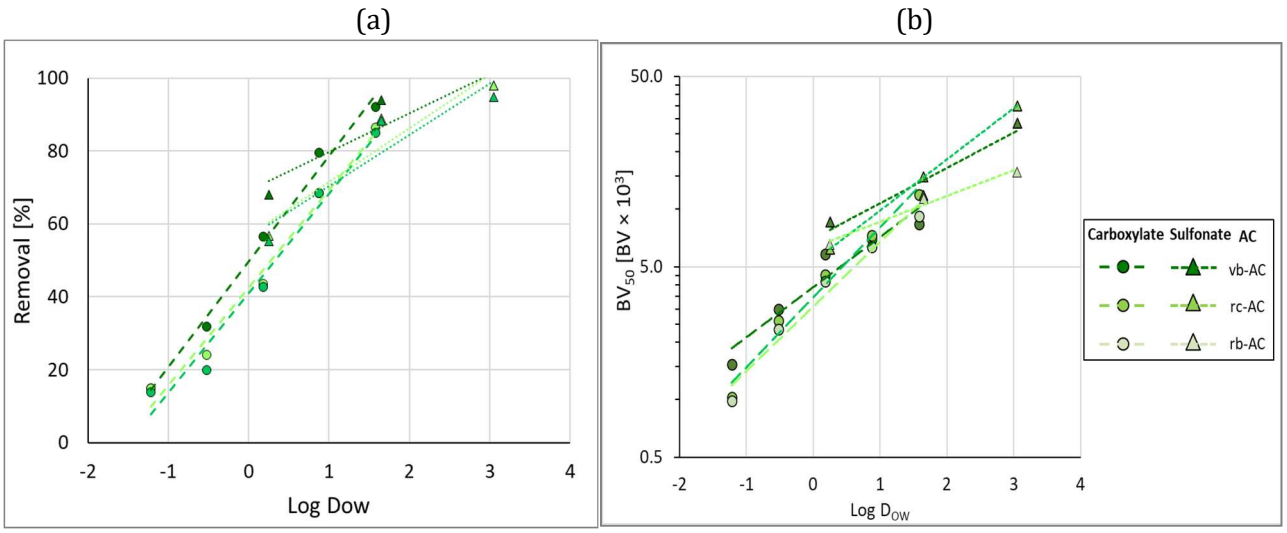

Figure S11. For each PFAS, functional group and positively charged AC: (a) removals achieved in batch experiments at an AC dose of 20 mg/L, and (b) RSSCT estimated 50% breakthrough throughput (BV_{50}), as a function of log Dow.

Table S7. Estimated linear correlation between the removals achieved in batch experiments at AC dose of 20 mg/L (y in batch), and the Log (BV_{50}) (y in RSSCTs) as a function of PFAS Log D_{OW} (x), for carboxylate and sulfonate PFAS, as a function of three positively-charged ACs.

Test scale	**Batch tests** (y=removal at AC dose of 20 mg/L; x=log Dow)			**RSSCTs** (y= Log(BV_{50}); x=log Dow)		
Activated carbon	**rc-AC**	**rb-AC**	**vb-AC**	**rc-AC**	**rb-AC**	**vb-AC**
Carboxylate PFAS	y = 26.8x +42.6 R^2 = 0.98	y = 27.3x + 41.1 R^2 = 0.97	y = 28.8x + 49.7 R^2 = 0.99	y = 0.34x + 3.5 R^2 = 0.97	y = 0.37x + 3.5 R^2 = 0.98	y = 0.26x + 3.6 R^2 = 0.92
Sulfonate PFAS	y = 14.7x + 56.8 R^2 = 0.91	y = 14.1x + 56.2 R^2 = 0.87	y = 10.7x + 69.0 R^2 = 0.84	y = 0.14x + 3.8 R^2 = 0.98	y = 0.27x + 3.72 R^2 = 0.99	y = 0.19x + 3.8 R^2 = 0.93

Section S9: RSSCTs results

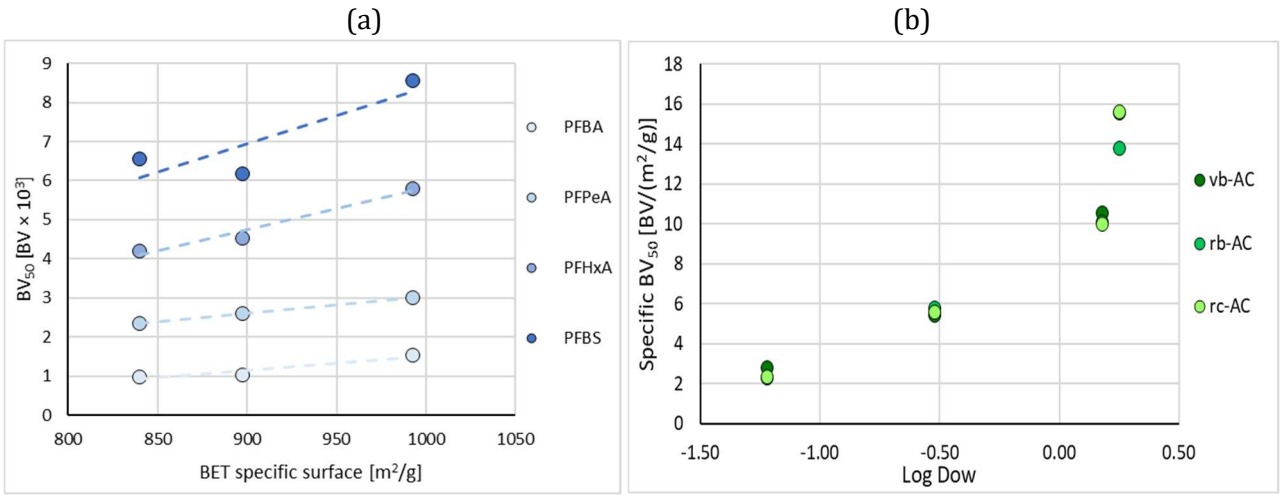

Figure S12. (a) Linear correlation between the estimated half saturation time (BV_{50}) and the BET specific surface area, (b) estimated specific BV_{50} as a function of PFAS Log D_{ow} for the three ACs.

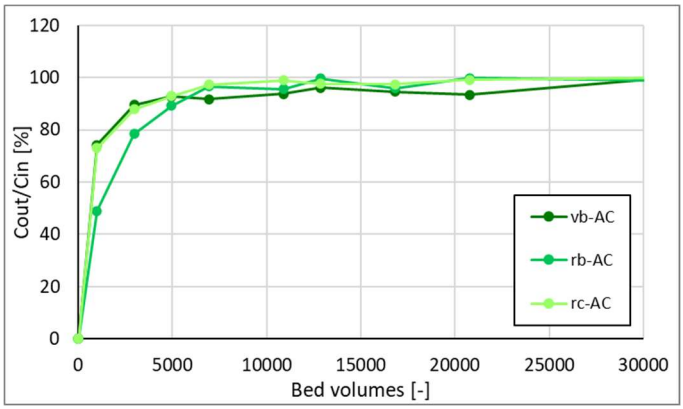

Figure S13. Breakthrough curves of UV_{254}-absorbance for the three positively-charged ACs.

Table S8. Estimated solid phase loading in ($\mu g_{PFAS}/mg_{AC}$) for each combination of PFAS and AC.

Activated carbon	PFBA	PFPeA	PFBS	PFHxA	PFHpA	PFOA	PFHxS	PFOS
vc_AC	3.4×10^{-3}	4.2×10^{-3}	3.9	1.3	5.5	15.2	13.8	14.8
vb_AC	9.4×10^{-3}	6.2×10^{-3}	24.98	12.78	21.6	47.6	43.6	74.5
rc_AC	5.4×10^{-3}	2.7×10^{-3}	8.9	1.4	12.9	37.5	26.6	65.5
rb_AC	7.7×10^{-3}	2.9×10^{-3}	13.7	6.9	13.8	43.3	38.3	82.6

CHAPTER 4

Predicting the fate of pharmaceutical active compounds (PhACs) in activated carbon adsorbers: influence of organic matter, activated carbon and PhACs structure

Abstract
The presence of pharmaceutical active compounds (PhACs) in fresh water is a source of growing concern for the negative effects they could have on both aquatic ecosystems and human health. Adsorption on activated carbon permits to achieve high removal efficiencies, but it is important to study factors affecting process performance, in order to optimize process reliability when a mixture of PhACs has to be treated. In the present work, to deepen the knowledge about the affecting factors, batch and column lab tests, according to RSSCT (Rapid Small Scale Column Tests), were performed on a mix of 8 PhACs, with different physical-chemical properties, varying: i) the aqueous matrix characteristics in terms of DOC (Dissolved Organic Carbon) and conductivity, ii) the activated carbon type, based on porosity and surface charge. Batch isotherms and breakthrough curves were fitted for each PhACs. Finally, an advanced statistical analysis, based on cluster analysis and regression modeling, was carried out for a comprehensive evaluation of the factors affecting the removal performance, considering mutual interections. The most important factors, which positively influence the adsorption process performance, are: i) high PhACs hydrophobicity, resulting in a greater affinity of the compound with the solid phase than the liquid phase, ii) activated carbon porosity, being the microporous one more efficient, iii) low concentration of DOC and conductivity, which implies reduced competitive effects. A predictive model for the value of BV_{50} (bed volumes corresponding to the 50% breakthrough) was developed, to support the selection of the best activated carbon to be adopted according to the target PhACs. Finally, the correlation between the removal of UVA_{254} (absorbance at 254 nm) and the removal of PhACs was verified both in the case of isotherms and RSSCT, highlighting that this correlation is independent from AC type and water matrix but depends on the test scale.

Keywords
Activated carbon adsorption; breakthrough curve prediction; natural organic matter; pharmaceuticals; rapid small-scale column tests; stochastic modeling.

The research work presented in this chapter was carried out during a research stay period of 3 months at the German Environmental Protection Agency (Umwelt Bundeamt – UBA), in collaboration with the Technical University of Berlin. The research work was carried out with the valuable supervision of Dr. Aki Sebastian Ruhl (UBA), the support of Pia Schumann (TU Berlin), Prof. Ilenia Epifani (Department of Mathematics, Politecnico di Milano) and one MSc student, Monica Mapelli. PhACs analyses described in this chapter were carried out with the helpful collaboration of TU Berlin lab technicians.

This chapter, once integrated with further simulations and discussion, will be prepared for submission to a peer-review international journal.

List of symbols and abbreviations

1/n	Freundlich exponent
AC	Activated Carbon
ANOVA	Analysis of variance
BET	Brunauer–Emmett–Teller
BT	Breakthrough
BV	Bed Volume
BV_{50}	Bed Volume of half saturation
C_e	Equilibrium concentration in solution
CECs	Contaminants of emerging concern
C_{IN}	RSSCT column inlet concentration
C_{OUT}	RSSCT column outlet concentration
DI	Deionized
DOC	Dissolved Organic Carbon
DOM	Dissolved Organic Matter
D_{ow}	Octanol-water partition coefficient
dp	Particle Diameter
DWTP	Drinking Water Treatment Plants
EBCT	Empty Bed Contact Time
FS	Full scale
GAC	Granular Activated Carbon
HPLC-MS	High Performance Liquid Chromatography Mass Spectrophotometry

k_C	RSSCT column constant
K_F	Freundlich adsorption constant
K_{ow}	octanol-water partition coefficient
LCOND	Low DOC and low conductivity water
LDOC	Low DOC water
LOQ	Limit Of Quantification
MTZ	Mass transfer zone
MW	Molecular weight
NOM	Natural organic matter
PAC	Powdered Activated Carbon
pH_{PZC}	pH of the Point of Zero Charge
PhACs	Pharmaceutical active compounds
q_e	Equilibrium concentration on solid phase
rb-AC	Reactivated bituminous AC
rc-AC	Reactivated coconut-based AC
RSSCT	Rapid Small-Scale Column Test
$SUVA_{254}$	Specific UV Absorbance at 254 nm
TAP	Tap water
UVA_{254}	Specific UV Absorbance at 254 nm
vb-AC	Virgin bituminous AC
vc-AC	Virgin coconut-based AC

1. Introduction

The effectiveness of activated carbon (AC) to remove pharmaceutical active compounds (PhACs) from various waters has been shown by numerous studies (*inter alia*, Summers et al., 1989; Ternes et al., 2002). However, the results from different studies are difficult to compare or to transfer, and usually extensive testing is necessary to investigate the potential of AC in each individual case. In fact, usually research studies evaluate the effect of one single factor on adsorption process not considering the combined effects of several factors that depend on the compound's properties, the nature of the activated carbon, and the characteristics of the aqueous matrix (Worch, 2012). The influence of PhACs characteristics is similar to the one of conventional organic micropollutants: adsorption extent increases with increasing molecular size of the adsorbates, as long as no size exclusion hinders the adsorbate molecules from entering the pore system. The adsorbability of organic substances onto activated carbon increases with decreasing polarity (solubility, hydrophilicity) of the adsorbate. Rivera-Utrilla et al. (2009) performed isotherms and kinetics tests on the adsorption of antibiotics (nitroimidazoles) on several activated carbons, finding an increase in the adsorption capacity with a decrease in the percentage of oxygen and an increase in the hydrophobicity of the compounds. The physical-chemical properties of the activated carbon, such as its pore size distribution, surface charge, specific surface, and functional groups, that are influenced by the source material (e.g. charcoal, wood, nutshells) and the manufacturing process (Li et al.; 2005), confer it a specific affinity towards certain compounds. In the study of Mailler et al. (2016) different ACs were compared in batch tests to evaluate the influence of the carbon properties on the removal efficiency of PhACs and other contaminants of emerging concern (CECs) in real wastewater at concentrations ranging from 6 to 1,632 ng/L. With an average removal of 52%, it emerges that the microporous AC, characterized by the highest specific surface, performs better than the mesoporous, with an average removal of 26%. This is due to the fact that microporous ACs have higher internal surface and, therefore, more active sites for CECs adsorption

(Newcombe et al., 2002; Li et al., 2005). As for the influence of water matrix characteristics, it is important to stress that in multicomponent systems, competitive adsorption takes place, resulting in a decreased adsorption of a considered compound in comparison with adsorption when it is present as single solute. Usually, PhACs and natural organic matter (NOM) are present simultaneously and they are adsorbed concurrently. Therefore, NOM constituents with molecular sizes similar to that of the target PhACs cause the largest decrease in PhACs adsorption capacity by bore blocking and competing directly with them for adsorption sites (Newcombe et al., 2002; Li et al., 2005). Kennedy et al. (2015) investigated AC adsorption of 30 CECs (including PhACs, personal care products, herbicides, insecticides, and a manufacturing additive) from four surface waters at the pilot scale. An increase in background dissolved organic matter (DOM) resulted in earlier breakthrough for most of the analyzed CECs. However, a systematic trend of increasing throughput with decreasing DOC (Dissolved Organic Carbon) concentration is not clearly evident for cotinine and methomyl. In fact, the magnitude of the decrease in adsorption capacity depends on other factors, such as the initial concentration of the CECs with respect to the one of the competing NOM (Knappe et al., 1998). The initial concentration effect is particularly important in drinking water treatment applications, where the concentration of NOM (mg/L) is about 3–6 orders of magnitude higher than the concentration of most CECs (Saravia and Frimmel, 2008).

Selecting an effective activated carbon for a given treatment objective remains a challenge because the combined effects of physical and chemical adsorbent characteristics on the adsorption of PhACs in the presence of NOM are not well understood. Therefore, this study aimed at developing a comprehensive performance prediction model to provide practical information and support in the selection of the best AC and in the optimal granular activated carbon (GAC) process design and management for drinking water treatment in the presence of a mixture of several PhACs in different water matrices. The concurrent removal of eight PhACs, having various physical-chemical properties, was firstly assessed by means of lab tests (i.e. batch isotherms and rapid small scale column tests, RSSCTs), comparing four ACs, differing in origin and activation state, in three water matrices, at different levels of DOC and conductivity. Experimental data have been then used to model PhACs breakthrough and evaluate the single and combined effects of the water and operating conditions on adsorption performance by means of advanced statistical techniques (i.e. factorial analysis, cluster analysis, regression analysis). As a result, a breakthrough prediction model was obtained. Moreover, we investigated the applicability of UVA_{254} as a surrogate parameter for PhACs removal in fixed-bed GAC applications.

2. Materials and methods

2.1. Activated carbons and reagents

All the experiments were performed using four GAC collected in full-scale adsorbers located in various drinking water treatment plants (DWTP) in a highly urbanized area in Italy. The ACs differ for: i) origin (two derive from coconut (Acticarbone NCL 1240, Arkema Group), two from bituminous coal (Cecarbon Gac 1240, Arkema Group)); ii) activation state (two are virgin, two are reactivated ACs). The adsorption capacities of the reactivated ACs have been restored through a steam-activation process to remove previously adsorbed pollutants. Abbreviations used to indicate the tested AC samples are summarized in Table 1, where their main characteristics are also reported: iodine number, BET (Brunauer–Emmett–Teller) specific surface area, micropore volume fraction and pH at point of zero charge (pH_{PZC}). Both for isotherm experiments and RSSCTs, AC samples were preliminarily milled: for isotherms, a powdered activated carbon (PAC) was obtained (44-53 μm particle size range), while for RSSCTs the fine fraction

of 90-125 µm particle size range was separated by sieving. PAC stock suspensions (2 g/L) were prepared for each AC in ultra-pure water and stored overnight for full wetting.

Table 1. Abbreviations (vc-AC: virgin coconut-based AC, rc-AC: reactivated coconut-based AC, vb-AC: virgin bituminous AC, rb-AC: reactivated bituminous AC) and main characteristics of the tested ACs.

Activated carbon	Activation state	Origin	Porosity status	Bulk density	Iodine number	BET specific surface area	Micropore volume fraction	pH_{PZC}
	-	-	-	mg/mL	mg/g	m^2/g	%	-
vc-AC	Activated	Coconut	Microporous	423.3	1072	1001.9	53.3	7.8
vb-AC	Activated	Bituminous coal	Microporous	451.0	1020	992.4	58.1	9.7
rc-AC	Reactivated	Coconut	Mesoporous	395.2	820	839.7	40.6	9.7
rb-AC	Reactivated	Bituminous coal	Mesoporous	370.0	871	897.3	35.0	9.8

A mix of eight PhACs (Sigma Aldrich, Germany, and Dr. Ehrenstorfer, Germany), listed in Table 2, was used for reagent preparation. The main chemical characteristics of the studied PhACs are reported in Table 2: origin, molar weight (MW), surface charge at the different tested pHs, octanol-water partition coefficient at pH 7.0 (log D_{ow}), octanol-water partition coefficient (log K_{ow}), maximum projection radius. All the reagents used were analytical grade. The eight analyzed PhACs were selected because of their different structure and chemical characteristics (Table 2) for which they can be classified in three different groups based on their hydrophobicity: i) hydrophilic PhACs, with log D_{ow} lower than 0 (group 1: GAB), ii) marginally hydrophobic PhACs, with log D_{ow} between 0 and 1 (group 2: SMX, FAA), and iii) hydrophobic PhACs, with log D_{ow} higher than 1 (group 3: GPL, VAL, DCF, PRI, CBZ). Moreover, they can be divided according to the surface charge assumed at the tested water pH between neutral CECs (GAB, FAA, GPL, PRI, CBZ) and negatively charged CECs (SMX, VAL, DCF).

Table 2. PhACs used in the experiments and their main physical-chemical characteristics.

Group	PhAC		Use	Formula	MW [α]	Charge [α] at pH [7.3; 7.8]	log D_{ow} [α]	log K_{ow} [α]	Maximum projection radius [α]
					[g/mol]				[Å]
1	Gabapentin	GAB	Antiepileptic	$C_9H_{17}NO_2$	171.2	0	-1.27	0.99	4.95
2	Sulfamethoxazole	SMX	Antibiotic	$C_{10}H_{11}N_3O_3S$	253.3	-0.95	0.00	0.79	7.55
	4-formylamino-antipyrine	FAA	Analgetics	$C_{12}H_{13}N_3O_2$	231.3	0	0.11	0.11	6.31
3	Gabapentin Lactam	GPL	Antiepileptic	$C_9H_{15}NO$	153.2	0	1.03	1.03	4.81
	Valsartan	VAL	Antihypertensivum	$C_{24}H_{29}N_5O_3$	435.5	-1.98	1.08	5.27	8.46
	Diclofenac	DCF	Anti-inflammatory	$C_{14}H_{11}Cl_2NO_2$	296.2	-1	1.10	4.26	6.01
	Primidone	PRI	Antiepileptic	$C_{12}H_{14}N_2O_2$	218.3	0	1.12	1.12	5.39
	Carbamazepine	CBZ	Antiepileptic	$C_{15}H_{12}N_2O$	236.3	0	2.77	2.77	5.82

[α] Data estimated through MarvinSketch 18.11.0 (ChemAxon Ltd., http://www.chemaxon.com/).

2.2. Test solutions

Both isotherm experiments and RSSCTs were performed on three water matrices: i) TAP, that is tap water derived from surface source water, ii) LDOC, that is tap water diluted five times with a salt solution

(SS) made of DI water with addition of salts at the same concentration of TAP, iii) LCOND, that is tap water diluted five times with deionized (DI) water only. The effect of NOM can be evaluated, comparing TAP and LDOC water matrices, having, respectively, DOC concentration of 5 mg/L (typical of surface water) and 1 mg/L (typical of groundwater) (see Table 3). In addition, it was evaluated the effect of conductivity on the adsorption to test whether the dilution made with the addition of the saline solution (LDOC) or with DI water (LCOND) results in different isotherms and breakthrough curves. The SS included the following salts and relative concentration: $CaCl_2$ (33.3 mg/L), $NaHCO_3$ (126.0 mg/L), KNO_3 (20.2 mg/L) (Merck, Germany), and $CaSO_4 \cdot 2H_2O$ (344.4 mg/L), $MgCl_2 \cdot 6H_2O$ (101.9 mg/L) (Carl Roth, Germany). Table 3 shows the tested water matrices main characteristics: DOC, conductivity, pH, specific UV absorbance at 254 nm ($SUVA_{254}$).
Water matrices were spiked with the stock solution containing eight PhACs, at 10 mg/L each one, to adjust single PhACs concentration at 1 μg/L in the solutions for both isotherm experiments and RSSCTs.

Table 3. Water matrices dilution volumes and measured parameters: mean ± standard deviation.

Water matrix	Tap	DI	SS	DOC	Conductivity	Measured pH	$SUVA_{254}$
	[%]	[%]	[%]	[mg L^{-1}]	[μS cm^{-1}]	[-]	[L mg^{-1} m^{-1}]
TAP	100	0	0	5.0 ± 0.07	736 ± 17.2	7.5 ± 0.16	2.1± 0.02
LCOND	20	80	0	1.3 ± 0.03	169 ± 1.5	7.3 ± 0.14	2.0± 0.05
LDOC	20	0	80	1.6 ± 0.10	712 ± 21.0	7.8 ± 0.20	1.7± 0.01

2.3. Batch isotherm experiments

Isotherm experiments were performed with PhACs-spiked test waters and the four AC at various doses (1, 2, 5, 10, 15, 20, 50 mg/L): specifically, different volumes of the PAC stock suspensions (homogenized by stirring) were pipetted into 50 mL of the PhACs-spiked test water, never exceeding a 3% dilution. Flasks were closed and agitated on a horizontal shaker allowing for continuous and full mixture of the test suspensions for 48 hours at room temperature, whereupon PAC was separated with a vacuum membrane filtration (0.45 μm regenerated cellulose, Macherey-Nagel, Germany). An additional flask only with PhACs-spiked test water was used as reference. Filtrated samples were analyzed for PhACs concentration, DOC, UVA_{254}, conductivity and pH.

2.4. Rapid small-scale column tests (RSSCTs)

RSSCTs were carried out with PhACs-spiked test waters and the four ACs in cylindrical borings in a acrylic glass block with an inner diameter and cross-sectional area of 7 mm and $3.85 \cdot 10^{-5}$ m^2, respectively. Each column was filled with 190 mg AC on supporting glass beads to prevent the grains from being washed out and AC was rinsed for 2 hours with deionized water prior to the RSSCT experiments. Since previous studies demonstrated that PhACs intra-particle diffusion is independent from adsorbent size in the tested tap water (Freihardt et al., 2017), the downscaling Eq. (1) for the case of constant diffusivity (Crittenden et al., 1991) was adopted for determining the empty bed contact time (EBCT) to be applied:

$$\frac{\mathrm{EBCT}_{RSSCT}}{EBCT_{FS}} = \left[\frac{\mathrm{d}_{p,RSSCT}}{d_{p,FS}}\right]^2 \qquad \text{(Eq. 1)}$$

where $EBCT_{RSSCT}$ and $EBCT_{FS}$ represent the EBCT values of the RSSCT and the full-scale adsorber. $EBCT_{FS}$ was set to 11 min, calculated as the average EBCT of fixed-bed GAC adsorbers located in 17 DWTPs in an urbanized area were the GAC samples were collected (see Figure S1 in the Supplementary Material).

The RSSCT mean particle diameter ($d_{p,RSSCT}$) was assumed 110 µm (as the mean value of the opening sizes of the two sieves), while the full-scale mean particle diameter ($d_{p,FS}$) is 1.2 mm. Therefore, the $EBCT_{RSSCT}$ was set to 5.5 s. Since each AC has a different bulk density (see Table 1), the volume of the AC bed in each column was different. Consequently, in order to guarantee the same $EBCT_{RSSCT}$, different flowrates were set for columns containing vc-AC, vb-AC, rc-AC and rb-AC corresponding to 0.29, 0.28, 0.31 and 0.34 L/h, respectively. RSSCTs column set-up details are reported in Table 4. The columns were operated in up-flow for seven days. The influent to each column was sampled every two days, while effluent sampling was performed every three hours by an automatic sampler. Collected samples were used for PhACs concentration, DOC, , UVA_{254}, conductivity and pH determination.

Table 4. RSSCTs columns set-up details for the different ACs: full-scale EBCT ($EBCT_{FS}$) and mean AC particle diameter ($d_{p,FS}$), RSSCT mean AC particle diameter ($d_{p,RSSCT}$) and calculated EBCT ($EBCT_{RSSCT}$), ACs bulk density, column volume and calculated flowrate.

Activated carbon	$EBCT_{FS}$	$d_{p,FS}$	$d_{p,RSSCT}$	$EBCT_{RSSCT}$	Bulk density	AC column volume	Flowrate
	min	mm	µm	sec	mg/mL	mL	L/h
vc-AC	11	1.2	110	5.5	423.3	0.448	0.29
vb-AC	11	1.2	110	5.5	451.0	0.421	0.28
rc-AC	11	1.2	110	5.5	395.2	0.481	0.31
rb-AC	11	1.2	110	5.5	370.0	0.514	0.34

2.5. Analytical methods

Iodine number was determined according to the standard ASTM4604. The pH_{PZC} was determined by the pH drift method (Lopez-Ramon et al., 1999): 0.3 g of carbon were added in 100 mL of 0.01 mol/L NaCl solution, after pH adjustment by means of 0.1 mol/L HCl or NaOH solutions; for each AC, 6 initial pH values were evaluated (in duplicate), measuring the final pH of the solution after 48 h; pH_{PZC} was determined by plotting initial vs. final pH values. Carbon surface area was determined according to the BET method (Brunauer et al., 1938), specific area and volume of micropores were determined by the t-Plot method (Barrett et al., 1951), pore size distribution was determined by the BJH method (Horvath et al., 1983). DOC was determined using a Vario TOC cube (Elementar Analysensysteme, Germany). Conductivity was measured using GMH 3410 (Greisinger electronic, Germany) and pH by a pH-meter pH537 (WTW, USA). UV absorption at 254 nm was measured with a Lambda 12 UV/vis spectrometer (Perkin- Elmer, USA) using quartz Suprasil 10 mm cuvettes (Hellma GmbH & Co. KG, Germany).
PhACs were measured by high performance liquid chromatography with tandem mass spectrometry (HPLC-MS/MS); sample volumes of 25 µL were separated using a on an XSelect HSS T3 HPLC column (2.5 µm particle size, 2.1*50 mm, Waters, USA) with a linear gradient (ultra-pure water with 5 vol.-% Methanol (HPLC grade, J.T. Baker, USA) and 0.1 vol.% formic acid (HPLC grade, Sigma Aldrich, Germany) versus 100% Methanol) running at 0.5 mL/min, and a TSQ Vantage (Thermo Scientific, USA) using ESI±. For each analyte, two mass fragments were chosen according to the DAIOS database (Wasserchemische Gesellschaft 2013). Deuterized isotopes (TRC, Canada, and Dr. Ehrenstorfer, Germany) were used for quantification. Limits of quantification (LOQ) were verified prior to the analysis by multiple measurement of spiked water samples at the concentration levels of LOQ according to ISO/TS 13530 Annex A. The analytical method LOQ was between to 0.05 µg/L and 0.1 µg/L depending on the PhAC.

2.6. Statistical analyses and software

Cluster analysis with k-means procedure was applied on Minitab to segment the data set and group the units that resemble each other. k-means is a clustering algorithm widely used in the context of unsupervised class division of data. The number of clusters in which the sample is divided is a parameter provided *a priori* to the algorithm. The cluster search is based on an iterative procedure. Firstly, the algorithm defines the centroids. The cluster in which each dot falls is defined through the minimization of the distance between the dot and each centroid: the dot falls into a given cluster if it is closer to its centroid than all other clusters' centroids. The algorithm then changes the centroids position iteratively, until a condition of convergence (Singh et al., 2004).

3. Preliminary results and discussion

The AC samples were selected for studying the influence of AC reactivation on PhACs adsorption kinetics and capacity, since it modifies their physical-chemical properties (Table 1). In detail, reactivation causes a decrease of both BET surface and micropore volume fraction, shifting the ACs from being microporous carbons to mesoporous carbons. Consequently, virgin carbons (vc-AC and vb-AC) should display a higher affinity towards small compounds, considering that the adsorption is favored when the sizes of pore and solute are similar (Newcombe et al., 2002). Additionally, vc-AC is characterized by a neutral surface, being the pH_{PZC} similar to the pH of the tested tap water, differently from the other ACs, which have a positively-charged surface.

3.1. Isotherm modeling

Isotherms data were fitted adopting the Freundlich model, which is an empirical relationship describing the adsorption of many compounds in diluted solutions (Schwarzenbach et al., 2003), widely used in the water field. The Freundlich model equation is:

$$q_e = K_F C_e^{\frac{1}{n}} \quad \text{(Eq. 2)}$$

where q_e (ng/mg) is the equilibrium concentration of the target compound on the solid phase (or loading), C_e (ng/L) is the equilibrium concentration in solution, K_F [(ng/mg)(ng/L)$^{-1/n}$] is the Freundlich adsorption coefficient and 1/n [-] is the Freundlich exponent which provides a measure for the sorption intensity (Ochoa-Herrera and Sierra-Alvarez, 2008). Isotherm parameters and the regression determination coefficients, R^2, for the two virgin ACs and all the combinations of water matrices and PhACs, are reported in Table 5. Values of the determination coefficient R^2 range from 0.001 to 0.999, with average equal to 0.504, indicating that these fittings cannot be used to make quantitative prediction of adsorption. Anyway, they are a useful tool to qualitatively compare AC performances and CECs removal extent, and to highlight competition phenomena. Adsorption isotherms data and related interpolation lines are reported in Figure 1 for GAB, SMX and CBZ, representative of hydrophilic (group 1), marginally hydrophobic (group 2) and hydrophobic (group 3) PhACs, for the two virgin ACs and the three tested water matrices.

Table 5. Freundlich isotherm constants and R^2 estimated for all the combinations of water matrices and PhACs with the two virgin ACs. Compounds are reported in order of increasing hydrophobicity.

Water Matrix	ACs	Models Coefficients	GAB	SMX	FAA	GPL	VAL	PRI	DCF	CBZ
TAP	vc-AC	K_F [(ng/mg)(ng/L)$^{-1/n}$]	26.86	83.77		4.60	0.89	31.34		21.15
		1/n [-]	-0.125	-0.092		0.421	0.103	0.227		0.528
		R^2	0.007	0.043		0.633	0.447	0.313		0.963
	vb-AC	K_F [(ng/mg)(ng/L)$^{-1/n}$]	0.458	151.74		8.52	60.12	41.61		122.40
		1/n [-]	0.547	-0.121		0.401	-0.044	0.271		0.286
		R^2	0.445	0.254		0.951	0.003	0.581		0.975
LDOC	vc-AC	K_F [(ng/mg)(ng/L)$^{-1/n}$]	0.001	12.77	49.5	4.32	13.65	41.52	30.92	55.24
		1/n [-]	1.587	0.359	0.152	0.573	0.332	0.320	0.316	0.298
		R^2	0.377	0.641	0.365	0.510	0.794	0.791	0.805	0.980
	vb-AC	K_F [(ng/mg)(ng/L)$^{-1/n}$]	0.016	18.90	0.00	10.47	19.74	49.00	27.70	53.04
		1/n [-]	1.279	0.284	2.25	0.476	0.367	0.292	0.344	0.283
		R^2	0.477	0.397	0.91	0.452	0.472	0.498	0.446	0.939
LCOND	vc-AC	K_F [(ng/mg)(ng/L)$^{-1/n}$]	0.075	38.68	22.7	41.00	18.32	138.13	56.87	75.33
		1/n [-]	0.984	0.007	0.25	0.472	0.323	0.309	0.103	0.341
		R^2	0.260	0.0002	0.95	0.163	0.284	0.999	0.066	0.944
	vb-AC	K_F [(ng/mg)(ng/L)$^{-1/n}$]	0.011	24.51	228.8	19.97	27.96	98.71	11.97	21.7
		1/n [-]	1.346	0.237	-0.029	0.424	0.271	0.287	0.509	0.733
		R^2	0.634	0.325	0.009	0.738	0.597	0.829	0.612	0.692

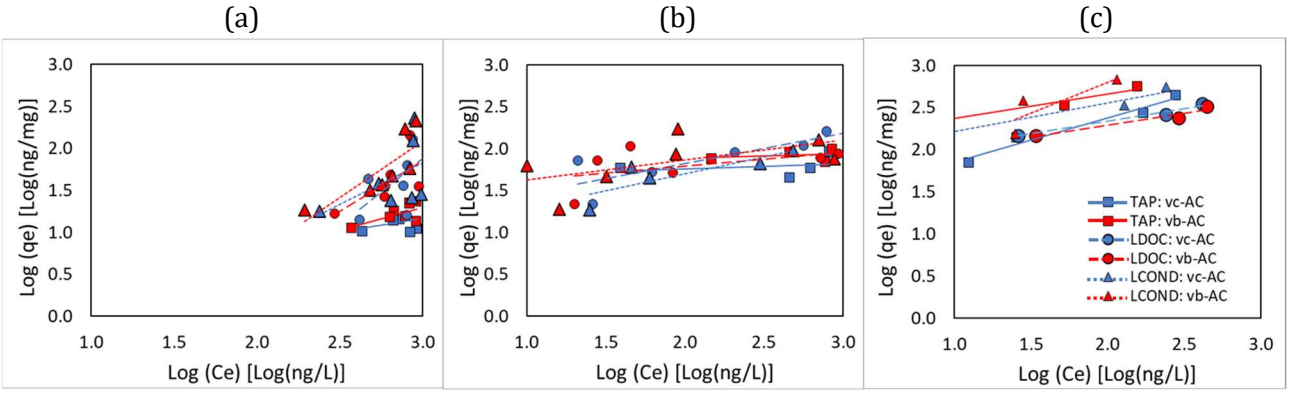

Figure 1. Estimated isotherms of the two virgin ACs in TAP, LDOC and LCOND water matrixes for: GAB (a), SMX (b), CBZ (c).

From a visual inspection, comparing the isotherm shapes found for GAB, SMX and CBZ for the two ACs in the three water matrices, it can be stated that the isotherm shapes are more sensitive to the analyzed PhACs compared to the selected AC or the tested water matrix. In particular, it can be observed that GAB

was characterized by higher equilibrium water concentrations (C_e) and lower equilibrium concentration in the solid phase (q_e) and, therefore, it was less adsorbed compared to SMX, which was in turn less adsorbed compared to CBZ. Therefore, as expected, adsorption capacity tends to increase with the hydrophobicity of the compound (described by its log D_{ow}), independently from the studied AC and water matrix. Actually, hydrophobic interactions relate primarily to the affinity between adsorbates and water: hydrophobic compounds are more likely to partition to the solid phase (Park et al., 2020). All isotherms are non-linear as the values of 1/n are in the range from -0.125 to 2.25. Isotherms non-linearity (having 1/n values different from 1) was explained in previous works by adsorbate–adsorbate interactions, such as electrostatic repulsion (Cheung et al., 2001). For the more hydrophilic compounds, this can be due to competition with more hydrophobic compounds. Finally, comparing the isotherms shape obtained for the same PhACs in TAP water with respect to the ones obtained in LDOC and LCOND waters, it emerges that in TAP water several PhACs (GAB, SMX, GPL, VAL, PRI) display isotherms with a more horizontal trend (lower 1/n values in Table 5) compared to the two matrices at low DOC. This finding confirms that competition with NOM can be seen as an additional reason of the lower adsorption, resulting in a detrimental effect of NOM in competing for adsorption active sites or in displaying steric blockage of micropores (Newcombe et al., 2002; Li et al., 2005; Kennedy et al., 2015).

3.2. RSSCT breakthrough curves modeling

The breakthrough (BT) curve resulting from the RSSCTs represents the ratio between the concentration at the outlet and inlet of the AC column as a function of the bed volume treated (volume of treated water at time t normalized with respect to AC bed volume) in the column. Analyzing the curves of the different compounds as a function of the different matrices and the different ACs, it is possible to note their effect on the trend of the curves.

The BT curve data have been fitted by the Lin and Huang model (Eq. 3):

$$t = BV_{50} + \frac{1}{k_C} ln\left[\frac{Cout\,(t)}{Cin - Cout\,(t)}\right] \qquad \text{(Eq. 3)}$$

where c_{in} and c_{out} are the concentrations of the individual PhACs, respectively, in the column influent and effluent at time t, here expressed in thousand bed volumes [BV×10^3], k_C is a column constant that is related to the slope of the breakthrough curve, while BV_{50} corresponds to the throughput in BV at which c_{out} reaches 50% of c_{in}. Some examples of the experimental data and estimated BT curves, are reported in Figure 2 for GAB, FAA and CBZ, representative of hydrophilic (group 1), marginally hydrophobic (group 2) and hydrophobic (group 3) PhACs, as a function of the ACs and water matrices.

Modeling was performed for each compound, for all the water matrices and all the ACs. The model well adapts to data since in general the R^2 values obtained are high, ranging between 0.58 to 0.96, with an average of 0.80.

As it was in the case of isotherms, also the BT curves shape seems to be more influenced by the PhACs than from the selected AC or the tested water matrix. It can be noted that the more hydrophilic compounds are removed less easily, with steeper curves that approach earlier the breakthrough and have a smaller active removal zone, compare to PhACs at increasing hydrophobicity. Moreover, in the case of synthetic matrices, such as the LDOC and LCOND, all the PhACs tend to have better adsorption. However, LDOC and LCOND BT curves for GAB are similar, while FAA and CBZ were better removed in water characterized by a lower conductivity. Considering every single PhAC and comparing the BT curve of the different ACs, it can be noted how the effect of the AC can change depending on the compound considered (Figure 2b, d, f).

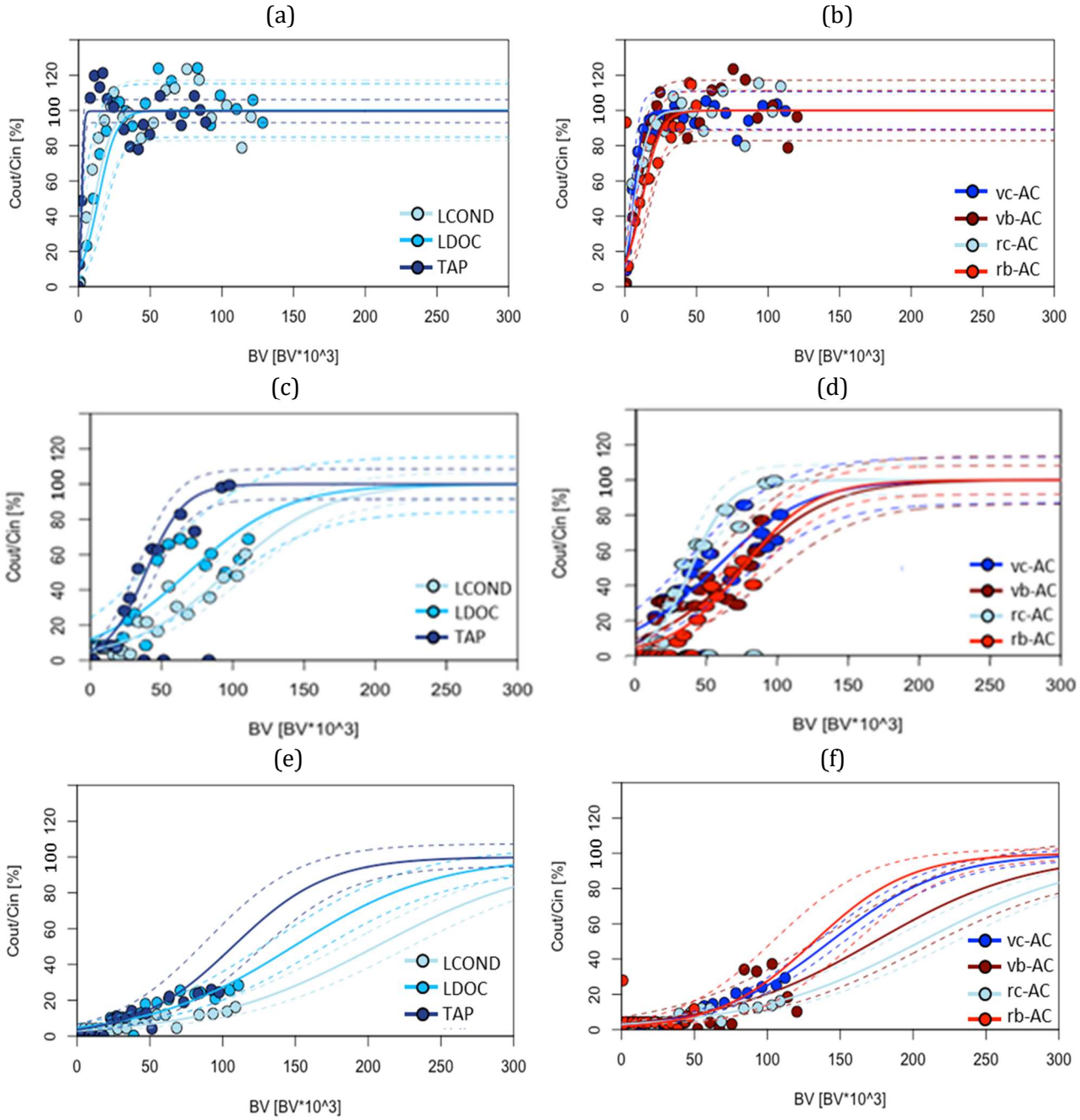

Figure 2. Breakthrough curves for the three water matrices (a, c, e) and for the four tested ACs (b, d, f) for GAB (obtained with vb-AC (a) and LCOND (b)), FAA (obtained with rc-AC (c) and TAP (d)) and CBZ (obtained with rc-AC (e) and LDOC (f)). Solid lines are the fitted models while dashed lines are the model 95% confidence intervals.

3.3. Influence of water and operating conditions on adsorption capacity

The previous results highlight that adsorption is a complex process affected by many factors, interacting one each other: the water quality, the AC type, the PhAC chemical characteristics and their interactions. Consequently, the goal of the statistical analysis was to understand which of these factors have more influence and how they interact affecting the adsorption process. The BT curves fitting modeling was used to derive, for each combination of PhAC, AC and water matrix, the two main indicators of adsorption capacity used for statistical analyses: BV_{50} and the Mass Transfer Zone (MTZ) extension. The

BV_{50} was chosen as an indicator of adsorption capacity, to which it is proportional if the concentration of target compound is low enough (in the range of µg/L or below) and DOM is present (Corwin and Summers, 2011). The MTZ extension, which is calculated as the difference between BV_{90} and BV_{10}, is an indicator of the slope of the breakthrough curve and the width of the active zone where the actual adsorption process takes place, so more it is extended, higher it is the level of competition to which a compound is subjected.

The BV_{50} and MTZ derived from BT curve fitting (section 3.2) were chosen as clustering factors in a cluster analysis performed to group in 4 clusters the experimental conditions that resemble each other and to understand the conditions that affect adsorption extent of the various PhACs (Figure 3).

The first cluster includes the experiments, characterized by the most disadvantaged conditions, with the lowest median BV_{50} (almost 21,000 BV) and MTZ (around 36,000 BV), followed by cluster 2, with median BV_{50} respectively of 75,000 BV and MTZ of 147,000 BV. Better performances are found for clusters 3 and 4 that are both characterized by comparable high BV_{50} (median values around 175,000 BV) but different MTZ (median values around 198,000 BV for cluster 3 and 145,000 BV for cluster 4). Actually, cluster 4 groups the PhACs and conditions for which less competitive effects are involved and adsorption is favored.

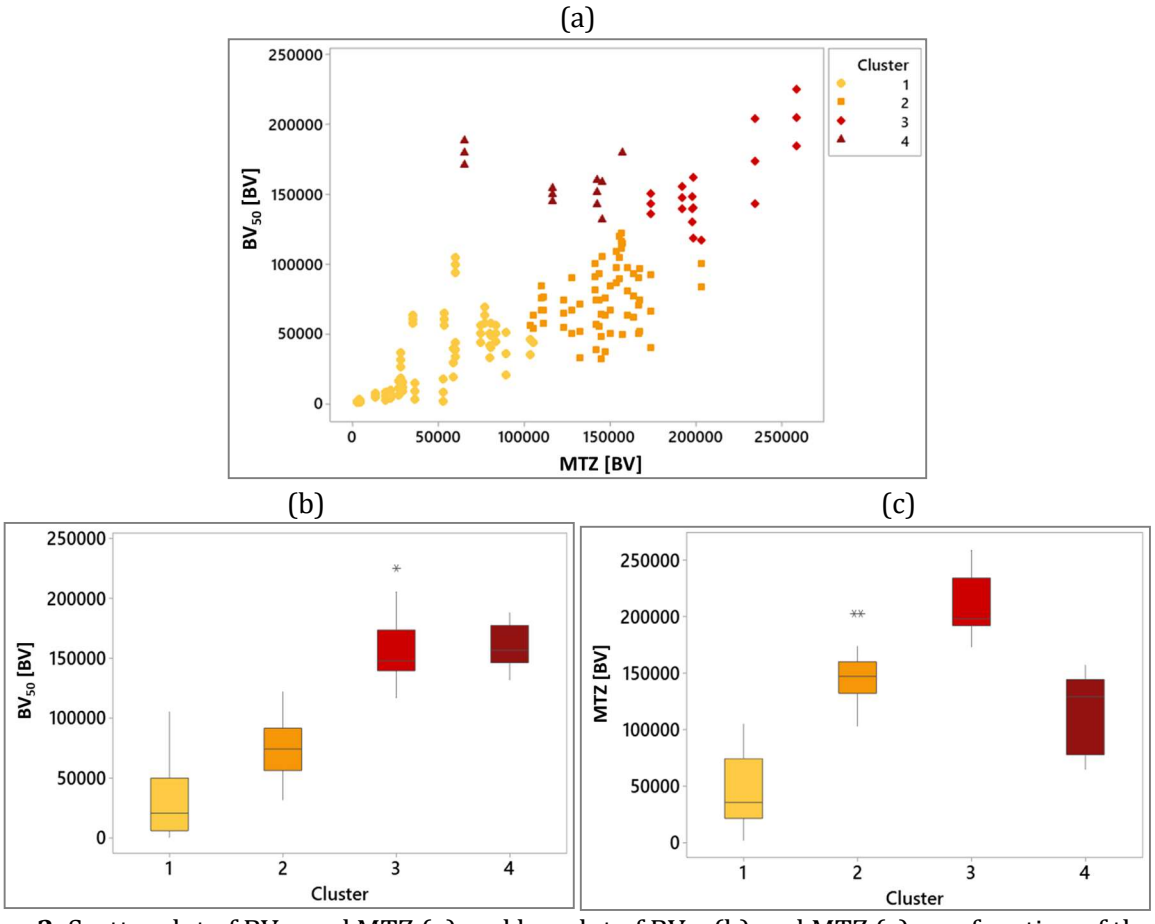

Figure 3. Scatterplot of BV_{50} and MTZ (a) and boxplot of BV_{50} (b) and MTZ (c) as a function of the four identified clusters.

For a more detailed evaluation, it is interesting to understand specifically how clusters are composed according to the starting variables to recognize how they influence adsorption process, as shown in Figure 4.

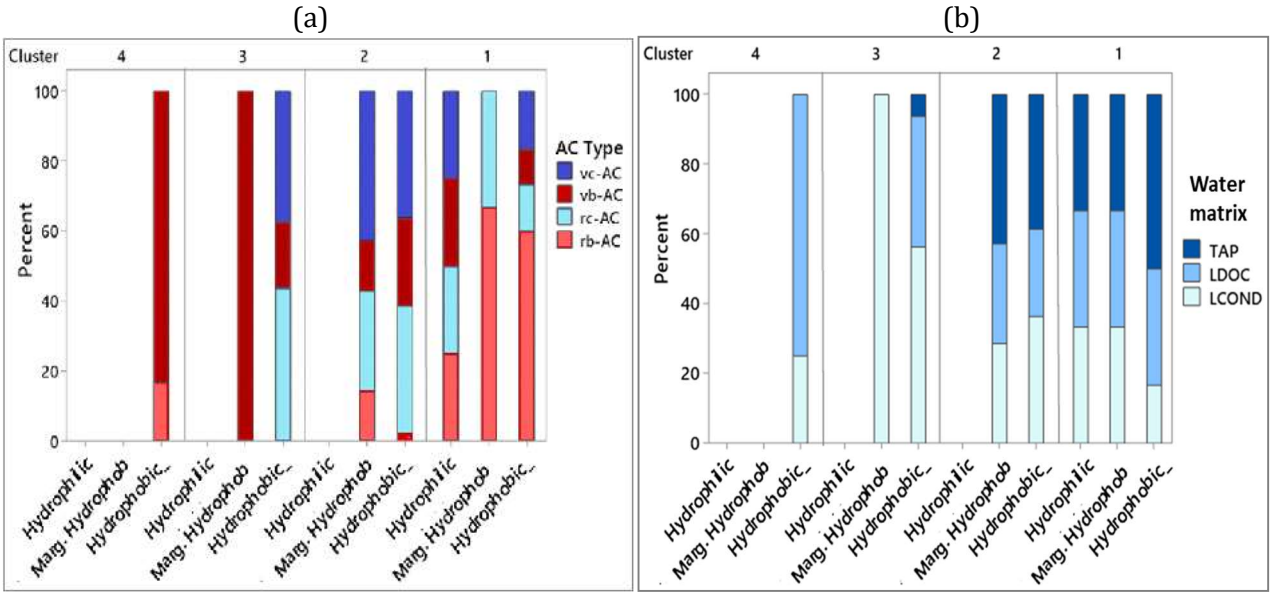

Figure 4. Bar chart of the four clusters as a function of PhACs hydrophobicity depending on: AC (a) and water matrix (b).

It can be observed that only hydrophobic PhACs fall in cluster 4, that groups the more favoring conditions, mainly in tests with vb-AC and in water matrices at low DOC concentration, mainly LDOC. In cluster 3 marginally hydrophobic PhACs can also be found, but only tested with vb-AC in LCOND water. No tests with mesoporous rb-AC can be found in cluster 3, since results with rb-AC mainly fall in cluster 1, describing disadvantaged conditions. Regardless the PhACs and ACs, tests in TAP water were characterized by worse adsorption compared to low DOC synthetic matrices, being the former more in cluster 1 and 2. Finally, regardless the AC and water matrix, BT curves of hydrophilic PhACs fall in cluster 1, characterized by the fastest breakthrough.

To support the AC selection based on the source water characteristics and the mixture of PhACs, a prediction model was built to predict the BV_{50} as a function of the following factors: i) source water characteristics (conductivity and DOC concentration), ii) ACs properties (BET surface, related to porosity distribution, and surface charge), iii) PhACs chemical characteristics (log D_{ow}, related to their hydrophobicity, charge and molar concentration), and iv) all the pairwise interactions between factors. The structure of the analyzed regression model is the following:

$$y = b_0 + \sum b_i \cdot x_i + \sum b_{ij} \cdot x_i \cdot x_j + \varepsilon \qquad \text{(Eq. 4)}$$

where b_0, b_i and b_{ij} are the coefficients to be estimated, while ε is the residual error term of the model; y represents BV_{50} while x the affecting factors. Table 6 reports the coded coefficients of the factors found to be significant in the prediction model, being their p-value lower than the significance level (α=0.05). The regression results are summarized in the Pareto charts (Figure 5), showing the standardized effects, that are indicators of the influence of the significant factors on the adsorption capacity, represented by the BV_{50}.

Table 6. Regression model coded coefficients, coefficients standard errors (SE Coef) and their 95% confidence interval for the linear and interaction factors found to be significant and their p-values.

Term	Coef	SE Coef	95% CI	t-value	p-value
Constant	73117	2180	(68813; 77421)	33,55	0,000
Log Dow	39576	2172	(35287; 43865)	18,22	0,000
Charge	11941	2305	(7388; 16493)	5,18	0,000
BET surface	13220	2159	(8956; 17485)	6,12	0,000
AC charge	8894	2152	(4644; 13143)	4,13	0,000
DOC	-6180	2373	(-10867; -1493)	-2,60	0,010
Conductivity	-5909	2300	(-10451; -1367)	-2,57	0,011
Inlet concentration micromol	-18415	2828	(-23999; -12830)	-6,51	0,000
Log Dow*DOC	-10154	2306	(-14707; -5600)	-4,40	0,000
Log Dow*Inlet concentration micromol	17106	4597	(8028; 26184)	3,72	0,000
Charge*AC charge	-4791	1975	(-8691; -890)	-2,43	0,016

The regression explains 75.47% of the variance (R^2 = 0.769, adjusted R^2 = 0.755, predicted R^2 = 0.739). The p-values under α=0.05 for all the predictors indicate that all linear effects are significant, differently to factors' interactions, considering that only three of them are significant.

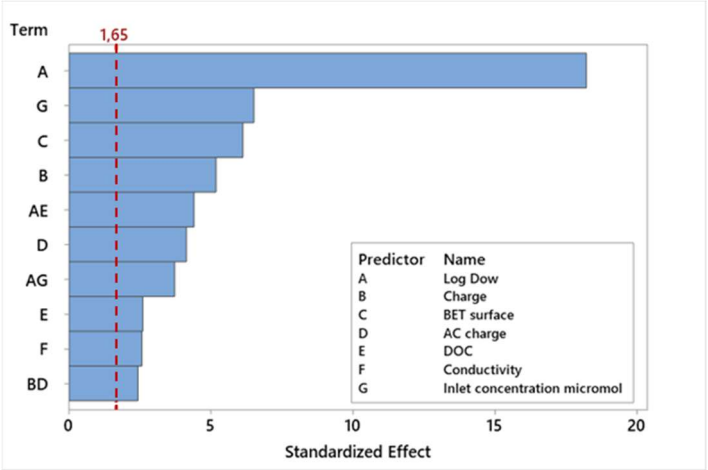

Figure 5. Pareto chart showing significant factors standardized effects on BV_{50}: the red dashed line represents the significance threshold at α=0.05

Looking at the standardized effects and coded coefficients, it can be stated that the main influencing factor (highest standardized effect and coefficient value) for BV_{50} is PhACs hydrophobicity (log D_{ow}). Since the coded coefficient for PhACs log D_{ow} is positive, it is confirmed the general evidence found in literature that adsorption capacity increases with compounds hydrophobicity. Moreover, this analysis allowed to conclude that the increase of BV_{50} with PhACs hydrophobicity (log D_{ow}) is influenced by its inlet molar concentration and the water DOC content, since significant interaction effects have been found. The AC properties were found to be influent with positive coded coefficients for both BET surface and AC charge, meaning that microporous positively-charged ACs tend to perform better than mesoporous neutral ones. It is interesting to see that there is a significant interaction factor between the PhACs and ACs surface charge, with a negative coded coefficient, suggesting that electrostatic interactions play an important role in determining adsorption. Finally, as for water characteristics, it was found that both DOC concentration and conductivity have a negative linear coefficient, meaning that

they negatively affect PhACs adsorption capacity. This finding has an important practical implication when designing a lab test. In fact, since the salt concentration affects the adsorption capacity, when preparing a synthetic matrix, either diluting tap water with DI water (for example to evaluate different levels of DOC) or adding to DI water the target compound (for example to avoid DOM competition), it is necessary to integrate salts in the solution.

3.4. UVA_{254} as surrogate parameter for PhACs removal monitoring

Previous studies have reported, for AC adsorption in laboratory-scale experiments, good correlations between compound removal and corresponding removal of UVA_{254} (Altmann et al., 2014; Zietzschmann et al., 2014). As UVA_{254} is usually easy to measure and monitor, it appears possible to monitor and predict CECs removal in large-scale applications using UVA_{254} measurements and the batch test correlations (Altmann et al., 2014).

Here, referring to batch experiments, the molar PhACs concentrations were summed up and used for the calculation of the overall PhACs removal that was then correlated with UVA_{254} removal for different ACs (Figure 6a) and water matrices (Figure 6b).

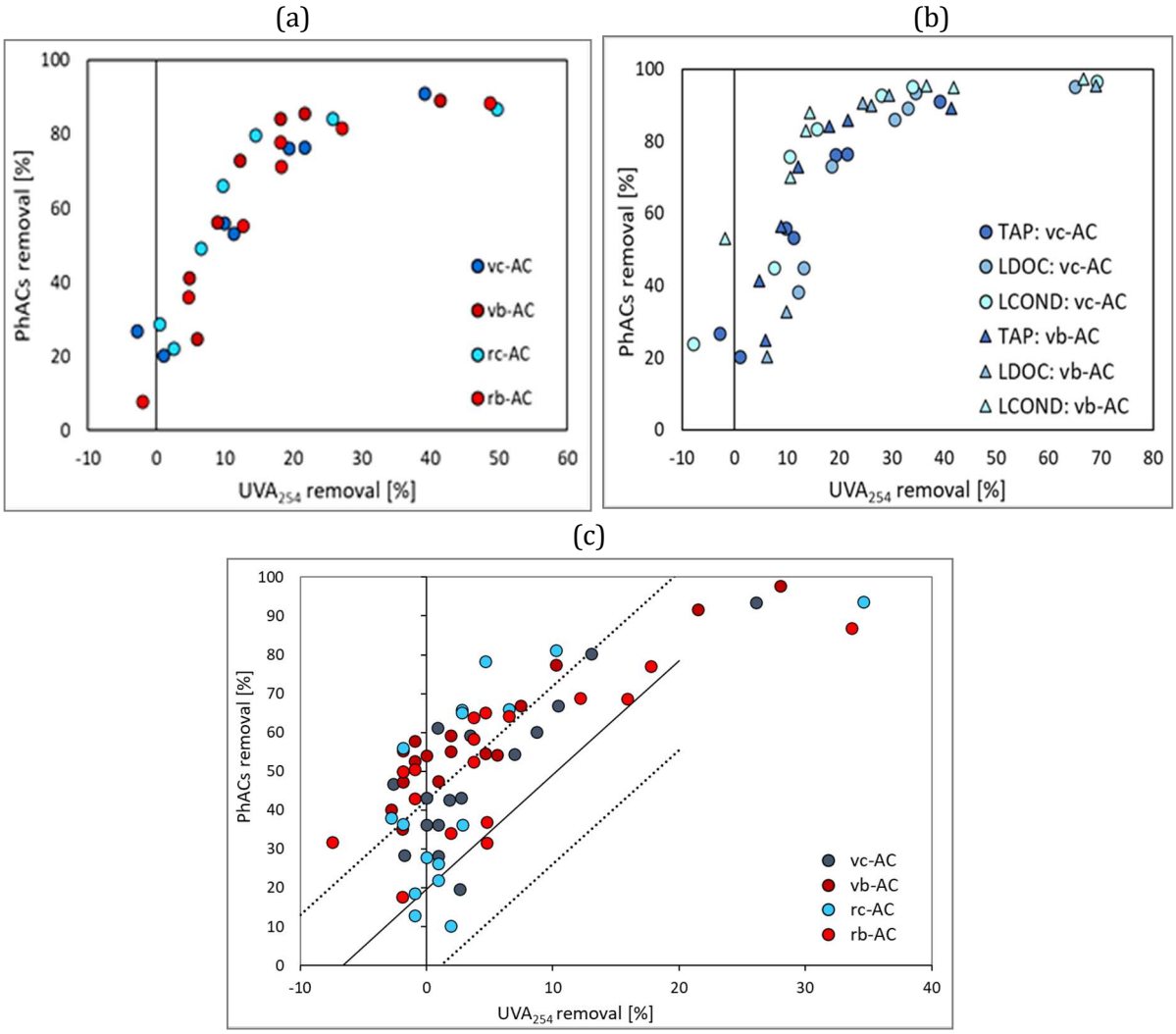

Figure 6. Correlation between PhACs removal and UVA_{254} removal for different ACs (a) and water matrices (b) with the two virgin ACs. (c) Comparison between the prediction line from batch experiments, reported as the black regression line with its 95% confidential interval, and experimental data, reported as dots, obtained by RSSCTs with different ACs in TAP water.

The relationship between PhACs removal and UVA_{254} removal assumes a saturation trend, with the plateau approached for UVA_{254} removal higher than 30%. For UVA_{254} removal lower than 30%, linear regressions well describe the relation between UVA_{254} removal and the sum of PhACs removal. Based on two-ways ANOVA outputs (significance level α=0.05), this correlation is not influenced by the AC type (p-value equal to 0.83) or the water matrix (p-value equal to 0.22), permitting to group together and fit all the isotherms data by a linear regression. The fitted line ($y=2.78 \cdot x + 25.5$) and its 95% confidence interval are plotted in Figure 6c, having a satisfactory R^2 value (0.873). Then, experimental data from RSSCTs were compared to the fitting line (Figure 6c), to verify if the correlation found in batch experiments can be used to predict PhACs breakthrough.

As for the comparison of batch and RSSCTs correlations, data could be grouped into two clusters: the first cluster is positioned around a null UVA_{254} removal value, comprising PhACs efficiency values up to 60%, the second cluster comprises data following the trend of the fitting line estimated from batch experiments, even if positioned close to the upper bound of the 95% confidential interval. The presence of the first cluster is due to the fact that UVA_{254} breakthrough curves rise faster than those of PhACs. In fact, the UVA_{254} BV_{50} is around 1,000-1,500 BV, that are earlier compared to PhACs ones, therefore UVA_{254} removal results to be null for most of the analyzed samples. The second is related to the beginning of the tests, when both UVA_{254} and PhACs were still removed. The RSSCT values are positioned on the upper bound of the confidence interval of the correlation found in the batch experiments, meaning that, for the same UVA_{254} removal, PhACs were better removed in RSSCTs compared to batch. This finding could be explained with the different test methods by which the adsorbent is contacted with water. In fact, compounds adsorption on AC can be explained through several consecutive steps (Caetano et al., 2009): i) the diffusion of solute through the liquid film surrounding the particle (Liquid Film Diffusion); ii) the diffusion of solute through the porous/polymeric matrix of the sorbent media (Particle Diffusion); iii) the chemical reaction. One of these steps usually offers much greater resistance than the others and may thus be considered as the rate-limiting step of the process. In batch experiments, the particle diffusion is the rate-limiting step, because only the equilibrium situation is taken into consideration after the step of liquid film diffusion is completed. The RSSCT experiments are useful to study the effect of liquid film diffusion, that is most likely rate-limiting for usually adopted flow rates (Weber, 1972; Xie et al., 2011). Therefore, the fact that PhACs were better removed in RSSCTs than in batch experiments, at a given UVA_{254} removal, suggests how the particle diffusion, as a limiting step, weighs more in terms of efficiency loss than the diffusion in the liquid film for PhACs adsorption on AC. Finally, the correlation found in batch experiments cannot be used in continuous-flow applications for the prediction and real time monitoring of PhACs removal by GAC adsorbers.

4. Conclusions

The adsorption behavior of eight PhACs in TAP water and in low DOC water matrices with two levels of conductivity was studied by batch tests and RSSCT with four ACs. Isotherms and breakthrough curves fitting allowed to evaluate combined effects of PhACs properties, ACs characteristics and water background conditions, by means of advanced statistical analyses. A cluster analysis on two BT curves parameters (BV_{50} and MTZ) allowed to group in 4 clusters the experimental conditions that resemble each other and to understand the conditions that affect adsorption extent of the various PhACs. Moreover, a regression model able to predict BV_{50} was developed as useful support for water utilities in order to select the optimal AC depending on the source water characteristics and the target PhACs to be removed. PhACs hydrophobicity was found to be the most important characteristic to be accounted for: hydrophobic compounds are better removed due to the higher affinity to the solid phase compared to the liquid one. As for AC type, the microporous carbons seem to have better affinity for the removal of

PhACs, with an effect of AC surface charge depending on PhACs charge. As for the water matrix, TAP water performed worse than low DOC synthetic matrices. Moreover, water conductivity was found to have an influence on PhACs adsorption, suggesting that the preparation of a synthetic water matrix must consider salts in the same concentration of fresh water. The correlation between UVA_{254} and PhACs removal resulted to be independent on the tested AC and water matrix, while it depends on the test method, meaning that correlations found in batch experiments cannot be used to predict PhACs in continuous-flow applications.

References

Altmann J., Bruebachb H., Sperlichb A., Jekela M. (2014). Removal of micropollutants from treated domestic wastewater by addition of powdered activated carbon to rapid filtration, Water Practice & Technology, vol. 9, no.3, 344-352.

Altmann J., Zietzschmann F., Geiling E.L., Ruhl A.S., Sperlich A., Jekel M. (2014). Impacts of coagulation on the adsorption of organic micropollutants onto powdered activated carbon in treated domestic wastewater, Chemosphere, 125 (2015), 198–204.

Altmann J., Massa L., Sperlich A., Gnirss R. (2016). UV_{254} absorbance as real-time monitoring and control parameter for micropollutant removal in advanced wastewater treatment with powdered activated carbon, Water Research, 94 (2016), 240-245.

Barrett, E.P., Joyner, L.G., Skold, R., 1951. The Determination of Pore Volume and Area Distributions in Porous Substances. II. Comparison between Nitrogen Isotherm and Mercury Porosimeter Methods. J. Am. Chem. Soc. 73, 3155–3158. https://doi.org/10.1021/ja01151a046

Brunauer, S., Emmett, P.H., Teller, E., 1938. Adsorption of gases in multimolecular layers. J. Am. Chem. Soc. 60, 309–319.

Caetano, M., Valderrama, C., Farran, A., & Cortina, J. L. (2009). Phenol removal from aqueous solution by adsorption and ion exchange mechanisms onto polymeric resins. Journal of Colloid and Interface Science, 338(2), 402-409.

Cheung, C.W., Porter, J.F., Mckay, G., 2001. Sorption kinetic analysis for the removal of cadmium ions from effluents using bone char. Water Res. 35, 605–612. https://doi.org/10.1016/S0043-1354(00)00306-7

Corwin C. J., Summers R. S. (2010). Scaling Trace Organic Contaminant Adsorption Capacity by Granular Activated Carbon, Environmental science & technology, vol. 44, no.14, 5403-5408.

Crittenden J.C., Reddy P.S., Arora H., Trynoski J., Hand D.W., Perram D.L. and Summers R.S. (1991) Predicting Gac Performance with Rapid Small-Scale Column Tests. Journal American Water Works Association 83(1), 77-87.

Freihardt J., Jekel M., Ruhl A. S. (2017). Comparing test methods for granular activated carbon for organic micropollutant elimination, Journal of Environmental Chemical Engineering, no. 5, 2542-2551.

Horvath, G. and Kawazoe, K., 1983. Method for calclualtion effective pore size distribution in molecular sieve carbon. J. Chem. Eng. Japan 16, 470.

Kennedy, A. M., Reinert, A. M., Knappe, D. R., Ferrer, I., & Summers, R. S. (2015). Full-and pilot-scale GAC adsorption of organic micropollutants. Water research, 68, 238-248.

Knappe D.R.U.;Matsui,Y.;Snoeyink,V.L.;Roche,P.;Prados, M. J.; Bourbigot, M. M. Predicting the capacity of powdered activated carbon for trace organic compounds in natural waters. Environ. Sci. Technol. 1998, 32 (11), 1694–1698.

Li L., Quinlivan P.A. and Knappe D.R.U. (2005) Predicting adsorption isotherms for aqueous organic micropollutants from activated carbon and pollutant properties. Environmental Science & Technology 39(9), 3393-3400.

Lin, S.H., Huang, C.Y., 1999. Adsorption of BTEX from aqueous solution by macroreticular resins. J. Hazard. Mater. 70, 21–37. https://doi.org/10.1016/S0304-3894(99)00148-X.

Lopez-Ramon, M. V., Stoeckli, F., Moreno-Castilla, C., Carrasco-Marin, F., 1999. On the characterization of acidic and basic surface sites on carbons by various techniques. Carbon N. Y. 37, 1215–1221. https://doi.org/10.1016/S0008-6223(98)00317-0.

Mailler R., Gasperia J., Coquetb Y., Deromea C., Buletéc A., Vullietc E., Bressyd A., Varraulta G., Chebbod.G., Rochere V. (2016). Removal of emerging micropollutants from wastewater by activated carbon adsorption: Experimental study of different activated carbons and factors influencing the adsorption of micropollutants in wastewater, Journal of Environmental Chemical Engineering, Volume 4, Issue 1, 1102-1109.

Newcombe G. and Cook D. (2002) Influences on the removal of tastes and odours by PAC. Journal of Water Supply Research and Technology-Aqua 51(8), 463-474.

Ochoa-Herrera, V., Sierra-Alvarez, R., 2008. Removal of perfluorinated surfactants by sorption onto granular activated carbon, zeolite and sludge. Chemosphere 72, 1588–1593. https://doi.org/10.1016/j.chemosphere.2008.04.029

Park, M., Wu, S., Lopez, I.J., Chang, J.Y., Karanfil, T., Snyder, S.A., 2020. Adsorption of perfluoroalkyl substances (PFAS) in groundwater by granular activated carbons: Roles of hydrophobicity of PFAS and carbon characteristics. Water Res. 170. https://doi.org/10.1016/j.watres.2019.115364

Rivera-Utrilla J., Prados-Joya G., Sánchez-Polo M., Ferro-García M. A., López-Peñalver J. J., Bautista-Toledo M. I. (2009). Removal of nitroimidazole antibiotics from water by adsorption/bioadsortion on activated carbon and advanced oxidation processes Trends in Chemical Engineering, 12 (2009), 51 – 69.

Saravia F., Frimmel F. H. (2008). Role of NOM in the performance of adsorption-membrane hybrid systems applied for the removal of pharmaceuticals, Desalination, 224(1), 168-171.

Schwarzenbach R.P., Escher B.I., Fenner K., Hofstetter T.B., Johnson C.A., von Gunten U., Wehrli B. (2006). The Challenge of Micropollutants in Aquatic Systems, Science, vol.13 (5790), 1072-1077.

Singh, K. P., Malik, A., Mohan, D., & Sinha, S. (2004). Multivariate statistical techniques for the evaluation of spatial and temporal variations in water quality of Gomti River (India)—a case study. Water research, 38(18), 3980-3992.

Summers, R. S.; Haist, B.; Koehler, J.; Ritz, J.; Zimmer, G.; Sontheimer, H. The influence of background organic-matter on GAC adsorption. J. Am. Water Works Assoc. 1989, 81 (5), 66-74.

Ternes, T., 2007. The occurrence of micropollutants in the aquatic environment: a new challenge for water management. Water Sci. Technol. 55 (12), 327e332.

Weber W.J. (1972). Physicochemical Processes for Water Quality Control. Wiley Interscience, New York, USA.

Worch E. (2012). Adsorption Technology in Water Treatment. Fundamentals, Processes, and Modeling. ISBN: 978-3-11-024022-1. De Gruyter, Third edition, 41, 77-79, 98-100, 104-111.

Xie Y., Jing K.J., Lu Y. (2011). Kinetics, equilibrium and thermodynamic studies of L-tryptophan adsorption using a cation exchange resin, Chemical Engineering Journal, 171(3), 1227-1233.

Zietzschmann F., Altmann J., Ruhl A. S., Dunnbier U., Dommisch I., Sperlich A., Meinel F., Jekel M. (2014). Estimating organic micro-pollutant removal potential of activated carbons using UV absorption and carbon characteristics, Water Research, 56 (2014), 48-55.

Zietzschmann F., Müller J., Sperlich A., Ruhl A. S., Meinel F., Altmann J., Jekel M. (2014). Rapid small-scale column testing of granular activated carbon for organic micro-pollutant removal in treated domestic wastewater. Water Science & Technology, 70 (7), 1271-1278.

CHAPTER 5

Human health risk due to bisphenol A leaching from epoxy resins in the drinking water distribution networks

Abstract: Monitoring and management of drinking water distribution networks (DWDNs), including possible leaching from materials in contact with drinking water, have been stressed as crucial to avoid re-contamination of drinking water leading to a potential increase of human health risk. Recent scientific studies and regulations clearly highlighted the leaching of bisphenol A (BPA) from plastic materials used to renovate DWDNs pipelines as one of the major hazardous events, resulting in severe consequences for human health. In this study, lab migration tests were performed on three commercial epoxy resins, designed with the Design of Experiments (DoE) method in order to build a BPA migration model as a function of water chemical stability, evaluated as aggressivity index (AI), and residual chlorine concentration. Tests lasted about 170 days to account for both short and long-term leaching. BPA migration over time was well described by a combination of two 1st-order kinetic models with an initial peak of leaching, a decrease and, then, a second increase due to resins' deterioration. Both chlorine concentration and AI values showed inverse proportionality with initial BPA concentration and BPA integral migration. However, measurements of free BPA content in epoxy resins proved that this is due to BPA transformation, not to a reduced leaching. The validated BPA migration model was combined with the hydraulic model of the DWDN in an urban area, through EPANET-MSX software. The model allowed to simulate the propagation of BPA in the DWDN, after the execution of a relining intervention, identifying the most vulnerable areas and permitting to customize a site-specific monitoring and intervention plan to minimize the health risk for final consumers.

Keywords: Bisphenol-A (BPA); design of experiment (DoE); drinking water distribution network; epoxy resins; fate modelling; migration tests.

The research work presented in this chapter was carried out with the valuable support of one MSc student, Anastasia Cappello Riguzzi. Epoxy resins free BPA content and BPA concentration in water were measured with the helpful support of Eurolab Analysis S.R.L. and the staff of MM S.p.A., respectively.

This chapter has been submitted for publication to "Science of the Total Environment"[4] and is now under review.

[4] Beatrice Cantoni, Anastasia Cappello Riguzzi, Andrea Turolla, Manuela Antonelli

Politecnico Milano, Department of Civil and Environmental Engineering (DICA) - Environmental Section, Piazza Leonardo da Vinci 32, 20133 Milano, Italy

List of symbols and abbreviations

ABS	Absorbance
AI	Aggressivity index
ANOVA	Analysis of variance
BADGE	Bisphenol A diglycidyl ether
BPA	Bisphenol A
BPA_0	Bisphenol A initial concentration
BPA_IM	Bisphenol A integral migration
BPF	Bisphenol F
BQ	Benchmark Quotient
CCF	Central composite face-centered
DEIO	Deionized water
DoE	Design of Experiments
DW	Drinking Water
DWDN	Drinking Water Distribution Network
DWTP	Drinking Water Treatment Plant

EFSA	European Food Safety Authority
HPLC-MS	High Performance Liquid Chromatography Mass Spectrophotometry
LOQ	Limit Of Quantification
MRM	Multiple reaction monitoring
NDMA	N-nitrosodimethylamine
NMSE	Normalized Mean Square Error
PCBs	Polychlorinated biphenyls
PE	Polyethylene
PET	Polyethylene teraphthalate
RfD	Reference Dose
RSM	Response Surface Methodology
TAP	Tap water
TCP	Trichlorophenol
THF	Tetrahydrofuran
U.S.EPA	United States Environmental Protection Agency

1. Introduction

Recent guidelines and regulations concerning drinking water production (e.g. EU Parliament, 2020; WHO, 2011) indicate a new approach for water system management based on health risk prevention through the whole supply chain. As a consequence, the accurate control of drinking water quality along drinking water distribution networks (DWDNs) is strongly recommended. In fact, a relevant deterioration of water quality can occur in DWDNs in case of micropollutants leaching from materials in contact with water (Bae et al., 2002). In particular, increasing attention is paid to epoxy resins, that are widely used for relining of damaged DWDN pipes (Palmiotto et al., 2015). Epoxy resins contain bisphenol A (BPA) and thus free BPA migration from such materials is one of the potential sources of BPA contamination in drinking water (Kosaka et al., 2012). BPA has been identified as an endocrine disruptor (Bae et al., 2002) and the most recent scientific opinion published by the European Food Safety Authority (EFSA) in 2015 on BPA reports a deterministic reference dose (RfD) for external oral exposure to BPA in humans of 4.0 $\mu g\ kg^{-1}day^{-1}$ (EFSA, 2015). Given the studies on BPA toxicity, in the revision of the European Directive on drinking water, BPA was introduced in the list of parameters to be monitored with a proposed limit equal to 2.5 μg/L (EU Parliament, 2020). Accordingly, recognizing BPA as an endocrine disruptor and its introduction in the revision of the Directive led to rethink the safety of the practice of relining (Palmiotto et al., 2015).

Two-component epoxy resins, so far adopted for relining, are formed by a resin pre-polymer and a hardener. The resin pre-polymer is designed to facilitate polymerization and it commonly is bisphenol A diglycidyl ether (BADGE), synthesized by the reaction between BPA and epichlorohydrin. The amount of BPA that does not react with epichlorohydrin for the synthesis of BADGE is found in the form of free BPA, which remains trapped by the resin lattice. The resins are then polymerized by reacting the BADGE with a hardening agent, such as polyamines (Pham and Marks, 2005). In addition to the correct selection of the components and their stoichiometry, it is important that a minimum hardening time is given to the epoxy resins, to assure a complete polymerization. In general, the incomplete polymerization of epoxy resins can enhance the leaching of BPA and all the other components, with consequent health risks (Amiridou and Voutsa, 2011). The more the formulation of all the components is stable and the lattice density is high, the higher is the probability that free BPA remains trapped within the lattice and its migration into water is difficult.

To best of authors' knowledge, there are only four available works analysing BPA leaching from epoxy resins, investigating the influence on BPA leaching of resin age, water temperature, residual chlorine in water and stagnation time, that is the time between two replacements of the contact water, simulating the water exchange in pipes. Bae et al. (2002) and Bruchet et al. (2014) performed leaching tests under static batch conditions on three resins in contact with test water without and with chlorine, respectively; these studies differ also for the monitoring periods (a short period of 6 to 24 hours for Bae et al., while a long period of 8 to 182 days for Bruchet et al.) and for the monitored parameters (BPA for Bae et al., and BPA, BPF (bisphenol-F) and chlorophenols for Bruchet et al.). Kosaka et al. (2012) measured the leaching rate of BPA and chlorinated BPAs in chlorinated water flowing in continuous through lined pipes, sampling the test water from 21 to 730 days from the beginning of the test. Finally, Rajasärkkä et al. (2016) reported the results of a BPA monitoring campaign on eight households with different pipe rehabilitations ages, ranging from three to ten years. However, none of these studies evaluated the BPA leaching trend in the first week after installation and none provided information on free BPA content in tested epoxy resins. Besides, there are no research studies assessing the fate of BPA in real DWDNs where epoxy resins are applied for pipes renovation.
In our work, lab migration tests have been performed on three epoxy resins in contact with several samples of tap waters to assess BPA leaching as a function of water conditions, such as water chemical stability, in terms of aggressivity index (AI), and residual chlorine concentration. Experiments were designed according to the Design of Experiments (DoE) technique to evaluate the role of those characteristics and also their interaction in causing BPA leaching. Results of lab tests have been used to calibrate a migration model as a function of the characteristics of both resins and water. The model was then validated against literature available data. Afterwards, the migration model was combined with the hydraulic model of a real DWDN, in a densely urbanised area, to highlight the potential of this modelling framework as supporting tool for the identification of the most vulnerable areas of a DWDN, useful for the optimization of the interventions in the whole DW supply system. Model outputs were compared with results of a monitoring campaign in the DWDN, where two renovated pipe segments were present, and they were used to assess human health risk for consumers drinking tap water in the specific area.

2. Materials and methods

2.1. Tested epoxy resins

Three epoxy resins were provided as cylindrical pipe sections by their manufacturers. All the provided resin samples were two-component epoxy resins, formed by BADGE as pre-polymer, synthesized by the reaction between BPA and epichlorohydrin, and polyamines as hardener. The main characteristics of the formulation and relining technique of the tested resins are reported in Table 1: all information was provided by the manufactures except for free BPA content which was measured (see section 2.4).

Table 1. Main characteristics of the formulation and relining technique of the tested epoxy resins.

Resin	Free BPA content [µg/g]	Stoichiometric ratio	Relining technique	Curing		Hardening	Relining	Cross-linking degree [%]
				T [°C]	Max time [days]	Max time [min]	Tot time [h]	
R1	92.1	BADGE excess	Spray-coat	20	3 - 4	1	1.5	< 96
R2	66.3	Polyamines excess	Felt-glass reinforced plastic pipe	20	7	3.5 - 5.5	7 - 8	96 - 97
R3	66.0	-	Felt-glass reinforced plastic pipe	20	-	7	-	-

2.2. BPA migration test and modelling

Migration tests on the three resins were performed according to standard method BS EN 12873-2:2005. Migration test procedure is reported in detail in Section S1 in Supplementary Materials. Keeping the migration time at 72 hours, water sampling and refilling was carried out for up to 171 days for a total of 12 samples per test. A stainless-steel filling cylinder was inserted in the resins samples to set the contact surface area of epoxy resins per sample volume equal to 5.4 dm^{-1} for all the tested resins. Blank tests were performed in parallel, where test waters were stored in a glass container with the stainless-steel filling cylinders. BPA was never detected in the blank samples.

The measured BPA concentrations in the 12 samples were used for calibrating the migration kinetic model, through MATLAB R2020a curve fitting function. The model was validated against literature data coming from the work of Bruchet et al. (2014) on BPA migration in tap water from two epoxy resins. The index used to verify the validity of the model is the NMSE (Normalized Mean Square Error), that is an estimate of the differences between observed and simulated values. The NMSE is dimensionless and has zero as optimal value.

2.3. Experimental plan for BPA migration tests

First, preliminary migration tests were carried out on the three epoxy resins with three water matrices (Table 2): (i) deionized water; (ii) tap water characterised by: temperature 15.6±1.6 °C, pH 7.5±0.1, alkalinity 203±13.9 mg/L, hardness 30.5±2.35 °F; (iii) tap water as in (ii) with chlorine at a concentration of 1 $mgCl_2/L$. A total of 9 experiments was carried out.

Then, the DoE methodology was applied (Lundstedt et al., 1998) to design the second set of experiments. The experimental dataset was established by a central composite face-centered (CCF) design, defined according to the Response Surface Methodology (RSM) (Table 2). Minitab 19 helped the construction of the DoE for the tests, indicating the number and order of experiments to be performed with different combinations of operating parameters and building the mathematical model correlating the responses to the operating parameters. Accordingly, a set of 12 experiments was performed on resin R1 with different test waters prepared from tap water (same characteristics of tap water in preliminary migration tests), varying chlorine concentration and water stability. Chlorine concentration was adjusted in a range between 0 and 0.4 $mgCl_2/L$ with a sodium hypochlorite solution, at a concentration of 17.1 $mgCl_2/L$ and a density of 1.22 kg/L. For each test water, the water stability was calculated through AI, which evaluates the acidity of the water and the solubility of calcium carbonate, using the following equation (Larson and Skold, 1958):

$$AI = pH + \log\left[(A) * (H)\right] \qquad \text{(Eq. 1)}$$

where A is the total alkalinity of the water (mg $CaCO_3/L$) and H is the hardness (°F). Test water AI was adjusted between 11.5 and 13.5 by changing the pH, dosing HCl [37% w/w] or NaOH [2 N], or by dosing calcium sulphate dihydrate ($CaSO_4 \cdot 2H_2O$) and sodium bicarbonate ($NaHCO_3$).

Table 2. Experimental plan for migration tests: migration tests abbreviation (names for tests performed in tap water are built as resin_chlorine_AI), tested resins, water characteristics and number of test replicates.

Design	Test abbreviation	Experimental Variables (Factors)				Replicates
		Resins	Water	[Cl_2]	AI	
Preliminary screening	R1_DEIO	R1	DEIO	0	11.5	1
	R1_0_12.5		TAP	0	12.5	1
	R1_1_12.5		TAP	1.00	12.5	1
	R2_DEIO	R2	DEIO	0	11.5	1
	R2_0_12.5		TAP	0	12.5	1
	R2_1_12.5		TAP	1.00	12.5	1
	R3_DEIO	R3	DEIO	0	11.5	1
	R3_0_12.5		TAP	0	12.5	1
	R3_1_12.5		TAP	1.00	12.5	1
RSM CCF design	R1_0_12.5	R1	TAP	0	12.5	1
	R1_0.06_11.8	R1	TAP	0.06	11.8	1
	R1_0.06_13.2	R1	TAP	0.06	13.2	1
	R1_0.2_11.5	R1	TAP	0.20	11.5	1
	R1_0.2_12.5	R1	TAP	0.20	12.5	4
	R1_0.2_13.5	R1	TAP	0.20	13.5	1
	R1_0.34_11.8	R1	TAP	0.34	11.8	1
	R1_0.34_13.2	R1	TAP	0.34	13.2	1
	R1_0.4_12.5	R1	TAP	0.40	12.5	1

2.4. Analytical methods

Water pH and temperature were measured with Hach HQ40D equipped with a PHC101 probe.

The procedure for determining the residual concentration of total chlorine in water was performed following the standard method ISO 7393-2:2017, correlating chlorine concentration to UV absorbance at 510 nm wavelength (10 mm optical path), using an Hach DR1900 spectrophotometer. Absorbance values (ABS) were then converted into total chlorine concentration through an ABS-concentration relation (6 calibration points in triplicates, determination coefficient R^2 of 0.96), in a validity range between 0.05 and 0.80 mgCl_2/L, while for concentrations above the calibration range a sample dilution was required.

For BPA analyses, samples were filtered using a 0.45 µm pore size syringe filter and stored in glass vials, refrigerated at 4 °C for at maximum 15 days. Afterwards, 1 mL of the sample was spiked in a glass vial with 10 µL of a deuterated BPA-d16 internal standard at 0.01 ng/µL (CAS 96210-87-6 from Ultra Scientific, c = 100 µg/mL in acetonitrile). BPA was analyzed using high performance liquid chromatography mass spectrometry (HPLC-MS/MS, Neera X2 from Shimadzu with a SPE online shim-pack column MAYI-ODS(G), a HALO-2 C18 100 mm x 2.1 mm x 2 µm column coupled with a HALO-2 C18 2.1 mm x 5 mm x 2 µm pre-coloumn (Shimatzu) and QTRAP 8060 MS/MS from Shimadzu) and evaluated by linear calibration with ten calibration points in the range of 0.015 to 0.6 µg/L (BPA CAS 80-05-7 from Ultra Scientific) and determination coefficients, R^2, for all analytes greater than 0.98. The mobile phases were (A) TEA 0.05% in MilliQ water and (B) acetonitrile, with mobile phase flux of 0.3 mL/min. The separation started with 30% (B), kept constant for 3 minutes, and increased to 100% (B) in 9 minutes and kept constant for another 1 min. Column reconditioning at 30% (B) takes place in 2 minutes, keeping it at 100% for 4 minutes. Total chromatographic run time is 19 minutes. Quantification was conducted using precursor-product ion multiple reaction monitoring (MRM) transitions. The transitions monitored by the mass spectrometer with their potentials (Q1 Prebias Q3 Prebias) and collision energies for BPA

were: 226.9-212.2 (12, 23, 20) and 226.9-133 (12, 14, 26); for BPA-d16 241.0-142 (12, 23, 20) and 241.0-142.0 (12, 14, 26). The quantification was done using the internal standard method with Software Lab Solutions 5.97. The Limit of Quantification (LOQ) was verified prior to the analysis by multiple measurement of spiked water samples at the concentration levels of LOQ according to ISO/TS 13530 Annex A. The analytical method LOQ was equal to 0.015 µg/L.
As for free BPA content in the epoxy resins, resin sample was dissolved and resin matrix precipitated in a tetrahydrofuran (THF)/hexane solution in 1:2 weight ratio. The solution was then diluted in methanol. Afterwards, 1 mL of the sample was spiked in a glass vial with 10 µL of a deuterated BPA-d16 internal standard at 0.01 ng/µL (CAS 96210-87-6 from Sigma-Aldrich, c = 100 µg/mL in acetonitrile). BPA was analyzed using high-resolution UPLC-Q-Exactive Orbitrap/MS (Thermo, Bremen, Germany) with a Raptor C18 50 mm x 2.1 mm x 2.8 µm column (Restek). The chromatographic system was coupled to the MS with a Heated Electrospray Ionization Source II (HESI II) in the negative ion polarity mode. The mobile phases were (A) MilliQ water and (B) methanol, with mobile phase flux of 0.4 mL/min. A full-scan acquisition was performed in the mass range of 150-900 m/z. The analytical method LOQ was equal to 0.01 µg/g.

2.5. Modelling and monitoring campaign of BPA fate in DWDN

For simulating BPA fate within a DWDN, a portion of a DWDN in a densely urbanized area was selected as case study. The studied portion of the DWDN is served by several drinking water treatment plants (DWTPs) and two segments (A and B) of pipes were renovated in February 2018 by the relining technique (Figure S2 in Supplementary Material). The already existing EPANET hydraulic model, developed to simulate a hydraulic scenario of average water consumption was used. In detail, EPANET-MSX (Multi-Species eXtension) was adopted to implement the BPA migration kinetics model within the studied DWDN. Simulation parameters were: free chlorine concentration at the DWTP outlet (0.1 $mgCl_2/L$), BPA concentration at the DWTP outlet (0 µg/L, being < LOQ), water AI (12.1) and pH (7.8). Details on the dimensional characteristics, and hydrodynamic conditions and the calculations used for the simulations are reported in Section S2 in Supplementary Materials. The BPA migration kinetic model was set in the hydraulic model as input in the two network nodes located downstream with respect to the two pipes containing the segments A and B. The relative BPA diffusivity was calculated as the ratio between BPA and chlorine diffusivities in water, that are respectively equal to $5.08 \cdot 10^{-10}$ m^2/s and $4{,}69 \cdot 10^{-6}$ m^2/s (Niesner and Heintz, 2000). The hydraulic and quality simulations have been performed over a time period of 190 days.
A monitoring campaign has been performed within the analyzed DWDN portion in collaboration with the water utility, to validate model outputs. The technical staff collected 10 samples, stored in polypropylene bottles at 4 °C until analysis for maximum 5 days, from April 2019 to February 2020.

2.6. Human health risk assessment

The human health risk has been assessed calculating the benchmark quotient (BQ), that is the ratio between the exposure BPA concentration and its health-based guideline level (Baken et al., 2018). Since a statutory drinking water guideline value is available for BPA in the revision to the European drinking water Directive, that is equal to 2.5 µg/L, this was used as health-based guideline level (Schriks et al., 2010). A BQ equal to 1 represents the risk threshold value that should not be exceeded. In fact, a BQ value higher than 1 in drinking water corresponds to a potential human health concern in case of water consumption over a lifetime period.

3. Results and discussion

Renovation of segments of DWDNs by relining is increasingly widespread technique, especially in densely populated urban area, allowing to reduce inconveniences associated to open-air construction sites and excavations. Since the water in contact with epoxy resins does not undergo a further treatment before the users tap, in view of minimizing human health risk, it is fundamental for water utility managers to: i) select the best epoxy resin depending on the resins characteristics and water conditions, ii) predict BPA migration in water and fate in the DWDN, iii) evaluate the DWDN area that is affected by a potential contamination, iv) estimate the current and potential human health risk, and v) optimize a monitoring and maintenance plan. The experimental plan here carried out and its combination with BPA fate modelling in DWDN and risk assessment satisfy these goals, being a supporting tool for water utilities to predict and minimize health risk associated to BPA in delivered drinking water.

3.1. Effect of resins' characteristics on BPA leaching

First of all, it is important to understand the role of epoxy resin characteristics in the extent of BPA release, since it affects the choice of the best resin to be selected and the expected quality of the drinking water delivered to the users taps. To evaluate this influence, the three epoxy resins listed in Table 1, characterized by different formulation, relining technique and installation procedure, have been compared. Results related to BPA migration over time are reported in Figure 1a for the three resins in contact with tap water without chlorine. The time trend of BPA concentration in both deionized and tap chlorinated water are reported in Figure S4 in Supplementary Materials.

Results in tap water show that a higher concentration of BPA was measured in water in contact with resin R1 over time compared to resins R2 and R3. In particular, it can be observed an initial peak concentration, of the order of 1.129 μg/L for resin R1 after 24 h from the start of the migration test, which drops to a minimum of 0.128 μg/L at 25 days, and then varies between 0.213 and 0.428 μg/L. The other two resins on average released a lower concentration of BPA over time, with values ranging from a minimum of 0.015 and 0.026 μg/L, and a maximum of 0.156 and 0.149 μg/L, respectively for resins R2 and R3.

Based on information provided by the manufacturers, resin R1 has a lower cross-linking degree than resin R2 (Table 1). The lower cross-linking degree, together with the shorter cross-linking time of the resin R1, determine "holes" inside the lattice in which free BPA, not reacted for the synthesis of BADGE, can accumulate to be then leached easily in the water. Resin R2 has been formulated in stoichiometric excess of hardener (polyamines), that gives it a final cross-linking degree up to 97% (Table 1): consequently, free BPA is better trapped inside the lattice and it is then more difficult to extract. These considerations are also confirmed by Vermeirssen et al., who reported that a more robust reaction process of the components of epoxy resins can reduce the free BPA available in the product and thus reduce BPA emissions (Vermeirssen et al., 2017). No considerations can be drawn about resin R3, since the manufactures didn't provide enough data to characterize both the resin and the relining process. These evidences are also in line with the measurement of free BPA content in the resin. In fact, due to its formulation and to the lower cross-linking degree, resin R1 has higher free BPA content (92.1±3.82 μg/g) compared to resin R2 (66.3 μg/g) and R3 (66.0 μg/g). This result has important implications for water utilities in the selection of the best resin to be applied in the DWDN. In fact, the measurement of free BPA content in the epoxy resin is fast to be measured and can be a first indication for resin selection in the screening phase.

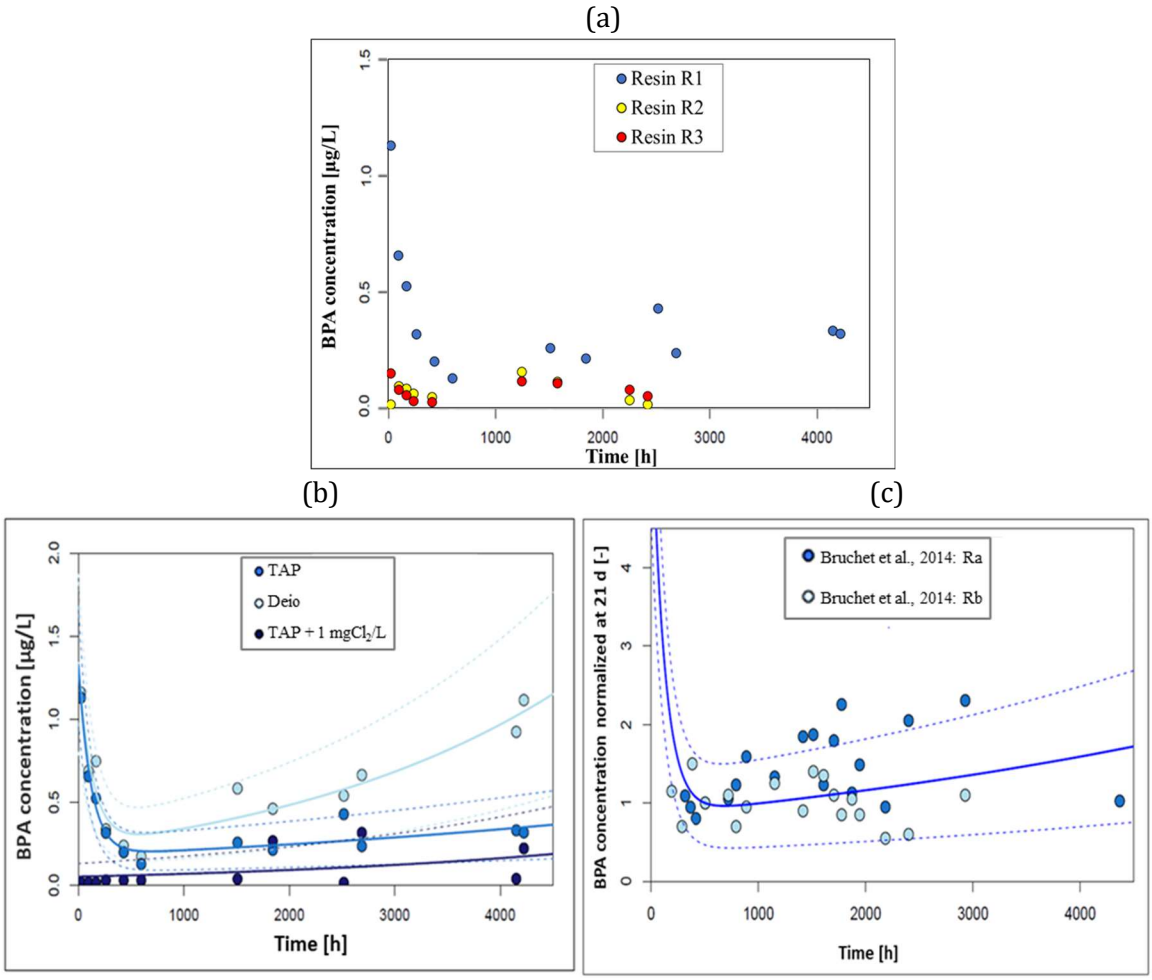

Figure 1. BPA migration over time: (a) experimental data in tap water without chlorine as a function of the tested resin; (b) experimental data with resin R1 as a function of the tested water matrix; (c) model validation of the normalized BPA leaching in tap water without chlorine: dots correspond to literature data from two epoxy resins (Bruchet et al., 2014). Solid lines indicate the estimated models, dashed lines represent the models 95% confidence intervals.

3.2. BPA migration modelling and validation

Actually, it is important to distinguish the definitions of BPA "release" and "migration". In fact, the released BPA can be partly transformed into by-products if a reactive species is present in water, leading to a lower BPA concentration in water (migrated BPA) compared to the released one. Therefore, the amount of BPA migrated in water corresponds to the released one in case no BPA-reactive species are present in water, as in the tests in deionized water or non-chlorinated tap water; while they differ in case of chlorinated tap water since chlorine can react with BPA transforming it into by-products and decreasing its concentration in water compared to the released one. Based on these considerations, since the kinetic model was built from the BPA concentration data in water, it is defined as migration kinetic model. The results on BPA migration from resin R1, considered the most critical one, in tap water, deionized water and tap water at 1 $mgCl_2/L$ are shown in Figure 1b, where lower BPA concentrations in water in presence of residual chlorine have been measured with respect to tests in tap and deionized water. Experimental data have been fitted and BPA migration from epoxy resins over time was well described by a model combining two first-order kinetics (Eq. 2):

$$BPA(t) = a \cdot e^{b \cdot t} + c \cdot e^{d \cdot t} \quad \text{(Eq. 2)}$$

where BPA(t) [µg/L] is the BPA concentration at time t [h]; *a+c* [µg/L] represents the initial migrated BPA concentration at time 0 (BPA_0); *b* and *d* [h^{-1}] are the parameters of the first-order kinetic describing, respectively, the initial decrease in the curve and the subsequent increase. The higher b and d are, in absolute value, the faster the BPA concentration varies. Estimated parameters for the preliminary screening experiments (see Table 2) are reported in Table 3.
In literature there are no articles reporting models describing BPA migration in water from epoxy resins. However, a first order kinetic equation was already used to describe the leaching of a compound from plastic materials. For instance, it was used by Fan et al. to describe BPA leaching from 16 different brands of PET (polyethylene teraphthalate) water bottles (Fan et al., 2014). A first order kinetic model was also adopted by Rungchang et al., to describe the leaching of antimony into water from PET plastic bottles of 80 different commercial brands (Rungchang et al., 2013), and by Endo et al. to model the leaching of PCBs (polychlorinated biphenyls) from marine plastic PE (polyethylene) pellets (Endo et al., 2013).

Table 3. Estimated parameters of the BPA migration kinetics model (resin R1), their 95% confidence interval and models R^2 values as a function of the tested conditions.

Design	Test	*a*	*b*	*c*	*d*	R^2	Adj. R^2
		µg/L	h^{-1}	µg/L	h^{-1}	-	-
Preliminary screening	R1_DEIO	1.097 (0.69, 1.50)	-0.00765 (-0.013, -0.002)	0.241 (0.11, 0.37)	0.00035 (2.0e-04, 5e-04)	0.890	0.849
	R1_0_12.5	1.147 (0.90, 1.40)	-0.00832 (-0.012, -0.004)	0.180 (0.08, 0.28)	0.00016 (-2.0e-05, 3e-04)	0.950	0.931
	R1_1_12.5	-15.05 (-15.1, -15.0)	0.00010 (-2.0e-04, 5e-04)	15.08 (15.3, 15.1)	0.00010 (-2.0e-04, 5e-04)	0.348	0.139
RSM CCF Design	R1_0.06_11.8	1.432 (0.75, 2.01)	-0.01249 (-0.032, 0.007)	0.282 (-0.42, 0.78)	-0.00002 (-1.9e-03, 2e-03)	0.775	0.691
	R1_0.06_13.2	0.777 (-0.11, 1.67)	-0.00783 (-0.026, 0.01)	0.636 (-0.289, 1.56)	-0.00082 (-2.3e-03, 7e-04)	0.926	0.888
	R1_0.2_11.5	0.805 (0.24, 1.37)	-0.01486 (-0.054, 0.023)	0.639 (0.401, 0.88)	-0.00034 (-6.5e-04, -3e-05)	0.950	0.929
	R1_0.2_12.5	1.292 (1.16, 1.43)	-0.01033 (-0.012, -0.009)	0.005 (-0.002, 0.01)	0.00137 (9.0e-04, 2e-03)	0.991	0.988
	R1_0.2_12.5b	0.983 (0.77, 1.17)	-0.0011 (-0.016, -0.006)	0.023 (-0.009, 0.12)	0.00040 (3.7e-05, 8e-04)	0.974	0.959
	R1_0.2_13.5	1.190 (0.97, 1.40)	-0.00826 (-0.012, -0.004)	0.110 (-0.035, 0.25)	0.00016 (-5.2e-04, 8e-04)	0.974	0.962
	R1_0.34_11.8	0.817 (0.18, 1.81)	-0.01983 (-0.193, 0.15)	0.577 (0.225, 0.93)	-0.00033 (-7.9e-04, 1e-04)	0.836	0.775
	R1_0.34_13.2	0.323 (0.142, 0.49)	-0.00847 (-0.033, 0.016)	0.614 (0.466, 0.96)	-0.00038 (-6.6e-05, -1e-04)	0.906	0.870
	R1_0.4_12.5	0.716 (0.21, 1.22)	-0.02443 (-0.053, 0.005)	0.186 (0.098, 0.27)	-0.00037 (-7.8e-04, 4e-05)	0.928	0.897

Looking at the results of the preliminary screening (Figure 1b and Table 3), both for tap and deionized water, the BPA concentration decrease after the instantaneous maximum concentration peak up to about 25 days can be well described according to a first-order kinetic: the rate of this decay is indicated by the parameter *b*, which is negative. The determination coefficients R^2 were satisfactory: 95% and 89% for tap and deionized water respectively. The initial peak can be attributed to an incomplete polymerization of the resins, seen as surface outcrops of all the parts that make up the mixture that have not finished reacting, including free BPA. The incomplete polymerization of epoxy resins could cause the leaching of free BPA, with consequent health risks (Amiridou and Voutsa, 2011). It can be assumed that

the BPA concentration decrease is due to the decrease in the amount of free BPA which can leach in water. In fact, BPA concentration decrease cannot be ascribed to reactions with other substances present in tap water, since comparable decay trends were observed for the resin immersed in tap and deionized water. This is confirmed by the similar values estimated for parameter *b* in the two tests R1_DEIO and R1_0_12.5, whose confidence intervals overlap. For the test in chlorinated water (R1_1_12.5), there is not an initial peak in BPA concentration in water (BPA_0 = a+c = 0.03 μg/L) compared to the results found in non-chlorinated tap water, whose initial peak is two orders of magnitude higher than the one measured in chlorinated tap water. This means that chlorine concentration in water has an influence on BPA migration. Since there is no initial peak, BPA concentration has a low increase, being parameter b positive and one order of magnitude lower than in deionized and non-chlorinated tap water.
From around 25 days onwards, the BPA concentration tends to increase again, according to a first-order kinetic, both in tap and deionized water; in fact, in this case, the parameter *d* of the model is positive. This trend is more marked in deionized water (R1_DEIO), that is more aggressive than tap water, as proved by the values of parameter *d*, higher than that of tap (R1_0_12.5) and chlorinated tap (R1_1_12.5). Deionized water exerts a more aggressive effect on the materials it comes into contact with (Jiang et al., 2019); thus, this could be a reason for possible greater BPA release. This means that water chemical stability, and hence water aggressivity, has an influence on BPA migration, especially in the second part of the kinetic model. The aging process of the epoxy coating and its influence on the increase in the migration of BPA has also been observed by Rajasärkkä et al. (2016); therefore, the same influence is hypothesized also in the results of this research, although the times evaluated in the study by Rajasärkkä et al. (2016) (2-8 years) are higher compared to those considered here.
The analysis of BPA migration trend over time, and especially in the first week, that has never been investigated in literature before, provides important insights on monitoring and management practices that water utilities should perform when renovating DWDN pipelines with epoxy resins. In fact, it is essential to monitor BPA concentration from the beginning of the installation of the resins and very frequently during the first week, as it was found that this is the period that involves the greatest leaching of BPA. Being the first week the most critical, it is crucial to monitor and prevent the risk of distributing water that is close to the BPA concentration level proposed in the EU DW Directive (2.5 μg/L). However, the BPA monitoring campaign must be carried out over time because materials deterioration can lead to an increase in the leaching of BPA and then to a risk to human health even in the long period.
The model on BPA migration over time in tap water was validated compared to data found in literature (Bruchet et al., 2014). As different conditions in terms of surface-to-volume ratio and stagnation time were tested by Bruchet et al. (2014) compared to this study, BPA leaching data from Bruchet et al. (2014) and data from the calibrated model in this study were normalized with respect to BPA concentration at 21 days, given in common between these two studies. The output of the validation is graphically shown in Figure 1c: it can be noted that the model is well suited to the experimental data of the study by Bruchet et al., being almost all the validating data points within the 95% confidence interval of the calibrated model, as confirmed by the NMSE value of 0.17.

3.3. Combined effect of residual chlorine and water stability

The results of the previous step have shown that the chemical stability, so water aggressivity, and the concentration of chlorine in water have an effect on BPA migration from epoxy resins. Consequently, their combined effect was studied on resin R1, exploiting the potential of DoE. As for residual chlorine in water, besides the tests performed in tap water without residual chlorine and with chlorine at 1 $mgCl_2/L$, four chlorine concentrations (0.06, 0.2, 0.34, 0.4 $mgCl_2/L$) were selected. The chlorine concentration value of 0.4 $mgCl_2/L$ is twice the limit set by the regulations for chlorine concentration in DW, but it can be considered representative of the washing with chlorinated water to which the relining

sections are subjected after the installation and before re-opening. As regards water stability, it was selected AI values in the range 11.55-13.55, according to drinking water chemical stability observed in the area selected as case study. AI values below 12.0 define a weakly aggressive water, while AI values above 12.0 indicate non-aggressive waters supersaturated with respect to solid calcium carbonate, which will tend to precipitate and form a scale. BPA leaching model parameters for all the migration tests performed according to the DoE experimental plan (see Table 2, RSM CCF design) are reported in Table 3. The initial migrated concentration of BPA (BPA_0) in the water in contact with the resin, and the BPA integral migration (BPA_IM), estimated integrating the BPA migration model over the tested period, were the two analysed responses by CCF design. The estimated responses for each test are reported in Table S2 in Supplementary Material. In fact, on one hand, the initial BPA concentration is fundamental to be estimated in order to describe the worst condition and to support water utilities in evaluating whether this concentration exceeds the regulation limit. On the other hand, since BPA has chronic health effects on human health, in addition to the initial BPA concentration, it is fundamental to evaluate the influence of water characteristics on the BPA integral migration in case of long-time exposures.
The response surface methodology (RSM) with CCF design allowed to build the model of the two responses, BPA_0 and BPA_IM, for resin R1, applying a full quadratic stepwise analysis, including all linear, quadratic and interaction effects of chlorine concentration and water stability (AI). The resulting trends are shown in Figure 2 and Figure S4 in Supplementary Material, while ANOVA results are summarized in Table 4 and the developed models are reported in Eq. 3 and 4.

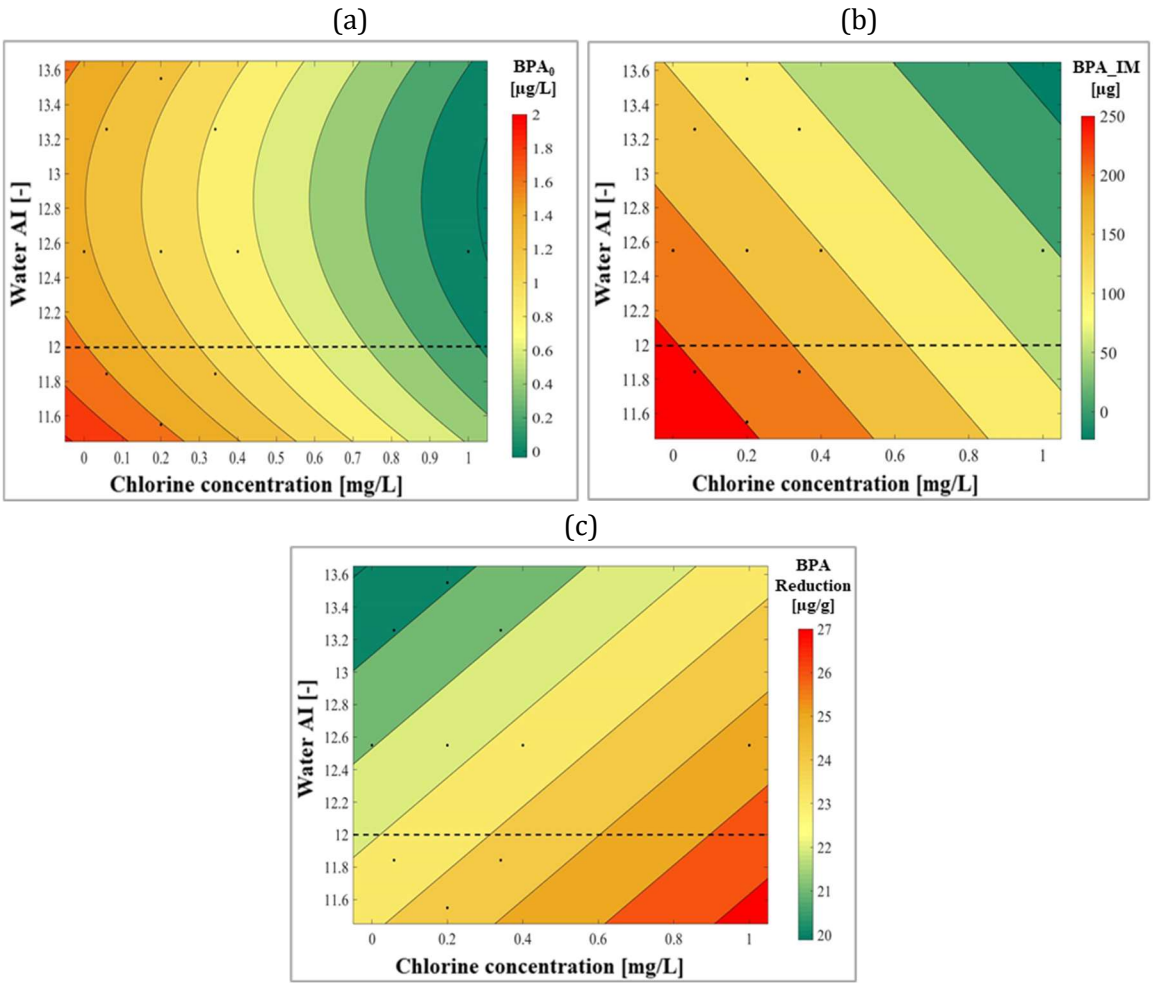

Figure 2. Contour plot of (a) initial BPA concentration, BPA_0, (b) BPA integral migration, BPA_IM, and (c) free BPA content reduction, BPA_Reduction, as a function of chlorine concentration and water AI.

Table 4. DoE ANOVA results (significance level, α=0.05) for the influence of chlorine concentration, water AI, and their interactions on initial BPA concentration (BPA_0), BPA integral migration (BPA_IM) and BPA content reduction (BPA_Reduction). p-values and standard effects of the significant parameters are reported in bold.

	BPA_0					**BPA_IM**					**BPA_Reduction**				
Term	**Coded Coef**	**SE Coef**	**t-value**	**p-value**	**Stand. Effect**	**Coded Coef**	**SE Coef**	**t-value**	**p-value**	**Stand. Effect**	**Coded Coef**	**SE Coef**	**t-value**	**p-value**	**Stand. Effect**
Constant	1.162	0.045	25.83	**0.000**		179.95	9.37	19.20	**0.000**		22.47	0.17	134.67	**0.000**	
[Cl_2]	-0.177	0.042	-4.20	**0.003**	**4.206**	-24.19	8.78	-2.75	**0.025**	**2.754**	0.495	0.16	3.16	**0.013**	**3.161**
AI	-0.120	0.043	-2.82	**0.023**	**2.816**	-45.59	8.91	-5.12	**0.001**	**5.119**	-1.232	0.16	-7.77	**0.000**	**7.771**
[Cl_2]^2	-0.004	0.009	-0.46	0.660	0.457	0.44	1.79	0.25	0.812	0.246	0.004	0.03	0.12	0.909	0.119
AI^2	0.139	0.046	3.05	**0.016**	**3.047**	6.82	9.49	0.72	0.493	0.719	0.292	0.17	1.73	0.122	1.728
[Cl_2]·AI	-0.039	0.061	-0.64	0.537	0.645	-3.6	12.6	-0.29	0.782	0.286	0.275	0.22	1.23	0.255	1.226

BPA_0 values (*a+c* in Table 3) vary between 1.17-1.71 µg/L depending on the combination of tested water characteristics. The BPA_0 model as a function of chlorine concentration ($mgCl_2/L$) and water AI (-) is:

$$BPA_0 = 48.1 - 1.37\,[Cl_2] - 7.27\,AI + 0.28\,AI^2 \quad \text{(Eq. 3)}$$

The R^2, the adjusted R^2 and the predicted R^2 were respectively 0.937, 0.918 and 0.826.
The model (Eq. 3) and the ANOVA results (Table 4) highlight that BPA_0 is affected by first order effects of chlorine concentration and AI, quadratic effect of water AI. The interaction between chlorine concentration and water AI was found to have a negligible effect on BPA_0.
BPA_IM values vary in the range of 60.8-275.7 µg depending on the combination of water characteristics. The BPA_IM model as a function of chlorine concentration and water AI is:

$$BPA\_IM = 1026 - 161.5\,[Cl_2] - 64.5\,AI \quad \text{(Eq. 4)}$$

The R^2, the adjusted R^2 and the predicted R^2 were respectively 0.869, 0.845 and 0.796.
The model (Eq. 4) and the ANOVA results (Table 4) highlight that the BPA_IM is affected by first order effects of chlorine concentration and water AI.
Both BPA_0 and BPA_IM decrease approximately linearly with increasing chlorine concentration, as demonstrated by the negative coded coefficients for [Cl_2] (Table 4). This decrease is even more evident by observing data collected in the test in tap water at 1 $mgCl_2/L$ (Figure 1b), which does not show an initial peak, confirmed by the very low value of BPA_0. Therefore, given that BPA is not detected at high chlorine concentration, it is of paramount importance that the initial BPA monitoring is carried out especially at the end of the chlorination phase, typically performed during the relining installation, to ensure that the actual leaching of BPA is assessed before re-opening of the renovated pipeline.
Several researchers justified the inverse proportion between BPA and chlorine concentrations in water, addressing their reaction to form chlorination by-products of BPA, such as trichlorophenol (TCP) and chloro-bisphenols BPA (Bruchet et al., 2014; Kosaka et al., 2012; Lane et al., 2015). In particular, Bruchet et al. (2014) found a higher concentration of TCP in water with chlorine than the concentration of BPA in water without chlorine, assuming a rapid attack of epoxy coatings by chlorine, and thus a faster deterioration of materials. To verify whether the lower BPA concentration at higher chlorine concentration is due to an actually lower release from epoxy resins or to BPA transformation in its chlorination by-products, free BPA content in the epoxy resins at the beginning and at the end of all the RSM-CCF tests has been analyzed. The response surface methodology (RSM) with CCF design was

applied to build the model correlating the reduction in free BPA content, for resin R1, applying a full quadratic stepwise analysis, including all linear, quadratic and interaction effects of chlorine concentration and water AI (Figure 2c). The reduction in free BPA content in the resins varied in the range of 20.7-25.4 μg/g depending on the combination of parameters. As suggested by ANOVA results, reported in Table 4, it was affected by first order effects of chlorine concentration and water AI; the quadratic effects and interaction between chlorine concentration and water AI were found to have a negligible effect. The corresponding free BPA reduction model as a function of chlorine concentration and water AI is:

$$\text{BPA\_Reduction} = 43.8 + 3.44\,[Cl_2] - 1.74\,AI \qquad \text{(Eq. 5)}$$

The R^2, the adjusted R^2 and the predicted R^2 were respectively 0.893, 0.874 and 0.834.
These results show that the reduction in resins BPA content throughout the test increases linearly with chlorine concentration. This is the opposite trend found looking at BPA concentration in contact water (Eq. 3 and Eq. 4). Hence, this is a confirmation that, the actual BPA release from epoxy resins is not decreasing with chlorine concentration but, the released BPA is then transformed in its chlorination by-products, causing a reduction in BPA concentration found in contact water.
Thus, it is crucial to study not only the leaching of BPA from epoxy resins, but also the formation, in disinfected waters, of the toxic chlorination by-products of BPA, which entail an additional risk for human health and also a degradation of the organoleptic properties of the water. In fact, TCP is able to bio-transform within the distribution network into 2,4,6-trichloroanisole, a compound with an intense odor of mildew. Moreover, it should be stressed that, in addition to BPA, also the other components of epoxy resins, such as epichlorohydrin, BADGE and polyamines, can leach into water, potentially leading to by-products in disinfected waters. For instance, the formation of nitrosamines should be carefully monitored, that are toxic chlorination by-products of polyamines, being classified by U.S.EPA as suspected cancerogenic (as for NDMA, a risk of 10^{-6} is set for 0.7 ng/L (IRIS U.S. EPA, 2002)). Then, all chlorination by-products should be monitored, in addition to the potentially leached resins' components, to assess the actual risk to human health in chlorinated water.
Looking at water chemical stability, AI has negative coded coefficients (Table 4), so there is an inverse proportionality between water AI and both BPA_0 and BPA_IM. This means that more aggressive water (AI<12) was found to intensify the release of BPA. Focusing on BPA_0, it is interesting to note that chlorine concentration has a greater effect compared to water AI (higher standard effect for $[Cl_2]$ than for AI in Table 4), affecting mainly the short-term behavior of the installed epoxy resin. On the contrary, water AI becomes more relevant than chlorine concentration when focusing on BPA_IM and on the reduction of free BPA content (higher standard effect for AI than for $[Cl_2]$ in Table 4), suggesting that water aggressivity has the main role in affecting epoxy resin behavior over a long-term period.

3.4. Combined migration and fate models in real DWDN for risk assessment

The validated BPA migration model was combined with the hydraulic model of a portion of a DWDN selected as case study, where two pipelines were renovated with a relining intervention. The simulated BPA concentration (Figure S4 in Supplementary Material) was normalized to the BPA proposed limit of 2.5 μg/L to assess the human health risk in terms of BQ in the analysed area (Figure 3). Several BQ threshold values (0.1, 0.6, 0.8, 1) were considered as interesting for the risk map visualization to support the prioritization in the areas needing more mitigation measures. In particular, if the BQ value is lower than 0.1, the human health risk is considered negligible, whereas when values are equal to or higher than 1, an adverse effect on human health is highly probable, especially if the exposure levels are

constant over a life-time period. For cases with BQ values between 0.1 and 1 further research and investigation are required (Baken et al., 2018; Schriks et al., 2010; Yang et al., 2017). Moreover, it is important to consider that water utilities usually adopt safety factors for the preventive control and management of hazards throughout the supply chain; in particular, it can be highlighted an attention threshold (assumed: BQ=0.6) and an alarm threshold (assumed: BQ=0.8), intended respectively to increase the monitoring campaign frequency and to stop operations to implement corrective actions.

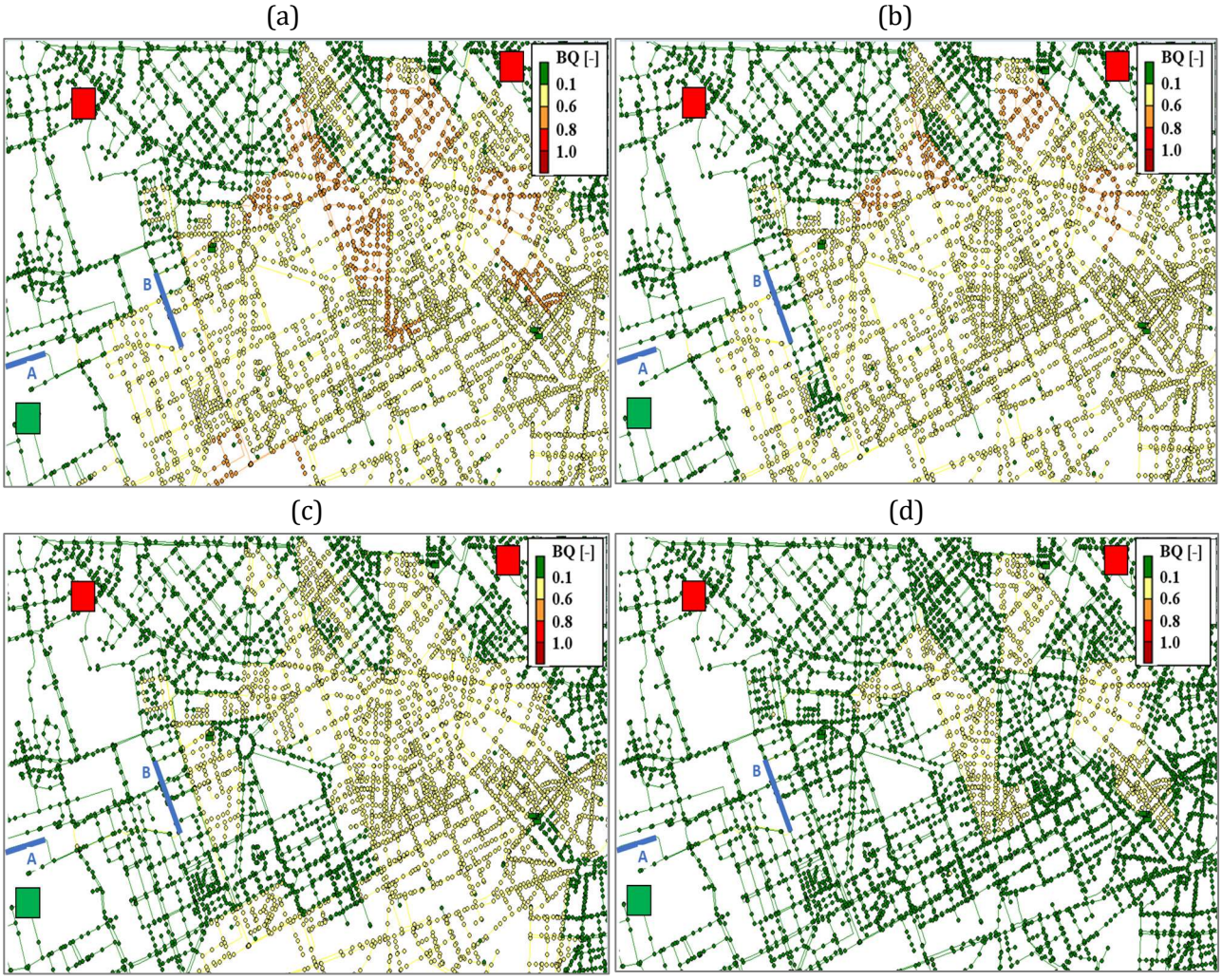

Figure 3. Estimated BQ due to BPA concentration in a portion of a DWDN in a densely urbanised area, where two pipe segments were renovated by epoxy resins relining (blue segments, identified by letters A and B) as a function of the time from installation: (a) after 1 day; (b) after 5 days; (c) after 30 days; (d) after 100 days. The DWTP feeding the renovated pipelines is reported as a green square. The DWTPs serving adjacent areas of the DWDN are reported as red squares.

The combination of BPA migration and hydraulic models, that has never been proposed in the literature, allowed to assess the BPA concentration in users tap water, as a consequence of the contact with the epoxy resins, as a function of time and characteristics of the water produced by the DWTP. Throughout the simulated period, BPA concentration in the affected area ranged from 0 to 1.65 µg/L, with a median concentration of 0.68 µg/L. It can be noted that, even after 100 days, there are still areas where BQ is higher than 0.1, that has been set by several studies as a first threshold value that implies the need for further investigations and mitigations.

A monitoring campaign was carried out to collect data about BPA concentration in the studied DWDN in various sampling points in the areas close to the installed epoxy resins. Over the ten collected samples, BPA concentration ranged from below the LOQ to 0.792 μg/L, being censored data (below the LOQ) 70% of the samples. The lower measured maximum concentration, compared to the simulated one, is probably due to the fact that the field monitoring campaign started after 290 days from the epoxy resins installation. Consequently, the initial BPA leaching peak, that is included in the model simulation, was not detected in the field monitoring campaign. Moreover, the presence of censored data could be due to the complete release of free BPA from the epoxy resin. In fact, if BPA migration is assumed to follow the developed kinetic model also after the tested period of 171 days, it can be estimated the time at which the whole available free BPA content is released. In this case, the whole available free BPA content in resin R1 (92.1 μg/g) is estimated to be released by the resin in 432 days. Thus, since the field monitoring campaign lasted from 290 to 596 days from the epoxy resins installation, this can be the reason for the presence of BPA concentration both higher and lower than the LOQ. Both the simulated and measured BPA concentrations in the studied area do not exceed the proposed regulation limit of 2.5 μg/L. However, according to the simulation, the maximum achieved concentration is 1.65 μg/L, corresponding to a BQ of 0.66. The exceedance of the BQ threshold of 0.6 highlights the need for frequent sampling and monitoring measurements.
The BPA spread is rapid: after ten days from the resin installation, BPA has spread through the whole area (around 8 km^2) served by the DWTP (green square in Figure 4). It is interesting to observe that, due to the hydraulic dynamics of the analysed DWDN portion, there are areas close to the installed resins (for example the area just north to pipes A and B) that are characterised by a low BPA concentration and, as a result, related human health risk. In fact, the hydraulic model allows to predict that, since those areas are served by other adjacent DWTPs (red squares in Figure 4), it is likely that water passing through the renovated pipelines is mixed and diluted with water not containing BPA. Moreover, within the studied area, the contamination does not spread like wildfire, but in patches; this kind of diffusion occurs due to the specific DWDN hydraulics. In fact, the directions of water flow that determine the transport of BPA play a fundamental role. The association of the descriptive quality model to the hydraulic model is, thus, essential for having a correct prediction of the areas of the DWDN in which human health risk is potentially higher, allowing the assessment of the spread of BPA contamination. The developed maps offer a support tool for assessing the risks associated with the renewal of one or more pipes with relining. Therefore, the EPANET-MSX model allowed to simulate the current fate of BPA in the DWDN, identifying the most vulnerable areas and the areas that are unlike to be affected by BPA risk; as a consequence, a monitoring and intervention plan can be site-specific customized to minimize the risk. Finally, this tool can be useful to simulate possible future relining scenarios in order to assess and minimize the risk.

4. Conclusions

In conclusion, this study was useful to define the test set-up and methods that the water utility can use for resins testing throughout the selection procedure.
The resin formulation and installation technique were found to influence BPA migration in contact water. In particular, the most critical resin was found to be the one with the highest free BPA content in the epoxy resin, this latter was found to be a useful first indicator for resin selection.
Moreover, this study was useful to provide indications on the DWDN monitoring plan. In particular, the decrease in BPA concentration due to the increase in chlorine concentration in water was found to be due to BPA transformation in its chlorination by-products. This evidence highlighted that it is important to analyze the migration of BPA, and all the other resins components, but also their chlorination by-

products, in order to have a complete evaluation of the human health risk. Since aggressive water was found to intensify BPA migration, it is important to evaluate the water stability of the area where the epoxy resins should be installed, in order to have accurate evaluation of BPA concentration trend in drinking water over time. Then, it was shown when to monitor, so at the initial peak, that should be monitored after the pipelines chlorination in order to avoid BPA release underestimation, but the system should be monitored also over time to assess the resins deterioration. Finally, the combination of the hydraulic and migration models was useful to identify the most vulnerable areas, characterized by the highest human health risk, that need for monitoring and can be used as supporting tool for future relining and intervention scenarios.

References

Amiridou, D., Voutsa, D., 2011. Alkylphenols and phthalates in bottled waters. J. Hazard. Mater. 185, 281–286. https://doi.org/10.1016/j.jhazmat.2010.09.031

Bae, B., Jeong, J.H., Lee, S.J., 2002. The quantification and characterization of endocrine disruptor bisphenol-A leaching from epoxy resin. Water Sci. Technol. 46, 381–387. https://doi.org/10.2166/wst.2002.0766

Baken, K.A., Sjerps, R.M.A., Schriks, M., Wezel, A.P. Van, 2018. Toxicological risk assessment and prioritization of drinking water relevant contaminants of emerging concern. Environ. Int. 118, 293–303. https://doi.org/10.1016/j.envint.2018.05.006

Bruchet, A., Elyasmino, N., Decottignies, V., Noyon, N., 2014. Leaching of bisphenol A and F from new and old epoxy coatings: Laboratory and field studies. Water Sci. Technol. Water Supply 14, 383–389. https://doi.org/10.2166/ws.2013.209

EFSA, 2015. Scientific Opinion on the risks to public health related to the presence of bisphenol A (BPA) in foodstuffs. EFSA J. 13. https://doi.org/10.2903/j.efsa.2015.3978

Endo, S., Yuyama, M., Takada, H., 2013. Desorption kinetics of hydrophobic organic contaminants from marine plastic pellets. Mar. Pollut. Bull. 74, 125–131. https://doi.org/10.1016/j.marpolbul.2013.07.018

EU Parliament, 2020. Directive of the European Parliament and of the Council on the quality of water intended for human consumption, in: Off. J. Eur. Union. 2020. https://doi.org/10.1017/CBO9781107415324.004

Fan, Y.-Y., Zheng, J.-L., Ren, J.-H., Cui, X.-Y., Luo, J., Ma, L.Q., 2014. Effects of storage temperature and duration on release of antimony and bisphenol A from polyethylene terephthalate drinking water bottles of China. Environ. Pollut. 192, 113–120. https://doi.org/10.1016/j.envpol.2014.05.012

Gama, M.C., Lanfranchi, E.A., Pan, Q., Jonoski, A., 2015. Water distribution network model building, case study: Milano, Italy. Procedia Eng. 119, 573–582. https://doi.org/10.1016/j.proeng.2015.08.910

IRIS U.S. EPA, 2002. U.S. Environmental Protection Agency. Integrated Risk Information System (IRIS), (CASRN62-75-9, N-nitrosodimethylamine). Integr. Risk Inf. Syst. Chem. Assess. Summ. 1–9.

Jiang, P., Blawert, C., Scharnagl, N., Zheludkevich, M.L., 2019. Influence of water purity on the corrosion behavior of Mg0.5ZnX (X=Ca, Ge) alloys. Corros. Sci. 153, 62–73. https://doi.org/10.1016/j.corsci.2019.03.044

Kosaka, K., Hayashida, T., Terasaki, M., Asami, M., Yamada, T., Itoh, M., Akiba, M., 2012. Elution of bisphenol A and its chlorination by-products from lined pipes in water supply process. Water Sci. Technol. Water Supply 12, 791–798. https://doi.org/10.2166/ws.2012.055

Lane, R.F., Adams, C.D., Randtke, S.J., Carter, R.E., 2015. Chlorination and chloramination of bisphenol A, bisphenol F, and bisphenol A diglycidyl ether in drinking water. Water Res. 79, 68–78. https://doi.org/10.1016/j.watres.2015.04.014

Larson, T.E., Skold, R. V., 1958. Laboratory Studies Relating Mineral Quality of Water To Corrosion of Steel and Cast Iron. Corrosion 14, 43–46. https://doi.org/10.5006/0010-9312-14.6.43

Lundstedt, T., Seifert, E., Abramo, L., Thelin C Å A, B., Nystrom, A., Pettersen, J., Bergma, R., 1998. Experimental design and optimization. Chemom. Intell. Lab. Syst. 42, 3–40.

Michel, M., Ferrier, E., 2020. Effect of curing temperature conditions on glass transition temperature values of epoxy polymer used for wet lay-up applications. Constr. Build. Mater. 231, 117206. https://doi.org/10.1016/j.conbuildmat.2019.117206

Niesner, R., Heintz, A., 2000. Diffusion coefficients of aromatics in aqueous solution. J. Chem. Eng. Data 45, 1121–1124. https://doi.org/10.1021/je0000569

Palmiotto, M., Bianchi, G., Brunelli, L., Lualdi, M., Lezzi, C., Manenti, A., Davoli, E., 2015. Safety Evaluation of New Polymer Materials Proposed for Relining Drinking Water Pipes in the City of Milano. Int. J. Anal. Mass Spectrom. Chromatogr. 03, 63–79. https://doi.org/10.4236/ijamsc.2015.34008

Pham, H.Q., Marks, M.J., 2005. Epoxy Resins. Ullmann's Encyclopedia of Industrial Chemistry. https://doi.org/10.1002/14356007.a09

Rajasärkkä, J., Pernica, M., Kuta, J., Lašňák, J., Šimek, Z., Bláha, L., 2016. Drinking water contaminants from epoxy resin-coated pipes: A field study. Water Res. 103, 133–140. https://doi.org/10.1016/j.watres.2016.07.027

Rungchang, S., Numthuam, S., Qiu, X., Li, Y., Satake, T., 2013. Diffusion coefficient of antimony leaching from polyethylene terephthalate bottles into beverages. J. Food Eng. 115, 322–329. https://doi.org/10.1016/j.jfoodeng.2012.10.025

Schriks, M., Heringa, M.B., Kooi, M.M.E. Van Der, Voogt, P. De, Wezel, A.P. Van, 2010. Toxicological relevance of emerging contaminants for drinking water quality. Water Res. 44, 461–476. https://doi.org/10.1016/j.watres.2009.08.023

WHO, 2011. Water quality for drinking: WHO Guidelines, Springer Reference. https://doi.org/10.1007/springerreference_30502

Yang, Y.Y., Toor, G.S., Wilson, P.C., Williams, C.F., 2017. Micropollutants in groundwater from septic systems: Transformations, transport mechanisms, and human health risk assessment. Water Res. 123, 258–267. https://doi.org/10.1016/j.watres.2017.06.054

Supporting material

Section S1

In this section the steps of the migration tests applied to all the resins samples are reported. A scheme of the procedure is illustrated in Figure S1.

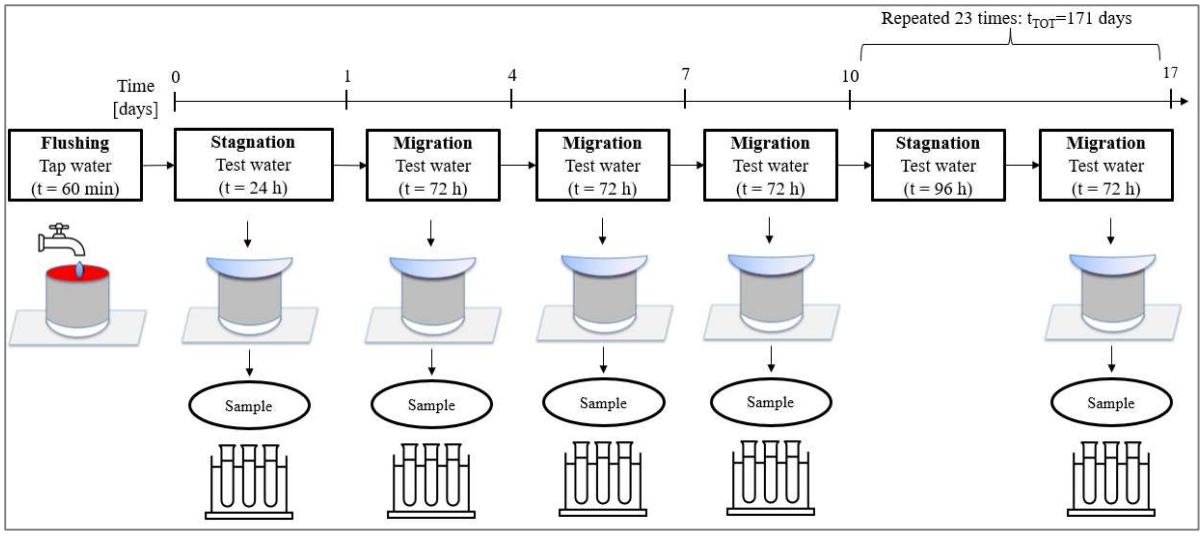

Figure S1. BPA migration test procedure and sampling scheme.

Firstly, the resins samples were flushed with flowing tap water for 60 min with a flushing speed of 1 m/min. Subsequently, the samples were filled with the test water and covered with a watch glass to avoid headspace formation and light intrusion for a 24 hours stagnation, at the end of which the test water was sampled for BPA analysis. The resin samples were then emptied and refilled with new test water. After the first stagnation, the test water was left in contact with the resin and then sampled for BPA measurement and replaced every 72 hours for three times. Subsequently, periods of stagnation of 96 hours, at the end of which the contact water was changed, were alternated with periods of migration of 72 hours at the end of which test water was sampled. This alternation between stagnation and migration was repeated for 23 times; therefore, the tests lasted for a total of 171 days.
The first 4 samples at 1, 4, 7 and 10 days were always analysed for BPA concentration. Over the other 23 collected samples, 8 samples were analysed for determination of BPA concentration. Therefore, for each test, a total of 12 samples was analysed and used for fitting the BPA leaching model over time.

Section S2

Figure S2 shows the urban area in which there are the two sections of piping, called A and B, renovated by relining with epoxy resins.

Figure S2. Representation of the urban area in which pipes A and B were renovated through relining with epoxy resins for which to assess the potential release of BPA. The DWTP feeding the renovated pipelines is reported as a green square. The DWTPs serving adjacent areas of the DWDN are reported as red squares.

The dimensional characteristics of the two pipe sections and the roughness values were provided by the water utility while the hydrodynamic conditions (flow rate, Q, and speed, v) in the two sections of the network where the relining is installed were obtained from the simulation of the EPANET hydraulic model. The values of the contact surface (S), volume (V) and water-pipe contact time (t_{cont}) of the pipe sections coated with epoxy resins are reported together with the dimensional and hydrodynamic characteristics of the two sections in Table S1.

Table S1. Installation date, dimensional and hydrodynamic characteristics of the pipe sections renovated by relining with epoxy resins.

Pipe	Installation date	Length	Diameter	Roughness	Q	v	S	V	t_{cont}
		[m]	[mm]	[µm]	[L/s]	[m/s]	[m²]	[m³]	[h]
A	28/02/2018	510	1200	1	600	0.53	1922.7	576.8	0.27
B	28/02/2018	605	1200	1	541	0.48	2280.8	684.2	0.35

About BPA diffusivity in water, in EPANET-MSX it was necessary to enter the relative diffusivity value, a parameter defined as:

$$D_{rel} = \frac{D_{BPA}}{D_{Cl,20°C}} \quad \text{(Eq. s1)}$$

where $D_{Cl,20°C}$ is the chlorine diffusivity at 20 °C, equal to $4{,}69 \cdot 10^{-6}$ m²/s (Niesner and Heintz, 2000).

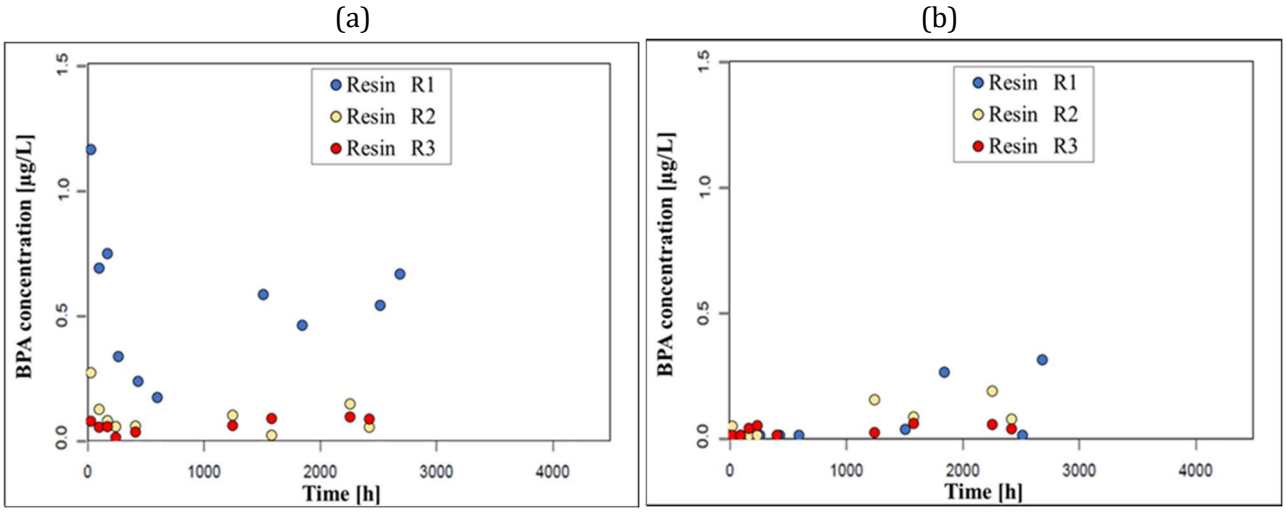

Figure S3. BPA migration over time as a function of the tested resin: (a) experimental data in deionized water, (b) experimental data in tap water with chlorine at 1 $mgCl_2/L$.

Table S2. Estimated responses (initial migrated concentration of BPA (BPA_0) and the BPA integral migration (BPA_IM)), and measured reduction in free BPA content in the epoxy resins for each test.

Design	Test	BPA_0	BPA_IM	BPA_Reduction
		µg/L	µg	µg/g
Preliminary screening	R1_0_12.5	1.327	216.6	21.5
	R1_1_12.5	0.030	60.8	25.4
RSM CCF Design	R1_0.06_11.8	1.714	226.9	24.2
	R1_0.06_13.2	1.412	160.6	20.7
	R1_0.2_11.5	1.443	275.7	24.4
	R1_0.2_12.5	1.297	171.4	21.8
	R1_0.2_12.5b	1.006	210.9	23.2
	R1_0.2_13.5	1.300	121.8	21.6
	R1_0.34_11.8	1.394	210.7	24.4
	R1_0.34_13.2	0.937	130.0	22.0
	R1_0.4_12.5	0.902	98.6	23.2

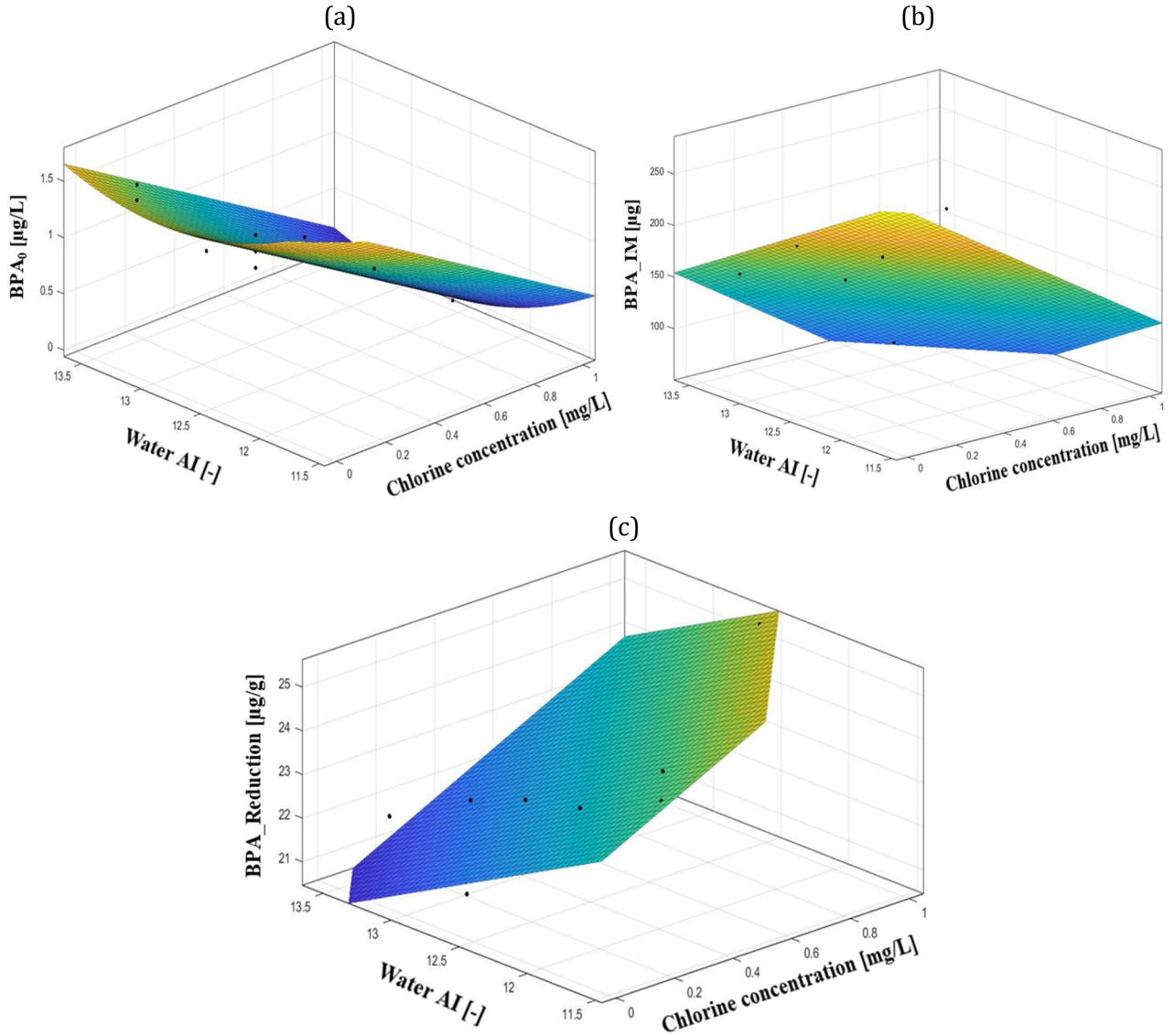

Figure S4. 3D models of (a) initial BPA concentration, BPA_0, (b) BPA integral migration, BPA_IM, and (c) free BPA content reduction, BPA_Reduction, as a function of chlorine concentration and water AI.

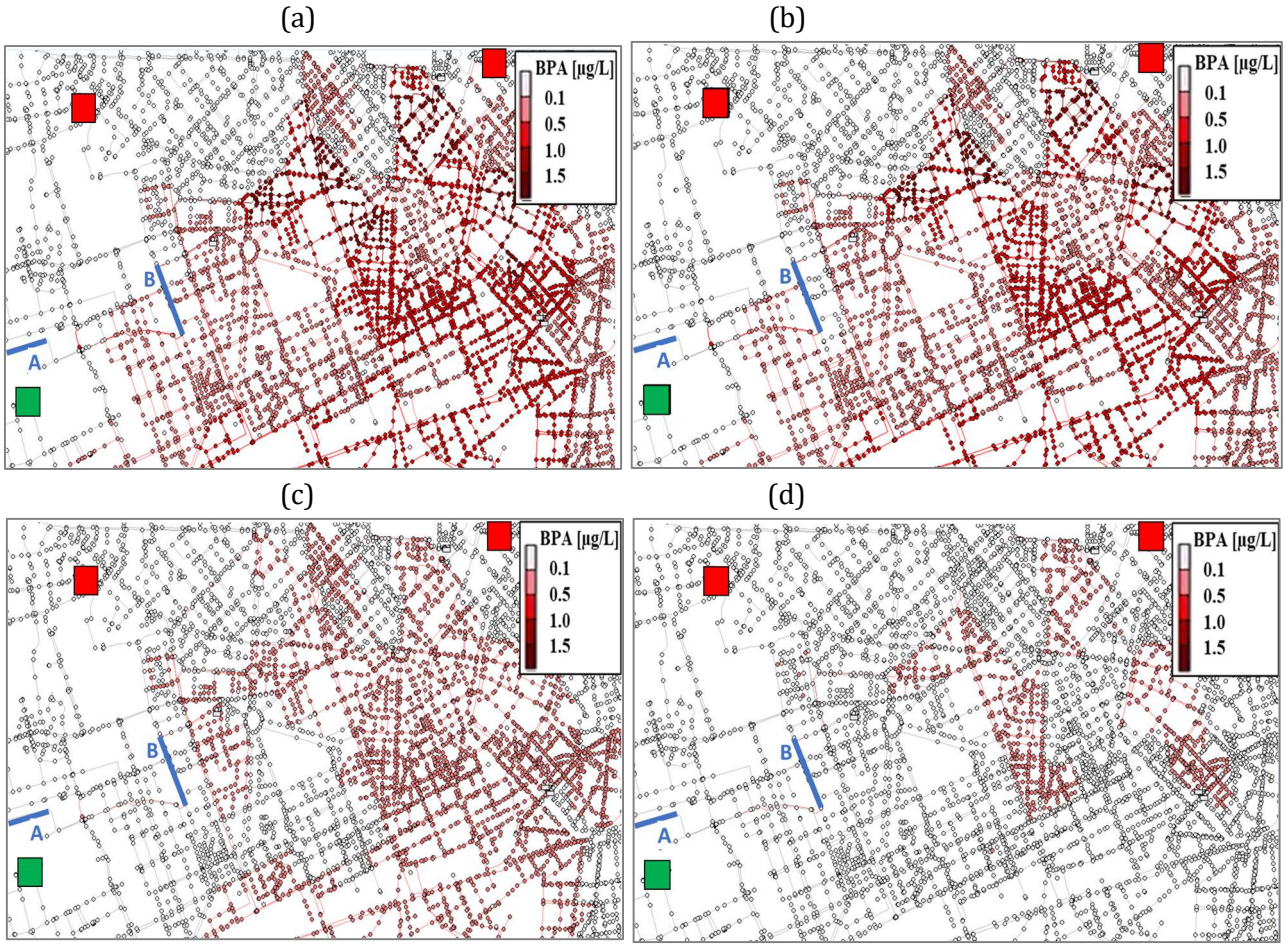

Figure S5. Modelled BPA concentration (µg/L) fate in a portion of the studied DWDN where two pipe segments were renovated by epoxy resins relining (blue segments in the graph, identified by letters A and B) as a function of the time from installation: (a) after 1 day; (b) after 5 days; (c) after 30 days; (d) after 100 days. The DWTP feeding the renovated pipelines is reported as a green square. The DWTPs serving adjacent areas of the DWDN are reported as red squares.

CONCLUSIONS

Drinking water (DW) supply systems should be managed with a risk-based approach to evaluate potential risks and devise preventive measures. The carried-out research works contributed to adapt and improve the application of risk assessment to contaminants of emerging concern (CECs) in DW supply systems. In fact, the application of risk assessment to CECs was found to be characterized by several knowledge gaps and high uncertainties that needed to be handled with new methods.

Several methods were developed and/or applied for the first time and were found to be fundamental in case of CECs presence in DW, considering their peculiar properties and very low concentrations with respect to other compounds usually present in DW. The following general conclusions could be derived:
- when dealing with CECs concentration databases, characterized by high percentages of censored data (data below the limit of quantification, LOQ), it is fundamental to use the advanced MLE_{LC} (maximum likelihood estimation for left censored data) method rather than traditional elimination or substitution methods, to accurately estimate CECs time trend, treatment removal efficiency and risk;
- the developed quantitative chemical risk assessment (QCRA) procedure allows the inclusion of CECs exposure and hazard uncertainties in the risk assessment, that is fundamental for a more precautionary risk management and can provide more insights, compared to the deterministic approach;
- the combination of lab experiments (i.e. isotherms, RSSCTs, and migration tests) designed with Design of Experiments (DoE) technique, advanced statistical data analyses (i.e. ANOVA, sensitivity, uncertainty, factorial, cluster analyses) and modelling tools (e.g. AquaPriori, Epanet-MSX, Response Surface Methodology, multivariate regression) enables the prediction of CECs fate through a full-scale GAC system and in the distribution network under different operating conditions, reducing the related uncertainties.

The work performed, integrating experimental and modeling features, has permitted to provide a supporting tool for:
- water utilities: that need to verify whether their current control measures are sufficient to meet new regulatory limits for CECs in DW and to elaborate intervention plans to minimize human health risks. In this context, the QCRA can be used to apportion the contribution of each phase of the supply chain to risk minimization in order to prioritize the interventions. The application of QCRA in combination with the simulation of GAC performance under different configurations and operating conditions allows to optimize GAC system up-grade and management. Finally, several practical indications were provided both on the criteria to be used in GAC and epoxy resins selection, and on planning monitoring systems to evaluate CECs removal by GAC system and to minimize recontamination events for DW contact with materials in the DW distribution network (DWDN);
- decision makers: that need to prioritize CECs to be included in regulations, beside the high uncertainty involved in this process. In this context, the QCRA can be effectively used to assess the exposure and hazard of different CECs, including the related uncertainties, to evaluate which CECs pose the highest risk for human health. Moreover, the study on epoxy resins could provide important supporting tools for decision makers to accurately regulate the characteristics of materials in contact with DW and tests manufacturers and water utilities should perform on the material before its installation in the DWDN;
- the scientific community: that needs to fill the knowledge gaps and reduce the uncertainties related to CECs exposure in DW and resulting health effect. In this context, this thesis provided indications on how to reduce estimation errors in different applications when analyzing databases characterized by high percentages of censored data. Additionally, the sensitivity and uncertainty analyses applied in combination to the QCRA can be useful to identify future needed research investigations and directions

in order to reduce uncertainties in risk estimation. Finally, this thesis showed how to combine experimental tests at different scales, prediction modeling tools and field monitoring to reduce the uncertainties related to CECs fate in GAC treatment systems and in the DWDN.

Currently, a further study has started on the application of the developed QCRA to assess and compare the human health risk due to the presence of several CECs (e.g. alkylphenols, BPA and phthalates) in tap and bottled waters.
Furthermore, possible future developments of this work involve the application of the developed QCRA to evaluate the effectiveness of different treatment trains to reduce the risk related to CECs in DW. Moreover, the QCRA can be used to select the optimal DW source to be fed to the DWTP, also in case of water reuse applications, which are among the topics of emerging interest.
Last but not least, another possible future development is related to the effect on water quality related to the interactions between water and materials, to deepen the work performed on bisphenol A release, in order to assess the release of other resins components and the formation of by-products due to water disinfection.